



The University of  
**Nottingham**

**Modelling the Linear Viscoelastic  
Rheological Properties of  
Bituminous Binders**

by

**Nur Izzi Md. Yusoff**

Thesis submitted to the University of Nottingham

For the degree of Doctor of Philosophy

April 2012

# Abstract

Rheology involves the study and evaluation of the flow and permanent deformation of time-and temperature-dependent materials, such as bitumen, that are stressed through the application of a force. The fundamental rheological properties of bituminous materials including bitumen are normally measured using a dynamic shear rheometer (DSR), from low to high temperatures. DSR is a powerful tool to measure elastic, viscoelastic and viscous properties of binders over a wide range of temperatures and frequencies, provided the tests are conducted in the linear viscoelastic region. Therefore, the study of bitumen rheology is crucial since it reflects the overall performance of a flexible pavement. However, it is well known that the DSR also has limitations, where the measurements are exposed to compliance (testing) errors particularly at low temperatures and/or high frequencies. In addition, conducting laboratory tests are known to be laborious, time consuming and require skilled personnel. Therefore, this research is conducted to elucidate a better understanding of the rheological properties and modelling procedures of bitumens and bituminous binders.

Various materials such as unmodified bitumens, polymer-modified bitumens (PMBs) and bitumen-filler mastics, unaged and aged samples, are used in this study. An extensive literature review was undertaken to identify reliable models that can be considered as a valuable alternative tool to describe or fit the rheological properties of bitumen. These properties are commonly presented in terms of complex modulus and phase angle master curves, together with the determination of shift factor values at a particular reference temperature. In general, the complex modulus and phase angle master curves can be modelled using different techniques; nomographs, mathematical equations and mechanical models. However, the nomographs have become obsolete in recent years and tended to be replaced by the two latter models.

Those models are able to satisfactorily describe the rheological properties of unmodified bitumen. However, the observations suggest a lack of agreement between measured and predicted rheological properties for binders that contain a

phase transition, such as found for highly crystalline bitumen, structured bitumen with high asphaltenes content and highly modified bitumen. An attempt was made to evaluate the validity of several mathematical equations and mechanical element approach using unaged and aged unmodified bitumens and PMBs database. It is observed that the Sigmoidal, Generalised Logistic Sigmoidal, Christensen and Anderson (CA), and Christensen, Anderson and Marasteanu (CAM) Models are able to satisfactorily describe the rheological properties of unmodified bitumens. Nevertheless, they suffer from the same drawbacks where the presence of highly EVA semi-crystalline and SBS elastomeric structures render breakdowns in the complex modulus master curves. Similar discrepancies are observed when one of the mechanical models (the 2S2P1D Model) is used.

To construct the master curves, different shifting methods are available. It is found that a numerical shift produced the best fit between measured and modelled data, followed by the *Laboratoire Central des Ponts et Chaussées* (LCPC) approach, William, Landel and Ferry (WLF), Modified Kaelble, Viscosity Temperature Susceptibility (VTS), Arrhenius and Log-Linear methods. A temperature range from 10 to 75°C is used in this study. It is worth mentioning that most of the methods are empirical and might not be applicable for all materials. Finally, the phase angle master curves must also not be neglected to yield a complete rheological properties of binders. The statistical analysis between measured and modelled data shows that the Fractional Model yielded the best correlation for a temperature range from 10 to 75°C, followed by the Al-Qadi and Co-workers, CAM, CA and Kramers-Kronig relationships. An anomaly is observed between measured and descriptive data of the Kramers-Kronig relationship particularly at high frequencies and/or low temperatures. The Fractional Model is not considered suitable for practical purposes due to the high number of coefficients that need to be solved.

# Acknowledgments

I need to thank and acknowledge the help and support of a lot of people, more than could be listed here. This thesis would never have been started without the help of my supervisor, Prof. Gordon Airey, who first introduced me to the mysteries of binder rheology and to the art of the scientific research.

I also owe a profound debt to those whose collective ideas and experiences have contributed greatly for writing the thesis: Prof. Emeritus Montgomery T. Shaw (University of Connecticut, USA), Prof. Hervé Di Benedetto (ENTPE, France), Dr. Geoffrey M. Rowe (Abatech Inc., USA) Dr. Tony T. Parry (NTEC, University of Nottingham), Mr. Adrian C. Pronk (Delft University of Technology, Netherland), Dr. Emmanuel Chailleux (LCPC, France), Mrs. Viviane Dupont (Eurobitume, Belgium), Dr. Jiantao Wu (Hohai University, China), Prof. Baosheng Wu (Tsinghua University, China), Prof. Che Husna Azhari (Universiti Kebangsaan Malaysia), Mr. Julien Van Rompu and Mr. Simon Pouget (ENTPE, France), Prof. Albert Molinas (Colorado State University, USA), Dr. Min Chi Liao (Taiwan), Mr. Ginoux Marc-Stéphane (LRPC, France), Mr. Pont Lawrence, Martyn Barret, Mr. Damien Mounier and Mrs. Angle Gilbert (NTEC, University of Nottingham).

My gratitude also goes to the Ministry of Higher Education (MOHE), Malaysia and Universiti Kebangsaan Malaysia for their financial support, without which it would have been impossible to complete this study. I especially want to acknowledge my wife, Hanna, and daughter, Suri, for their tolerance of the widespread piles of research papers and their encouragement at those bleak times when thoughts were not gel coherently. I would also like to thank all my family members for their precious supports and sacrifice.

Special thanks also given to all my research fellows in NTEC, with whom I have shared many memorable moments together. Thanks to all those who have helped me in some way but are not mentioned above by name.

# **Declaration**

The work described in this thesis was conducted at the University of Nottingham, Department of Civil Engineering between July 2007 and April 2012. I declare that the work is my own and has not been submitted for a degree of another university.

# Table of Contents

	<b>Page</b>
<b>Abstract</b>	i
<b>Acknowledgements</b>	iii
<b>Declaration</b>	iv
<b>Table of Contents</b>	v
<b>List of Figures</b>	xii
<b>List of Tables</b>	xvi
<b>1 Introduction</b>	<b>1</b>
1.1 Background	1
1.2 Bitumen Chemistry and Structure	2
1.3 Problem Statement	4
1.4 Objectives of Research	6
1.5 Thesis Structure	6
<b>2 Literature Review</b>	<b>8</b>
2.1 Background	8
2.2 Empirical Testing	9
2.2.1 The penetration test	9
2.2.2 The softening point test	10
2.2.3 Viscosity tests	11
2.2.4 The Fraass breaking point test	12
2.3 Fundamental Testing	13
2.3.1 Dynamic shear rheometer test	13
2.3.2 Bending beam rheometer test	15
2.4 Ageing	18
2.4.1 Thin film oven test	19
2.4.2 Rolling thin film oven test	19
2.4.3 Pressure ageing vessel test	20
2.5 Viscoelastic Behaviour of Bitumen	21
2.6 Dynamic Mechanical Analysis	23
2.7 Time-Temperature Superposition Principle	28
2.8 Master Curves	31
2.9 Shift Factors Laws	33
2.9.1 Numerical, non-linear least squares shift	34
2.9.2 The Williams, Landel and Ferry (WLF) equation	34
2.9.3 The Arrhenius equation	35
2.9.4 The Log-Linear Equation	36
2.9.5 The Viscosity Temperature Susceptibility (VTS) equation	36
2.9.6 The Laboratoire Central des Ponts et Chaussées approach	37
2.10 Rheological Data Representation	38
2.10.1 Isochronal plots	38
2.10.2 Isothermal plots	39
2.10.3 Black diagrams	39
2.10.4 Cole-Cole diagrams	40
2.11 Glassy Modulus	41

2.12	Bitumen Modification	44
2.13	Polymer-Modified Bitumens	45
2.13.1	Plastomer	47
2.13.2	Elastomer	48
<b>3</b>	<b>Rheological Models</b>	<b>51</b>
3.1	Background	51
3.2	Nomographs	52
3.2.1	Van der Poel's Nomograph	52
3.2.2	Modified Van der Poel's Nomograph	56
3.2.3	McLeod's Nomograph	60
3.3	Mathematical Models	64
3.3.1	Jongepier and Kuilman's Model	64
3.3.2	Dobson's Model	66
3.3.3	Dickinson and Witt's Model	69
3.3.4	Christensen and Anderson (CA) Model	70
3.3.5	Fractional Model	76
3.3.6	Christensen Anderson Marasteanu (CAM) Model	78
3.3.7	Bahia and Co-workers' Model	79
3.3.8	Al-Qadi and Co-workers' Model	82
3.3.9	Polynomial Model	85
3.3.10	Sigmoidal Model	85
3.3.11	The LCPC Master Curve Construction Method	86
3.3.12	New Complex Modulus and Phase Angle Predictive Model	89
3.3.13	Generalised Logistic Sigmoidal Model	90
3.4	Mechanical Models	90
3.4.1	Huet Model	91
3.4.2	The Huet-Sayegh Model	92
3.4.3	Di Benedetto and Neifar (DBN) Model	94
3.4.4	The 2S2P1D Model	95
3.5	Summary	100
<b>4</b>	<b>Experimental Programs</b>	<b>102</b>
4.1	Background	102
4.2	Materials	102
4.2.1	Unaged unmodified bitumens	102
4.2.2	Aged unmodified bitumens	103
4.2.3	Unaged polymer-modified bitumens	103
4.2.4	Aged Polymer-Modified bitumens	104
4.2.5	Unaged bitumen-filler mastics	104
4.2.6	Aged bitumen-filler mastics	104
4.3	Dynamic Shear Rheometer	105
4.3.1	Basic principle	105
4.3.2	Strain limit	106
4.3.3	Testing procedure	108
4.4	Solver Function	110
4.5	Statistical Analysis	110
4.5.1	Graphical method	111
4.5.2	Standard error ratio, $S_e/S_y$	111
4.5.3	Coefficient of determination, $R^2$	112

4.5.4	The discrepancy ratio ( $r_i$ )	112
4.5.5	The mean normalised error ( $MNE$ )	113
4.5.6	The average geometric deviation ( $AGD$ )	113
<b>5</b>	<b>Shift Factor Equations</b>	<b>114</b>
5.1	Background	114
5.2	Results and Discussion	115
5.2.1	Graphical comparisons	115
5.2.2	Goodness-of-fit statistics	120
5.2.3	WLF coefficients	125
5.3	Summary	126
<b>6</b>	<b>Mathematical Models</b>	<b>128</b>
6.1	Background	128
6.2	Detailed Procedure	129
6.3	Results and Discussion	130
6.3.1	The Sigmoidal Model	130
6.3.2	The Generalised Logistic Sigmoidal Model	137
6.3.3	Christensen and Anderson (CA) Model	142
6.3.4	Christensen Anderson and Marasteanu (CAM) Model	145
6.3.5	Statistical Analysis	152
6.3.6	Measurement errors	161
6.4	Summary	167
<b>7</b>	<b>Mechanical Models</b>	<b>168</b>
7.1	Background	168
7.2	Results and Discussion	169
7.2.1	Unaged unmodified bitumens	169
7.2.2	Unmodified bitumen-filler mastics	173
7.2.3	Unaged polymer-modified bitumens	176
7.2.4	Aged unmodified bitumen	180
7.2.5	Aged bitumen-filler mastics	183
7.2.6	Aged polymer modified bitumens	186
7.3	Statistical Analysis	189
7.3.1	Graphical comparisons	189
7.3.2	Goodness-of-fit statistics	191
7.4	Summary	194
<b>8</b>	<b>Phase Angle Equations</b>	<b>195</b>
8.1	Background	195
8.2	Phase Angle Equations	196
8.2.1	Kramers-Kronig Relationship	196
8.2.2	Christensen and Anderson (CA) Model	197
8.2.3	Fractional Model	197
8.2.4	Christensen, Anderson and Marasteanu (CAM) Model	197
8.2.5	Al-Qadi and co-workers Model	198
8.3	Construction of the Phase Angle Master Curves	198
8.4	Results and Discussion	199
8.4.1	Graphical comparisons	199
8.4.2	Statistical analysis	207

8.3 Summary	214
<b>9 Conclusions and Recommendations</b>	<b>215</b>
9.1 Conclusions	215
9.2 Recommendations for Future Work	217
<b>References</b>	<b>219</b>
<b>Appendix A</b>	<b>233</b>
<b>Appendix B</b>	<b>246</b>
<b>Appendix C</b>	<b>258</b>
<b>Appendix D</b>	<b>273</b>
<b>Appendix E</b>	<b>301</b>
<b>Appendix F</b>	<b>311</b>

# List of Figures

	<b>Page</b>
Fig. 1.1: Schematic representation of (a) SOL type and (b) GEL type bitumen structure [Read and Whiteoak, 2003]	3
Fig. 2.1: The penetration test [Read and Whiteoak, 2003]	10
Fig. 2.2: The ring-and-ball softening point test [Read and Whiteoak, 2003]	10
Fig. 2.3: Rotational viscometer	12
Fig. 2.4: The Fraas breaking point test [Read and Whiteoak, 2003]	12
Fig. 2.5: Schematic of dynamic shear rheometer testing configuration	13
Fig. 2.6: Definitions of $T$ , $\theta$ , $r$ and $h$	14
Fig. 2.7: Bending beam rheometer [Rowe <i>et al.</i> , 2001]	15
Fig. 2.8: Determination of $S(60)$ and $m$ -value [Rowe <i>et al.</i> , 2001]	16
Fig. 2.9: A comparison of inverse compliance to relaxation modulus of Polyisobutylene [Rowe <i>et al.</i> , 2001]	18
Fig. 2.10: Schematic diagram of rolling thin film oven test	20
Fig. 2.11: Schematic diagram of vessel ageing pressure [Petersen <i>et al.</i> , 1994]	21
Fig. 2.12: Viscoelastic response of bitumen under creep loading [Airey, 1997]	22
Fig. 2.13: Dynamic oscillatory stress-strain functions	25
Fig. 2.14: Dynamic test outputs from dynamic mechanical analysis (DMA)	25
Fig. 2.15: Relationship between $ G^* $ , $G'$ , $G''$ and $\delta$ [Airey and Hunter, 2003]	27
Fig. 2.16: Time-temperature superposition principle [Airey, 1997]	29
Fig. 2.17: Time-temperature superposition principle in the construction of a master curve [Anderson <i>et al.</i> , 1994]	31
Fig. 2.18: Construction of the $ G^* $ and $\delta$ master curves	32
Fig. 2.19: Isochronal plots for $ G^* $ and $\delta$ [Airey, 2002a]	38
Fig. 2.20: Isothermal plots for $ G^* $ and $\delta$ [Airey, 2002a]	39
Fig. 2.21: Example of the Black diagrams [Airey, 2002a]	40
Fig. 2.22: The Cole-Cole diagram	40
Fig. 2.23: Black diagram for two spindle geometries [Airey, 2002a]	42
Fig. 2.24: Complex modulus versus $\log(1 + \tan \delta)$ for two spindle geometries [Airey, 2002a]	43
Fig. 2.25: EVA copolymer structures [SpecialChem, 2012]	47
Fig. 2.26: SBS copolymer structures [Airey, 1997]	49
Fig. 2.27: Typical effect of SBS on the softening point of bitumen with different content of asphaltenes [Asphalt Academy, 2007]	50
Fig. 3.1: Van der Poel's non-linear multivariable model [Van der Poel, 1954]	53
Fig. 3.2: $S_m/S$ as a function of $S$ and $C_v$ [Heukolem and Klomp, 1964]	57
Fig. 3.3: Modified Van der Poel's non-linear multivariable model [Heukelom, 1973]	59
Fig. 3.4: Correlation between viscosity at 135°C and penetration at 25°C [McLeod, 1972]	61
Fig. 3.5: Suggested modification of Heukolem's version of Pfeiffer's and Van Doormaal's Nomograph [McLeod, 1972]	62
Fig. 3.6: Suggested modification to determine stiffness modulus of bitumen [McLeod, 1972]	63
Fig. 3.7: Definition of the CA Model [Christensen and Anderson, 1992]	71

Fig. 3.8: Modelling using the CA Model [Silva <i>et al.</i> , 2004]	73
Fig. 3.9: Comparison between measured (dotted) and descriptive (lines) data using the Fractional Model [Stastna <i>et al.</i> , 1996]	77
Fig. 3.10: Modelling using the CAM Model [Silva <i>et al.</i> , 2004]	79
Fig. 3.11: Definition of the Bahia and Co-workers' Model [Bahia <i>et al.</i> , 2001]	80
Fig. 3.12: Comparison between measured and descriptive $ G^* $ and $\delta$ master curves using Al-Qadi and Co-workers Model [Elseifi <i>et al.</i> , 2002]	84
Fig. 3.13: Definition of the Sigmoidal Model [Pellinen <i>et al.</i> , 2002]	86
Fig. 3.14: Example of plot $d \log  G^*  / d \log \omega$ versus $\delta/90$ [Chailleux <i>et al.</i> , 2006]	88
Fig. 3.15: The Huet Model [Huet, 1963]	91
Fig. 3.16: The Huet-Sayegh Model [Sayegh, 1966]	93
Fig. 3.17: The Di Benedetto and Neifar (DBN) Model [Di Benedetto <i>et al.</i> , 2007]	94
Fig. 3.18: Calibration of the DBN Model using the 2S2P1D Model	95
Fig. 3.19: Representation of the 2S2P1D Model	96
Fig. 3.20: Graphical representation of the model's parameters in terms of the Cole-Cole diagram	99
Fig. 3.21: Graphical representation of the model's parameters in terms of the Black diagram	102
Fig. 4.1: Illustration of the DSR set-up [Airey, 1997]	105
Fig. 4.2: Strain sweep used to determine the LVE region [Anderson <i>et al.</i> , 1994]	107
Fig. 4.3: (a) The DSR body and (b) 8 mm and 25 mm plates	108
Fig. 5.1: Comparisons between $a_T$ (numerical shift) and $a_T$ (model) of different shift factor equations of the unaged samples ( $T_{ref} = 25^\circ\text{C}$ )	118
Fig. 5.2: Comparisons between $a_T$ (numerical shift) and $a_T$ (model) of different shift factor equations of the aged samples ( $T_{ref} = 25^\circ\text{C}$ )	119
Fig. 5.3: Black diagram for unaged, RTFOT and PAV aged EVA PMB	120
Fig. 6.1: Comparisons between measured and model of unaged and aged unmodified bitumen data using the Sigmoidal Model	132
Fig. 6.2: Comparisons between measured and model of the unaged EVA PMBs data using the Sigmoidal Model	134
Fig. 6.3: Comparisons between measured and model of the RTFOT and PAV EVA PMBs data using the Sigmoidal Model	135
Fig. 6.4: Comparisons between measured and model of the unaged SBS PMBs data using the Sigmoidal Model	136
Fig. 6.5: Comparisons between measured and model of the PAV SBS PMBs data using the Sigmoidal Model	136
Fig. 6.6: Comparisons between measured and model of the unaged and aged unmodified bitumen data using the Generalised Logistic Sigmoidal Model	138
Fig. 6.7: Comparisons between measured and model of the unaged EVA PMBs data using the Generalised Logistic Sigmoidal Model	140
Fig. 6.8: Comparisons between measured and model of the PAV SBS PMBs data using the Generalised Logistic Sigmoidal Model	141
Fig. 6.9: Comparisons between measured and model of the unaged and aged	143

unmodified bitumens data using the CA Model	
Fig. 6.10: Comparisons between measured and model of the RTFOT and PAV EVA PMBs data using the CA Model	145
Fig. 6.11: Comparisons between measured and model of the unaged and aged unmodified bitumen data using the CAM Model	147
Fig. 6.12: Comparisons between measured and model of the unaged EVA PMBs data using the CAM Model	149
Fig. 6.13: Comparisons between measured and model of the unaged unmodified bitumen data using the CA and CAM Models	150
Fig. 6.14: Comparisons between measured and model of the unaged SBS PMBs data using the CAM Model	151
Fig. 6.15: Comparisons between measured and model of the PAV SBS PMBs data using the CAM Model	151
Fig. 6.16: Comparisons between measured and modelled the unmodified bitumens	154
Fig. 6.17: Comparisons between measured and modelled of PMBs	158
Fig. 6.18: Errors from the DSR measurements	161
Fig. 7.1: (a) Complex modulus, (b) phase angle and (c) Black diagrams of unaged unmodified bitumens	172
Fig. 7.2: (a) Complex modulus (b) phase angle and (c) Black diagrams of unaged bitumen-filler mastics	175
Fig 7.3: (a) Complex modulus, (b) phase angle and (c) Black diagrams of unaged PMBs	180
Fig. 7.4: (a) Complex modulus, (b) phase angle and (c) Black diagrams of aged unmodified bitumen	182
Fig. 7.5: (a) Complex modulus, (b) phase angle and (c) Black diagrams of aged bitumen-filler mastics	186
Fig. 7.6: (a) Complex modulus, (b) phase angle and (c) Black diagrams of aged PMBs	189
Fig. 7.7: Graphical comparison between measured and modelled $ G^* $	190
Fig. 7.8: Graphical comparison between measured and modelled $\delta$	191
Fig. 8.1: Measured versus descriptive $\delta$ data of the unaged unmodified bitumens	201
Fig. 8.2: Measured versus descriptive $\delta$ data of the aged unmodified bitumens	202
Fig. 8.3: Measured versus descriptive $\delta$ data of the unaged PMBs	203
Fig. 8.4: Measured versus descriptive $\delta$ data of the aged PMBs	204
Fig. 8.5: A comparison between measured and descriptive $\delta$ of the unaged unmodified bitumen	205
Fig. 8.6: A Comparison between measured and descriptive $\delta$ of the aged PMB using the Fractional Model	206
Fig. 8.7: A comparison between measured and descriptive $\delta$ of the aged PMB using the Al-Qadi and co-workers Model	207

# List of Tables

	<b>Page</b>
Table 2.1: General classification of bitumen additives and modifiers [Airey, 2009]	46
Table 2.2: Advantages of the EVA PMB	48
Table 2.3: Advantages of the SBS PMB	49
Table 3.1: The 2S2P1D parameters functions	99
Table 4.1: Linear viscoelastic strain limits (%)	109
Table 4.2 : Criteria of the goodness-of-fit statistics [Tran and Hall, 2005]	112
Table 5.1: Summary of the $S_e/S_y$ , $R^2$ , $r_i$ , $MNE$ and $AGD$ goodness-of-fit for unaged samples	123
Table 5.2: Summary of the $S_e/S_y$ , $R^2$ , $r_i$ , $MNE$ and $AGD$ goodness-of-fit for aged samples	124
Table 5.3: Shifting coefficients of the WLF equation	125
Table 6.1: The Sigmoidal parameters for unmodified bitumens	130
Table 6.2: The Sigmoidal parameters for the EVA PMBs	133
Table 6.3: The Sigmoidal parameters for the SBS PMBs	133
Table 6.4: The Generalised Logistic Sigmoidal parameters for unmodified bitumens	137
Table 6.5: The Generalised Logistic Sigmoidal parameters for EVA PMBs	139
Table 6.6: The Generalised Logistic Sigmoidal parameters for SBS PMBs	141
Table 6.7: The CA Model parameters for unmodified bitumens	142
Table 6.8: The CA Model parameters for the EVA PMBs	144
Table 6.9: The CA Model parameters for the SBS PMBs	144
Table 6.10: The CAM Model parameters for unmodified bitumens	146
Table 6.11: The CAM Model parameters for the EVA PMBs	148
Table 6.12: The CAM Model parameters for the SBS PMBs	148
Table 6.13: SSE for the unaged and aged unmodified bitumens	156
Table 6.14: SSE for the unaged EVA PMBs	156
Table 6.15: SSE for the RFTOT aged EVA PMBs	157
Table 6.16: SSE for the PAV aged EVA PMBs	157
Table 6.17: SSE for the unaged SBS PMBs	158
Table 6.18: SSE for the RTFOT aged SBS PMBs	158
Table 6.19: SSE for the PAV aged SBS PMBs	159
Table 6.20: The goodness-of-fit statistics for unmodified bitumens	159
Table 6.21: The goodness-of-fit statistics for PMBs	160
Table 6.22: Measurement error (%) of the unaged and aged unmodified bitumens	163
Table 6.23: Measurement error (%) of the unaged EVA PMBs	163
Table 6.24: Measurement error (%) of the RTFOT aged EVA PMBs	164
Table 6.25: Measurement error (%) of the PAV aged EVA PMBs	164
Table 6.26: Measurement error (%) of the unaged SBS PMBs	165
Table 6.27: Measurement error (%) of the RTFOT aged SBS PMBs	165
Table 6.28: Measurement error (%) of the PAV aged SBS PMBs	166

Table 7.1: The model parameters for unaged unmodified bitumens	170
Table 7.2: Comparisons between NTEC and Di Benedetto <i>et al.</i> 's Model parameters	170
Table 7.3: The model parameters for bitumen filler mastics (40% by volume)	173
Table 7.4: The model parameters for bitumen-filler mastics (by weight)	173
Table 7.5: The model parameters for bitumen filler mastics obtained by Delaporte <i>et al.</i> [2009] (40% by volume)	176
Table 7.6: The model parameters for unaged polymer-modified bitumens	178
Table 7.7: The model parameters for the aged unmodified bitumens	184
Table 7.8: The model parameters for the aged bitumen-filler mastics (40% by volume)	184
Table 7.9: The model parameters for the aged polymer modified bitumens	190
Table 7.10: Statistical analysis for the complex modulus master curves	196
Table 7.11: Statistical analysis for the phase angle master curve	196
Table 8.1: SSE values for the unaged and aged unmodified bitumens	210
Table 8.2: SSE values for the unaged EVA PMBs	210
Table 8.3: SSE values for the RTFOT aged EVA PMBs	211
Table 8.4: SSE values for the PAV aged EVA PMBs	211
Table 8.5: SSE values for the unaged SBS PMBs	212
Table 8.6: SSE values for the RTFOT aged SBS PMBs	212
Table 8.7: SSE values for the PAV aged SBS PMBs	212
Table 8.8: The goodness-of-fit statistics for the unaged and aged unmodified bitumens	213
Table 8.9: The goodness-of-fit statistics for the unaged and aged PMBs	213

## **1.1 Background**

Bitumen is a civil engineering construction material manufactured from crude oil through a series of distillation processes undertaken during the refining of petroleum. One of the characteristics and advantages of bitumen as an engineering construction and maintenance material is its great versatility. Although a semi-solid at ordinary temperatures, bitumen may be liquified by applying heat, dissolving in solvents, or emulsifying it. Bitumen is a strong cement that is readily adhesive and highly waterproof and durable, making it useful in road building. It is also highly resistive to the actions of most acids, alkalis, and salts [Minnesota Asphalt Pavement Association, 2003].

The principle use of bitumen is as a binder in the road construction industry where it is mixed with graded aggregate to produce asphalt mixture. This mixture is then laid as the structural pavement layers of a road. The main function of these 'bitumen-bound' layers is to spread loads (caused by the trafficking of vehicles) evenly over the unbound pavement layers of the road and natural sub-grade to prevent overstressing. In addition to providing stiffness and bearing capacity, asphalt mixture must be able to resist two primary modes of flexible pavement distress, namely, excessive permanent deformation (rutting) and fatigue cracking. As the mechanical properties of asphalt mixture are strongly dependent upon the properties of the binder, it has to fulfil certain mechanical and rheological requirements to ensure the integrity of the road [Airey, 2009].

First, the bitumen must be fluid enough at high temperature (approximately 160°C) to be pumpable and workable to allow for a homogeneous coating of the

aggregates upon mixing. Second, it has to become stiff enough at the highest pavement temperature to resist rutting deformation (approximately around 60°C, depending on the local climate). Finally, it must remain soft enough at lower temperatures (down to -20°C, depending on the local climate) to resist cracking. Therefore, it is difficult to obtain bitumen that would work under all possible climates. To surmount this problem, different types of bitumens including modified binders are available. The softer and harder binders are normally used for colder and hotter climate regions respectively [Lesueur, 2009].

It should be noted that the word "bitumen" in the European sense is used, when referring to the binder, throughout this thesis and not "asphalt" or "tar". The word "asphalt" brings a similar meaning to "bitumen" in North America but in Europe, "asphalt" refers to the complex mixture composed of various selected aggregates bound together with different percentages of air voids. Meanwhile, "tar" is a liquid obtained when natural organic materials such as coal or wood are carbonised or destructively distilled in the absence of air [Read and Whiteoak, 2003]. The word asphalt mixture is used in the whole thesis, not "hot mix asphalt concrete (HMA or HMAC)" or "asphalt (or asphaltic) concrete pavement (AC)" or "bituminous asphalt concrete (bituminous mixture)" when referring to the mixture.

## **1.2 Bitumen Chemistry and Structure**

In general, bitumen can be divided into two broad chemical groups; namely asphaltenes (which are insoluble in *n*-heptane) and maltenes. The maltenes can be further split into saturates, aromatics and resins [Corbett, 1970]. The asphaltene content has a large effect on the rheological properties of bitumen and related to a number of physical parameters such as the glass transition and bitumen viscosity [Corbett, 1970; Halstead, 1987]. An increase of the asphaltenes content will generally produce harder bitumen with a lower penetration, higher softening point and higher viscosity [Scholz, 1995]. In general, asphaltenes represent between 5–25% of the bitumen and are the heaviest constituents with molecular weights ranging from 600 to 30,000 [Read and Whiteoak, 2003; Lesueur, 2009]. Resins, with molecular weights ranging from 500 to 50,000, act as dispersing agents or peptisers for the asphaltenes and their proportion to asphaltenes determines the

structural character of the bitumen [Nellensteyn, 1924]. Aromatics are the major dispersion medium for peptised asphaltenes and constitute between 40–65% of the bitumen and have molecular weights ranging from 300 to 2000. Saturates are non-polar viscous oils, consisting of 5–20% of overall bitumen [Read and Whiteoak, 2003; Airey, 2009].

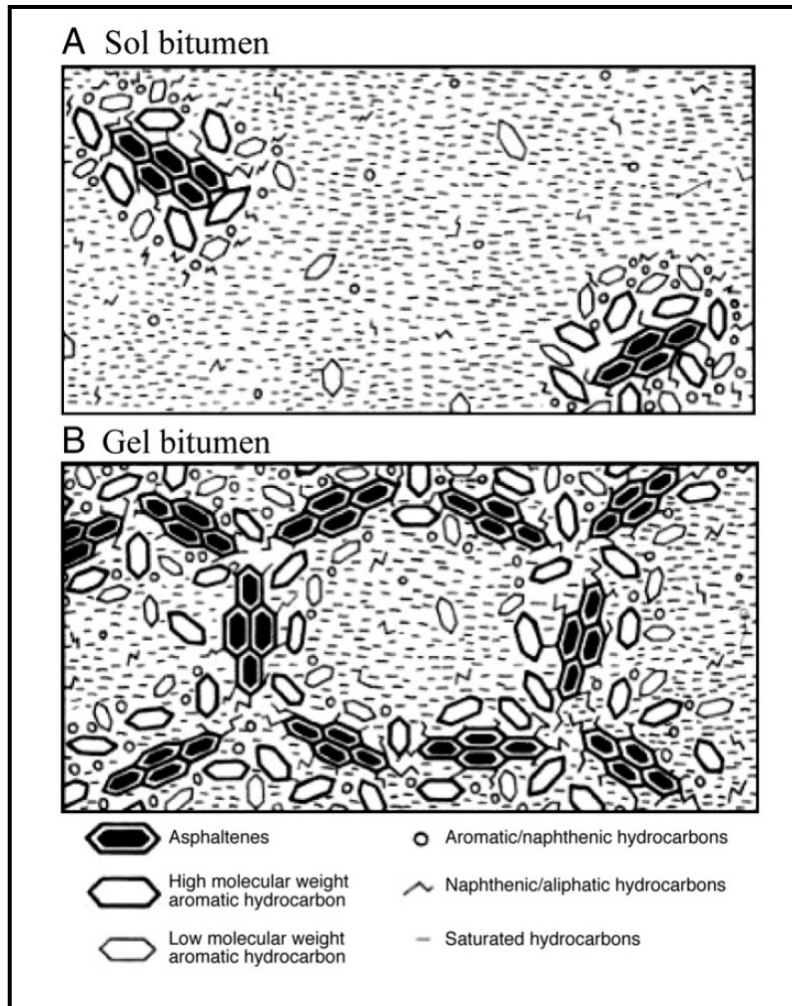


Fig. 1.1: Schematic representation of (a) SOL type and (b) GEL type bitumen structure [Read and Whiteoak, 2003]

In terms of its structure, bitumen is traditionally regarded as a colloidal system consisting of high molecular weight asphaltene micelles dispersed or dissolved in a lower molecular weight oily medium [Read and Whiteoak, 2003; Airey, 2009]. There are two distinct types of bitumens namely the well dispersed solution (SOL) type and the gelatinous (GEL) type, as shown in Fig. 1.1 [Pfeiffer and Saal, 1940]. SOL type bitumens are those which have sufficient quantities of

resins and aromatics of adequate solvating power leading to fully peptized, well-dispersed asphaltenes that do not form extensive associations. GEL type bitumens are that which the resins aromatic fraction is insufficient to fully peptize the micelles and the asphaltenes form large agglomerations or even continuous networks [Read and Whiteoak, 2003].

The Index of Colloidal Instability (CI), which is defined as the ratio of the amount of asphaltenes and saturates to the amount of resins and aromatics, is sometimes used to describe the stability of the colloidal structure. The higher the CI, the more the bitumen is regarded as GEL type bitumen. The lower the CI, the more stable the colloidal structure, therefore the bitumen is regarded as SOL type bitumen [Airey, 2009]. Other structural models had been proposed including a conceptual microstructural model during the Strategic Highway Research Program (SHRP) [Petersen *et al.*, 1994] and a thermodynamic solubility model [Redelius, 2006]. Irrespective of their differences, all these models have one common goal of attempting to establish a correlation between the chemical composition of the bitumen and its physical properties. The physical, mechanical and rheological properties of bitumens are determined and defined by both the constitution (chemical composition) and the structure (physical arrangement of the molecules in the material) [Nellensteyn, 1924; Corbett, 1970; Petersen, 1984; Airey, 2009]. In this study, emphasis is given to the rheological properties of bituminous binders.

### **1.3 Problem Statement**

The rheological properties of bituminous binders including bitumens are typically determined by means of dynamic mechanical analysis (DMA) using an oscillatory type, dynamic shear rheometer (DSR) tests. In general, the test is conducted within the linear viscoelastic (LVE) region [Airey, 2002a]. Research into the rheological properties of bitumen has been growing and importance in specifications in the USA since the early 1990's following the Strategic Highway Research Program (SHRP). The DSR instrument, however, does have its limitations where the measured rheological data are exposed to the measurement error particularly at low temperatures and/or high frequencies. Alternatively, other

equipments such as a bending beam rheometer (BBR) and a direct tension test (DT) can be used at this region.

The use of models can be a valuable tool to fit or describe the rheological properties of bituminous binders and asphalt mixtures [Mohammad *et al.*, 2005]. Development of the models started in the 1950s when Van der Poel developed his first nomograph [Van der Poel, 1954]. Since then, a reasonable number of studies have been conducted to describe dynamic data master curves of binders and asphalt mixtures. The dynamic data collected at different temperatures can be shifted relative to the frequency (time of loading), so that the various curves can be aligned to form a single and continuous line called a master curve [Pellinen *et al.*, 2002]. The amount of shifting required at each temperature to form the master curve is termed as the shift factor,  $a_T$ . It is found that different shift factor methods are available such as a random shift, William Landel and Ferry (WLF), Arrhenius, Log-Linear, Viscosity Temperature Susceptibility (VTS) and *Laboratoire Central des Ponts et Chaussées* (LCPC) methods [Anderson *et al.* 1994; Pellinen *et al.* 2002; Chailleux *et al.* 2006].

In general, the rheology models established can be divided into three main groups; namely nomographs, mathematical and mechanical models. Some of the models are applicable for both viscoelastic liquids (binders) and viscoelastic solids (asphalt mixtures). One of them is the 2S2P1D Model developed by Di Benedetto *et al.* [Olard and Di Benedetto, 2003; Olard *et al.*, 2003; Delaporte *et al.*, 2007]. This model, a combination of two springs, two parabolic elements and one dashpot, is a unique model as its parameters are relatable to the construction of master curves, the Black diagram and the Cole-Cole diagram. Di Benedetto *et al.* conducted dynamic tests using an annular shear rheometer (ASR) and validated the data using the 2S2P1D Model [Olard and Di Benedetto, 2003; Olard *et al.*, 2003; Delaporte *et al.*, 2007]. However, none of the studies have been conducted to validate the dynamic test data from other rheometers like the DSR.

## **1.4 Objectives of Research**

In general, this research is conducted to elucidate a better understanding of the rheological properties and modelling procedures of bitumens and bituminous binders. Considering the problem statement above, the main objectives of this research can be summarised as follows:

- Review the published literature on rheology models used to characterise the rheological properties of bitumens and bituminous binders.
- To verify different shifting factor techniques on constructing complex modulus master curves using the Nottingham Transportation Engineering Centre (NTEC) DSR database.
- To verify several mathematical and mechanical models using the NTEC DSR database.
- To verify different phase angle models using the NTEC DSR database.

## **1.5 Thesis Structure**

The thesis structure is arranged as follows:

- Chapter 1 provides a brief background on chemical and structural properties of bitumen are that normally used in asphalt mixture paving construction. The problem statement and research objectives are also included.
- Chapter 2 deals with the basic concept of bitumen rheology and overview of the construction of a master curve.
- Chapter 3 reviews various rheological models used to describing or fitting the rheological properties of bituminous binders. Three groups of models; namely the nomographs, mathematical and mechanical models, including their advantages and drawbacks, are discussed.
- Chapter 4 describes the experimental design section and various types of materials used in this study, the introduction of the DSR tests, the use of Solver function and statistical analysis.

- Chapter 5 deals with six shifting techniques; namely a numerical, non-functional form shift approach, the Williams, Landel and Ferry (WLF), a *Laboratoire Central des Ponts et Chaussées* (LCPC), a Viscosity Temperature Susceptibility (VTS), the Arrhenius and a Log-linear approaches have been used together with a large rheological database held by the NTEC laboratory.
- Chapter 6 investigates the use of four mathematical models; namely the Sigmoidal Model, the Generalised Logistic Sigmoidal Model, the Christensen and Anderson (CA) Model and Christensen, Anderson and Marasteanu (CAM) Model to fit or describe the rheological properties of bituminous binders. Graphical and goodness-of-fit statistics methods are used to correlate between measured and descriptive data.
- Chapter 7 evaluates the suitability of the 2S2P1D Model to describe the rheological properties of NTEC database. Correlations between measured and descriptive data are evaluated using both graphical and goodness-of-fit statistical analysis methods.
- Chapter 8 attempts to evaluate the validity of several phase angle equations on NTEC DSR dataset. Correlations between measured and descriptive data are evaluated using both graphical and goodness-of-fit statistical analysis methods.
- Chapter 9 summarises the conclusions obtained from this study and presents several potential recommendations for future work.

## Literature Review

---

### 2.1 Background

Physically, bitumen can be classified as a thermoplastic material that shows glass-like behaviour at (elastic and brittle response to loading) at low temperatures ( $<0^{\circ}\text{C}$ ) and fluid-like behaviour at high temperatures ( $>60^{\circ}\text{C}$ ). At intermediate temperatures ( $0^{\circ}\text{C}$  to  $60^{\circ}\text{C}$ ), bitumen processing both elastic and viscous properties (viscoelastic response), with the relative proportion of these two responses depending on temperature and loading rate. It is this fundamental rheological (flow) property of bitumen that defines its physical nature and makes it such a versatile binder for paving mixture in virtually all of the habitable climates found on earth [Airey, 2009]. In the measurement of the physical properties of bitumen, emphasis is given to the characterisation of the rheological behaviour of bitumen.

Rheology, by definition, involves the study and evaluation of the flow and permanent deformation of time- and temperature-dependent materials, such as bitumen, that are stressed (usually shear stress or extensional stress) through the application of force [Barnes *et al.*, 1989; Airey, 1997; Saleh, 2007]. The word rheology is believed originally from the Greek words "ῥεω", which can be translated as "*the river, flowing, streaming*", and "λογία" meaning "*word, science*" and therefore literally means "*the study of the flow*" or "*flow science*" [Airey, 1997; Mezger, 2006]. Therefore, the rheology of bitumen can be defined as the fundamental measurements associated with the flow and deformation characteristics of bitumen. Understanding the flow and deformation (rheological properties) of bitumen in an asphalt mixture is important in terms of pavement performance. Asphalt mixture that deforms and flows too readily may be susceptible to rutting

and bleeding, whereas those that are too stiff may be susceptible to fatigue and cracking.

The physical properties of bitumen are complex and to describe its properties over a wide range of operating conditions (temperature, loading rate, stress and strain) normally require a large number of tests. To avoid this and to simplify the situation, the mechanical behaviour and rheological properties of bitumen have traditionally been described using empirical tests and equations. Two consistency tests normally required to characterise different grades of bitumen are the needle penetration test and the ring and ball softening point test. These two tests provide an indication of the consistency (hardness) of the bitumen without completely characterising the viscoelastic response and form the basis of the bitumen specification [Airey, 2009].

## **2.2 Empirical Testing**

### **2.2.1 The penetration test**

The penetration test can be considered as an indirect measurement of the viscosity of the bitumen at 25°C, to specify different grades of bitumens. In the penetration test, a needle penetrates a sample of bitumen under a load of 100 grams at a temperature of 25°C for a known loading time of 5 seconds. The test apparatus is shown in Fig. 2.1. The definition of penetration, which is measured in tenths of a millimetre (decimillimetre, dmm) is the distance travelled by the needle into the bitumen sample under the loading conditions. Under these conditions, typical values for paving grade bitumen range between 15 and 200 dmm. For penetration less than 30 dmm, the bitumen is generally said to be hard. On the contrary, penetration values higher than 100 dmm correspond to soft bitumens [Lesueur, 2009]. For example, a 40/60 penetration grade bitumen has a penetration value at 25°C ranging from 40 to 60 in units dmm. Therefore, a variety of bitumens can be easily graded and specified based on the penetration results.



Fig. 2.1: The penetration test [Read and Whiteoak, 2003]

### 2.2.2 The softening point test

The ring and ball softening point test is usually conducted to determine the consistency of bitumens by measuring the equi-viscous temperature at the beginning of the fluidity range of bitumens. In this test, a steel ball (weight 3.5 g) is placed on a bitumen sample contained in a brass ring that is suspended in a water or glycerine bath, in which the bath temperature is raised at 5°C per minute. Water is used for bitumen with a softening point of 80°C or below. Meanwhile, glycerine is used for softening points greater than 80°C [Read and Whiteoak, 2003].

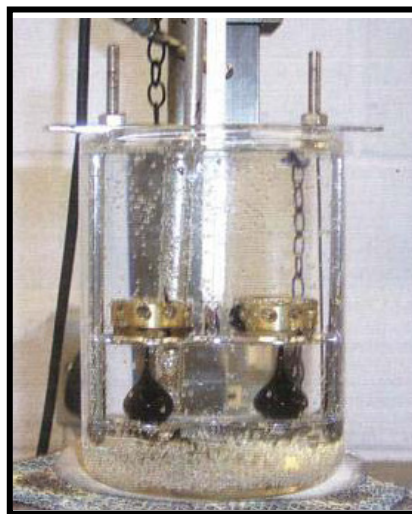


Fig. 2.2: The ring-and-ball softening point test [Read and Whiteoak, 2003]

The softening point is the temperature measurement when the bitumen softens and eventually deforms slowly with the ball through the ring to touch a base plate 25 mm below the ring. The test set-up is shown in Fig. 2.2. Under these conditions, typical values for paving grade bitumen range between 35°C and 65°C. A hard bitumen generally has a softening temperature close to 60°C while a softer grade will typically have a softening temperature around 40°C [Lesueur, 2009].

### 2.2.3 Viscosity tests

Viscosity is a measure of the resistance to flow of a liquid and is defined as the ratio between the applied shear stress and the rate of shear strain measured in units of pascal seconds (Pa.s). It is a fundamental characteristic of bitumens and determines how the material will behave at a given temperature and over a temperature range. In addition to absolute or dynamic viscosity, viscosity can also be measured as kinematic viscosity in units of  $\text{m}^2/\text{s}$  or more commonly  $\text{mm}^2/\text{s}$  with  $1 \text{ mm}^2/\text{s}$  is equal to 1 centistoke (cSt). The viscosity of bitumen can be measured with a variety of devices in terms of its absolute and kinematic viscosities. In general, specifications are based on a measure of absolute viscosity at 60°C and a minimum kinematic viscosity at 135°C using vacuum and atmospheric capillary tube viscometers respectively. Absolute viscosity can also be measured using a fundamental method known as the sliding plate viscometer. The sliding plate test monitors force and displacement on a thin layer of bitumen contained between parallel metal plates at varying combinations of temperature and loading time.

The rotational viscometer test (ASTM D 4402-02) is presently considered to be the most practical means of determining the viscosity of bitumen. The Brookfield rotational viscometer and Thermocel system, as shown in Fig. 2.3, allows the testing of bitumen over a wide range of temperatures (more so than most other viscosity measurement system). The operation of the rotational viscometer consists of one cylinder rotating coaxially inside a second (static) cylinder containing the bitumen sample, all contained in a thermostatically controlled environment. The material between the inner and the outer cylinder (chamber) is therefore analogous to the thin bitumen film found in the sliding plate viscometer. The torque on the rotating cylinder or spindle is used to measure the relative resistance to rotation of the

bitumen at a particular temperature and shear rate. The torque value is then altered by means of calibration factors to yield the viscosity of the bitumen [Airey, 2009].

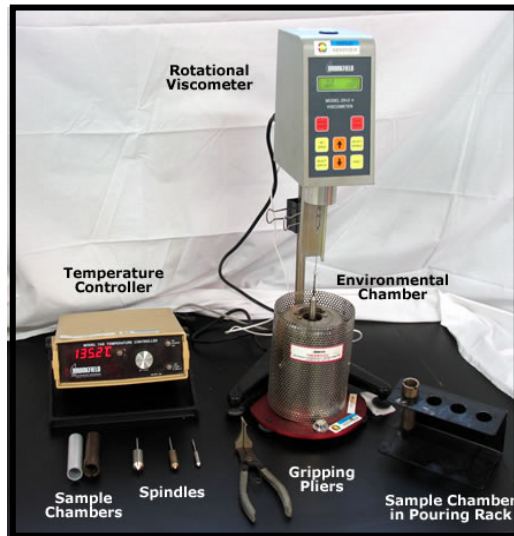


Fig. 2.3: Rotational viscometer

#### 2.2.4 The Fraass breaking point test

The Fraass test (Fig. 2.4) is an empirical means of obtaining an estimate of the temperature at which a thin film of bitumen might crack. The test involves the flexing of a sample of bitumen contained on a spring steel plaque at successively lower temperatures until it cracks. The temperature at which the sample cracks is termed the breaking point and represents an equi-viscous temperature [Airey, 2009].

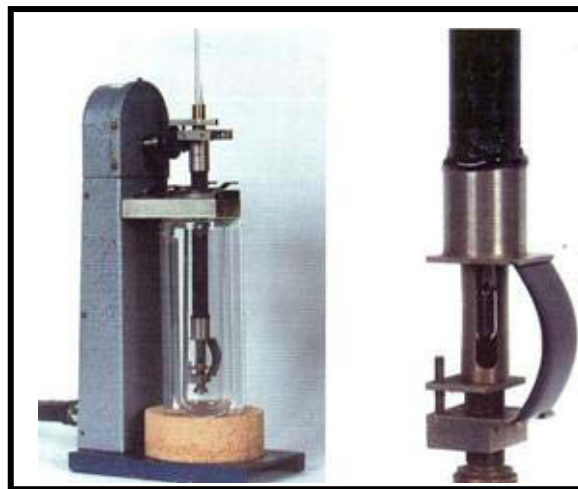


Fig. 2.4: The Fraass breaking point test [Read and Whiteoak, 2003]

## 2.3 Fundamental Testing

The performance of asphalt pavements are not easily characterised by physical properties as they are subjected to complex environmental and loading conditions. In addition, various modified binders cannot necessarily be characterised by empirical properties. It is important to understand the stress-strain behaviour of bituminous binders over a wide range of temperatures and loading time conditions. Thus, fundamental tests were introduced and developed to investigate mechanical properties and viscoelasticity of binders under different environmental conditions. The Strategic Highways Research Program (SHRP), developed in the United States of America, was a coordinated effort to produce binder specifications which were classified based on a performance-grade system in accordance with fundamental testing results [Petersen *et al.*, 1994; Anderson *et al.*, 1994].

### 2.3.1 Dynamic shear rheometer test

The dynamic shear rheometer (DSR) test (AASHTO T315–02) is used to measure the elastic, viscoelastic and viscous nature of bituminous binders within the linear viscoelastic (LVE) region over a wide range of temperatures and frequencies (time of loadings). The schematic diagram of DSR testing configuration is shown in Fig. 2.5.

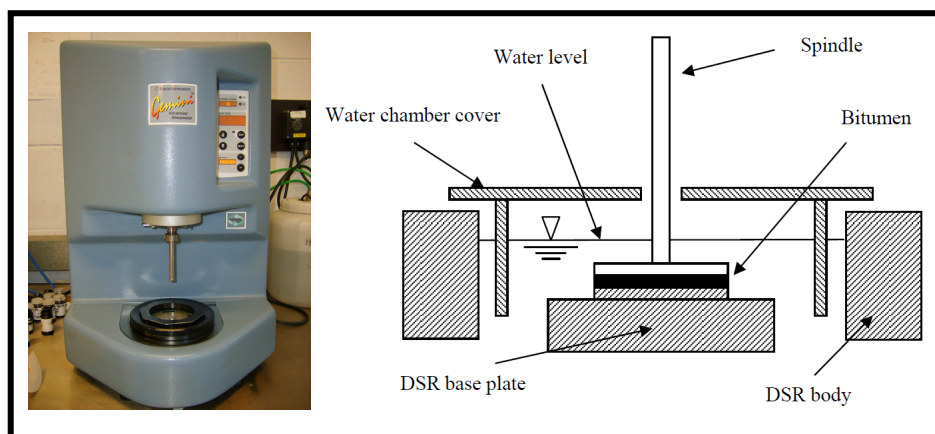


Fig. 2.5: Schematic of dynamic shear rheometer testing configuration

The oscillatory-type test is conducted on binders at different temperature, frequency, stress and strain levels. In the test, a bitumen sample sandwiched between two parallel plates is subjected to a sinusoidal torque or a sinusoidal angular displacement of constant angular frequency. Various rheological parameters are converted from the measurements of the torque applied to a specimen in response to the applied shear stresses or strains. The amplitude of the responding stress is measured by determining the torque transmitted through the sample in response to the applied strain. Therefore, the stress and strain parameters can be calculated as:

$$\sigma = \frac{2T}{\pi r^3} \quad (2.1)$$

and

$$\gamma = \frac{\theta r}{h} \quad (2.2)$$

where  $\sigma$  is a shear stress,  $T$  is a torque,  $r$  is radius of parallel discs,  $\gamma$  is shear strain,  $\theta$  is deflection angle and  $h$  is a gap between parallel discs. They are shown in Fig. 2.6.

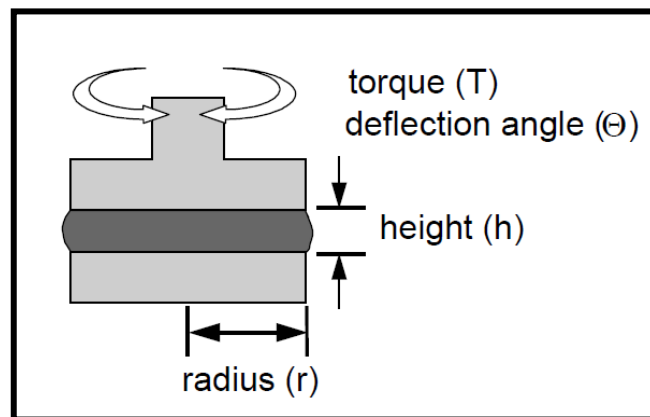


Fig. 2.6: Definitions of  $T$ ,  $\theta$ ,  $r$  and  $h$

The shear stress and strain in Equations 2.1 and 2.2 are dependent on the radius of the parallel discs and vary in magnitude from the centre to the perimeter of the disc. The shear stress, shear strain and complex modulus, which is a function of the radius to the fourth power, are calculated for the maximum value of radius. The

phase angle,  $\delta$ , is measured by the instrument by accurately determining the sine wave forms of the strain and torque.

The strains that are applied during the dynamic testing must be kept small to ensure that the test remains in the LVE region. Strain sweeps can be used to verify that testing occurs in the LVE region. In general, the strain must be less than 0.5 percent at low temperatures but can be increased at high temperatures. Various parallel disc sizes can be used during dynamic mechanical testing. The size of the disc that should be used to test the bitumen decreases as the expected stiffness of the bitumen increases. In other words, the lower the testing temperature, the smaller the diameter of the disc that needs to be used to accurately determine the dynamic properties of bituminous binders [Goodrich, 1988].

### 2.3.2 Bending beam rheometer test

The bending beam rheometer (BBR) test (AASHTO: T313-02) is used to measure the creep response of binders at low/cold temperatures. The testing mode of this equipment is illustrated schematically in Fig. 2.7. In the test, a constant load is applied to a prismatic bitumen beam measuring 125 mm by 12.5 mm by 6.25 mm in simple bending at its midpoint.

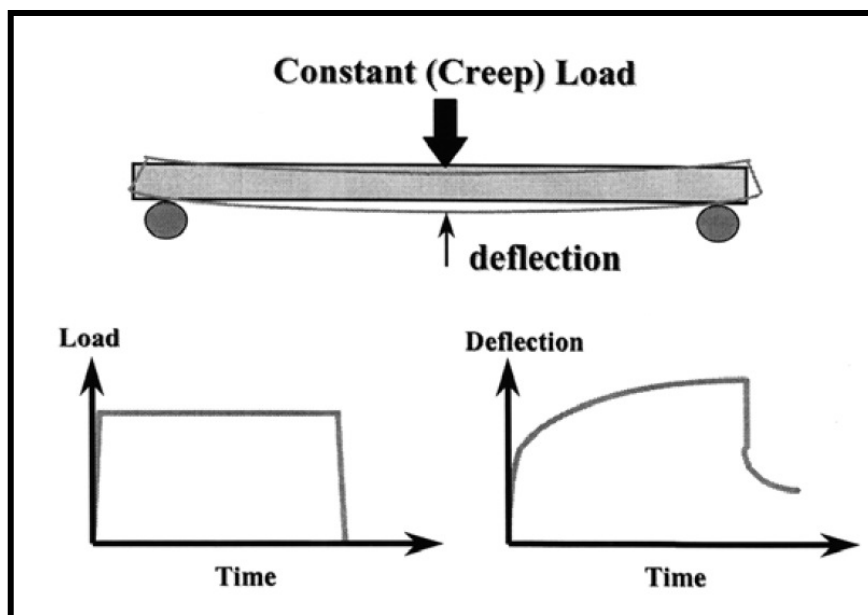


Fig. 2.7: Bending beam rheometer [Rowe *et al.*, 2001]

Creep stiffness values are obtained at several loading times ranging from 8 to 240 seconds (six loading times: 8, 15, 30, 60, 120 and 240). The  $m$  value is the slope of the log creep stiffness versus log time curve. The stiffness and the slope of the stiffness curve ( $m$ -value have been used in the Superpave specification as illustrated in Figure 2.8 [Rowe *et al.*, 2001].

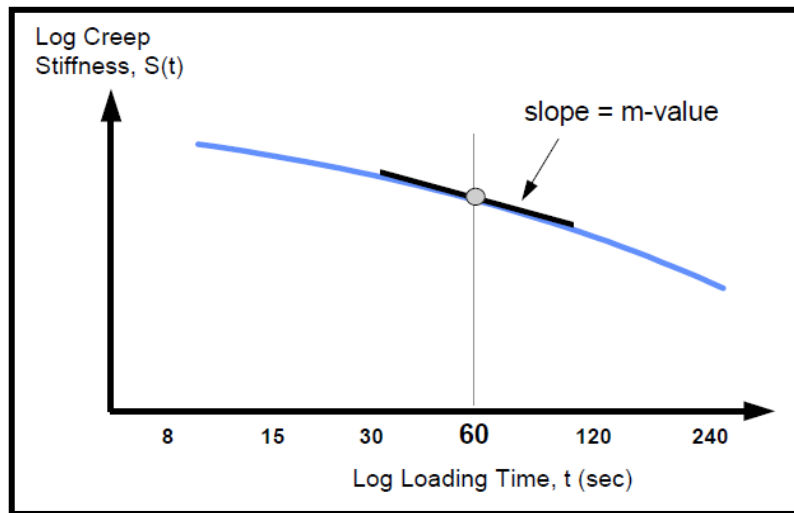


Fig. 2.8: Determination of  $S(60)$  and  $m$ -value [Rowe *et al.*, 2001]

The SHRP binder specification states if the creep stiffness is less than or equal to 300 MPa together with the  $m$  value being greater than 0.30, the binder meets the specification [Petersen *et al.*, 1994].

$$S(t) = \frac{PL^3}{4bh^3\Delta(t)} \quad (2.3)$$

where  $S(t)$  is the creep stiffness modulus at time,  $t$  ( $t = 60$  seconds is used as standard),  $P$  is applied constant load (normally 100 g),  $L$  is distance between beam supports (102mm),  $h$  is beam thickness (6.25 mm) and  $\Delta(t)$  is deflection at time ( $t$ ).

Bouldin *et al.* [2000] and Rowe *et al.* [2001] provided a detailed discussion on the BBR data analysis. The steps are discussed as follows; First,  $S(t)$  master curve must be created. Next the  $S(t)$  master curve must be fitted to a functional relationship before the relaxation modulus,  $E(t)$ , can be determined. According to Rowe *et al.* [2001], by using two BBR data sets to obtain a master curve, best

results were obtained by fitting the Christensen, Anderson and Marasteanu (CAM) Model. Details of the CAM Model can be found later in Chapter 3. The relaxation modulus can be determined using an approximation method, known as Hopkins and Hamming [1957] technique. This technique provide a numerical solution to the convolution integral required to convert BBR creep stiffness (compliance,  $D(\zeta)$ ) is first computed using the CAM parameters, with  $D(\zeta) = 1/S_{\text{BBR}}(\zeta)$  to  $E(t)$  [Bouldin *et al.*, 2000].

Mathematically, the convolution integral can be shown as follows [Bouldin *et al.*, 2000]:

$$\int_0^t E(\zeta)D(t-\zeta)d\zeta = 1 \quad (2.4)$$

where  $E(\zeta)$  is the relaxation modulus at reduced time ( $\zeta$ ) and  $t$  is the physical loading time. The Hopkins and Hamming solution is:

$$E(t_{n+1/2}) = \frac{t_{n+1} - \sum_{i=0}^{n-1} E(t_{i+1/2})[f(t_{n+1}+t_i) - f(t_{n+1}-t_{i+1})]}{f(t_{n+1}-t_n)} \quad (2.5)$$

where

$$f(t_{n+1}) = f(t_n) + \frac{1}{2}[D(t_{n+1}) + D(t_n)][t_{n+1} - t_n]$$

The initial value of  $f(t)$  at zero time is set as zero [Rowe *et al.*, 2001]. Fig. 2.9 shows the importance of this step. According to Rowe *et al.* [2001], the simple inversion does not fit the data really well even though for much less complex materials when the material exhibit any real changes of the relaxation modulus (i.e. when the material becomes more viscous). Most binders show significant changes of the modulus with increasing time (or temperature) and consequently, the resulting error is significant [Bouldin *et al.*, 2000; Rowe *et al.*, 2001].

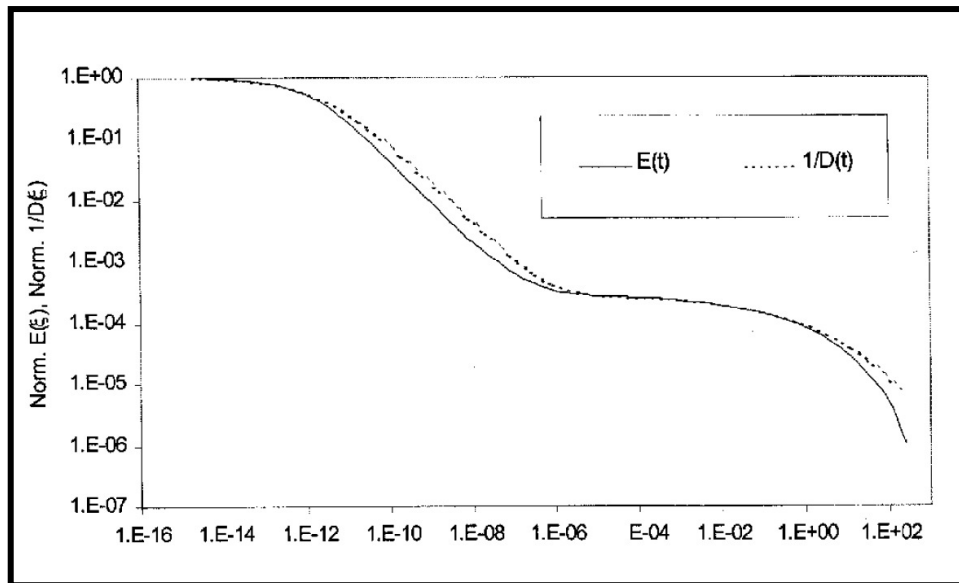


Fig. 2.9: A comparison of inverse compliance to relaxation modulus of Polyisobutylene [Rowe *et al.*, 2001]

## 2.4 Ageing

Bitumen is also affected by the presence of oxygen, ultraviolet radiation and by changes in temperature. These external influences result in the phenomenon known as ageing and cause changes in the chemical composition and therefore the rheological and mechanical properties of the bitumen [Petersen, 1984]. Ageing is primarily associated with the loss of volatile components and oxidation of the bitumen during asphalt mixture production (short-term ageing) and progressive oxidation of the in-place material in the road (long-term ageing). Both factors cause and increase in viscosity (or stiffness) of the bitumen and subsequently stiffening of the asphalt mixture. Other factors such as molecular structuring over time (steric hardening) and actinic light (primarily ultraviolet radiation, particularly in desert conditions) may also contribute to ageing [Traxler, 1963, Vallerga *et al.*, 1957].

Ageing can have two effects, either increasing the load bearing capacity (strength) and permanent deformation resistance of the pavement by producing a stiffer material or reducing pavement flexibility. These result in the formation of cracks with the possibility of total failure. Therefore, ageing at moderate levels is generally accepted and can even enhance performance. However, ageing at

significant levels results in embrittlement of the bitumen, significantly affecting its adhesive characteristics and usually resulting in reduced cracking resistance of the asphalt mixture under repeated loading [Airey, 2009].

Test related to ageing of bitumen can be broadly divided into two categories; namely tests performed on neat bitumens and test performed on asphalt mixtures. Much of the research into the ageing bitumen utilises thin film oven ageing to age the bitumen in an accelerated manner. These tests are typically used to simulate the relative hardening that occurs during the mixing and laying process (short-term ageing). The thin film oven ageing is typically combined with the pressure oxidative one to include long-term hardening in the field [Airey, 2009].

#### **2.4.1 Thin film oven test**

The thin film oven test, TFOT (ASTM Test Method D1754 (ASTM, 1998)) is a method of ageing bitumen by subjecting it to conditions approximating those that occur during normal hot-mix plant operations. Samples of the bitumen are placed in pans on a rotating shelf in an oven at 163°C for five hours. The aged residue may be tested to determine the effects of hardening due to ageing.

#### **2.4.2 Rolling thin film oven test**

The rolling thin film oven test, RTFOT (ASTM Test Method D2872 (ASTM, 1998)) is a modification of the thin film oven test. Instead of samples being placed in pans on a rotating shelf, they are poured into specially designed bottles. The bottles are placed horizontally into a vertically rotating rack in an oven maintained at 163°C for 75 minutes. As the bottles are rotated, fresh films of bitumen are exposed. Once during each rotation, the bottle opening passes before an air jet that purges accumulated vapours from the bottle and exposes the bitumen to additional air to intensify the ageing effect. The residue from the rolling thin film oven test is subsequently tested for the effects of ageing. A schematic diagram of the RTFOT is shown in Fig. 2.10.

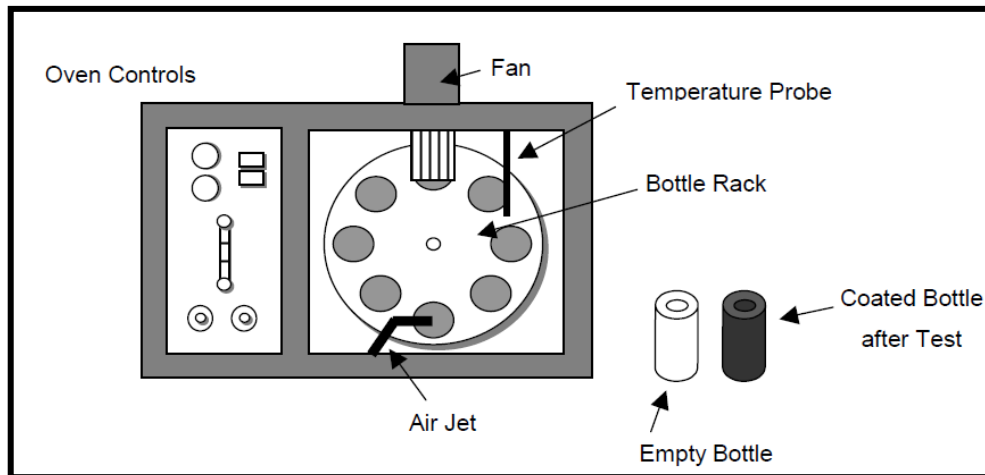


Fig. 2.10: Schematic diagram of rolling thin film oven test

### 2.4.3 Pressure ageing vessel test

The pressure ageing vessel test (PAV), shown in Fig. 2.11, is used to simulate the physical and chemical property changes that occur in bitumens as a result of long-term, in-service oxidative ageing in the field [Petersen *et al.*, 1994]. After the bitumen has first been aged in the rolling thin film oven, it may be aged in the PAV. This test consists of ageing 50 g of bitumen placed in a pan within a heated vessel pressurised with air to 2.1 MPa for 20 hours at temperatures of 90, 100 and 110°C<sup>1</sup>. However, this particular ageing temperature is dependent on the climatic region where the binder will be put in service and is selected from the SHRP performance graded binder specification [Harrigan *et al.*, 1994].

<sup>1</sup> Within the industry, there is considerable concern that ageing materials at temperatures in this range is too far removed from the temperature experienced in service and that such an approach may give misleading results [Read and Whiteoak, 2003].

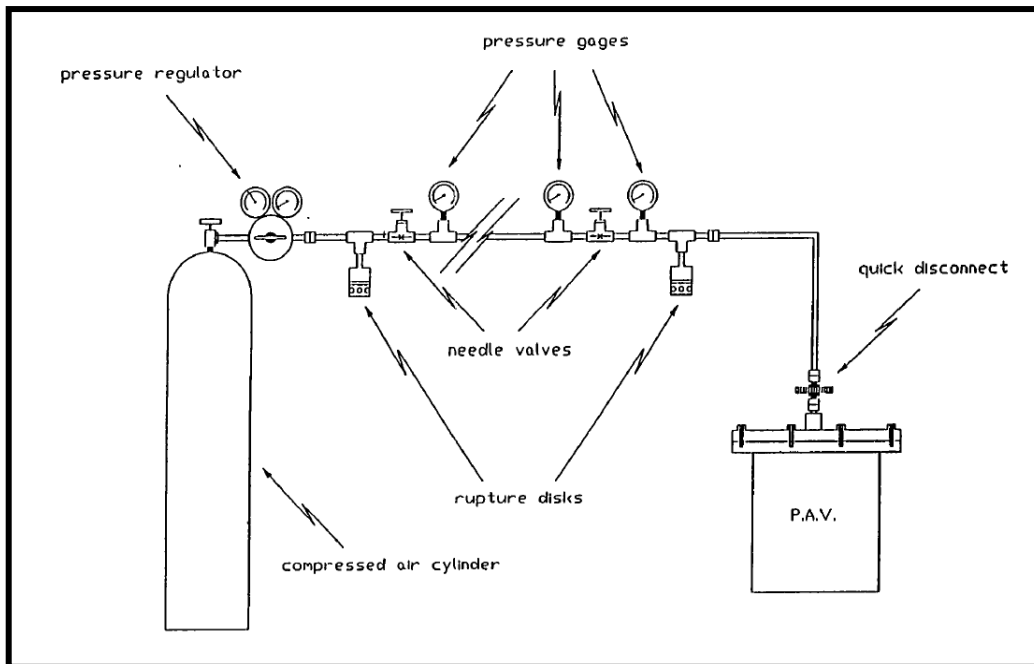


Fig. 2.11: Schematic diagram of vessel ageing pressure [Petersen *et al.*, 1994]

The PAV test accounts for temperature effects but is not intended to account for mixture variables such as air voids, type of aggregates and as well as aggregate adsorption [Petersen *et al.*, 1994]. After the PAV test, the residue is normally used for DSR, BBR and direct tension tests.

## 2.5 Viscoelastic Behaviour of Bitumen

Bitumen is a thermoplastic liquid that behaves as a viscoelastic material. The term viscoelastic behaviour refers to the mechanical properties of the bitumen, which, in two extremes, can result in the bitumen behaving either as an elastic solid or a viscous liquid, depending on temperature and time of loading. At low temperatures elastic properties dominate. At high temperatures, the bitumen behaves like a liquid, usually with Newtonian viscous flow properties. At normal pavement temperatures, the bitumen has properties that are in the viscoelastic region [Dukatz and Anderson, 1980]. Therefore, at these temperatures the bitumen exhibits both viscous and elastic behaviour and displays a time dependent relationship between applied stress or strain and resultant strain or stress [Goodrich, 1988].

The intermediate range of temperatures and loading times, at which the viscoelastic behaviour occurs, is indicative of the typical conditions experienced in service. Another viscoelastic representation of the behaviour of bitumen is represented in Figure 2.12, where three regions of behaviour is observed, namely linear elastic, delayed elastic and viscous regions [Airey, 1997].

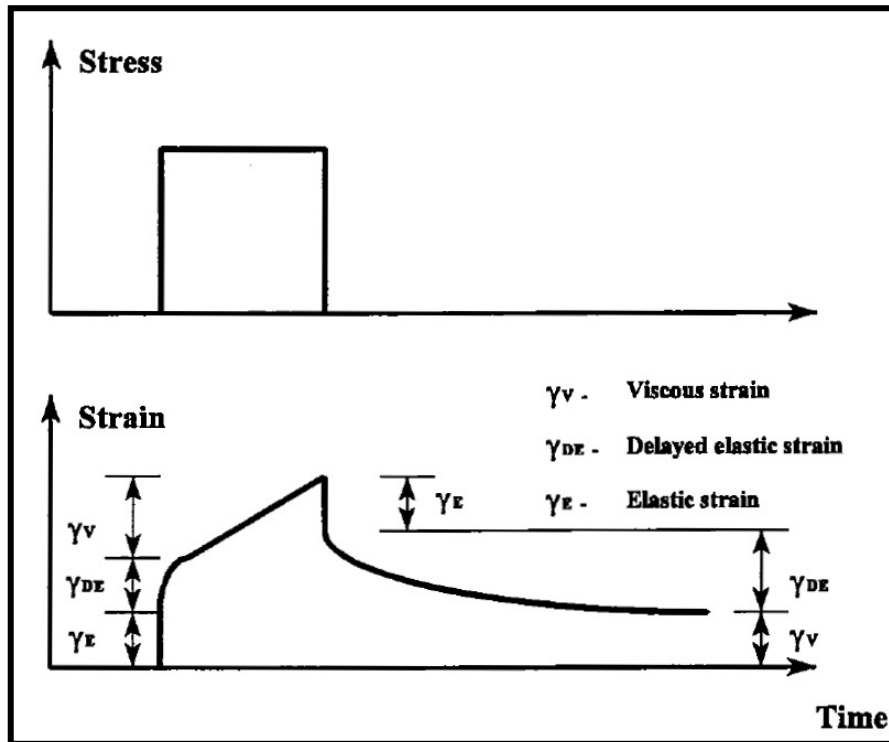


Fig. 2.12: Viscoelastic response of bitumen under creep loading [Airey, 1997]

The viscous portion is solely responsible for non-recoverable deformation experienced when the bitumen or asphalt mixture incorporating the bitumen loaded. However, the elastic and delayed elastic strain are totally recoverable once the load and applied stress are released. The elastic response of the bitumen dominates at short loading times and/or high temperatures. Meanwhile, at intermediate loading times and/or high temperatures, the delayed response dominates. The purely viscous and delayed elastic components constitute the time dependent deformation of the viscoelastic material [Airey, 1997].

Although none of the viscous deformation is recovered once the load is removed, the delayed elastic deformation is recovered but not immediately as with the purely elastic deformation. Because the relative magnitude of the three

components change with loading time and temperature, both the magnitude and the shape of the creep curve in Fig. 2.13 will change with loading time and temperature [Anderson *et al.*,1991].

The descriptions given of elastic, viscous and viscoelastic response are for a linear response; that is the deformation at any time and temperature is directly proportional to the applied load. Non-linear response, especially for viscoelastic materials, is extremely difficult to characterise in the laboratory or to model in practical engineering applications [Anderson *et al.*, 1994]. For this reason, models are generally limited to the LVE region. Within this region, the inter-relation of stress and strain and stiffness is not influenced by the magnitude of stress. To ensure the testing remains within this LVE region, the strain (or deformation), that is applied to the bitumen must remain within limits.

## **2.6 Dynamic Mechanical Analysis**

Various forms of dynamic mechanical analysis (DMA) are used to measure the rheological properties of bituminous binders, usually by means of oscillatory-type DSR testing. The principle used with the DSR is to apply sinusoidal, oscillatory stresses and strains to a thin disc of bitumen, which is sandwiched between the two parallel plates of the DSR (previously shown in Fig. 2.5). The test can be either stress or strain-controlled, depending on which of these variables is controlled by the test apparatus. The controlled-strain test is normally used to determine the dynamic rheological properties of the bitumen [Goodrich, 1988; Pink *et al.*, 1980].

Normally the tests are conducted over a wide range of temperatures and frequencies if complete characterisation of the viscoelastic properties of binders needs to be obtained. In addition, the tests are usually conducted by inducing small strain (within the LVE region) to enable the rheological data to be transposed between frequencies and temperatures using the time-temperature superposition principle (TTSP) [Airey and Hunter, 2003] The TTSP will be discussed in greater detail in section 2.7.

The sinusoidally varying stress can be shown as [Airey and Hunter, 2003]

$$\sigma(t) = \sigma_o \sin \omega t \quad (2.6)$$

and the resulting strain as

$$\gamma(t) = \gamma_o \sin(\omega t + \delta) \quad (2.7)$$

where  $\sigma_o$  is the peak stress (Pa),  $\gamma_o$  is the peak strain,  $\omega$  is the angular frequency (rad/s),  $t$  is the time (seconds) and  $\delta$  is the phase angle of the measured material response in degrees. The angular frequency,  $\omega$ , also known as the rotational frequency, is expressed as

$$\omega = 2\pi f \quad (2.8)$$

where  $f$  is the frequency (Hz) at which the test was measured. The sinusoidally varying stress and strain can also be presented in complex notation as

$$\sigma^* = \sigma_o e^{i\omega t} \quad (2.9)$$

and

$$\gamma^* = \gamma_o e^{i(\omega t + \delta)} \quad (2.10)$$

The phase angle,  $\delta$ , is defined as the phase difference between stress and strain and is also called the loss angle or the phase lag. For purely elastic materials, the phase angle will be  $0^\circ$ , whereas for purely viscous materials, the phase angle will be  $90^\circ$ . Therefore, the phase angle is important in describing the viscoelastic properties of a material.

The sinusoidal, oscillatory, stress and strain waveforms and the resulting dynamic test outputs are shown in Figs 2.13 and 2.14.

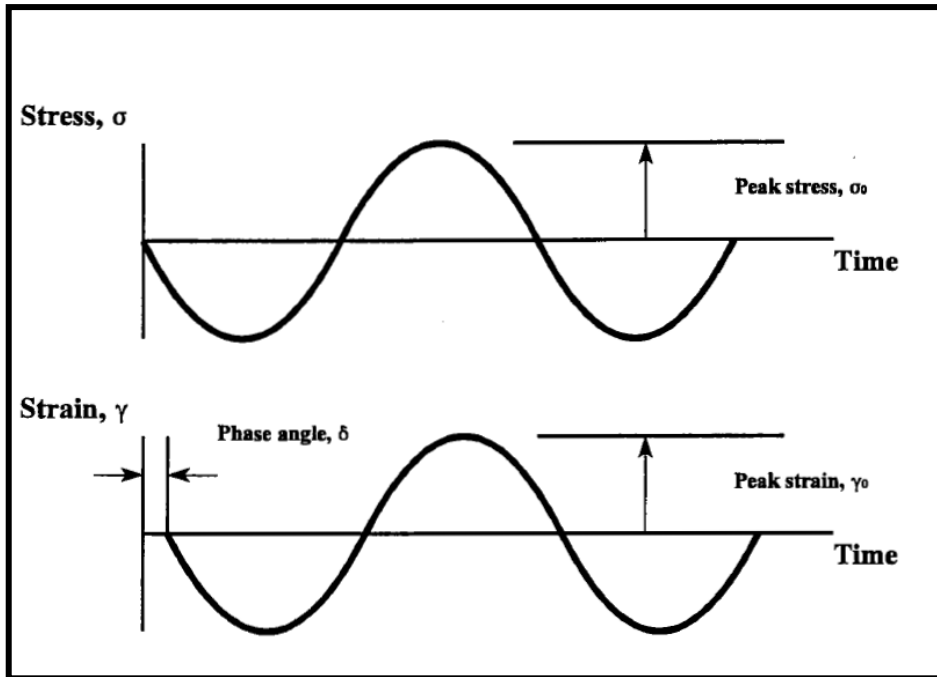


Fig. 2.13: Dynamic oscillatory stress-strain functions [Airey, 1997]

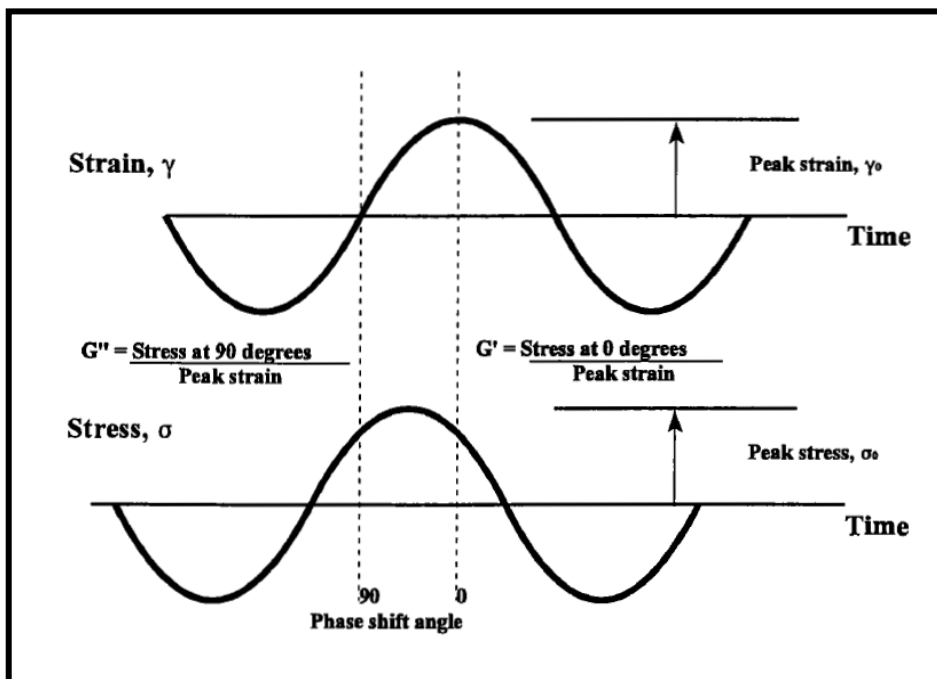


Fig. 2.14: Dynamic test outputs from dynamic mechanical analysis (DMA) [Airey, 1997]

The ratio of the resulting stress to the applied strain is called the complex shear modulus,  $G^*$ , defined as

$$G^* = \frac{\sigma^*}{\gamma^*} = \frac{\sigma_o}{\gamma_o} e^{i\delta} \quad (2.11)$$

Equation 2.11 can also be written as

$$G^* = \left( \frac{\sigma_o}{\gamma_o} \right) \cos \delta + i \left( \frac{\sigma_o}{\gamma_o} \right) \sin \delta \quad (2.12)$$

which corresponds to the definition for the complex shear modulus,  $|G^*|$ , given in the Eurobitume glossary of rheological terms [Eurobitume, 1996].

$$G^* = G' + iG'' \quad (2.13)$$

where  $G'$  is the storage modulus (Pa),  $G''$  is the loss modulus (Pa) and the other symbols are as previously defined.

The magnitude of the complex modulus,  $|G^*|$  (Fig. 2.13) can be calculated as the square root of the sum of squares of the two components

$$|G^*| = \sqrt{G'^2 + G''^2} \quad (2.14)$$

The in-phase component or the real part of  $|G^*|$  is called the (shear) storage modulus. The storage modulus equals to the stress that is in phase with the strain divided by the strain, or:

$$G' = |G^*| \cos \delta \quad (2.15)$$

The storage modulus describes the amount of the energy that is stored and released elastically in each oscillation and is therefore also known as the elastic modulus, or the elastic component of the complex modulus [Airey, 1997].

The (shear) loss modulus is the out-of-phase component or the imaginary part of  $|G^*|$ . This equals the stress  $90^\circ$  out of phase with the strain divided by the strain, or:

$$G'' = |G^*| \sin \delta \quad (2.16)$$

The loss modulus describes the average energy dissipation rate in the continuous steady oscillation found in the dynamic test. The loss modulus is also referred to as the viscous modulus or the viscous component of the complex modulus. The loss tangent is defined as the ratio of the viscous and elastic components of the complex modulus or simply the tangent of the phase angle:

$$\delta = \tan^{-1} \left( \frac{G''}{G'} \right) \quad (2.17)$$

Fig. 2.15 shows a relationship between  $|G^*|$ ,  $G'$ ,  $G''$  and  $\delta$  [Airey and Hunter, 2003].

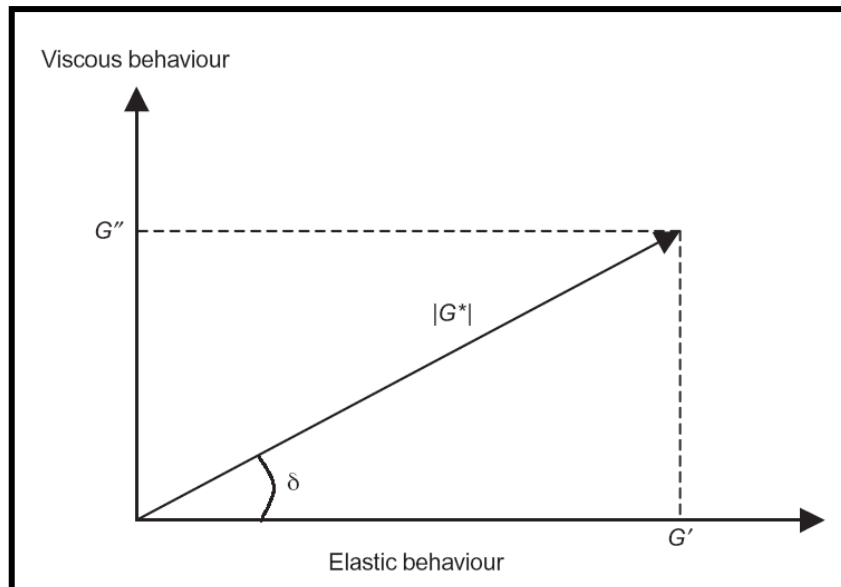


Fig. 2.15: Relationship between  $|G^*|$ ,  $G'$ ,  $G''$  and  $\delta$  [Airey and Hunter, 2003]

The storage and loss moduli are sometimes misinterpreted as the elastic and viscous modulus respectively. In reality, the elastic component of the response only represents part of the storage modulus and the viscous response only part of the loss modulus. In addition, viscoelastic materials exhibit a significant amount of delayed elastic response that is time dependent but completely recoverable. The storage and loss modulus both reflect a portion of the delayed elastic response [Airey, 1997].

In addition, a viscosity value for the bitumen can also be obtained from dynamic oscillatory test. The viscosity is known as the complex viscosity (Pa.s) and is defined as the ratio of the complex modulus and the angular frequency:

$$\eta^* = \frac{|G^*|}{\omega} \quad (2.18)$$

Since the complex viscosity is a function of complex number pair, a real and an imaginary part of the complex viscosity can also be defined. The real part of the  $\eta^*$  is termed the dynamic viscosity and defined as:

$$\eta' = \frac{G''}{\omega} \quad (2.19)$$

where  $\eta'$  is dynamic viscosity (Pa.s) and the other parameters are as previously defined. The imaginary part of the  $\eta^*$  is called out-of-phase component of  $\eta^*$  and defined as:

$$\eta'' = \frac{G'}{\omega} \quad (2.20)$$

where  $\eta''$  is out of phase component of  $\eta^*$  (Pa.s) [Airey, 1997].

## 2.7 Time-Temperature Superposition Principle

In principle, the complete modulus versus time behaviour of any polymer at any temperature can be measured [Shaw and MacKnight 2005]. Work done by various researchers has shown that there is an inter-relationship between temperatures and frequencies (or temperatures and times of loading) through the time-temperature shift factor may bring measurements done at different temperatures to fit one overall continuous curve at a reduced frequency (or time scale) [Monismith *et al.* 1966; Dickinson and Witt, 1974; Goodrich, 1988; Airey, 2002a]. This curve, known as a master curve, represents bituminous binders' or asphalt mixtures' behaviour at a given temperature over a wide range of frequencies. The principle that is used to relate the equivalency between frequency (time) and temperature and thereby produce the master curve is known as the time-temperature

superposition principle (TTSP or tTS) [Airey, 1997]. A material for which data can be reduced to a master curve in this way is said to be thermo-rheologically simple. This terminology was firstly introduced in 1952 by Schwarzl and Staveman [Dealy and Larson, 2006].

According to Airey [1997], modulus curves at low temperatures crowd together at high frequency/low temperature values and at very high frequencies they nearly all coincide with one horizontal asymptote. At this region, the modulus is called the glassy modulus,  $G_g$ . Under viscous conditions, however, there is no convergence to a single viscous asymptote as viscosity depends on temperature and therefore each temperature gives rise to a separate viscous flow asymptote. This is shown in Fig. 2.16.

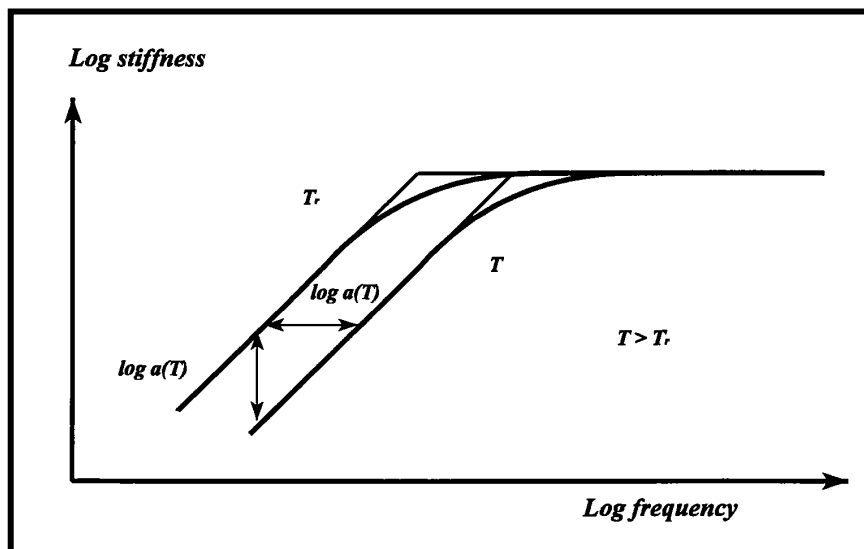


Fig. 2.16: Time-temperature superposition principle [Airey, 1997]

Airey [1997] also noted that because the limiting viscous behaviour is strongly temperature dependent and the elastic behaviour is not, it is possible to separate the influence of frequency and temperature. The concept of time-temperature superposition (Fig. 2.17) which shows an asymptote pair for an arbitrary reference temperature,  $T_{ref}$  (or  $T_r$ ). If the temperature is increased from  $T_{ref}$  to  $T$  there is a decrease in viscosity by a factor  $a_T$ . Therefore, the viscous asymptote at  $T$  lies an amount of  $\log a_T$  below that of  $T_{ref}$ . However, the elastic asymptote is negligibly changed during the temperature rise. The result is that the asymptote pair

appears to be shifted a distance  $\log a_T$  along the  $\log \omega$  axis, because the viscous asymptote has unit slope. The viscoelastic response of a bitumen is a transition between the asymptotic viscous and elastic response and is represented by the curve for  $T_{\text{ref}}$ . If a change in temperature causes the modulus curve to shift together with its asymptotes over the same distance  $\log a_T$ , the material behaves as a thermorheologically simple one [Airey, 1997].

A reference temperature can be chosen and the next higher modulus curve shifted coincides with the reference temperature curve to obtain a value for the horizontal shift factor  $\log a_T$  and a more extended modulus curve. This procedure is repeated for all curves in succession to obtain a master curve. The effect of temperature on complex modulus is, therefore, to shift the curve of  $\log |G^*|$  versus  $\log \omega$  axis without changing its shape. This permits the reduction of isotherms of  $\log |G^*|$  versus  $\log \omega$  measured over a wide range of temperatures to a single master curve [Airey, 1997].

The extended frequency scale used in a master curve is referred to as the reduced frequency scale and defined as:

$$\log f_r = \log f + \log a_T \quad (2.21)$$

where  $f_r$  is reduced frequency (Hz),  $f$  is frequency (Hz) and  $a_T$  is the shift factor.

The amount of shifting required at each temperature to form the master curve is called the shift factor,  $a_T$ . A  $\log a_T$  plot versus temperature with respect to the reference temperature curve is generally prepared in conjunction with a master curve. This plot gives a visual indication of how the properties of viscoelastic material change with temperature [Anderson *et al.*, 1994]. Fig. 2.17 shows the process involved in constructing a master curve.

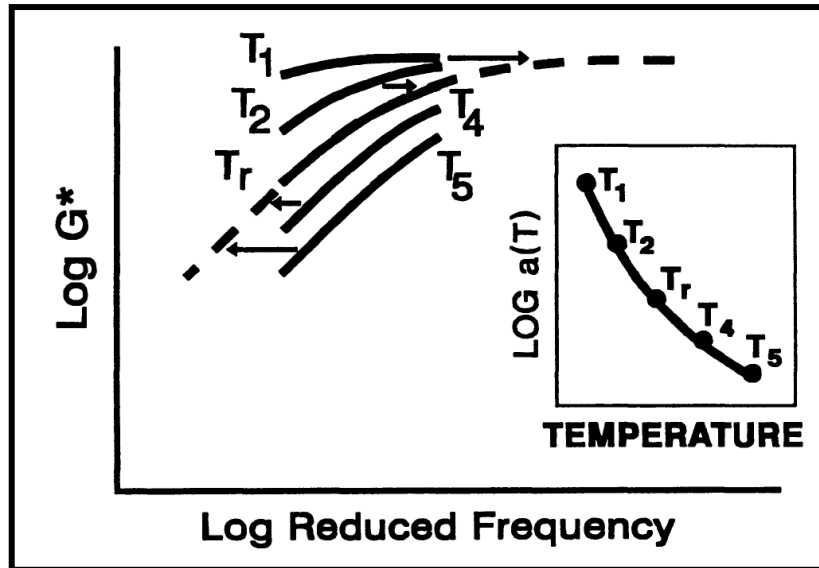


Fig. 2.17: Time-temperature superposition principle in the construction of a master curve [Anderson *et al.*, 1994]

## 2.8 Master Curves

According to Rowe and Sharrock [2000], the construction of master curves is a powerful tool to understand how binder type and chemical make up affects the viscoelastic behaviour of the binders. As aforementioned, it is difficult to measure the dynamic data over a frequency (or time) window of more than about four decades in practical work [Shaw and MacKnight, 2005]. Once the master curve is established, it is possible to derive interpolated values of property of any combination of temperature ( $T$ ) or frequency inside the range covered by the measurement. In addition, this gives the possibility of comparing the results obtained by two laboratories with different sets of test conditions such as frequencies and temperatures [Pellinen *et al.*, 2002]. Additionally, master curves can also be used to describe the rheological properties of asphalt mixtures [Garcia and Thompson, 2007].

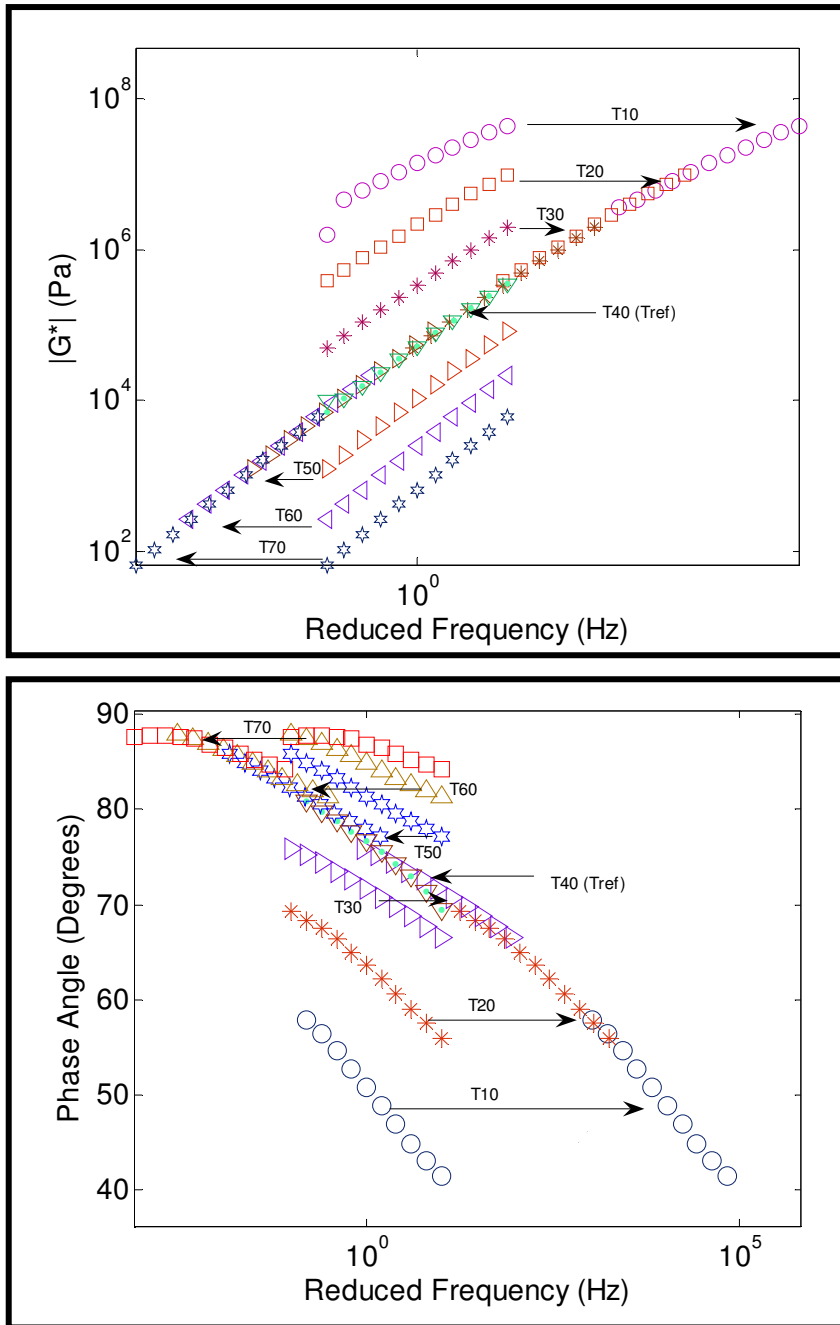


Fig. 2.18: Construction of the  $|G^*|$  and  $\delta$  master curves

Details of this  $|G^*|$  master curve (Fig. 2.18) are described as follows. Firstly, the dynamic data was collected over a range of temperatures and frequencies (e.g. 10–70°C with temperature intervals of 10°C and 0.10, 0.16, 0.25, 0.40, 0.63, 1.00, 1.58, 2.51, 3.98, 6.31 and 10.00 Hz). This combination produced 77 data sets. Secondly,  $T_{\text{ref}}$  is chosen, usually arbitrarily, say  $T_{40}$  (temperature at 40°C). Any temperature may be chosen as the reference temperature. All the curves at the temperature higher than  $T_{40}$  (i.e.  $T_{50}$ ,  $T_{60}$ , and  $T_{70}$ ) are manually shifted to the left.

The temperatures lower than  $T_{40}$  (i.e.  $T_{10}$ ,  $T_{20}$  and  $T_{30}$ ) are manually shifted to the right. The shifting process is repeated until the curves merge into a smooth and continuous master curve.

It has to be emphasised that at  $T_{ref}$ , the shift factor is equal to 1 (or 0 in logarithmic scale). If  $T_{50}$  had been chosen with shift factor equal to 0,  $T_{60}$  and  $T_{70}$  would have been shifted to the left with the shift factors larger than 0. Meanwhile  $T_{10}$ ,  $T_{20}$ ,  $T_{30}$  and  $T_{40}$  would have been shifted to the right with the shift factors smaller than 0. It is not necessary to use one of the experimental temperatures as the reference temperatures; any value within the temperature range can be used simply by interpolation [Shaw and MacKnight, 2005]. A similar procedure is also used on the other dynamic data such as  $\delta$  (Fig. 2.19),  $G'$  and  $G''$ .

Master curves can also be determined from creep test data. The individual creep curves can be combined into a single master curve by translating the curves along the time axis to obtain a creep curve at a single reference temperature [Airey, 1997].

## 2.9 Shift Factors Laws

The temperature dependency of the viscoelastic behaviour of bitumen is indicated by means of shift factors and can be expressed as:

$$a_T = a_T(T, T_{ref}) \quad (2.23)$$

and therefore depends, for a given system, only on the temperature. In general, several different  $a_T$  functions can be used to model the TTSP relationship of bitumens and asphalt mixtures. Most of the functions only involve horizontal line movements and do not take vertical shifts into account. The vertical shift,  $b_T$ , represents temperature induced density changes and involves shifts along the modulus axis [Rouse, 1953]. A vertical shift factor,  $b_T$  can be shown by the following:

$$b_T = \frac{T_0 \times \rho_0}{T \times \rho} \quad (2.2.4)$$

where  $b_T$  is the vertical shift factor,  $T$  is temperature,  $T_0$  is reference temperature,  $\rho$  is density and  $\rho_0$  is density at reference temperature. However, most research to date on binders and bituminous materials master curve construction does not normally consider the vertical shift factor based on temperature adjustment. Horizontal shifting will be discussed in the following sections.

### 2.9.1 Numerical, non-linear least squares shift

In the numerical, non-functional form shift approach, all the shift factors are solved simultaneously with the coefficients of a model using a non-linear least squares fitting. This is achieved with the aid of the Solver function in the MS Excel Spreadsheet, without assuming any functional form for the relationship of  $a_T$  versus temperature [Pellinen *et al.*, 2002].

### 2.9.2 The Williams, Landel and Ferry (WLF) equation

The WLF equation, after it's discovers Williams, Landel and Ferry, has been widely used to describe the relationship between the  $a_T$  and temperature dependency and thereby determine the  $a_T$  of bitumens [Williams *et al.*, 1955]:

$$\log a_T = \frac{-C_1(T - T_{\text{ref}})}{C_2 + (T - T_{\text{ref}})} \quad (2.24)$$

where  $T$  is temperature,  $T_{\text{ref}}$  is the reference temperature,  $C_1$  and  $C_2$  are taken as constants. The other parameters are as previously defined. This method is found to be applicable for both bitumens [Dobson, 1969; Goodrich, 1988; Chailleux *et al.*, 2006; Garcia and Thompson, 2007] and asphalt mixtures [Levenberg and Shah, 2008].

The WLF equation requires three constants to be determined namely  $C_1$ ,  $C_2$  and  $T_{\text{ref}}$ . The constants  $C_1$  and  $C_2$  can be calculated with respect to the reference

temperature,  $T_{\text{ref}}$ , from the slope and intercept of the linear form of the WLF equation [Airey, 1997]:

$$-\frac{T - T_{\text{ref}}}{\log a_T} = \frac{C_2}{C_1} + \frac{1}{C_1}(T - T_{\text{ref}}) \quad (2.25)$$

The temperature dependency of bitumens can be described by one parameter,  $T_{\text{ref}}$  if universal constants are used for  $C_1$  and  $C_2$  in the WLF equation. Williams *et al.* [1955] proposed that  $T_{\text{ref}}$  is suitably chosen for each material then  $C_1$  and  $C_2$  could be allotted universal values of 8.86 and 101.6 respectively. Brodnyan *et al.* [1961] showed that for bitumens the universal parameters fitted the data for  $T - T_{\text{ref}} > -20^\circ\text{C}$ , but at lower temperatures the predicted shift factors were too great.

Anderson *et al.* [1994] have found that for unaged and aged bitumens, the constants in the WLF equation are all essentially the same value, with  $C_1$  and  $C_2$  equal to 19 and 92 respectively, based on a defining temperature,  $T_d$ , which is bitumen specific. These values were also obtained by Jongepier and Kuilman [1975]. Unfortunately,  $T_d$  is difficult to determine. Brodnyan *et al.* [1961] suggested that  $T_{\text{ref}}$  is very similar to the softening point. Williams *et al.* [1955] proposed that  $T_{\text{ref}}$  is related to the glass transition temperature ( $T_g$ ) by the relationship:

$$T_r - T_g = 50^\circ\text{C} \quad (2.26)$$

Nielsen [1995] states that due to the nature of the WLF equation, the reference temperature cannot be chosen arbitrarily, but must be determined by iteration.

### 2.9.3 The Arrhenius equation

The Arrhenius equation can be described by the following:

$$\log a_T = C \left( \frac{1}{T} - \frac{1}{T_{\text{ref}}} \right) = \frac{0.4347 E_a}{R} \left( \frac{1}{T} - \frac{1}{T_{\text{ref}}} \right) \quad (2.27)$$

where  $C$  is a constant,  $E_a$  is the activation energy (J/mol) and  $R$  is the ideal gas constant (8.314 J/mol.K). The other parameters are as previously defined. In the

literature, different values such as 10920 K, 13060 K and 7680 K were reported for the constant  $C$  [Medani and Huurman, 2003]. The Arrhenius expression requires only one constant to be determined,  $E_a$ , which describes the minimum energy needed before any intermolecular movement can occur.

Anderson *et al.* [1994] found that for aged and unaged bitumen, the Arrhenius equation is better than the WLF equation at relating shift factors to temperature at low temperatures, below a bitumen specific defining temperature,  $T_d$ . Both the Arrhenius and WLF equations are based on the theoretical considerations and therefore their parameters provide some insight into the molecular structure of bitumen [Marasteanu and Anderson, 1996].

#### 2.9.4 The Log-Linear Equation

Equation 2.28 shows the form of the equation with the concept of reference temperature:

$$\log a \left( \frac{T}{T_{\text{ref}}} \right) = \beta(T - T_{\text{ref}}) \quad (2.28)$$

where  $\beta$  is the slope of the straight line relationship between  $\log a_T$  and temperature [Pellinen *et al.* 2002]. As discussed by Garcia and Thompson [2007], the Log-Linear equation is normally only used for asphalt mixture. However, this equation has been used in this study as a comparison to the other methods.

#### 2.9.5 The Viscosity Temperature Susceptibility (VTS) equation

In the Mechanistic-Empirical Pavement Design Guide (MEPDG),  $a_T$  was expressed as a function of binder viscosity to allow ageing over the life of the pavement to be considered using a global ageing model [Mirza and Witczak, 1995]. Later, Mirza and Witczak revised the shift factor equation used in the MEPDG, termed the viscosity temperature susceptibility (VTS) equation [Bonaquist and Christensen, 2005]:

$$\log a_T = c \left( 10^{A+VTS \log T_R} - 10^{A+VTS \log(T_R)_0} \right) \quad (2.29)$$

where  $T_R$  is temperature (Rankine),  $T_{R0}$  is the reference temperature (Rankine),  $A$  is the regression line intercept,  $VTS$  is regression line slope (called VTS coefficient) and  $c$  is a constant.

### 2.9.6 The *Laboratoire Central des Ponts et Chaussées* (LCPC) approach

Chailleux *et al.* [2006] from the LCPC, France, established a mathematical based procedure in order to construct master curves from dynamic measurements. Using the Kramers-Kronig relations<sup>2</sup> and when two close frequencies are considered ( $f_i$  and  $f_j$ ), they show that

$$\delta_{\text{avr}}^{(f_i, f_j)} \cdot \frac{2}{\pi} = \frac{\log(|G^*(T, f_j)|) - \log(|G^*(T, f_i)|)}{\log(f_j) - \log(f_i)} \quad (2.30)$$

where  $\delta_{\text{avr}}^{(f_i, f_j)}$  is the average of two angles measured at  $f_i$  and  $f_j$  (for temperature  $T$ ) and  $|G^*(T, f)|$  represents the complex modulus. A shift factor,  $a_{(T_1, T_2)} = f_2/f_1$  exists as the TTSP is presumably valid. For two close temperatures, Equation 4.7 can be written;

$$\delta_{\text{avr}}^{(T_1, T_2)}(f_2) \cdot \frac{2}{\pi} = \frac{\log(|G^*(T_1, f_2)|) - \log(|G^*(T_2, f_2)|)}{\log(a_{(T_1, T_2)})} \quad (2.31)$$

where  $\delta_{\text{avr}}^{(T_1, T_2)}$  is the average of two angles measured at  $T_1$  and  $T_2$  (for  $f_2$ ). Shift factors can be calculated using Equation 4.8 for close isotherms, at only one frequency. Considering the measurements are carried out at temperatures  $T_1, T_2 \dots T_i, T_{i+1} \dots, T_n$ , master curve construction related to a  $T_{\text{ref}}$  (with reference between 1 to  $n$ ) will be made using the cumulative sum of  $\log(a_{(T_i, T_{i+1})})$ . Hence, the shift factor needed to be applied for an isotherm  $T_i$  according to  $T_{\text{ref}}$  will be:

<sup>2</sup> The Kramers-Kronig relationship is the integral transform relationship between the real and imaginary parts of a complex function, and gives one of the several relations as;  $\delta(\omega) \approx \frac{\pi}{2} \cdot \frac{d \log|G^*(\omega)|}{d \log(\omega)}$ .

$$\log(a_{(T_i, T_{i+1})}) = \sum_{j=i}^{j=\text{ref}} \log(a_{(T_j, T_{j+1})}) \quad (2.32)$$

then

$$\log(a_{(T_i, T_{\text{ref}})}) = \sum_{j=i}^{j=\text{ref}} \frac{\log(|G^*(T_j, f)|) - \log(|G^*(T_{j+1}, f)|)}{\delta_{\text{avr}}^{(T_j, T_{j+1})}(f)} \times \frac{\pi}{2} \quad (2.33)$$

The calculation of the shift factor using the LCPC approach derives only from measurements of  $(|G^*(j, T)|$  and  $\delta(j, T)$  and does not need any adjustable coefficients. This technique is based on linear viscoelastic theory.

## 2.10 Rheological Data Representation

The DSR data obtained need to be represented in a useful form to enable study on the rheological properties of bituminous binders.

### 2.10.1 Isochronal plots

An isochronal plot is defined as an equation or a curve on a graph representing the behaviour of the system at a constant frequency (time of loading). Curves of  $|G^*|$  (or  $\delta$ ) as a function of temperature at constant frequency are isochrones [Eurobitume, 1996]. Examples of the isochronal plots for  $|G^*|$  and  $\delta$  are shown in Fig. 2.19.

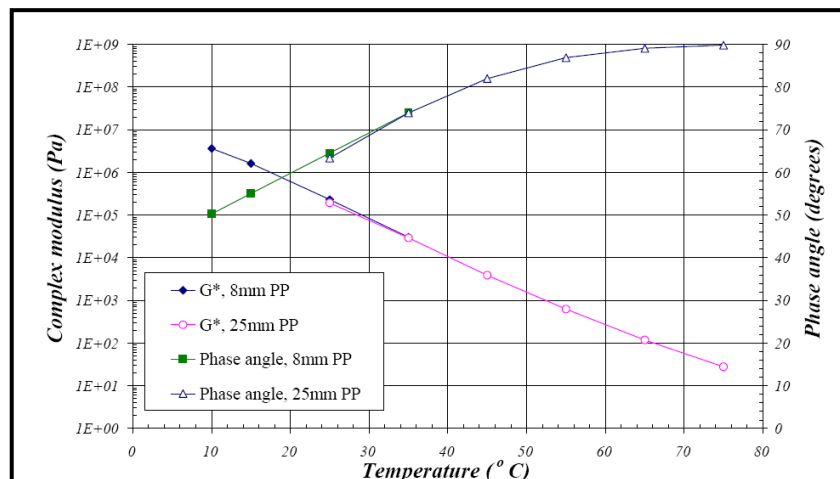


Fig. 2.19: Isochronal plots for  $|G^*|$  and  $\delta$  [Airey, 2002a]

### 2.10.2 Isothermal plots

An isothermal plot is described as an equation or a curve on a graph representing the behaviour of a system at a constant temperature. Curves of  $|G^*|$  (or  $\delta$ ) as a function of frequency at constant temperature are isotherms [Eurobitume, 1996]. Examples of the isothermal plots for  $|G^*|$  and  $\delta$  are shown in Fig. 2.20.

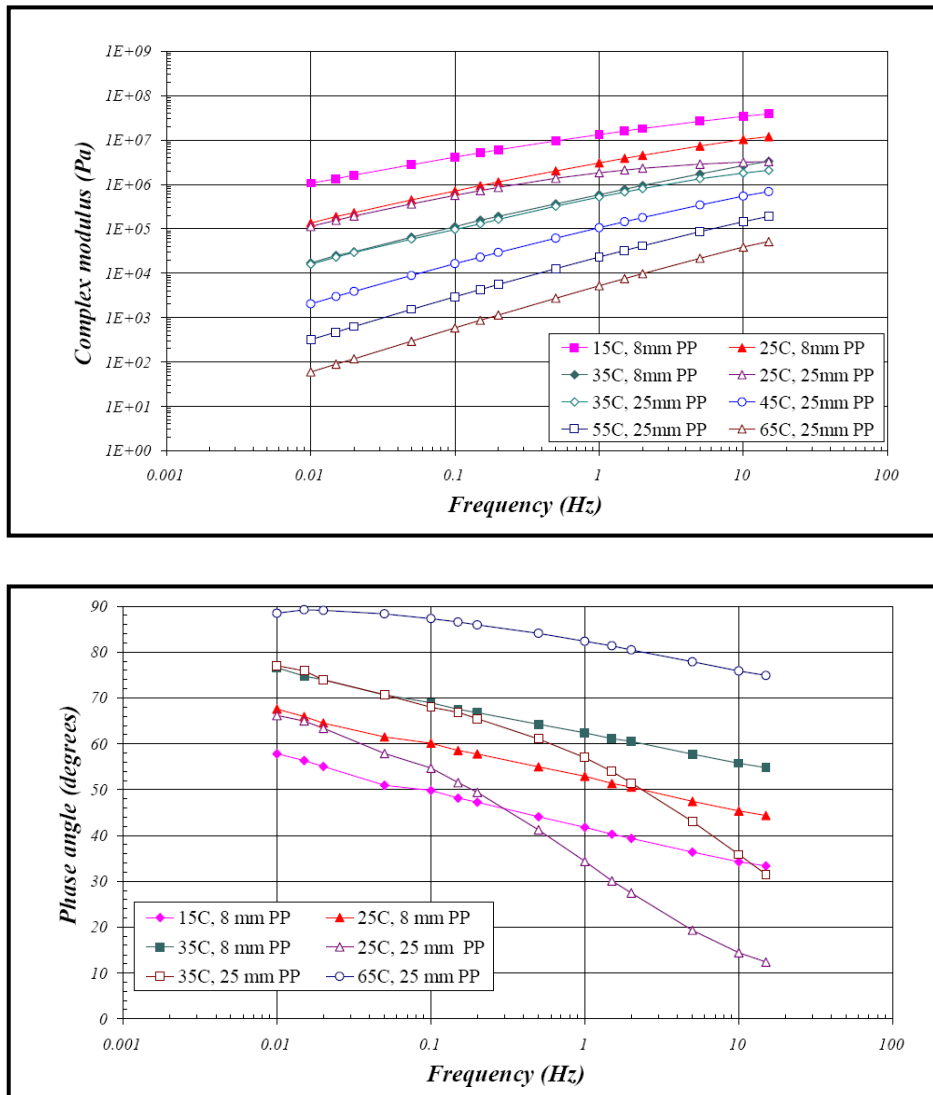


Fig. 2.20: Isothermal plots for  $|G^*|$  and  $\delta$  [Airey, 2002a]

### 2.10.3 Black diagrams

For a dynamic experiment, a graph of the magnitude (or norm) of the complex shear modulus ( $|G^*|$ ) versus the phase angle ( $\delta$ ) is called a Black diagram

[Eurobitume, 1996]. An example of the Black diagram is shown in Fig. 2.21 [Airey, 2002a].

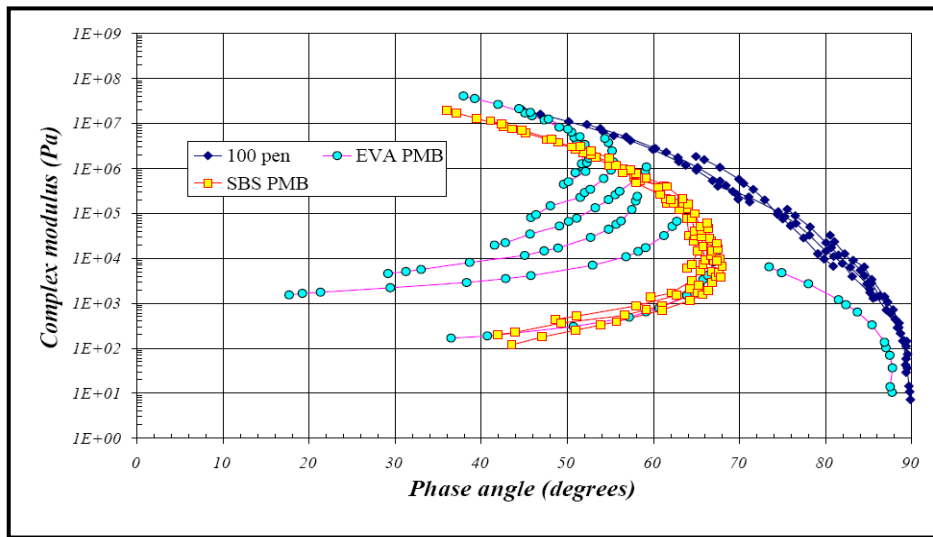


Fig. 2.21: Example of the Black diagrams [Airey, 2002a]

#### 2.10.4 Cole-Cole diagrams

In pavement engineering practise, a Cole-Cole diagram is defined as a graph of  $G''$  as a function of  $G'$  [Eurobitume, 1996; Airey, 1997]. The Cole-Cole diagram provides a means of presenting the viscoelastic properties of the bitumen without incorporating frequencies and/or temperatures as one of the axes [Airey, 1997]. An example of the Cole-Cole diagram is shown in Fig. 2.22.

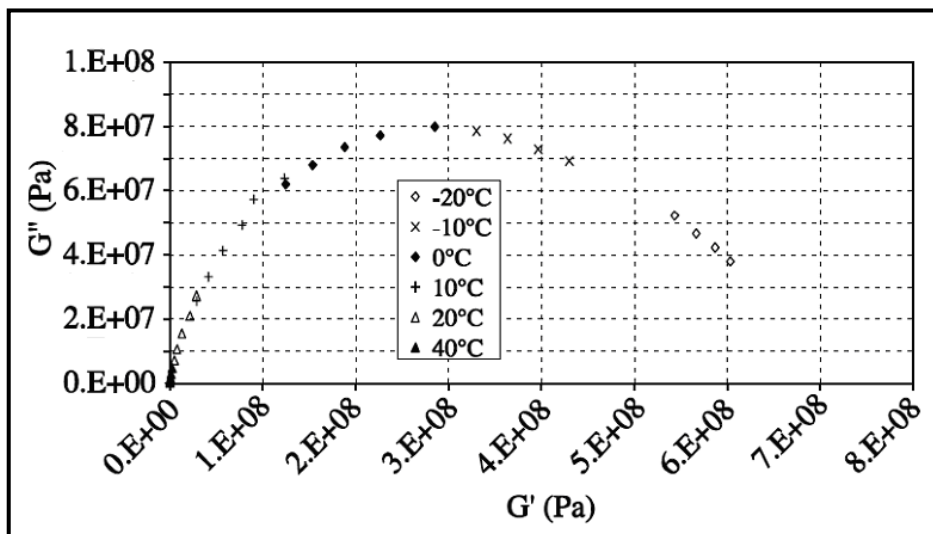


Fig. 2.22: The Cole-Cole diagram

## 2.11 Glassy Modulus

The glassy modulus,  $G_g$  is defined as the value which  $|G^*|$  approaches at low temperatures and/or high frequencies [Anderson *et al.*, 1992]. However, it appears quite hard to obtain  $G_g$  via experimental work because materials such as bitumens become harder and subsequently brittle at a very low temperature. For example, Sui [2008] conducted rheological tests using the advanced rheometric expansion system (ARES) rheometer. He observed that the  $G_g$  value was approximately  $0.5 \times 10^9$  Pa at a very low temperature. This value was a bit low as it is recommended to use the  $G_g$  values of  $1 \times 10^9$  (in shear) and  $3 \times 10^9$  Pa (in extension or flexure) for most engineering purposes [Anderson *et al.*, 1992; Christensen and Anderson, 1992].

Graphical and modelling methods are normally used to calculate the  $G_g$  value for bituminous binders and asphalt mixture, with the absence of dynamic data at a low temperature. The graphical method is done by plotting the measured  $|G^*|$  as a function of  $\delta$  for the values of the phase angle less than approximately  $10^\circ$ . The intercept on such a plot is  $G_g$  [Anderson *et al.*, 1992; Lu *et al.*, 1998]. Lu *et al.* [1998] found the  $G_g$  values vary from  $0.5 \times 10^9$  to  $1 \times 10^9$  Pa for unmodified bitumens and PMBs. The influence of polymer modification at a low temperature is too small and can be neglected. Edwards *et al.* [2006] observed the  $G_g$  values were between  $0.42 \times 10^9$  and  $0.56 \times 10^9$  Pa when they added commercial waxes and a polyphosphoric acid to three 160/220 penetration grade bitumens.

Airey [2002a] used a similar method on unmodified bitumens, ethylene vinyl acetate (EVA) and styrene butadiene styrene (SBS) PMBs. The values of  $|G^*|$  and  $\delta$ , measured with the different sample geometries, have also been plotted in the form of a Black diagram in Fig. 2.23. The Black diagram shows a separation of the rheological data from the two plate geometries at  $|G^*|$  values greater than  $5 \times 10^5$  Pa (temperatures below  $35^\circ\text{C}$  and high frequencies). In addition, the Black diagram provides a reliable means of evaluating the suitability of the DSR testing configurations. Extrapolating lines to the y-axis indicate different values of limiting stiffness for the 25 mm and 8 mm geometries. The 25 mm configuration indicates a limiting stiffness of approximately  $5 \times 10^6$  Pa, which is considerably lower than the

traditionally recognised value of  $2 \times 10^9$  Pa (glassy modulus) indicated by the 8 mm configuration. The lower value of complex modulus indicates that the data are exposed to measurement error.

The upper limit of stiffness can also be estimated by using a linear relationship between the logarithm of  $(1 + \tan \delta)$ , within the range of 0 to 1, and the logarithm of  $|G^*|$  [Dobson, 1969]. This approach allows more rheological data to be used in the estimation of limiting stiffness. The plot for the 50 penetration grade bitumen is shown in Fig. 2.24, where, firstly, the limiting stiffness can be readily extrapolated and secondly, the divergence of the two geometries can be identified. The 8 mm configuration can be extrapolated to a limiting stiffness of approximately  $2 \times 10^9$  Pa, but the value for the 25 mm configuration is limited to  $2.5 \times 10^7$  Pa. The point of divergence of the 8 mm and 25 mm geometries occurs between  $10^5$  to  $10^6$  Pa [Airey, 2002a].

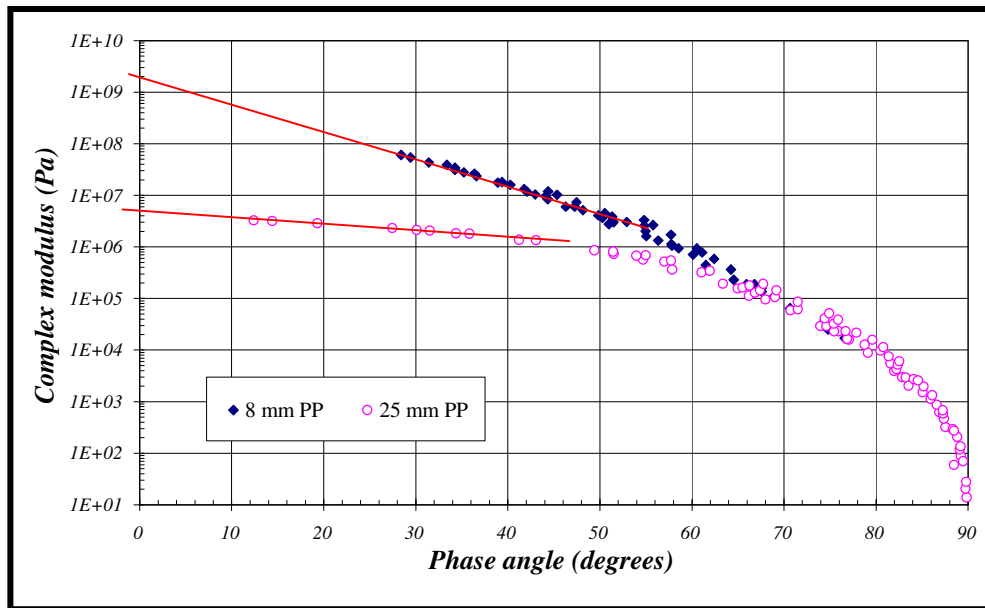


Fig. 2.23: Black diagram for two spindle geometries [Airey, 2002a]

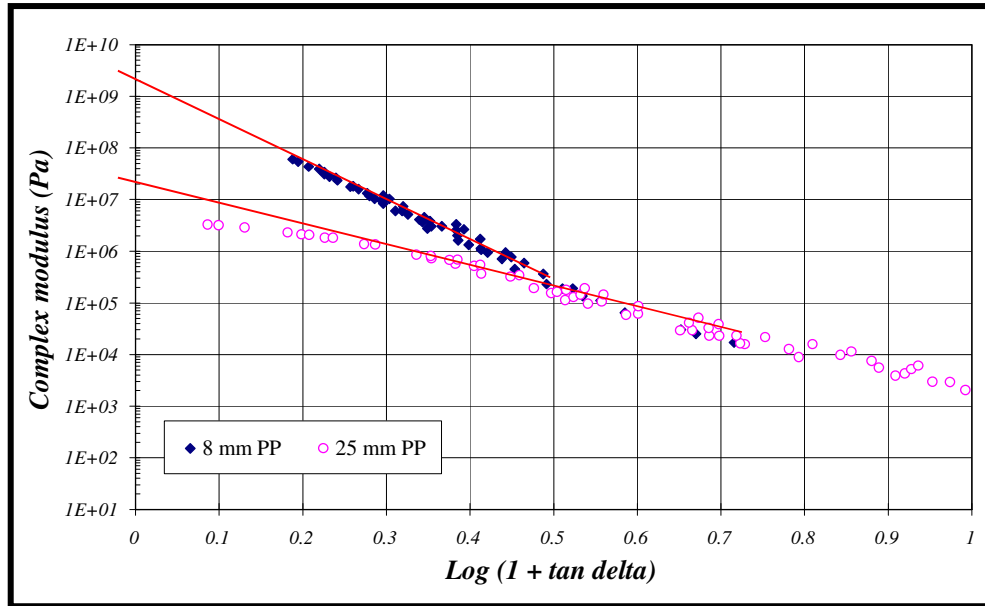


Fig. 2.24: Complex modulus versus  $\log (1 + \tan \delta)$  for two spindle geometries [Airey, 2002a]

Findings shown in Figs. 2.23 and 2.24 are in good agreement with Anderson *et al.* [1994]. Based on the work conducted on RMS 803, Anderson *et al.* [1994] recommend that 8 mm and 25 mm parallel plates should be used when  $1 \times 10^5 < |G^*| < 10 \times 10^7$  Pa and  $1 \times 10^3 < |G^*| < 10 \times 10^5$  Pa respectively.

The DSR experiments with the 25 mm and 8 mm geometries show that with wide frequency sweeps at different temperatures it is necessary to use both spindle configurations when performing dynamic shear testing within the transitional stiffness region between  $10^5$  Pa and  $10^6$  Pa. This overlapping allows the differences in  $|G^*|$  and  $\delta$ , as measured by the two configurations, to be identified and the appropriate values to be selected for the rheological characterisation of the bitumen. Black diagrams of  $|G^*|$  versus  $\delta$  provide a useful means of identifying these appropriate values and, therefore, aid the selection of suitable disc configurations (testing geometries) [Airey, 2002a].

On the other hand,  $G_g$  can also be obtained using a rheological model. Di Benedetto *et al.*, for example, used a model to describe the rheological properties of unmodified bitumens, PMBs and bitumen-filler mastics. They found that the  $G_g$

values of unmodified bitumens and PMBs were between  $0.8 \times 10^9$  and  $2 \times 10^9$  Pa [Olard and Di Benedetto, 2003; Olard *et al.*, 2003; Delaporte *et al.*, 2007]. However, the  $G_g$  values for bitumen-filler mastics were slightly higher, between  $1.9 \times 10^9$  to  $8.5 \times 10^9$  Pa. These values depend on the percentage of the mineral fillers used. Stastna *et al.* [1997] suggested allowing the  $G_g$  value to be a free parameter in order to obtain a better fit of master curves. This can be done with the aid of the Solver function in MS Excel, a tool for performing an optimisation with non-linear least squares regression technique. This method also has a disadvantage where the  $G_g$  value is determined statistically and in many cases, can be under or overestimated. If the data is affected by the measurement error, the shape of the model will follow that from original data and subsequently, the  $G_g$  will be lower than the suggested value.

## **2.12 Bitumen Modification**

Conventional bituminous materials have tended to perform satisfactorily in most highway pavement and airfield runway applications [Airey, 1997]. However, in recent years, increased traffic levels, larger and heavier trucks, new axle designs and increased type pressure, have added to the already severe demands of load and environment of the highway system, resulting in the need for enhancement of the properties of existing asphalt material [Brown *et al.*, 1990]. The modifiers that are commercially available fall into various categories, including naturally occurring materials, industrial by products and waste materials as well as carefully engineered products. Some of the more common categories include reclaimed rubber products, fillers, fibres, catalysts, extenders and polymers (natural and synthetic) [Airey, 1997]. Polymer-modified bitumen, normally abbreviated as PMB, tended to be the most popular.

The PMB is produced by mixing bitumen and polymer using a low or high shear mixer. Typical polymers include styrene-butadiene-styrene (SBS), styrene-butadiene-rubber (SBR), ethylene-vinyl acetate (EVA) and polyethylene among others [Isacsson and Lu, 1995]. In terms of overall performance, PMBs tend to have greater elastic response, improved cohesive and fracture strength, greater ductility

and are able to resist the pavement distress mechanisms of permanent deformation and fatigue cracking [Airey, 2009]. A wide range of additives and modifiers can be used to enhance the properties of conventional bitumen as listed in Table 2.1.

### **2.13 Polymer-Modified Bitumens**

A polymer is defined as a substance composed of molecules with large molecular mass composed of repeating structural units called monomers, connected by covalent chemical bonds. The word polymer is originally derived from the Greek words, *πολυ*, *polu*, "many" and *μέρος*, *mares*, means "part" [Taylor and Airey, 2008a]. Meanwhile, the term "polymerisation" is used to describe the process of linking the small molecules or monomers together. PMBs that have been used in road construction can be divided into two main groups, namely the elastomeric and plastomeric substances.

According to Airey [2003], and Taylor and Airey [2008b], approximately 75% of PMBs can be classified as elastomeric, 15% as plastomeric with the remaining 10% being either rubber or miscellaneous modified used worldwide. The PMB is produced by mixing bitumen and polymer using a low or high shear mixer. The use of PMBs could be expected to have a resistance to traffic at least four times greater than unmodified bitumens and better performance in extreme climatic conditions [Lenoble and Nahas, 1994].

Table 2.1: General classification of bitumen additives and modifiers [Airey, 2009]

Type		Generic examples
1	Fillers	<ul style="list-style-type: none"> <li>• Mineral fillers: Crusher fines</li> <li>• Lime</li> <li>• Portland cement</li> <li>• Fly ash</li> <li>• Carbon black</li> </ul>
2	Extenders (chemical modifiers)	<ul style="list-style-type: none"> <li>• Organo-metallic compounds</li> <li>• Sulphur</li> <li>• Lignin</li> <li>• Polymers</li> </ul>
3	Rubbers (thermoplastic elastomers) a. Natural latex b. Synthetic latex c. Block copolymer d. Reclaimed rubber	<ul style="list-style-type: none"> <li>• Natural rubber</li> <li>• Styrene-butadiene-rubber (SBR)</li> <li>• Polychloroprene latex</li> <li>• Styrene-butadiene-styrene (SBS)</li> <li>• Styrene-isoprene-styrene (SIS)</li> <li>• Crumb-rubber modifier</li> </ul>
4	Plastic (thermoplastic polymers)	<ul style="list-style-type: none"> <li>• Polyethylene (PE)/polypropylene (PP)</li> <li>• Ethylene acrylate copolymer</li> <li>• Ethylene vinyl acetate (EVA)</li> <li>• Polyvinyl chloride (PVC)</li> <li>• Ethylene propylene or EPDM</li> <li>• Polyolefins</li> </ul>
5	Combinations	<ul style="list-style-type: none"> <li>• Blends of polymers in 3 and 4</li> </ul>
6	Fibres	<ul style="list-style-type: none"> <li>• Natural: asbestos</li> <li>• Rock wool</li> <li>• Man-made: polypropylene</li> <li>• Polyester</li> <li>• Glass-fibre</li> <li>• Mineral</li> <li>• Cellulose</li> </ul>
7	Oxidants	<ul style="list-style-type: none"> <li>• Manganese salts</li> </ul>
8	Antioxidants	<ul style="list-style-type: none"> <li>• Lead compounds</li> <li>• Carbon</li> <li>• Calcium salts</li> <li>• Amines</li> </ul>
9	Hydrocarbons	<ul style="list-style-type: none"> <li>• Recycling and rejuvenating oils</li> <li>• Hard and natural asphalt (gilsonite, TLA)</li> </ul>
10	Anti-stripping agents (adhesion improvers)	<ul style="list-style-type: none"> <li>• Amides</li> <li>• Lime</li> </ul>
11	Waste materials	<ul style="list-style-type: none"> <li>• Roofing shingles</li> <li>• Recycled tyres</li> <li>• Glass</li> </ul>
12	Miscellaneous	<ul style="list-style-type: none"> <li>• Silicones</li> <li>• De-icing calcium chloride granules</li> </ul>

### 2.13.1 Plastomer

In general, a plastomer can be divided into thermosets (thermosetting resins) and thermoplastics (Table 2.1), where the latter is commonly used in pavement applications. Thermoplastics are characterised by softening on heating and hardening on cooling. Thermoplastic polymers, when mixed with a base bitumen, associate below certain temperatures increasing the viscosity of bitumen. However, they do not significantly increase the elasticity of the bitumen and when heated they can separate which may give rise to a coarse dispersion on cooling [Taylor and Airey 2008a]. Accepting these limitations, ethylene vinyl acetate (EVA) is the most widespread plastomer used with bitumen, because the less expensive polyethylene (PE) and polypropylene (PP) have been observed to exhibit low compatibility with bitumen [Polacco *et al.*, 2003, 2004]. Yeh *et al.* [2010] found that the PE PMB increases rutting resistance at high temperatures but does not significantly improve elastic resilience.

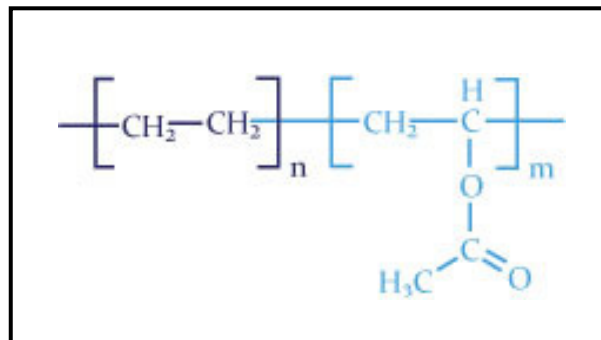


Fig. 2.25: EVA copolymer structures [SpecialChem, 2012]

EVA is basically built from two monomers, ethylene and vinyl acetate, as shown in Fig. 2.25. Table 2.2 lists the advantages of using this EVA modifier. According to Sengoz *et al.* [2009], EVA characteristics lie between those of low density polyethylene (LDPE), semi rigid, translucent product and those of a transparent and rubbery material similar to plasticised polyvinyl chloride (PVC) and certain types of rubbers. EVA copolymer alters the rheological characteristics of unmodified bitumens by increasing the temperature and frequency (or time of loading) dependent binder stiffness ( $|G^*|$ ), binder elasticity ( $G'$ ) and elastic response

(reduced  $\delta$ ) with the larger increases being experienced by polymeric dominant modified bitumens.

Table 2.2: Advantages of the EVA PMBs

Advantages	References
<ul style="list-style-type: none"> <li>• Improves workability of the bitumen during compaction</li> <li>• Improves deformation resistance to rutting</li> <li>• Improves compatibility</li> <li>• Safer handling</li> <li>• Easily blended into bitumens using a simple low-shear mixing machine</li> <li>• Thermally stable at normal temperatures</li> <li>• Increases the resistance to damage caused by fuel spillages</li> <li>• Increases stability and air voids</li> <li>• Improves stripping properties</li> <li>• Decrease flow value and unit weight</li> <li>• Heat stable and does not deteriorate at high temperatures</li> </ul>	<p>Isacson and Lu [1995]; Airey [1997]; Panda and Mazumdar [1999]; Read and Whiteoak [2003]; Asphalt Academy [2007]; Taylor and Airey [2008a]</p>

The properties of EVA vary for different grades depending on the chain length and molecular weight of the polymer, the vinyl acetate (VA) monomer content and the crystallinity. For the EVAs, the VA content and melt flow rate (MFR) are as important as the styrene content and linear or radial structure in SBS, when determining specific properties. EVA modified bitumen is also more heat stable and does not deteriorate at elevated temperatures during storage as fast as SBR and SBS modified bitumen products. Therefore, its storage stability is better compared to SBS and SBR [Asphalt Academy, 2007].

### 2.13.2 Elastomer

An elastomer is a polymer capable of recovery after high deformation. It has been used to modify bitumen. Examples of elastomers are shown previously in Table 2.1. Of these groups, the styrenic block copolymers (e.g. styrene butadiene styrene, SBS) have the greatest potential when blended with unmodified bitumens [Airey, 1997]. Fig. 2.26 depicts the copolymer structure of SBS.

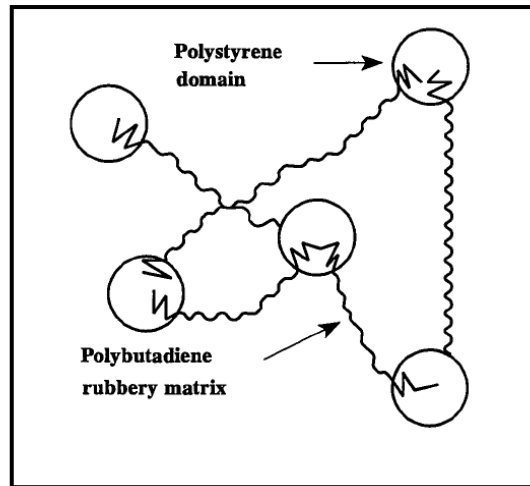


Fig. 2.26: SBS copolymer structures [Airey, 1997]

When the SBS copolymer is added to hot bitumen, it absorbs maltenes from bitumen and swells by up to nine times its initial value [Sengoz *et al.*, 2009]. A critical or continuous network can be formed throughout bitumen with a suitable concentration of SBS, normally around 5 to 6% (by mass) [Isacsson and Lu, 1995]. Once the critical networks begin to form, no significant property increase can be observed, even though the polymer content is elevated [Chen *et al.*, 2002]. The use of more than 8% of SBS concentration is generally impractical in road construction [Wojciech and Mieczyslaw, 1996]. Cong *et al.* [2008] observed the addition of more than 8% of SBS in bitumen resulted in storage instability. The minimum content (or percentage) of polymer modification also depends on the nature of unmodified bitumens [Lu and Isacsson, 1999a; Airey, 2004]. Advantages of the SBS PMBs are shown in Table 2.3.

Table 2.3: Advantages of the SBS PMB

Advantages	References
<ul style="list-style-type: none"> <li>• The ability to resist permanent deformation</li> <li>• Enhances low temperature crack resistance</li> <li>• Enhances high temperature rutting resistance of asphalt mixtures</li> <li>• Easily manufactured by blending powder with conventional bitumens using low to medium- shear mixing.</li> <li>• Improves the low temperature properties of bitumens</li> <li>• Reduces creep stiffness and limiting stiffness temperature of bitumens</li> <li>• Decreases the pavement layers by almost half</li> </ul>	Ait-Kadi <i>et al.</i> [1996]; Lu <i>et al.</i> [1998]; Lu and Isacsson [1999b]; Airey [1997, 2004]; Ho and Zanzotto [2005]; Asphalt Academy [2007]; Vlachovicova <i>et al.</i> [2007]; Yildirim [2007].

The effect of an increase of SBS polymer on the softening point of a base bitumen with varying asphaltene contents is shown in Fig. 2.27. The rate of increase rate in the softening point and thus, the shape of the curve is dependent mainly on the asphaltene content of the base bitumen, the type and grade of the SBS polymer and the percentage thereof. Typically, the curve assumes an S shape as the SBS structure changes from a fragmented form to a continuous network in the modified binder [Asphalt Academy, 2007].

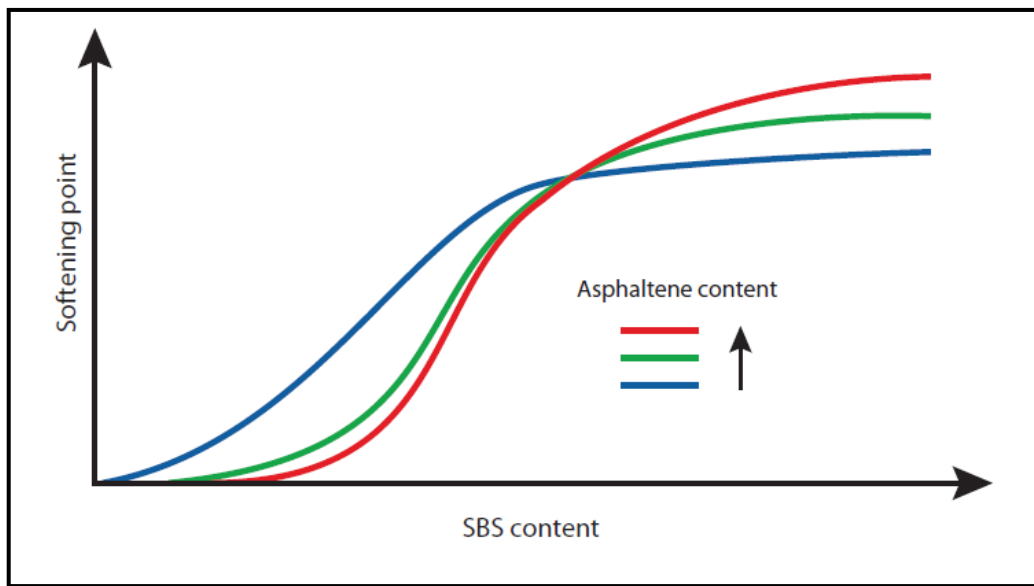


Fig. 2.27: Typical effect of SBS on the softening point of bitumen with different content of asphaltenes [Asphalt Academy, 2007]

There is a direct correlation between elastic recovery and deformation resistance where an increase in elastic recovery provides higher resistance to deformation. Cohesive strength also increases with the increase of elastic recovery. SBS PMBs are generally preferable due to the higher softening points and higher elastic recovery properties, which in turn can be applied at lower temperatures as a result of the lower relative viscosities. At these temperatures, the addition of SBS improves the flexibility of the bitumen which inhibits cracking and improves the resistance of the binder to crack reflection [Asphalt Academy, 2007].

### 3.1 Background

The use of a model can be a valuable alternative tool to fit or describe the rheological properties of bituminous binders. Using this approach, the rheological parameters ( $|G^*|$ ,  $\delta$ , etc.) at any particular temperature and frequency of a bitumen can be described using the rheological models to an accuracy that is acceptable for most purposes. In the 1950s and 60s, nomographs were used to describe the rheological properties of bitumen [Van der Poel, 1954; Heukelom and Klomp, 1964]. These nomographs (for example the Van der Poel's Nomograph) use methods like a penetration test to estimate binder's stiffness. The penetration test has a very complex variable stress state and cannot be used reliably as a measure of stiffness that would relate to a test conducted in shear at a known rate. A significant change in measurement accuracy when compared to the 1950s and subsequently the invention of computational techniques have caused this method be replaced by mathematical and mechanical models.

In the mathematical approach, a mathematical formulation is adjusted and fitted to the experimental main curve. On the other hand, in the mechanical element approach, use is made of the fact that the linear viscoelastic properties of material can be represented by a combination of spring and dashpot models, resulting in a particular mathematical formulation [Eurobitume, 1995]. Most of the rheological models rely on the construction of stiffness/complex modulus ( $|G^*|$ ) and phase angle ( $\delta$ ) master curves and the determination of temperature shift factor. They imply that the time-temperature superposition principle (TTSP) concept holds for the binders [Dobson, 1969; Jongepier and Kuilman, 1969; Dickinson and Witt, 1974; Christensen and Anderson, 1992; Anderson *et al.*, 1994; Lesueur *et al.*, 1996].

The use of nomographs will be firstly discussed, followed by the mathematical and mechanical models. In this study, stress is given to the use of models on viscoelastic liquids, even though some of them can be used for viscoelastic solids as well.

## 3.2 Nomographs

### 3.2.1 Van der Poel's Nomograph

As early as the 1950's, Van der Poel introduced the concept of bitumen stiffness modulus as a function of temperature and time of loading into a nomograph [Van der Poel, 1954, 1955]. This model, based upon 20 years of laboratory work [Yoder and Witczak, 1975], used the empirical tests, penetration and ASTM Ring-and-Ball softening point ( $T_{R\&B}$ ), as input parameters [Van der Poel, 1954, 1955]. According to Van der Poel, a simple concept of Young's modulus,  $E$ , can be applied to viscoelastic materials and can be shown as the following [Van der Poel, 1954; Heukolem 1966]:

$$E = \frac{\sigma}{\varepsilon} = \frac{\text{tensile stress}}{\text{total strain}} \quad (3.1)$$

The "stiffness modulus" of bitumen, normally abbreviated as  $S$ , is defined as the ratio between stress and strain [Heukolem, 1966; Heukolem and Klomp, 1964; Yoder and Witczak, 1975]:

$$(S)_{t,T} = \left( \frac{\sigma}{\varepsilon} \right)_{t,T} \quad (3.2)$$

where  $S$  is denoted as stiffness modulus and depends on loading procedure, frequency (time of loading) and temperature. It is worth mentioning that the term  $S$  was firstly coined by Van der Poel and is now widely used among bitumen and asphalt mixture technologists [Heukolem, 1966; Airey, 1997].

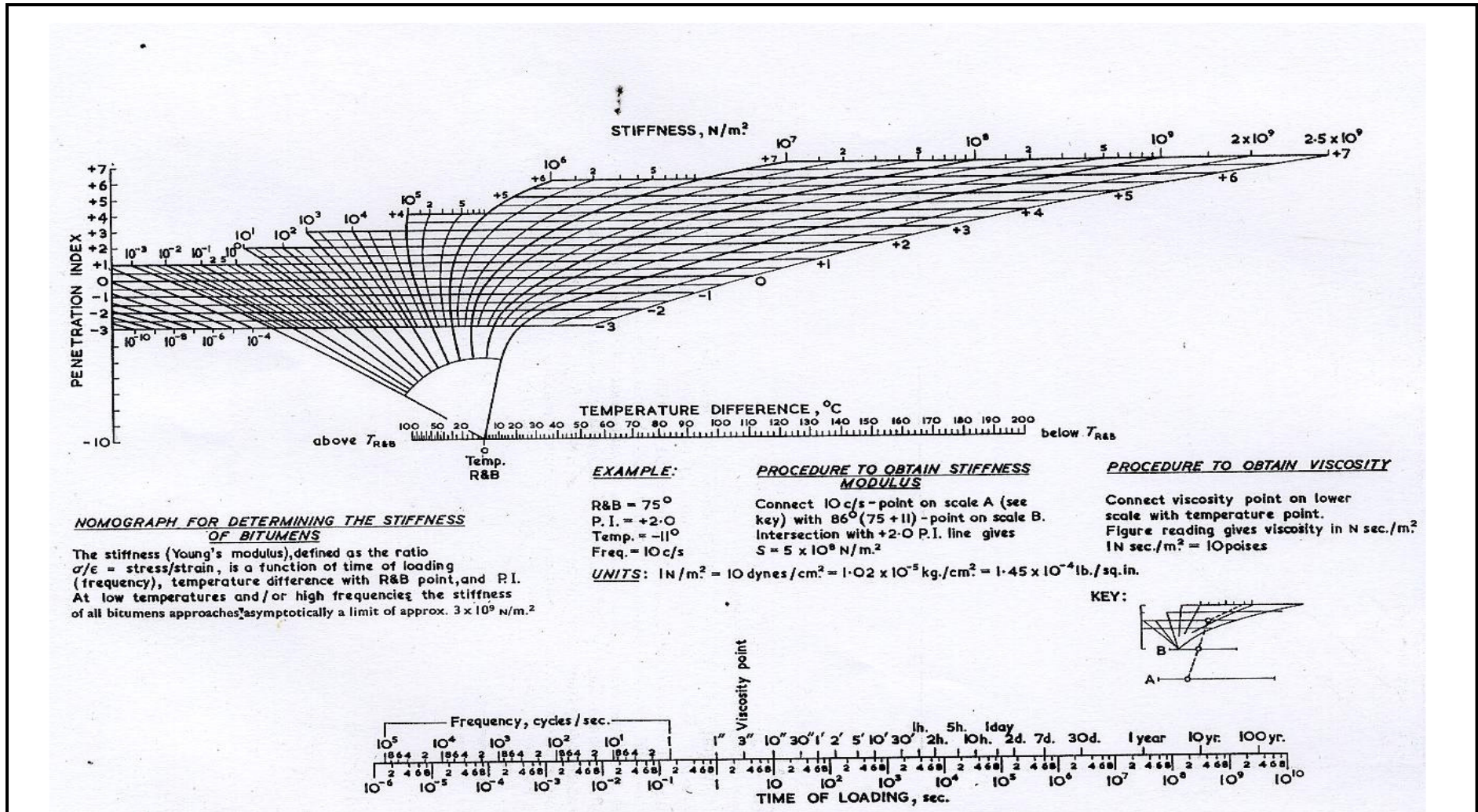


Fig. 3.1: Van der Poel's Nomograph [Van der Poel, 1954]

In this work, a total of 47 bitumen samples from different sources were tested with Penetration Index (PI) values ranging from  $-2.3$  to  $+6.3$  at different temperatures and frequencies. In addition, Van der Poel indicated that  $S$  depends on four variables: [a] time of loading or frequency, [b] temperature, [c] hardness of bitumen and [d] rheological type of bitumen. The rheological stiffness property of bitumen could therefore be estimated by entering the following information; [a] temperature, [b] softening point, [c] loading time and [d] PI into the nomograph. The hardness of bitumen can be completely characterised by the Ring-and-Ball softening point and the PI determines the rheological characteristics.

Meanwhile, for purely viscous behaviour, differences in hardness can be eliminated by a choice of temperature where the viscosities of all bitumen are equal. The bitumen stiffness modulus,  $S$ , is a function of time of loading ( $s$ ), the  $T_{\text{diff}} = (T_{\text{R\&B}} - T)$  and PI. The PI can be used to characterise the rheological type and can be determined from the following equation:

$$\frac{20 - \text{PI}}{10 + \text{PI}} = 50 \times \left( \frac{\log 800 - \log \text{penetration}}{T_{\text{R\&B}} - T} \right) \quad (3.3)$$

where the  $T_{\text{R\&B}}$  is ring-and-ball softening point temperature ( $^{\circ}\text{C}$ ) and  $T$  is penetration temperature (normally taken at  $25^{\circ}\text{C}$ ) and the penetration value of 800 dmm corresponds to the penetration at softening point temperature for bitumens. Therefore, obtaining test results from one penetration test and the ring-and-ball softening point test,  $S$  can be found from the nomograph for any given temperature. Van der Poel's Nomograph is shown in Fig. 3.1.

It can be recapitulated that  $S$  at any temperature condition and time of loading, within a factor of two, can be described solely on penetration and softening point data [Van der Poel, 1954; Bonnaure *et al.*, 1977]. Van der Poel employed the TTSP in the construction of his nomograph even though it was not clearly written in his paper [Anderson *et al.*, 1994]. According to Van der Poel, the accuracy of this nomograph which covers a temperature range of  $300^{\circ}\text{C}$ , is amply sufficient for engineering purposes. It was found that at lower temperatures, all bitumens behaved elastically in

the classical sense, with  $S$  being equal to  $3 \times 10^9$  Pa. This value is equal to the glassy modulus, in extension or flexure, of bitumen [Christensen and Anderson, 1992].

The precision of mathematical functions used by Van der Poel in developing the nomograph was never described in any publication [Anderson *et al.*, 1994]. However, the following approximation formula (only) matches a limited portion of the nomograph [Ullidtz, 1979; Thom, 2008]:

$$S = 1.157 \times 10^{-7} \times t^{-0.368} \times e^{-PI} \times (T_{R\&B} - T)^5 \quad (3.4)$$

where  $S$  is bitumen stiffness (in MPa),  $t$  is loading time (seconds) and  $T$  is temperature ( $^{\circ}\text{C}$ ). The other symbols are as previously defined. However, this equation is restricted to a range of input parameters;  $t$  between 0.01 and 0.1 seconds; PI between  $-1.0$  and  $+1.0$ ; and temperature difference ( $T_{R\&B} - T$ ) between  $10^{\circ}\text{C}$  and  $70^{\circ}\text{C}$  [Ullidtz 1979; Ullidtz and Larsen, 1983].

Van der Poel's Nomograph has been widely adopted in pavement design by various researchers and in fact, efforts have been made to modify this nomograph [Heukolem, 1966, 1973; McLeod, 1972]. Those modifications, however, are largely minor and cosmetic and will be discussed in the following section [Anderson *et al.*, 1994]. As it stands, the nomograph is a convenient and easily accessible method for practical use. This model can be used to estimate  $S$  over a wide range of temperature and loading times to an acceptable accuracy [Gershoff *et al.*, 1999].

Nevertheless, Van der Poel and other researchers found several shortcomings when using this nomograph. For example, this nomograph is clearly unable to describe the behaviour of unmodified bitumen which contains more than 2% waxy elements [Van der Poel, 1954; Kong *et al.*, 1979]. This model is principally developed on unmodified bitumens and not suitable to be used for polymer-modified bitumens (PMBs) [Anderson *et al.*, 1992; Read and Whiteoak, 2003]. It is well known that modified bitumens are more complex in terms of their rheological behaviour and thus this nomograph could be misleading. The modified binder data lies almost exclusively below the equivalency line and clearly indicates the inability of the nomograph to

describe the stiffness of modified bitumen from the penetration and softening point of these materials [Airey, 1997].

In addition, the discrepancies between stiffness values measured and predicted with the nomograph for modified bitumen tend to be more significant at the lower temperatures and longer loading times [Kong *et al.*, 1979; Anderson *et al.*, 1992, 1994]. Moreover, this method is not readily amendable to numerical calculation since it involves the usage of a nomograph [Dobson, 1969]. Although the nomograph method seems to be effectively used, it is not convenient for analysis involving computers due to the lack of mathematical expressions [Zeng *et al.*, 2001]. However, it must be noted that a computerised version of the nomograph produced by Shell is also available in the market.

### 3.2.2 Modified Van der Poel's Nomograph

As previously mentioned, Van der Poel's Nomograph has been widely used by various researchers for describing the stiffness of bitumen. In conjunction with this model, Heukelom and Klomp [1964] developed a relationship between stiffness of bitumen,  $S$  and the modulus of asphalt mixture,  $S_m$ , irrespective of the combination of loading time (frequency) and temperature underlying the value of  $S$ . A semi-empirical formula of this relation can be shown as follows:

$$S_m = S \left[ 1 + \left( \frac{2.5}{n} \right) \left( \frac{C_v}{1 - C_v} \right) \right]^n \quad (3.5)$$

where  $S_m$  is asphalt mixture stiffness ( $N/m^2$ ) and  $S$  is bitumen stiffness ( $N/m^2$ ).  $C_v$  (volume concentration of aggregates) and  $n$  are calculated using the following equations:

$$C_v = \frac{V_A}{V_A + V_B} \quad (3.6)$$

and

$$n = 0.83 \times \log\left(\frac{4 \times 10^4}{S}\right) \quad (3.7)$$

where  $V_A$  and  $V_B$  are percentage volume of aggregate and bitumen respectively. Heukolem and Klomp [1964] studied Van der Poel's method in detail and then modified the relationship between  $S$ ,  $S_m$ , and  $C_v$  using Equations 3.5 to 3.7, as shown in Fig. 3.2. However, the stiffness equation suffers from various shortcomings, one of which is that it is only applicable for air void contents of about 3% and  $C_v$  values from 0.6 to 0.9.

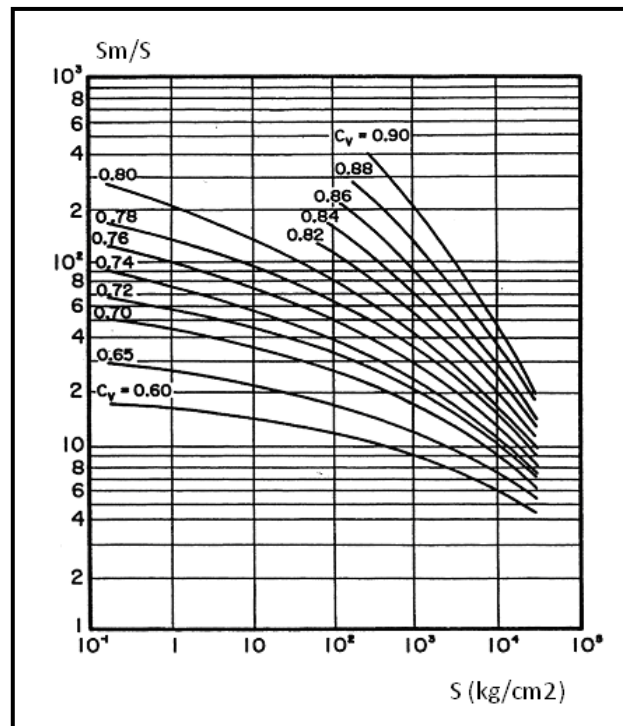


Fig. 3.2:  $S_m/S$  as a function of  $S$  and  $C_v$  [Heukolem and Klomp, 1964]

It is recommended to use  $C_v'$  if the air voids content is larger than 3% [Bonnaure *et al.*, 1977; Ullidtz, 1979; Ullidtz and Larsen, 1983]:

$$C_v' = \frac{C_v}{0.97 + 0.01 \times (100 - (V_A + V_B))} \quad (3.8)$$

However, this correction is applicable only to asphalt mixture having bitumen volume concentration factor,  $C_b$  satisfying the following equation [Yoder and Witczak, 1975]:

$$C_b \geq \frac{2}{3}(1 - C_v') \quad (3.9)$$

where  $C_b = \frac{V_B}{V_A + V_B} = 1 - C_v'$ .

In 1966, Heukelom re-shaped Van der Poel's Nomograph with a slight correction at very low PI values [Heukolem, 1966]. To validate the modification, Heukolem [1966] checked the model described against the data for hundreds of bitumens representing a variety of grades from different sources. He found that as in the original version, the accuracy is comparable with the distance between lines, or better.

This new revised nomograph was used to describe stiffness of bitumen for roughly seven years until Heukelom found uncertainty when reviewing the original data on a few hundred bitumens. An extensive study of the penetration at the softening point revealed that considerable departures from 800 dmm penetration may occur with bitumen having high softening points and high PI values [Heukolem, 1973]. In the few cases where there was a real departure, Heukolem replaced softening point ( $T_{R\&B}$ ) with softening point temperature at penetration of 800 dmm. Consequently, PI (pen/pen) is preferred to PI (pen/R&B). Fig. 3.3 shows the revised nomograph [Heukolem, 1973]. Heukelom used this new nomograph to describe the stiffness of bitumen, particularly for blown bitumen<sup>1</sup> The revised version of Van der Poel's Nomograph is no different from the original ones but with additional or more adequate text as discussed by Heukelom. The key change is the  $T_{R\&B}$  axis becomes  $T_{800pen}$ .

Heukelom found that the results corresponded with the experimental values within 10 to 15%, which is the average of repeatability of the measurements. The use of  $T_{R\&B}$  and PI (pen/R&B), in contrast, gave errors which were 4 to 10 times larger.

---

<sup>1</sup>Blown bitumen is produced via an oxidation process that involves passing air through the short residue, either on a batch or a continuous basis, with the short residue at a temperature between 240°C and 320°C [Read and Whiteoak, 2003].

The revised nomograph can be used for dynamic loading conditions if the frequency,  $f$  is replaced by an effective loading time of  $t = 1/2\pi f$ .

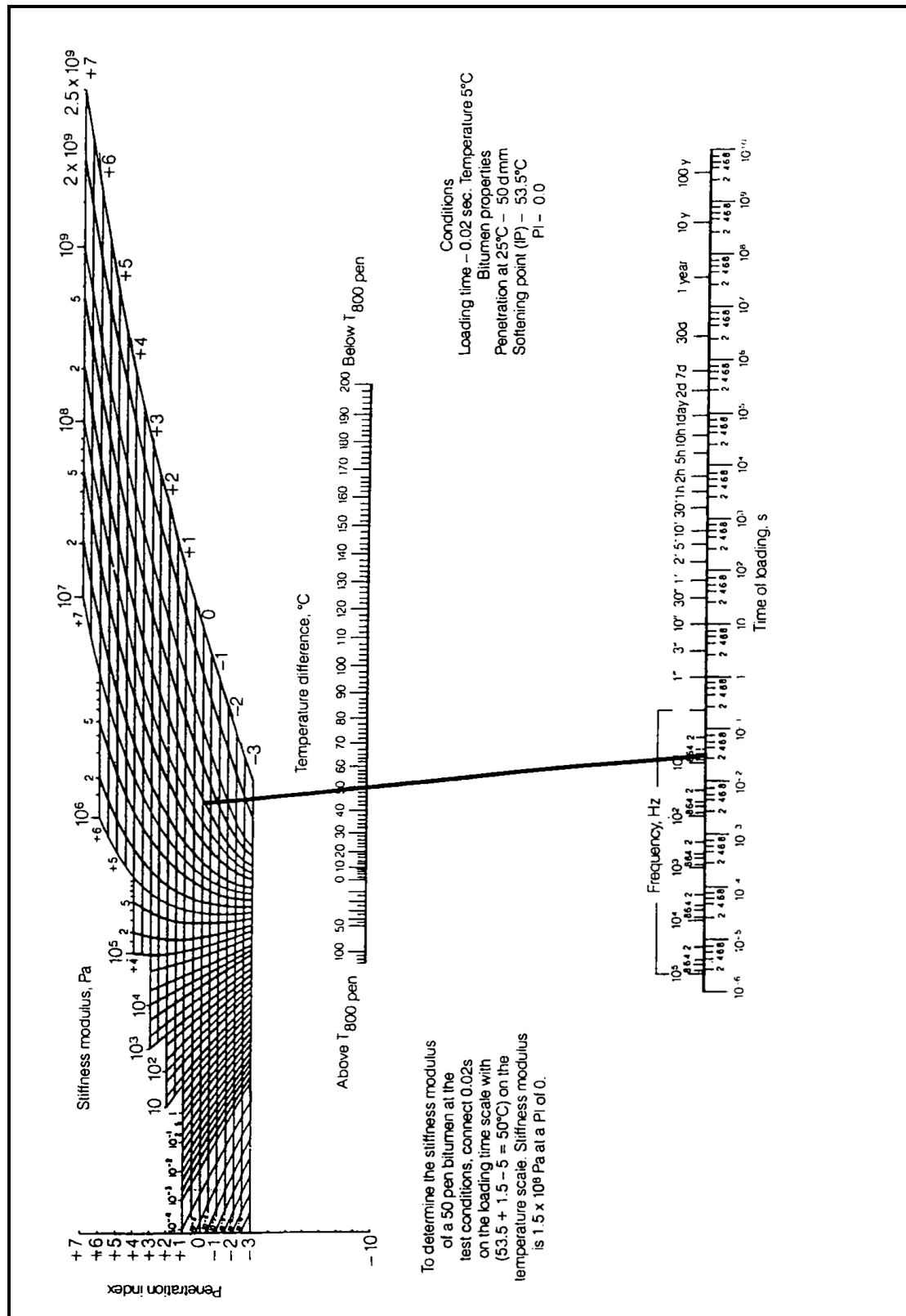


Fig. 3.3: Modified Van der Poel's Nomograph [after Heukelom, 1973]

However, for a complete description of the dynamic behaviour of bitumen, the phase angle between stress and strain is needed; needless to say, its value cannot be obtained from the nomograph [Heukelom, 1973].

### 3.2.3 McLeod's Nomograph

McLeod found that it was impossible to obtain a fixed relationship between Pfeiffer and Doormaal's PI for bitumens and low temperature transverse pavement cracking performance due to penetration of many bitumens at their softening point varying widely from 800 dmm penetration [McLeod, 1972]. He established a different method to measure a quantitative difference of the variation in temperature susceptibility for bitumen. McLeod [1976] defines temperature susceptibility as the rate at which the consistency of bitumen changes with a change in temperature. This method uses the penetration of bitumen at 25°C and its viscosity in centistokes at 135°C (or in poise at 60°C) [McLeod, 1972]. Therefore, the term "pen-vis number" (PVN) is used by McLeod instead of PI as a quantitative measure of temperature susceptibility. The PVN has been designated because the temperature susceptibility of bitumen is based on penetration and viscosity values. The PVNs are numerically similar to, and must be numerically identical with PI values for most types of bitumen because of the way in which it is derived. The PVN can be obtained by using the following equation [McLeod, 1972, 1976, 1987]:

$$PVN = -1.5 \times \frac{(L - X)}{(L - M)} \quad (3.10)$$

where X is log viscosity (centistokes) measured at 135°C, L is log viscosity in (centistokes) at 135°C for a PVN of 0.0 and M is log viscosity (centistokes) at 135°C for a PVN of -1.5. Fig. 3.4 shows a correlation between viscosity at 135°C and penetration at 25°C for various PVN values.

The following equations (based on a least squares line) could be used to calculate more accurate values of L and M [McLeod, 1976; Roberts *et al.*, 1996; Saleh, 2007]:

$$L = 4.258 - 0.7967 \log (\text{Penetration at } 25^{\circ}\text{C}) \quad (3.11)$$

and

$$M = 3.46289 - 0.61094 \log (\text{Penetration at } 25^{\circ}\text{C}) \quad (3.12)$$

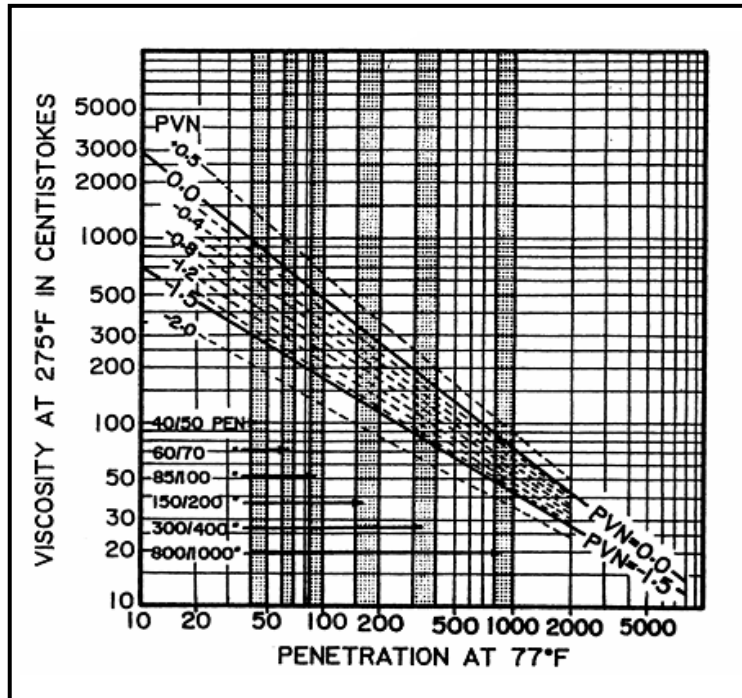


Fig. 3.4: Correlation between viscosity at 135°C and penetration at 25°C [McLeod, 1972]

The lower PVN values indicate that bitumens are more susceptible to temperature [Roberts *et al.*, 1996]. The PVN values for bitumen are normally between +0.5 and -2.0 with a good range between +1 and -1 [Saleh, 2007]. For example, bitumen has a penetration of 100 dmm at 25°C and a viscosity of 400 centistokes at 135°C. From McLeod's chart (Fig. 3.4), L and M are taken as 450 and 180 centistokes, respectively. Using Equation 2.12, the PVN value is calculated equal to -0.19. Fig. 3.5 shows the suggested modification of Heukolem's version of Pfeiffer and Doormaal's chart used to obtain the base temperature. Supposing that the penetration of bitumen and the PVN are 90 and -1.0, respectively (calculated from Equation 2.12), a straight line intercept gives a value of 20°C which is 25°C (the temperature at which the penetration test was made) below the base temperature of bitumen. Therefore, the base temperature for this sample is 45°C.

After having established the base temperature, the stiffness of bitumen for any specific temperature and rate of loading could be obtained using Fig. 3.6 [McLeod, 1973, 1976]. Graphically, this model is more or less similar to Van der Poel's Nomograph, but has a slight modification where McLeod used the PVN and temperature correlation to obtain stiffness of bitumen. For instance, it is assumed that the loading time is 20 000 seconds at  $-28.9^{\circ}\text{C}$ . The service temperature is  $45 + 28.9 = 73.9^{\circ}\text{C}$ , with the base temperature of bitumen being  $45^{\circ}\text{C}$ . By drawing a straight line intercept at 20 000 seconds,  $73.9^{\circ}\text{C}$  and the PVN of  $-1.0$ ,  $S$  is found equal to 49 MPa. Finally, McLeod used another graph that correlates the stiffness of bitumen with the stiffness of asphalt mixture via  $C_v$  curves [McLeod, 1976, 1987].

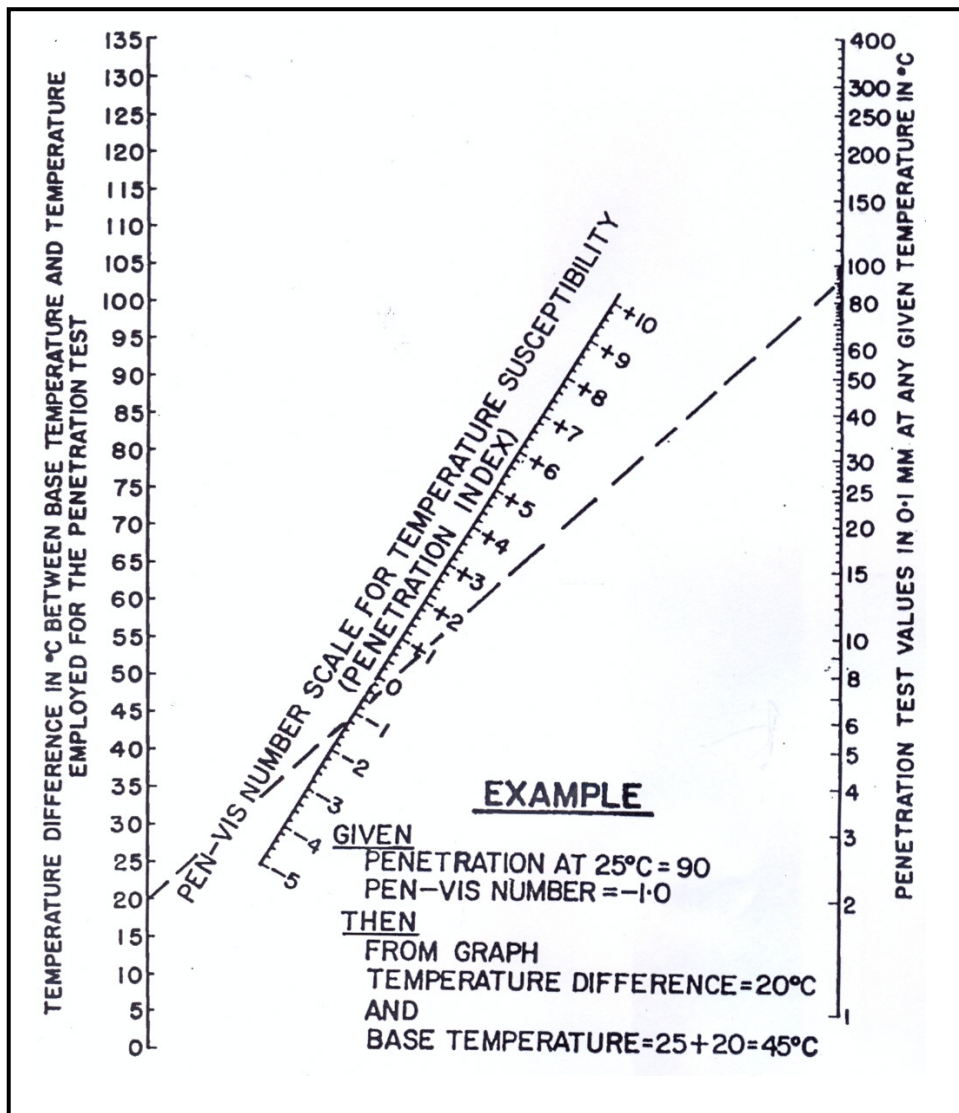


Fig. 3.5: Suggested modification of Heukolem's version of Pfeiffer's and Van Doormaal's Nomograph [McLeod, 1972].

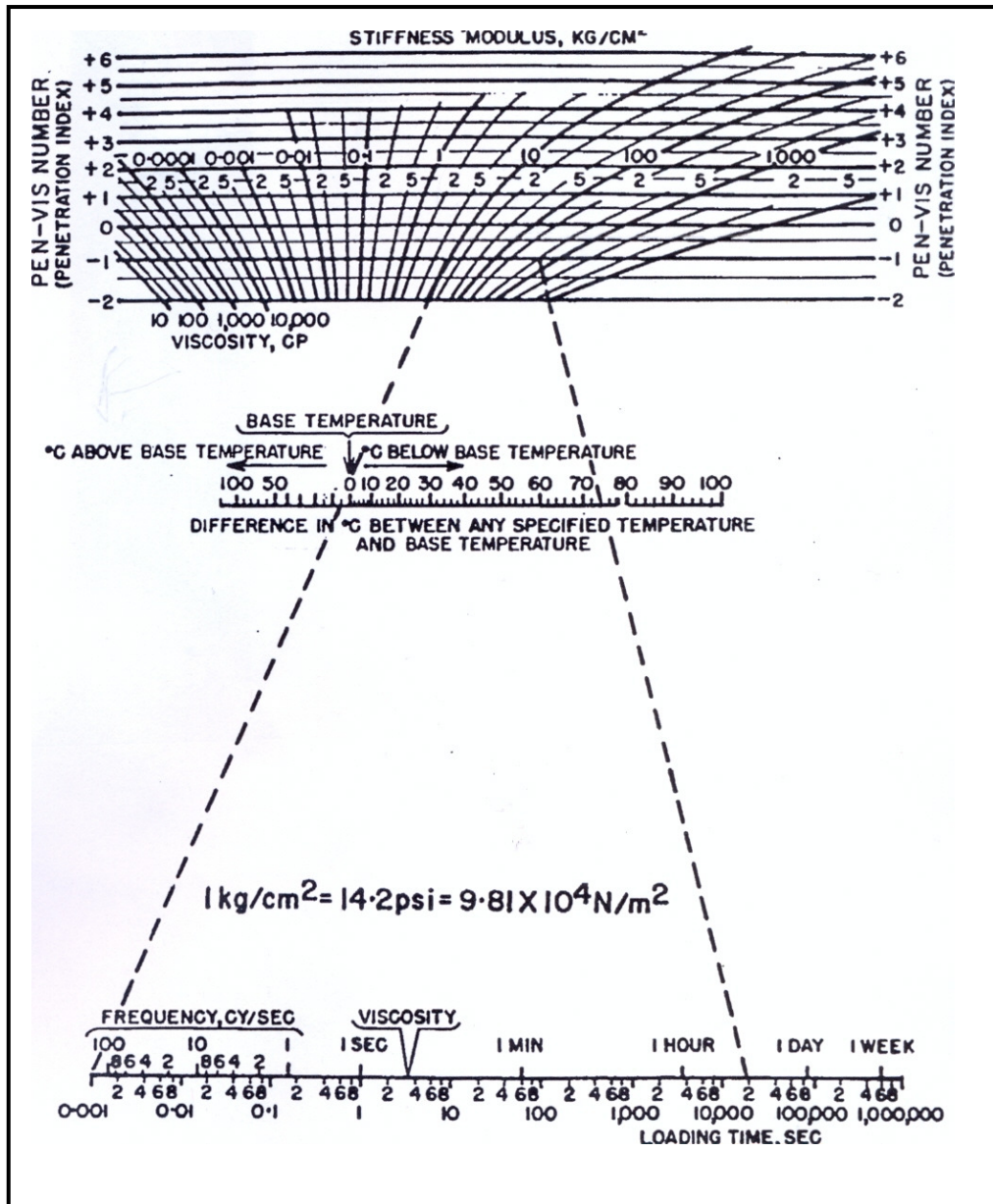


Fig. 3.6: Suggested modification to determine stiffness modulus of bitumen [McLeod, 1972]

McLeod's suggestion of using the relationship between viscosity and base temperature rather than the Ring-and-Ball softening point temperature is a significant deviation from Van der Poel's Nomograph. The disadvantage of this model is its inability to describe the rheological properties of PMBs since it was not developed for that type of material. As discussed by Robert *et al.*, [1996], one noticeable difference between PI and PVN is that the PI changes on ageing (during mixing and subsequently in service) whereas PVN remains substantially the same. In general, Van der Poel, Heukolem and McLeod's nomographs suffer from similar

shortcomings and their use should be avoided if other, more rational and accurate methods of characterisation are available. Anderson *et al.* [1994] found the discrepancies between measured and predicted values were more noticeable at lower temperatures and longer times of loading. When such nomographs are used, the proper metric and conversion values are essential [Yoder and Witzak, 1975].

### 3.3 Mathematical Models

#### 3.3.1 Jongepier and Kuilman's Model

Various researchers have used explicit mathematical models to describe or fit master curves of complex modulus for bitumen. Among them, Jongepier and Kuilman [1969] developed a mathematical model, suggesting that the relaxation spectrum of bitumen is approximately log normal in shape. Based on this assumption, they derived various rheological functions [Jongepier and Kuilman, 1969, 1970; Soleymani *et al.*, 1999]. The relaxation spectrum was derived from experiments using the Weissenberg rheometer operating from  $-20^{\circ}\text{C}$  to  $160^{\circ}\text{C}$  at frequencies from  $5 \times 10^{-4}$  to 50 Hz (from  $3 \times 10^{-3}$  to 32 rad/s) [Lesueur *et al.*, 1996]. A total of 14 samples from different sources such as "pitch type bitumens" (strongly temperature susceptible), "road bitumens" and "blown type bitumens" (rubbery grades) were used in this study.

However, this approach requires the use of integral equations and/or transforms, which can only be solved using numerical methods. The relaxation spectra of bitumen, although close to a log normal distribution at long loading times, deviated significantly from a log normal distribution at short loading times [Anderson *et al.*, 1994]. The Jongepier and Kuilman's Model is based on the distributions of relaxation time and expressed mathematically using a relatively complex set of equations.

First, the frequency has been replaced by a (dimensionless) relative frequency:

$$\omega_r = \frac{\omega \eta_0}{G_g} \quad (3.13)$$

where  $\omega_r$  is reduced frequency (rad/s),  $\eta_0$  is zero shear viscosity (Pa.s) and  $G_g$  is the glassy modulus (Pa). The logarithmic relaxation time distribution of the log normal type is given by:

$$H(\tau) = \frac{G_g}{\beta\sqrt{\pi}} \exp\left\{-\left[\frac{\ln \tau / \tau_m}{\beta}\right]^2\right\} \quad (3.14)$$

where  $H(\tau)$  is the relaxation spectrum distribution,  $\beta$  is the width parameter,  $\tau$  is relaxation time (s) and  $\tau_m$  is a time constant (which determines the position of the spectrum along the relaxation time  $\tau$  axis at a given temperature).  $G_g$  is defined as [Jongepier and Kuilman, 1970]:

$$G_g = \int_{-\infty}^{\infty} H(\tau) d \ln \tau \quad (3.15)$$

and the parameter  $\tau_m$  is given as:

$$\tau_m = \frac{\eta_0}{G_g} \exp\left(\frac{\beta^2}{4}\right) \quad (3.16)$$

Jongepier and Kuilman found the parameter  $\beta$  depends strongly on the type of bitumen. Moreover,  $\beta$  for a particular bitumen can only be found by curve fitting. The storage and loss moduli are expressed by Equations 3.17 and 3.18 after the following substitution:  $u = \ln \omega t$  and  $x = \frac{2}{\beta^2} \ln \omega_r$ ,

$$G'(x) = \frac{G_g}{\beta\sqrt{\pi}} \exp\left\{-\left[\frac{\beta\left(x - \frac{1}{2}\right)}{2}\right]^2\right\} \times \int_0^{\infty} \exp\left(-\left(\frac{u}{\beta}\right)^2\right) \frac{\cosh\left(x + \frac{1}{2}\right)u}{\cosh u} du \quad (3.17)$$

and

$$G''(x) = \frac{G_g}{\beta\sqrt{\pi}} \exp\left\{-\left[\frac{\beta\left(x - \frac{1}{2}\right)}{2}\right]^2\right\} \times \int_0^{\infty} \exp\left(-\left(\frac{u}{\beta}\right)^2\right) \frac{\cosh\left(x - \frac{1}{2}\right)u}{\cosh u} du \quad (3.18)$$

The  $\tan \delta$  (loss tangent), is simply the ratio of  $G''$  to  $G'$  [Jongepier and Kuilman, 1969, 1970; Anderson *et al.*, 1994].

They numerically integrated Equations 3.17 and 3.18 for a range of  $\beta$  values to produce  $|G^*|$  and  $\delta$  master curves. The factor  $\beta$  was found to characterise the shape of the relaxation spectrum, and was thus determined to be a rational parameter for characterising bitumen. Additionally,  $\beta$  was observed to be strongly correlated with the composition of bitumen. It is reported that values from this model fit the observed data to within the experimental error; but that the accuracy of the model was not as good for bitumen with large  $\beta$  values as for bitumen with small  $\beta$  values [Anderson *et al.*, 1994].

Jongepier and Kuilman [1969] relied upon the WLF equation to describe the temperature dependence of bitumens. In general, the Jongepier and Kuilman's Model is reasonably accurate in its treatment of the viscoelastic properties of bitumens. Brodynan *et al.* [1960] suggested that the relaxation times are not log normally distributed since they found relaxation spectrum highly skewed on a logarithmic scale distribution. It is also reported that the Jongepier and Kuilman's Model makes use of integral equations which makes practical calculations with this model impossible [Christensen and Anderson, 1992; Anderson *et al.*, 1994; Elseifi *et al.*, 2002]. In addition, no details concerning the precise determination of the model parameters were presented by the researchers [Anderson *et al.*, 1994].

### 3.3.2 Dobson's Model

Dobson developed a mathematical model for fitting a master curve, based on the empirical relationship between  $|G^*|$  and  $\delta$  for bitumen [Dobson, 1969, 1972; Soleymani *et al.*, 1999]. However, Dobson does not express modulus in term of frequency, but the reverse. He presented the results in terms of a universal master curve, with the intention to characterise bitumen by graphical comparison with this master curve [Anderson *et al.* 1994]. He described how the stiffness of bitumen under any conditions of temperature and rate of loading may be calculated from three fundamental parameters; [a] a viscosity, [b] temperature dependence and [c] rate dependence [Dobson, 1969, 1972]. The temperature dependence and viscosity

parameters are obtained by using a new viscosity-temperature chart, and the rate dependent parameter is obtained from measurement of apparent viscosity at two levels of shear stress.

The viscosity measurements were made at 60°C by a vacuum capillary viscometer and at 25°C by a conical-cylindrical viscometer. The fundamental assumption of this model, which was based on the empirical observations of dynamic data on a range of bitumens, is that the log-log slope of the  $|G^*|$  with respect to loading frequency is a function of the loss tangent and the width of the relaxation spectrum [Dobson, 1969; Anderson *et al.*, 1994]:

$$\frac{dy}{dx} = \frac{\tan \delta}{(1 + \tan \delta)(1 - 0.01 \times \tan \delta)} \quad (3.19)$$

where  $y = \log(|G^*|/G_g)$ ,  $|G^*|$  is the complex modulus magnitude,  $G_g$  is glassy modulus,  $x = \log(\eta_0 \omega a_T / G_g)$ ,  $\eta_0$  is the steady state or Newtonian viscosity and  $a_T$  is the shift factor. Dobson also observed a linear relationship between  $\tan \delta$  and  $|G^*|$  which can be expressed in the following form:

$$\log(1 + \tan \delta) = -by \quad (3.20)$$

where  $b$  is a parameter describing the width of the relaxation spectrum. It may also be regarded as a shear susceptibility index and is related to the PI [Dobson, 1969]. Equations 3.19 and 3.20 can be combined to give a new equation for relating reduced frequency and complex modulus:

$$\log \omega_r = \log G_r - \frac{1}{b} \left[ \log(1 - G_r^b) + \frac{20.5 - G_r^{-b}}{230.3} \right] \quad (3.21)$$

or by rearranging:

$$\log \omega_r^{-b} = \log(G_r^{-b} - 1) + \frac{20.5 - G_r^{-b}}{230.3} \quad (3.22)$$

where  $\omega_r = \eta_0 \omega a_T / G_g$  and  $G_r = |G^*| / G_g$ .  $\omega_r^{-b}$  is a unique function of  $G_r^{-b}$ . All the equations above are applicable for the value of  $\tan \delta \leq 9.5$ . Dobson developed an

instrument to measure the complex shear modulus of 45-mg bitumen samples over a frequency range from 2 to 200 Hz and over a continuously variable temperature range [Dobson, 1967]. This equipment was based on a plate measuring geometry. He used the value of  $G_g$  as  $1 \times 10^9$  Pa ( $1 \times 10^{10}$  dynes/cm<sup>2</sup>) at  $\tan \delta \geq 9.5$ ,  $dy/dx = 1$ . It was found that the model exhibited good agreement with experimental data.

Like Jongepier and Kuilman, Dobson described the effect of temperature on viscoelastic properties using the WLF equation. He found that a single set of coefficients could be used to fit the shift factor data for a range of bitumens, but a different coefficient set was needed for two extreme temperatures. The simple form of the WLF equation with two sets of constants: For  $T - T_s < 0$ ,  $C_1 = 12.5$  and  $C_2 = 142.5$  has been used. Meanwhile for  $T - T_s > 0$ , use was made with  $C_1 = 8.86$  and  $C_2 = 101.6$ .  $T_s$  is equivalent to the reference temperature, with  $T_s = T_g - 50$ .  $T_g$  was probably determined from dilatometric measurements [Anderson *et al.*, 1994].

In general, Dobson's method for describing the temperature dependency appears to be reasonably accurate. He also presents a practical means for applying this part of his model to rheological data on bitumen. Nevertheless, this model also has several shortcomings. Maccarrone [1987] studied the Dobson Model for describing temperature dependence of  $a_T$  and found the WLF equation with Dobson's coefficients over described the  $a_T$  at temperatures below 20°C when applied to aged bitumens. It is difficult to assess the accuracy of Dobson's Model since he only made a few comparisons of measured and described  $|G^*|$  and  $\delta$  values. In addition, the failure to express modulus as an explicit function of reduced frequency is a serious shortcoming, as is the lack of a well-defined procedure for determining the constants in his equation for the modulus [Anderson *et al.*, 1994]. In addition, the development of this model was not applied to modified bitumen.

### 3.3.3 Dickinson and Witt's Model

Dickinson and Witt performed dynamic mechanical testing on 14 different bitumens and developed analytical expressions for the  $|G^*|$  and  $\delta$  in terms of their frequency dependencies. They proposed the following equation [Dickinson and Witt, 1974; Christensen *et al.*, 1992]:

$$\log G_r^* = \frac{1}{2} \left\{ \log \omega_r - \left[ (\log \omega_r)^2 + (2\beta)^2 \right]^{\frac{1}{2}} \right\} \quad (3.23)$$

where  $|G_r^*|$  is relative complex modulus at frequency,  $\omega$  (i.e.,  $G_r^* = |G^*|/G_g$ ),  $\omega_r$  is the relative angular frequency ( $\omega_r = \omega \eta_0 a_T / G_g$ ) and  $\beta$  is a shear susceptibility parameter, which is defined as the distance on a logarithmic scale between  $G_g$  and the modulus at  $\omega_r = 1$ . Meanwhile the phase angle ( $\delta$ ) can be expressed as the following:

$$\delta = \delta' + \frac{\pi - 2\delta'}{4} \left\{ 1 - \log \omega_r \left[ (\log \omega_r)^2 + (2\beta)^2 \right]^{-\frac{1}{2}} \right\} \quad (3.24)$$

where  $\delta$  is the phase angle and  $\delta'$  is the limiting phase angle at infinite frequency [Dickinson and Witt, 1974; Anderson *et al.*, 1994]. By eliminating  $\log \omega_r$  in Equations 3.23 and 3.24 a relationship between complex modulus and phase angle was established by Dickinson and Witt, treated as a hyperbola model:

$$\log |G_r^*| = -\beta \left[ \frac{2(\delta - \delta')}{\pi - 2\delta} \right]^{\frac{1}{2}} \quad (3.25)$$

Because of the limited temperature range examined, they used the same coefficients as Dobson to describe temperature dependence of the  $a_T$  for their bitumen (see Dobson's Model). The standard errors (SE) of fit of  $|G^*|$  obtained ranged from 0.008 to 0.025 on the logarithmic scale, corresponding to a maximum error of about 10%. The accuracy of the  $\delta$  was not reported by Dickinson and Witt although it can be seen that the accuracy was comparable to the experimental error

in determining the phase angle [Christensen *et al.*, 1992; Anderson *et al.*, 1994]. In addition, Dickinson and Witt observed that the spectra were unsymmetrical with respect to the maximum value and disputed Jongepier and Kuilman's assumption of a log Gaussian distribution of relaxation times.

The reported values of  $\log G_g$  ( $G_g$  in Pa), ranged from 9.5 to 10.6, which are similar to the values of 9.7 or 10, reported by other researchers like Dobson [1969] and Jongepier and Kuilman [1970]. Maccarrone evaluated various models for describing the dynamic properties of bitumen based on 39 aged and 2 original bitumen samples. It was found that the Dickinson and Witt's Model fits the rheological data quite well with a standard error of estimate ( $S_e$ ) of  $\log |G^*|$  ranging from 0.001 to 0.012 [Maccarrone, 1987]. In general, this model is more practical and simpler than either Dobson's Model or Jongepier and Kuilman's Model but  $G_g$  and viscosity in the model are determined statistically and in many cases, overestimated [Anderson *et al.*, 1994; Airey, 1997].

### 3.3.4 Christensen and Anderson (CA) Model

During the Strategic Highway Research Program (SHRP) A-002A study, Christensen and Anderson performed dynamic mechanical analysis (DMA) on 8 SHRP core bitumens for the purpose of developing a mathematical model that described the viscoelastic behaviour of bitumen. The model will be referred to as the Christensen and Anderson (CA) Model. They noted that four primary parameters (the glassy modulus,  $G_g$ , the steady state viscosity,  $\eta_0$ , the crossover frequency,  $\omega_c$ , and the rheological index,  $R$ ) are needed to fully characterise the properties of any bitumen [Christensen and Anderson, 1992; Anderson *et al.*, 1994]:

- *The glassy modulus ( $G_g$ )* is the value that the complex modulus or stiffness modulus approaches at low temperatures and high frequencies (short loading times).  $G_g$  is normally very close to  $1 \times 10^9$  Pa in shear loading for most bitumens and can be used for most purposes.
- *The steady-state viscosity ( $\eta_0$ )* is the steady-state, or Newtonian viscosity. In dynamic testing, it is approximated as the limit of the complex viscosity,

$|\eta^*|$ , as the phase angle approaches  $90^\circ$ . The  $45^\circ$  line that the dynamic master curve approaches at low frequencies is often referred to as the viscous asymptote. It is indicative of the steady-state viscosity, and the value of  $\eta_0$  is binder specific.

- *The crossover frequency ( $\omega$ ) or crossover time ( $t_c$ )* is the frequency at a given temperature where  $\tan \delta$  is 1. At this point, the storage and loss moduli are equal. For most bitumens, the crossover frequency is nearly equal to the point at which the viscous asymptote intersects the glassy modulus. The crossover frequency can be thought of as a hardness parameter that indicates the general consistency of a given bitumen at the selected temperature and is binder specific. The crossover frequency is the reciprocal of the crossover time,  $t_c = 1/\omega_c$ .
- *The rheological index ( $R$ )* is the difference between the glassy modulus,  $G_g$ , and the dynamic shear complex modulus at the crossover frequency,  $|G^*(\omega_c)|$ . The rheological index is directly proportional to the width of the relaxation spectrum and indicates rheologic type.  $R$  is not a measure of temperature but reflects the change in modulus with frequency or leading time and therefore is a measure of the shear rate dependency of bitumen.  $R$  is binder specific.

Fig. 3.7 shows some of the parameters mentioned above.

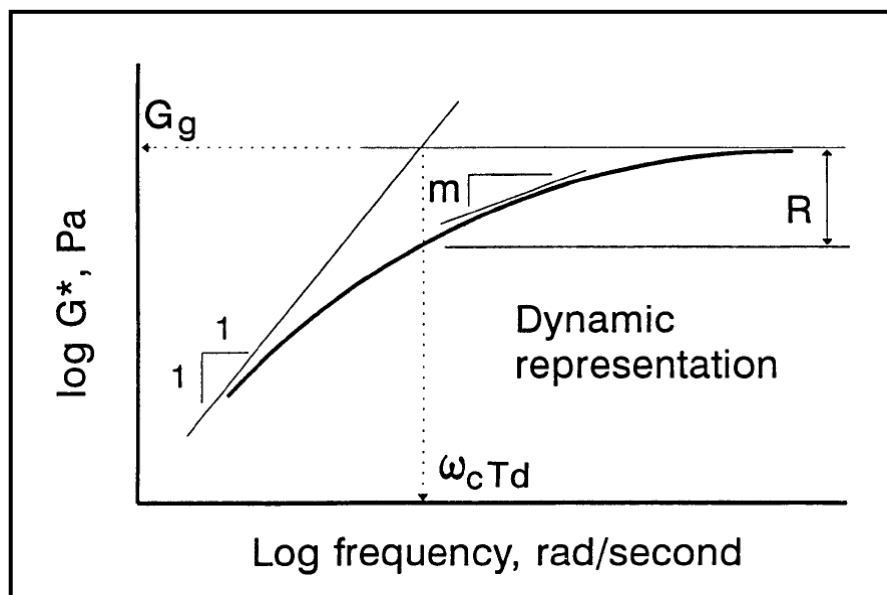


Fig. 3.7: Definition of the CA Model [Christensen and Anderson, 1992]

The CA Model is presented as a series of equations for the primary dynamic viscoelastic functions. For  $|G^*|$ , the following mathematical function can be used:

$$|G^*| = G_g \left[ 1 + \left( \frac{\omega_c}{\omega} \right)^{\frac{(\log 2)}{R}} \right]^{\frac{R}{\log 2}} \quad (3.26)$$

where  $\omega_c$  is the crossover frequency and  $R$  is a rheological index. The other parameters are as defined previously. Bitumen with larger values of  $R$  exhibit wider relaxation spectra. Meanwhile  $\delta$  (in degrees) can be taken as:

$$\delta = \frac{90}{\left[ 1 + \left( \frac{\omega}{\omega_c} \right)^{\frac{(\log 2)}{R}} \right]} \quad (3.27)$$

The other parameters are as defined above [Christensen and Anderson, 1992; Marasteanu and Anderson, 1996; Zeng *et al.*, 2001; Silva *et al.*, 2004]. Christensen and Anderson combined Equations 3.26 and 3.27 to define  $R$  as:

$$R = \frac{(\log 2) \times \log \left( \frac{|G^*|}{G_g} \right)}{\log \left( 1 - \frac{\delta}{90} \right)} \quad (3.28)$$

where the parameters are as previously defined. They found this equation is quite useful when the value of  $R$  is desired, but it is impossible to obtain data at the region when  $\delta = 90^\circ$ . In using this equation to calculate the  $R$  value,  $G_g$  can be taken as  $1 \times 10^9$  Pa in shear and  $3 \times 10^9$  Pa in extension (or flexure).

It was reported that Equation 3.28 is reasonably accurate within the region where  $\delta$  is between  $10^\circ$  to  $70^\circ$  and the best results are obtained near the crossover point, where  $\delta = 45^\circ$  [Anderson *et al.*, 1994]. This model is not recommended to be used at temperatures and frequencies where  $\delta$  approximates  $90^\circ$ . The CA Model was validated using the SHRP core bitumens (unaged), thin film oven test (TFOT) aged and pressure ageing vessel (PAV) aged. It can generally be used over a wide range

of frequencies and temperatures extended well into the glassy region [Christensen and Anderson, 1992]. Silva *et al.* [2004] found the model presented lack of fit particularly at high temperatures and/or long loading times (Fig. 3.8).

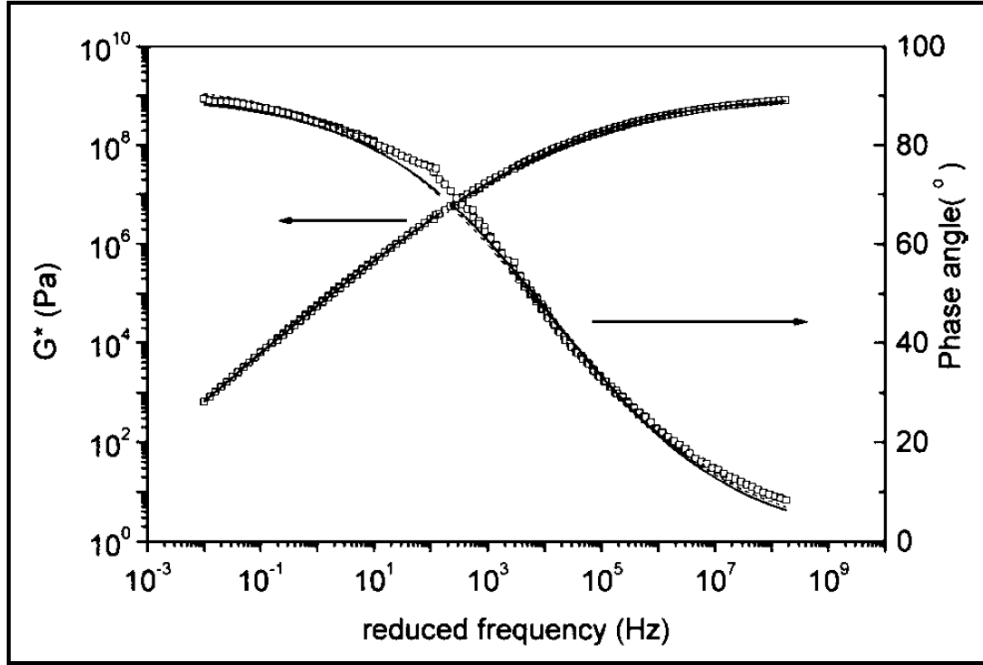


Fig. 3.8: Modelling using the CA Model [Silva *et al.*, 2004]

To surmount this inconsistency, Christensen and Anderson suggested calculating a second set of parameter values for the secondary region in which the value of  $R$  is set equal to 0.81 when Newtonian flow is approached. They have manipulated the equations above to generate a series of equations from which the LVE parameters for the secondary viscoelastic region can be calculated [Christensen and Anderson, 1992; Anderson *et al.*, 1994]. The most important of these calculations is for determination of  $\delta_v$ , which divides the primary and secondary regions:

$$\delta_v = 90 \left( \frac{\eta_0 \omega_c}{G_g} \right)^{\frac{\log 2}{(R-0.81)}} \quad (3.29)$$

where  $\delta_v$  is transition phase angle (degrees),  $\eta_0$  is the steady-state viscosity (Pa.s),  $\omega_c$  is the crossover frequency (rad/s),  $G_g$  is the glassy modulus (Pa) and  $R$  is the rheological index.

From Equation 3.29, it is clear that the value of  $G_g/\omega_c$  must be equal to or less than the value of the steady-state viscosity,  $\eta_0$ , which is always the case for unmodified bitumens. If the value of these parameters is equal, it means that the same LVE parameters apply throughout the entire region of behaviour. This phenomenon will sometimes occur in bitumens having very high asphaltene contents. Once  $\delta_v$  is known, it can be used in conjunction with the primary LVE parameters to estimate the appropriate values for the viscous flow region [Anderson *et al.*, 1994].

For estimating,  $G_{gv}$ ,

$$G_{gv} = G_g \left[ \frac{90}{(90 - \delta_v)} \right]^{0.81 - \frac{R}{\log 2}} \quad (3.30)$$

where  $G_{gv}$  is the limiting modulus in the viscous flow region and the other parameters are as previously defined.

For estimating  $\omega_{cv}$ ,

$$\omega_{cv} = \omega_c \left[ \frac{(90 - \delta_v)}{\delta_v} \right]^{\frac{R}{\log 2} - 0.81} \quad (3.31)$$

where  $\omega_{cv}$  is the location parameter for the viscous flow region (rad/s) and the other parameters are as previously defined.

These two parameters,  $G_{gv}$  and  $\omega_{cv}$  can be used in conjunction with the standard value of  $R$  in the viscous region (0.81) to generate all viscoelastic functions at high temperatures and/or low frequencies. The primary set of parameters should be used when the phase angle is below  $\delta_v$ , the secondary parameters (for viscous flow), when the phase angle is above  $\delta_v$ . In many cases, it is tedious to first estimate the phase angle, compare it with  $\delta_v$ , and then determine if the proper set of parameters has been used. Therefore, a fourth parameter, the transition frequency,  $\omega_v$  is useful:

$$\omega_v = \omega_c \left[ \frac{(90 - \delta_v)}{\delta_v} \right]^{\frac{R}{\log 2}} \quad (3.32)$$

when estimating the modulus or phase angle from the LVE parameters, it is first necessary to check whether the loading frequency is above or below  $\omega_v$ . If the loading frequency is above the  $\omega_v$ , the primary LVE parameters are used. If the loading frequency is below  $\omega_v$ , the values for the viscous flow region are used.

Although the division of the master curve into two regions with two set of parameters may seem unnecessarily complicated, it has been found that this method is the only way to achieve reasonable accuracy in mathematical modelling while still maintaining the use of the explicit parameters that characterise the master curve. In practice, the primary parameters are of more interest and can be applied with confidence to temperatures up to about 45°C under typical traffic loading times. At higher temperatures, the only property that is of practical interest is the steady-state viscosity, which is one of the explicit parameters from the master curve therefore, in practical applications, it is generally not necessary to use the parameters for the viscous flow region. These parameters were developed and presented here in the interest of completeness. In research and detailed pavement modelling applications, it may also be desirable to have a comprehensive and accurate model for the LVE behaviour of bitumens [Anderson *et al.*, 1994].

The WLF equation is used above the defining temperature,  $T_d$  and in the Newtonian region.  $T_d$  is a characteristic parameter for each bitumen. It is reported that the values of  $C_1 = 19$  and  $C_2 = 92$  can be used for all bitumens. However, it is recommended to obtain the  $C_1$  and  $C_2$  by optimisation process from experimental data. No universal values can, a priori, be applied. Meanwhile, for the temperatures below  $T_d$  and in the Newtonian region, an Arrhenius function is used to describe  $a_T$ . The activation energy ( $E_a$ ) for flow below  $T_d$  was reported to be 261 kJ/mol. In general, the CA Model is relatively simple in shape and reasonably accurate as compared to the previous models. However, the sensitivity analysis showed the use of only parameters related to the shape of the relaxation spectrum (rheological index) is not enough to describe bitumen behaviour [Silva *et al.*, 2004]. In addition,

the model is not able to model the rheological properties of modified bitumen [Airey, 1997].

### 3.3.5 Fractional Model

Stastna *et al.* proposed a simple model for  $|G^*|$  and  $\delta$  to describe the behaviour of bitumen. The model, called the Fractional Model, is based on the generalisation of the Maxwell Model [Stastna *et al.*, 1985, 1994, 1996, 1997, 1999a, 1999b; Lesueur, 1999]. This model has a relatively low number of parameters and requires only half the parameters compared to the generalised Maxwell Model.  $|G^*|$  represents the response function of viscoelastic materials and can be described by a general power of a rational fraction. Models of this type have been studied by Stastna *et al.* [1985] and comparison with experimental data for polymeric solutions can be found in the study of Stastna *et al.* [1994].  $|G^*|$  can be shown as the following:

$$|G^*| = \eta_0 \omega \left[ \frac{\prod_{k=1}^m (1 + (\mu_k \omega)^2)^{\frac{1}{2(n-m)}}}{\prod_{k=1}^n (1 + (\lambda_k \omega)^2)} \right] \quad (3.33)$$

where  $\mu_k$  and  $\lambda_k$  are the relaxation times ( $\mu_k > 0$ ,  $\lambda_k > 0$ ) and  $m$  and  $n$  are the numbers of relaxation time ( $n > m$ ). Stastna *et al.* found the Fractional Model is much more flexible than the generalised Maxwell Model and is easily manageable. A phase angle,  $\delta$  can be expressed as:

$$\delta = \frac{\pi}{2} + \frac{1}{(n-m)} \left[ \sum_{k=1}^m a \tan(\mu_k \omega) - \sum_{k=1}^n a \tan(\lambda_k \omega) \right] \quad (3.34)$$

where  $a$  is the Fourier transform of the Dirac delta function. They performed DMA on 19 unmodified and 5 modified bitumen samples from different sources. For almost all cases and with the reference temperature set at 0°C, the Fractional Model generates excellent fitting of  $|G^*|$  and  $\delta$  master curves, for both the unmodified and modified bitumens (Fig. 3.9).

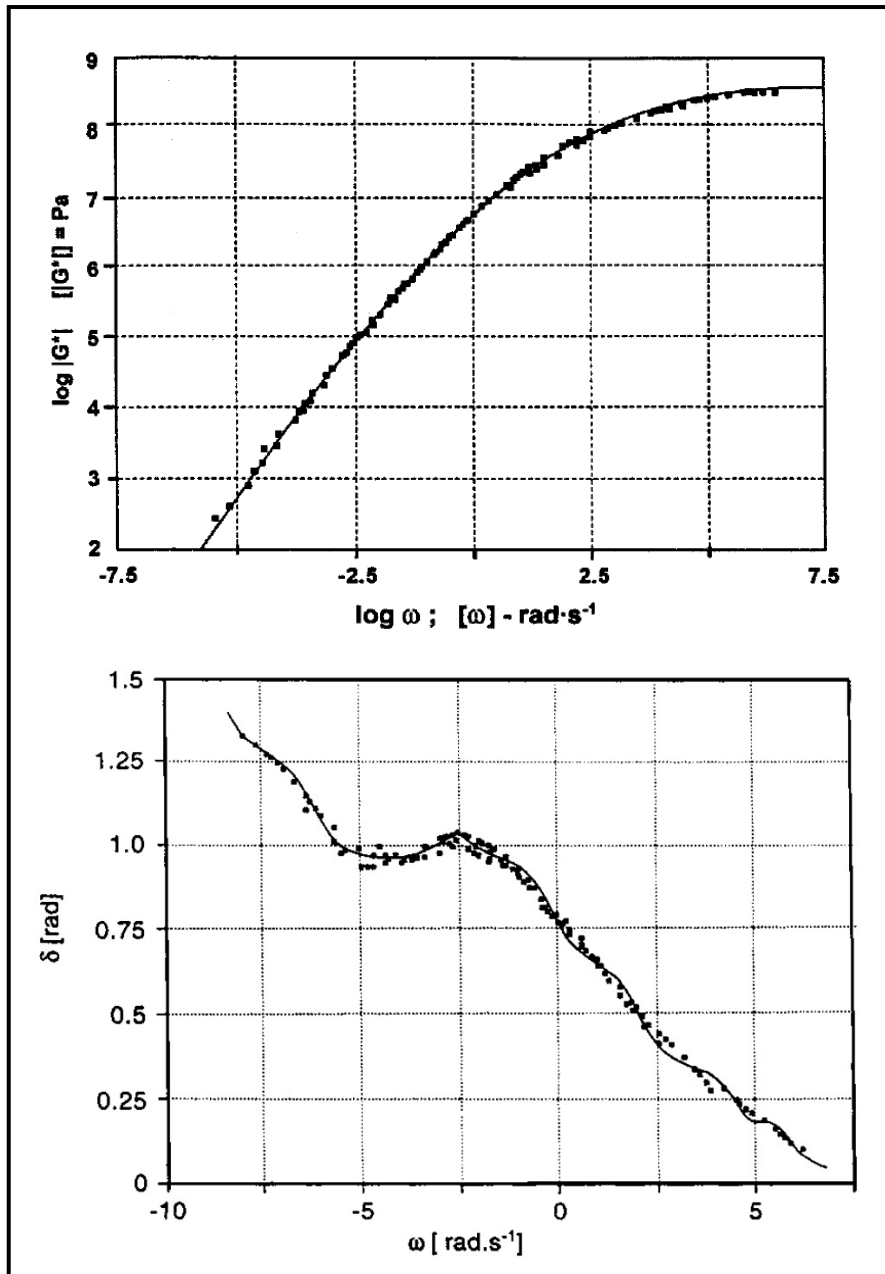


Fig. 3.9: Comparison between measured (dotted) and descriptive (lines) data using the Fractional Model [Stastna *et al.*, 1997]

Stastna *et al.* [1999] in their study employed both the WLF and Arrhenius equations for shifting purposes but stress was given to the earlier equation for a better fit. Nevertheless, no details concerning the precise determination of the parameters were presented in their papers. Marasteanu and Anderson [1999a] reported this model lacks statistical robustness because of the number of unknown parameters (10 to 15) approaches the number of observations. Indeed it is difficult to interpret a model with so many parameters on a phenomenological basis.

However, they found the degree of flexibility offered by the model is very useful when simulating plateaus or other irregularities in the master curves. This, however, can also lead to the fitting of anomalous portions of the master curve that are the result of testing error, rather than real rheological properties of binders [Marasteanu and Anderson, 1999a].

### 3.3.6 Christensen Anderson Marasteanu (CAM) Model

Marasteanu and Anderson [1999a] developed a new model by modifying the CA Model to improve the fitting particularly in the lower and higher zones of the frequency range of bitumens. The model known as the CAM Model after Christensen, Anderson and Marasteanu, attempts to improve the descriptions of both unmodified and modified bitumen. The researchers applied the Havriliak and Nagami Model to the initial CA Model and proposed the following equation for  $|G^*|$  [Marasteanu and Anderson, 1999a; Li *et al.*, 2006].

$$|G^*| = G_g \left[ 1 + \left( \frac{\omega_c}{\omega} \right)^v \right]^{-\frac{w}{v}} \quad (3.35)$$

where  $v = \log 2/R$  and  $R$  is the rheological index.  $\delta$  is defined as:

$$\delta = \frac{90w}{\left[ 1 + \left( \frac{\omega_c}{\omega} \right)^v \right]} \quad (3.36)$$

The introduction of  $w$  parameter addresses the issue of how fast or how slow the  $|G^*|$  data converge into the two asymptotes (the  $45^\circ$  asymptote and the  $G_g$  asymptote) as the frequency goes to zero or infinity [Marasteanu and Anderson, 1999a].

During the work, Marasteanu and Anderson tested their model using 38 unmodified and modified bitumens. The fitted  $|G^*|$  values of the measured values for the CAM Model and CA Model were within 10–35%, respectively. They found that typically the lack of fit occurred at the two asymptotes of the master curves and

it was believed that the departure from the thermorheologically simplicity is bitumen dependent and is strongly related to bitumen composition, especially the presence of waxy elements and higher asphaltenes. Marasteanu and Anderson did not clearly specify the equation for describing the temperature dependence of bitumen. The degree of precision in modeling  $|G^*|$  and  $\delta$  was greater than the original CA Model. However, anomalies were still seen in the construction of a smooth master curve when test bitumens behaved as thermorheologically complex materials. Like the CA Model, Silva *et al.* [2004] found the CAM Model presented lack of fit particularly at high temperatures as shown in Fig. 3.10.

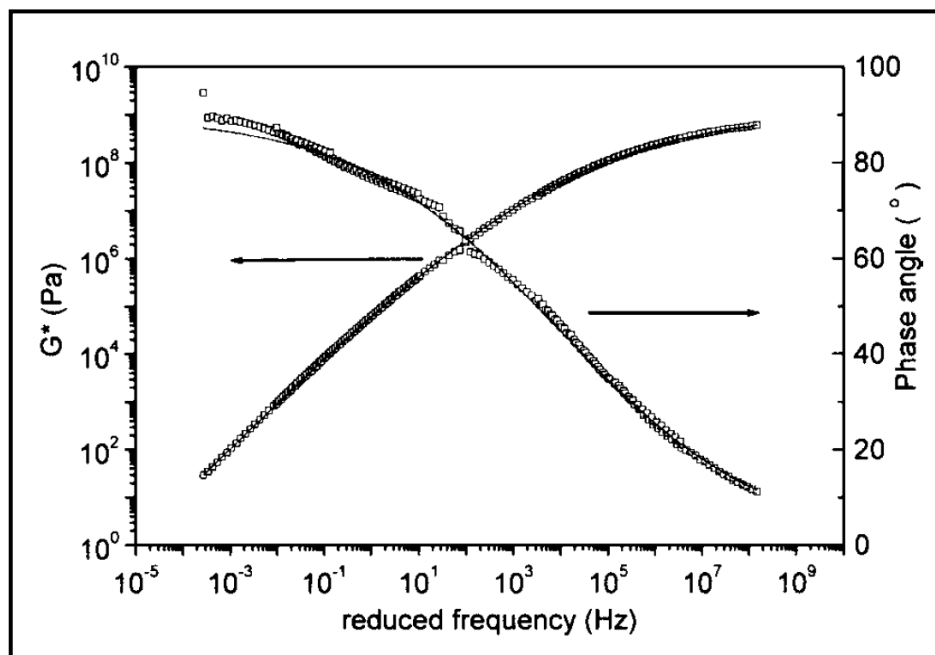


Fig. 3.10: Modelling using the CAM Model [Silva *et al.*, 2004]

### 3.3.7 Bahia and Co-workers' Model

Bahia and co-workers [Bahia *et al.*, 2001; Zeng *et al.* 2001] developed mathematical equations to characterise the unmodified and modified bitumen and asphalt mixture with bitumen modification under dynamic shear loading over a wide range of frequencies, temperatures and strains. The model is composed of four formulations for the  $|G^*|$  and  $\delta$  master curves, temperature and strain dependencies. This model is capable of modelling the behaviour of bitumen as a viscoelastic fluid, and also for asphalt mixture as a viscoelastic solid in a universal form. However, in this study, stress is given to the use of a model on viscoelastic fluids. The  $|G^*|$

equation is based on a generalisation of the CAM Model and generalised law model [Bahia *et al.*, 2001; Zeng *et al.*, 2001]:

$$|G^*| = G_e + \frac{G_g - G_e}{\left[1 + \left(\frac{f_c}{f'}\right)^k\right]^{\frac{m_e}{k}}} \quad (3.37)$$

where  $G_e = |G^*|(f \rightarrow 0)$  with  $G_e = 0$  for bitumen,  $G_g = |G^*|(f \rightarrow \infty)$ ,  $f_c$  is a location parameter with dimensions of frequencies and  $f'$  is reduced frequency, function of both temperature and strain and  $k$  and  $m_e$  are the shape parameters (dimensionless).  $f_c$  is equal to crossover frequency in the CA Model and CAM Model. Fig. 3.11 shows a schematic diagram of the Modified CAM Model.

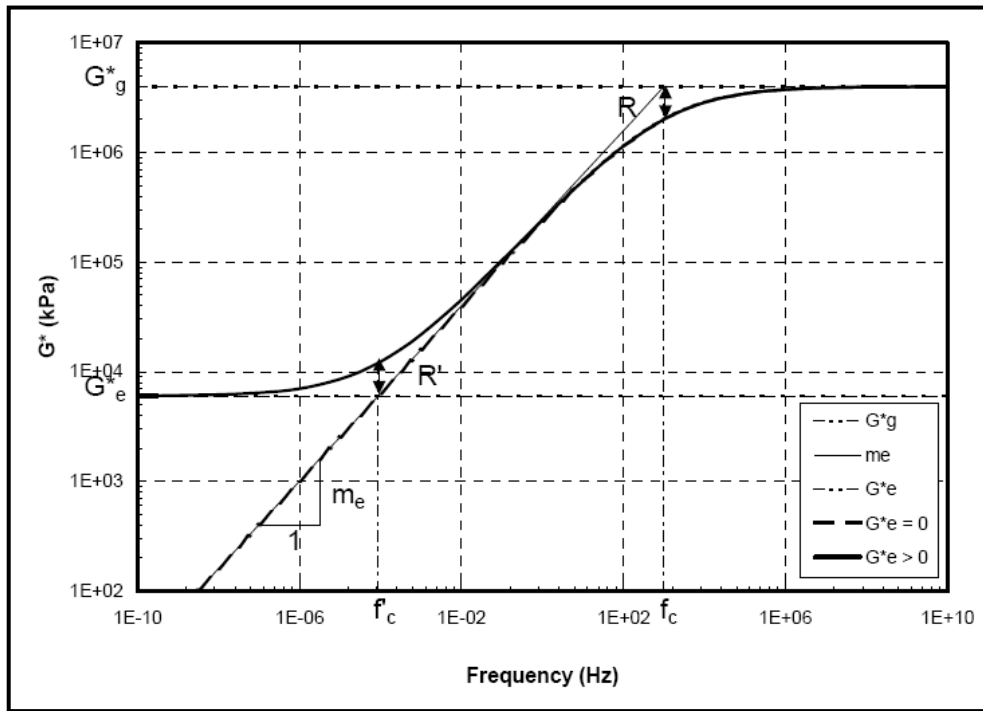


Fig. 3.11: Definitions of the Bahia and Co-workers' Model [Bahia *et al.*, 2001]

It is seen that  $G_g$  and  $G_e$  are horizontal asymptotes when frequencies approach infinity and zero, respectively. The third asymptote is the one with the slope of  $m_e$ . The  $G_g$  and  $m_e$  asymptotes intercept at  $f_c$ .  $G_e$  and  $m_e$  asymptotes intercept at:

$$f_c' = f_c \left( \frac{G_e}{G_g} \right)^{\frac{1}{m_e}} \quad (3.38)$$

For binders,  $f_c' = 0$ . According to Bahia *et al.* [2001], the distance (one logarithmic decade being unity) between  $|G^*| (f_c)$  and  $G_g$  for bitumen is given by:

$$R = \log \frac{2^{m_e/k}}{1 + (2^{m_e/k} - 1)G_e/G_g} \quad (3.39)$$

For binders,  $R = m_e/k \log 2$ . The distance between  $|G^*| (f_c')$  and  $G_e$  is given by:

$$R' = \left\{ 1 + \left( \frac{G_g}{G_e} - 1 \right) \times \left[ 1 + \left( \frac{G_g}{G_e} \right)^{k/m_e} \right]^{-m_e/k} \right\} \quad (3.40)$$

For binders,  $R' = \log 2$ . The physical meanings of the parameters are shown as the following [Bahia *et al.*, 2001; Zeng *et al.*, 2001]:

- The glass modulus,  $G_g$  is the maximum asymptote modulus in shear that represents the response at very high frequencies or low temperatures of the material.
- The equilibrium modulus,  $G_e$  is the minimum modulus that a mixture can offer in shear at very low frequencies and/or high temperatures. In the case of asphalt mixture, this asymptotic value is considered to represent the ultimate interlock between aggregates when the contribution of the binder in a mixture is negligible.
- The location parameter,  $f_c$  (also called crossover frequency) represents the frequency at which the storage component  $G'$  is approximately equal to the loss component  $G''$  of the complex modulus in the case of the binder. A higher  $f_c$  value is an indication of a higher phase angle and thus a more overall viscous component in the behaviour.
- The two shape parameters  $k$  and  $m_e$  are related to  $R$  in Equation 3.39, which is a shape or rheological index. This index is an indicator of the width of the relaxation spectrum. A higher value of  $R$  is an indication of a more gradual transition from the elastic behaviour to the viscous behaviour. This gradual

transition suggests less sensitivity to frequency changes, lower  $|G^*|$  values and higher phase angles in the intermediate range of frequency.

Meanwhile, the phase angle,  $\delta$  (in degrees) is shown as:

$$\delta = 90I - (90I - \delta_m) \left\{ 1 + \left[ \frac{\log(f_d/f')}{R_d} \right]^2 \right\}^{m_d/2} \quad (3.41)$$

where  $\delta_m$  is the phase angle constant at  $f_d$ , the value at the inflexion (or inflection point) for bitumens,  $f'$  is the reduced frequency,  $f_d$  is a location parameter with dimensions of frequency at which  $\delta_m$  occurs and  $R_d$  and  $m_d$  are the shape parameters. Zeng *et al.* [2001] did not explicitly provide the definition of  $I$  but showed  $I = 0$  if  $f > f_d$  and  $I = 1$  if  $f \leq f_d$  for bitumen. For asphalt mixture,  $I$  is always equal to zero.

Equation 3.41 satisfies the requirement that  $\delta$  varies from  $90^\circ$  to  $0^\circ$  when the frequency is elevated from zero to infinity for bitumen [Zeng *et al.*, 2001]. Like others, Zeng *et al.* [2001] used the WLF equation to describe the shift factor of bitumens. In addition, they have suggested the Arrhenius function should be used if low temperatures are involved. Zeng *et al.* [2001] conducted the dynamic test by means of the DSR and Simple Shear Test (SST) for bitumen and asphalt mixture respectively. Analysis of data involving 9 modified bitumens, 36 asphalt mixtures and 4 types of aggregates over various ranges of frequency, temperature and strain indicated that the model fits the measurements very well. They found a good agreement between measured and modelled  $|G^*|$  master curves.

### 3.3.8 Al-Qadi and co-workers' Model

Al-Qadi and co-workers proposed a new model of  $|G^*|$  and  $\delta$  for describing the rheological behaviour of unmodified and modified bitumens in the LVE region [Elseifi *et al.*, 2002]. They performed DMA using a DSR with parallel plate geometry at frequencies between 0.01 and 30 Hz and temperatures ranging from 5–

75°C. The proposed  $|G^*|$  based on the Havriliak and Negami function as follows [Elseifi *et al.*, 2002]:

$$|G^*| = G_g \left[ 1 - \frac{1}{\left[ 1 + \left( \frac{\omega}{\omega_0} \right)^v \right]^w} \right] \quad (3.42)$$

where  $\omega_0$  is the scale parameter that defines the location of the transition along the frequency axis,  $v$  and  $w$  are the dimensionless model parameters. In addition, the proposed  $\delta$  model (in degrees) can be shown as:

$$\delta = \frac{90}{\left[ 1 + \left( \frac{\omega}{\omega_0} \right)^v \right]^w} \quad (3.43)$$

where the symbols are as previously defined. Fig. 3.12 shows the comparison between measured and modelled  $|G^*|$  and  $\delta$  master curves.

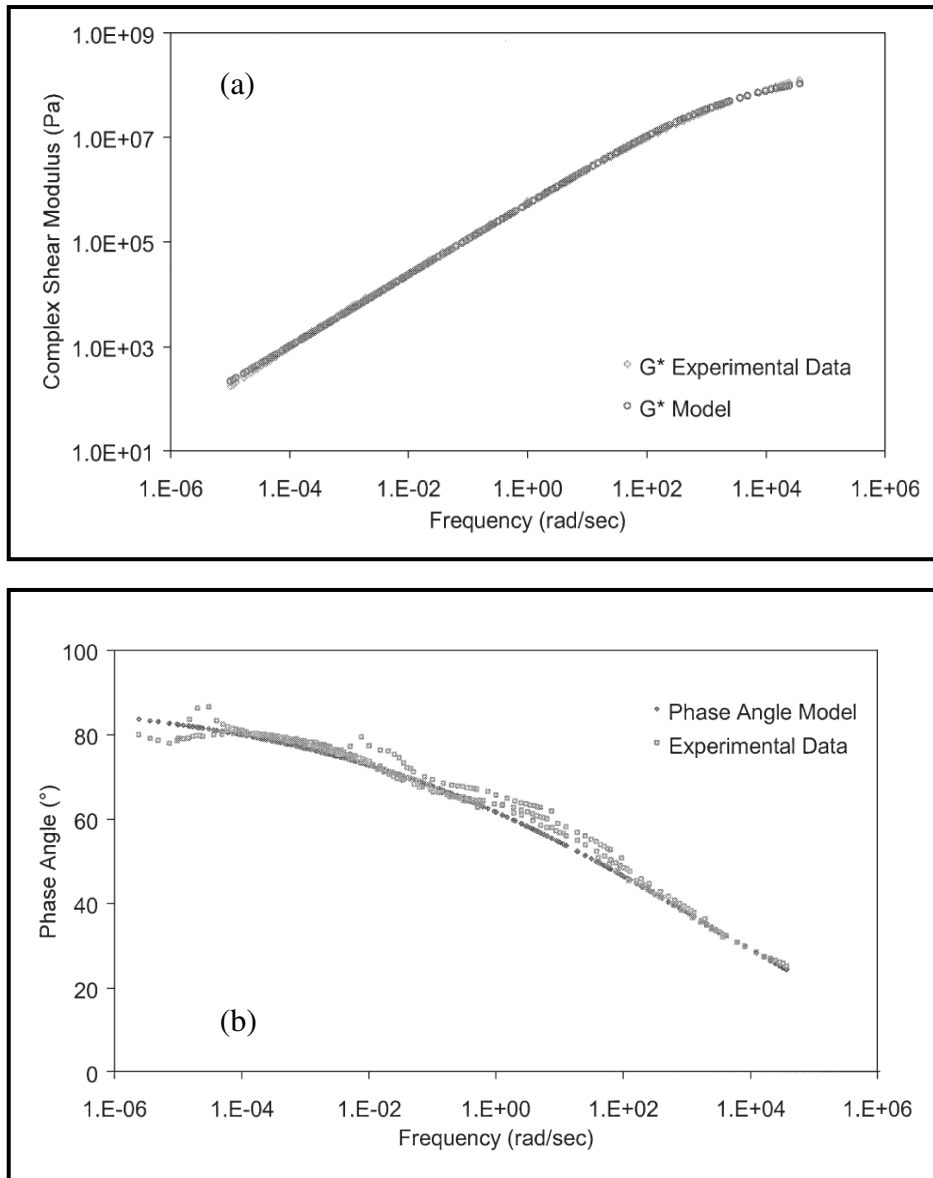


Fig. 3.12: A comparison between measured and descriptive  $|G^*|$  and  $\delta$  master curves using Al-Qadi and Co-workers Model [Elseifi *et al.*, 2002]

The WLF equation has been used by Al-Qadi and co-workers to show the temperature dependency of bitumens. From the study, they found a good agreement between the measured and modelled values for  $|G^*|$ . Meanwhile the  $\delta$  model was found to be adequately described for unmodified bitumen with small percentage errors ( $< 5\%$ ). Nevertheless, anomalies can still be seen where the proposed model could not simulate the small plateau region observed in the  $\delta$  master curve of modified bitumen in an accurate way. The difference, however, between the modelled and measured values was less than 10% which was within the acceptable range in such a test.

### 3.3.9 Polynomial Model

The Polynomial Model was originally developed to describe the complex modulus master curves of asphalt mixture. For practical purposes, a simpler polynomial function may be used to express the  $|G^*|$  master curve constructed from a dynamic modulus test [Mohammad *et al.*, 2005]. This model, however, also can be used for describing the complex modulus for bituminous binders. In general, the form of the Polynomial Model can be shown as the following:

$$\log |G^*| = A(\log f)^3 + B(\log f)^2 + C(\log f) \quad (3.44)$$

where  $f$  is reduced frequency and  $A$ ,  $B$  and  $C$  are the shape parameters. This model generally can fit the test data from low to moderate temperatures satisfactorily. As the temperature increases or decreases, the curves tend to skew, depending on the degree of freedom in the equation used [Bonaquist and Christensen, 2005]. A single Polynomial Model cannot be used for fitting the whole master curve. The rheological properties of bitumen seem incomplete since the model does not take the behaviour of  $\delta$  into account.

### 3.3.10 Sigmoidal Model

A new dynamic modulus function, the Sigmoidal Model, has been introduced in the Mechanistic-Empirical Pavement Design Guide (ME PDG) developed in the National Cooperative Highway Research Program (NCHRP) Project A-37A. In the ME PDG, the Sigmoidal Model is used to describe the rate dependency of the modulus master curve [Pellinen *et al.*, 2002, Pellinen and Witczak, 2002; Bonaquist and Christensen, 2005; Medani and Huurman, 2003; Medani *et al.*, 2004; Biswas and Pellinen, 2007]. Mathematically, the Sigmoidal Model can be shown as the following:

$$\log |G^*| = v + \frac{\alpha}{1 + e^{\beta + \gamma \{\log(\omega)\}}} \quad (3.45)$$

where  $\log \omega$  is log reduced frequency,  $v$  is the lower asymptote,  $\alpha$  is the difference between the values of the upper and lower asymptote,  $\beta$  and  $\gamma$  define the

shape between the asymptotes and the location of the inflection point (inflection point obtained from  $10^{(\beta/\gamma)}$ ) [Rowe *et al.*, 2009]. In the ME PDG,  $a_T$  is expressed as a function of the bitumen viscosity to allow ageing over the life of pavement. The definition of each parameter is shown in Fig. 3.13.

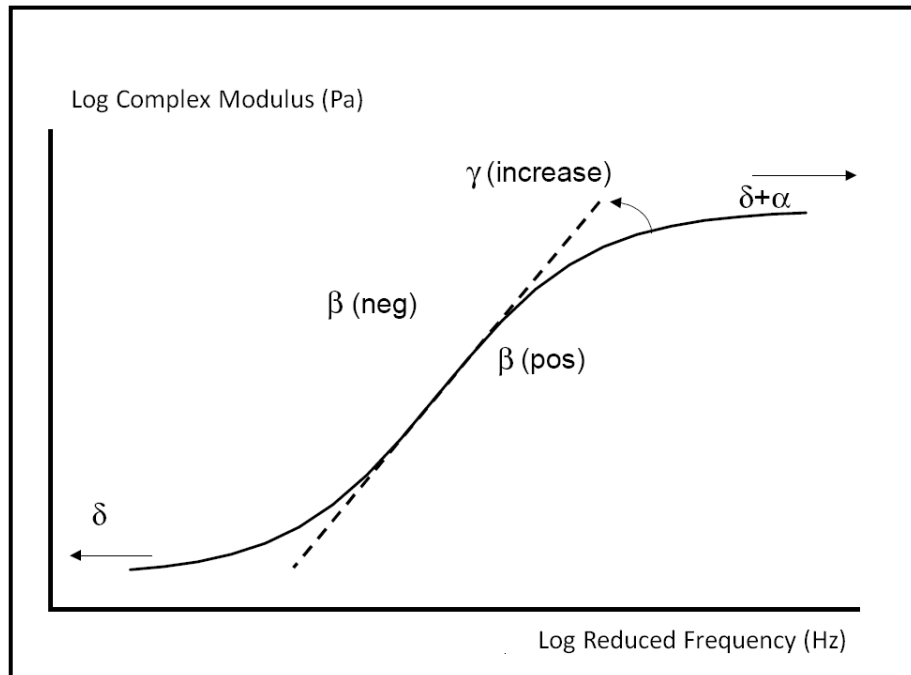


Fig. 3.13: Definition of the Sigmoidal Model [Pellinen *et al.*, 2002]

The Sigmoidal Model has been widely used by many researchers to describe the complex modulus master curve of asphalt mixture [Pellinen *et al.*, 2002; Pellinen and Witczak, 2002; Bonaquist and Christensen, 2005; Medani and Hurman, 2003; Medani *et al.*, 2004; Biswas and Pellinen, 2007]. However, in this study, the Sigmoidal Model is used for describing complex modulus master curve of bituminous binders.

### 3.3.11 The LCPC Master Curve Construction Method

Chailleux *et al.* from the *Laboratoire Central des Ponts et Chaussées* (LCPC), France adapted a mathematical equation in order to construct master curves from complex modulus measurements [Chailleux *et al.*, 2006]. The researchers applied the Kramers-Kronig relations, based on previous work done by Booij and Thoone [1982], linking  $|G^*|$  and  $\delta$  of a complex function. The integral

transform relationships between the real and imaginary parts of this function are generally known as the Kramers-Kronig relations.

Booij and Thoone [1982] carried out experiments on a polyvinyl-acetate sample involving oscillation measurements in a Mechanical Spectrometer at 5 different frequencies and temperatures between 22.85 to 119.85°C. Superimposed curves of both  $G'$  and  $G''$  versus frequency were produced. This was done by means of time-temperature shift factors on both master curves at a reference temperature of 34.85 °C. Booij and Thoone also tested this relation for other materials as well, including a number of dielectric data. It appears that the relation invariably holds with standard deviation (SD) never exceeding 5% [Booij and Thoone, 1982]. The Kramers-Kronig approximations give the following equations for  $|G^*|$  and  $\delta$  [Chailleux *et al.*, 2006]:

$$\log |G^*(\omega)| - \log |G^*(\infty)| = -\frac{2}{\pi} \int_0^{\infty} \frac{u \cdot \delta(u) - \omega \cdot \delta(\omega)}{u^2 - \omega^2} du \quad (3.46)$$

and

$$\delta = \frac{2\omega}{\pi} \int_0^{\infty} \frac{\log |G^*(u)| - \log |G^*(\omega)|}{u^2 - \omega^2} du \quad (3.47)$$

where  $u$  is defined as a dummy variable. Equation 3.47 becomes exactly:

$$\delta = \frac{\pi}{2} \times \frac{d \log |G^*|}{d \log \omega} \quad (3.48)$$

Chailleux *et al.* used the following shift factor relationship to characterise temperature dependence of bitumen:

$$\log a_{(T_i, T_o)} = \sum_{j=i}^{j=\text{ref}} \frac{\log |G^*(r_j)| - \log |G^*(r_{j+1})|}{\delta_{\text{avr}}^{(T_j, T_{j+1})}} \times \frac{\pi}{2} \quad (3.49)$$

where  $\delta_{\text{avr}}$  is the average of two angles measured at  $\omega_j$  and  $\omega_{j+1}$ . In order to validate the possible use of this methodology, they applied the model to 3 unmodified

bitumens, 1 SBS PMB and 2 asphalt mixtures using DMA. They proposed to plot  $d \log |G^*|/d \log \omega$  versus  $\delta/90$  to verify both the Booij and Thoonen equation and the Kramers-Kronig relations (Fig. 3.14).

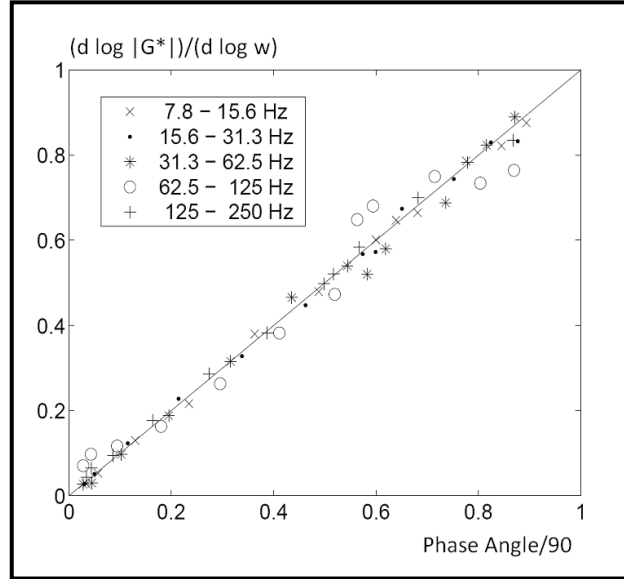


Fig. 3.14: Example of plot  $d \log |G^*|/d \log \omega$  versus  $\delta/90$  [Chailleux *et al.*, 2006]

Earlier, Marasteanu and Anderson applied the same Booij and Thoonen approximation to analyse the dynamic shear data for a set of 71 unmodified and modified bitumens [Marasteanu and Anderson, 1999b]. The validity of the Booij and Thoonen relation was examined by calculating the slopes of the logarithmic plots of  $|G^*|$  versus  $\omega$ , as the ratio of the difference of the logarithm of two consecutive  $|G^*|$  values divided by the difference of the logarithm of their corresponding frequencies. The  $\delta$  was, subsequently, calculated as the average of the two corresponding phase angles. No rheological model was assumed and the slope was obtained by means of simple calculations. This method is also known as approximate differential method. Furthermore, the Booij and Palmen approximation was also used to calculate the relaxation spectra. This approximation can be shown as below:

$$H(\tau) \cong \frac{1}{\pi} \left[ |G^*| \sin 2\delta \right]_{\omega=1/\tau} \quad (3.50)$$

where  $\tau$  is the relaxation time and  $H(\tau)$  is the strength of relaxation at  $\tau$  for discrete spectra. From this study, a smooth master curve was produced when applying this

equation to the data at different temperatures from frequency sweep tests. This approximation plays a significant role in modelling DSR data and in generating rheological master curves for bitumens. This model fits data ranging from intermediate to high temperatures satisfactorily [Marasteanu and Anderson, 1999b].

### 3.3.12 New Complex Modulus and Phase Angle Predictive Model

To surmount the limitations of the current models used in the ME PDG, Bari and Witczak developed a new predictive model for  $|G^*|$  and  $\delta$  [Bari and Witczak, 2007]. A database containing 8,940 data points from 41 different unmodified and modified bitumens was used in this study. The equation for  $|G^*|$  is shown as follows:

$$|G^*| = 0.0051 f_s \eta_{f_s, T} (\sin \delta) 7.1542 - 0.4929 f_s + 0.0211 f_s^2 \quad (3.51)$$

where  $f_s$  is the dynamic shear loading frequency to be used with  $|G^*|$  and  $\delta$ ,  $\eta_{f_s, T}$  is viscosity of bitumen (cP) as a function of both loading frequency ( $f_s$ ) and temperature ( $T$ ), and  $\delta$  is the phase angle (degrees). The value of  $|G^*|$  is limited to a maximum value of  $1 \times 10^9$  Pa.  $\delta$  is obtained from a non-linear optimisation technique in the form of the following equation:

$$\delta = 90 + (b_1 + b_2 \text{VTS}') \times \log(f_s \times \eta_{f_s, T}) + (b_3 + b_4 \text{VTS}') \times \left\{ \log(f_s, \eta_{f_s, T}) \right\}^2 \quad (3.52)$$

where  $\text{VTS}' = 0.9699 f_s^{-0.0575} \times \text{VTS}$ ,  $f_s$  is loading frequency in dynamic shear (Hz),  $b_1$ ,  $b_2$ ,  $b_3$ , and  $b_4$  are the fitting parameters ( $-7.3146$ ,  $-2.6162$ ,  $0.1124$  and  $0.2029$ ). The fitting parameters will change slightly as a function of the type of bitumen (crude source and grade).

To evaluate the model's performances, Bari and Witczak used the ratio of standard error of estimates over standard deviation ( $S_e/S_y$ ) and coefficient of determination ( $R^2$ ) to measure the goodness-of-fit statistics between measured and predicted data. The criteria of the goodness-of-fit statistics used will be discussed in Chapter 4. In general, Bari and Witczak found a good correlation between measured and model data. This new  $\delta$  model has a very good correlation for unmodified

bitumens compared with that of the modified bitumens. They concluded that modified bitumens used in this study had higher variability in stiffness characteristics as a result of their type and amount of modification. However, the overall variation from all 41 bitumens is practically negligible and the predicted plots are very close to the equality line. More bitumen modifications are needed for future development as the current model only includes a small sample of modified bitumens [Bari and Witczak, 2007].

### 3.3.13 Generalised Logistic Sigmoidal Model

Rowe *et al.* introduced a generalisation of the Sigmoidal Model, called the Generalised Logistic Sigmoidal Model (or Richards Model) to describe the stiffness of asphalt mixture. This equation is also applicable to bituminous binders and other materials the Generalised Logistic Sigmoidal Model can be shown as the following [Rowe, 2008; Rowe *et al.*, 2009]:

$$\log|G^*| = v + \frac{\alpha}{[1 + \lambda e^{(\beta + \gamma \{\log(\omega)\})}]^{1/\lambda}} \quad (3.53)$$

where the symbols are as previously defined. The  $\lambda$  parameter allows the curve to take a non-symmetrical shape for the master curve. When  $\lambda$  reduces to one, Equation 3.53 reduces to the standard sigmoidal function as represented in Equation 3.45.

## 3.4 Mechanical Models

It is useful to consider the simple behaviour of analogue models constructed from linear springs and dashpots to get some feeling for LVE behaviour of bitumen. The spring (Hooke's Model) is an ideal elastic element obeying the linear force extension relation while the dashpot (Newton's Model) is an ideal viscous element that extends at a rate proportional to the applied stress. A number of different models with various arrays of spring and dashpot arrangements, such as the Jeffery, Zener and Burgers' Models, are available to facilitate the mathematical expression of the viscoelastic behaviour of engineering materials. However, none of these

models is itself sufficient to represent the behaviour of bitumens [Monismith *et al.*, 1969].

### 3.4.1 Huet Model

The Huet Model was initially conceived by Christian Huet in order to describe the behaviour of both bitumens and asphalt mixtures [Huet, 1963]. This model consists of a combination of a spring and two parabolic elements ( $k$  and  $h$ ) in series as illustrated in Fig. 3.15.

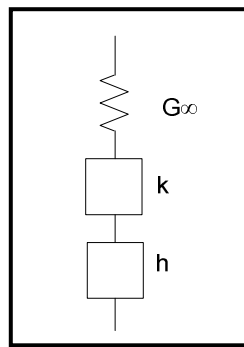


Fig. 3.15: The Huet Model [Huet, 1963]

According to Olard and Di Benedetto [2003], the parabolic element is an analogical model with a parabolic creep function with equations for creep compliance and complex modulus as follows:

$$J(t) = a \left( \frac{t}{\tau} \right)^h \quad (3.54)$$

and

$$G^* = \frac{(i\omega\tau)^h}{a\Gamma(h+1)} \quad (3.55)$$

where  $J(t)$  is the creep function,  $h$  is the exponent such as  $0 < h < 1$ ,  $a$  is a dimensionless constant,  $\Gamma$  is gamma function,  $t$  is the loading time,  $\tau$  is the characteristic time (which value varies only with temperature),  $i$  is the complex number ( $i^2 = \sqrt{-1}$ ) and  $\omega$  is the angular frequency.

This model, in addition, has a continuous spectrum and can be presented by an infinite number of Kelvin-Voigt elements in series or Maxwell elements in parallel [Olard and Di Benedetto, 2003]. The analytical expression of  $G^*$  can be shown as follows [Huet, 1963; Sayegh, 1967; Olard and Di Benedetto, 2003; Blab *et al.*, 2006]:

$$G^* = \frac{G_\infty}{1 + \alpha(i\omega\tau)^{-k} + (i\omega\tau)^{-h}} \quad (3.56)$$

where  $G^*$  is the complex modulus,  $G_\infty$  is the limit of the complex modulus,  $h$  and  $k$  are exponents such as  $0 < h < k < 1$ ,  $\alpha$  is a dimensionless constant. The other symbols are as previously defined. The Huet equation accounts for the non-symmetric shape of the frequency response.

The WLF equation has been used by Huet to describe the temperature dependency of bitumen. He presented the results obtained under monotonic loading by means of the Cole-Cole diagram. It was seen that the Huet Model is well suited for the description of this kind of loading. However, it is believed that this model is unable to model modified bitumen correctly. Another drawback is that the original model does not contain a viscous element for simulating permanent deformation, in contrast with the Burger's Model, a combination of the Maxwell and a Kelvin-Voigt unit in serial connection (4 parameters model) [Pronk, 2003a, 2005].

### 3.4.2 The Huet-Sayegh Model

Sayegh developed a model based on the generalisation of the Huet Model but modified by adding a spring of small rigidity compared with  $G_\infty$  in parallel [Sayegh, 1967]. This model consists of the combination of two springs ( $G_0$  and  $G_\infty - G_0$ ) and two parabolic creep elements ( $k$  and  $h$ ) are presented in Fig. 3.16.

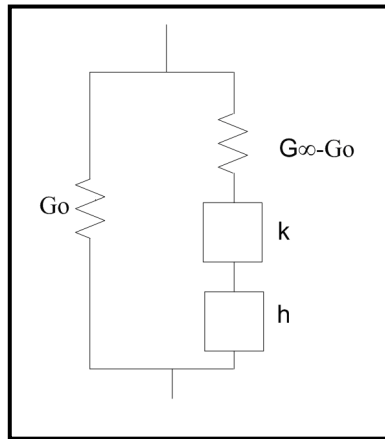


Fig. 3.16: The Huet-Sayegh Model [Sayegh, 1967]

If the  $G_0$  is equal to zero, then the Huet-Sayegh Model is identical to the Huet Model. As a matter of fact, the Huet-Sayegh Model looks like a Zener Model but instead of one linear dashpot, it has two parabolic dashpots [Pronk, 2003a, 2003b, 2005]. The model can be described mathematically using the following formula:

$$G^* = G_0 + \frac{G_\infty - G_0}{1 + \alpha(i\omega\tau)^{-k} + (i\omega\tau)^{-h}} \quad (3.57)$$

with  $G_0$  is the elastic modulus and  $\alpha$  is a dimensionless constant. The other symbols are as previously defined.  $a$ ,  $b$ , and  $c$  can be determined implicitly using  $\tau$  which is referred to as the characteristic time and it is calculated using the following equation [Pronk, 2003a, 2003b; Adams *et al.*, 2006]:

$$\ln \tau = a + bT + cT^2 \quad (3.58)$$

where  $a$ ,  $b$  and  $c$  are regression parameters representing the material characteristics. This model was originally developed for asphalt mixture, but it can also be used for unmodified bitumens.

Unlike the Huet Model, no analytical expression of the creep function of the Huet-Sayegh Model is available in the time domain. Olard and Di Benedetto attempted to fit the data both on bitumen and asphalt mixture using the Huet-Sayegh Model and they found the model is unsuitable for bitumens at the very low

frequencies where it is equivalent to a parabolic element instead of a linear dashpot [Olard and Di Benedetto, 2003].

### 3.4.3 Di Benedetto and Neifar (DBN) Model

The DBN Model is a rheological model specially developed by Di Benedetto and Neifar for asphalt mixture [Olard and Di Benedetto, 2005a, 2005b; Blab *et al.*, 2006; Di Benedetto *et al.*, 2007]. However, this equation also can be used to describe the rheological properties of bituminous binders. The DBN Model, abbreviated from Di Benedetto and Neifar, takes into account the linear viscoelastic behaviour in the small-strain domain, as well as plastic flow for large strain values. To find a compromise between the complexity of the development and a close description of the material behaviour, the number of considered bodies must be reasonable.

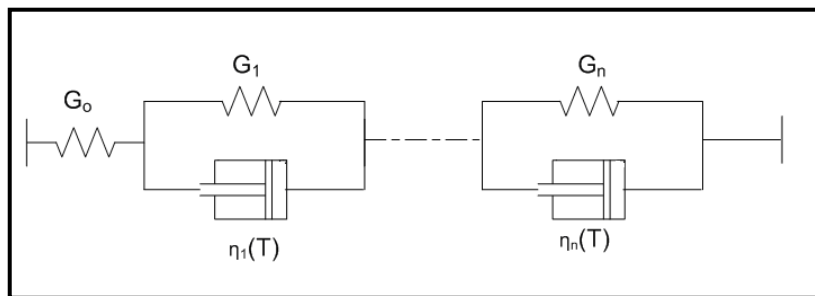


Fig. 3.17: The Di Benedetto and Neifar (DBN) Model [Di Benedetto *et al.*, 2007]

The DBN Model, which is depicted in Fig. 3.17, can also be used for describing the rheological properties of bitumens in the linear viscoelastic region. The  $G^*$  function of the DBN Model can be written as:

$$G^* = \left( \frac{1}{G_0} + \sum_{i=1}^n \frac{1}{G_i + i\omega\eta_i(T)} \right)^{-1} \quad (3.59)$$

where  $G_0$  is the elastic modulus of the single spring,  $\eta_i$  is a viscosity function of the temperature ( $T$ ) and  $\omega = 2\pi f$ . The number  $n$  of the elementary body can be arbitrarily chosen.

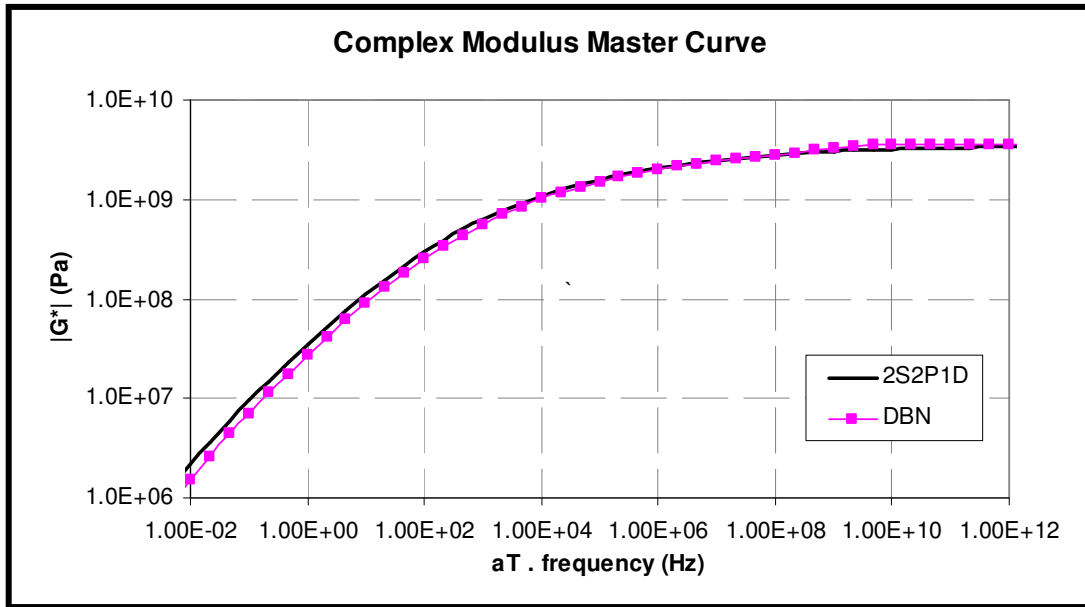


Fig. 3.18: Calibration of the DBN Model using the 2S2P1D Model

Di Benedetto and Neifar used the 2S2P1D Model (section 2.9.4) to calibrate the DBN Model and found good agreement between the two models and experimental data using an optimisation process. An example of the DBN and 2S2P1D complex modulus master curves is shown in Fig. 3.18. However, as reported by Blab *et al.* the calibration of the DBN Model based on the 2S2P1D Model means that uncertainties associated with the 2S2P1D Model will also lead to uncertainties in the DBN Model [Blab *et al.*, 2006].

#### 3.4.4 The 2S2P1D Model

Normally, the rheological models used to describe the rheological properties of bituminous binders consists of three basic elements namely; a spring, dashpot (or damper) and parabolic (nonlinear dashpot) element. The spring is normally expressed as  $G^*(i\omega)$ . The parabolic element is an analogical model with a parabolic creep function [Olard and Di Benedetto, 2003]:

$$J(t) = a \left( \frac{t}{\tau} \right)^h \quad (3.61)$$

and the  $|G^*|$  equation is shown as the following

$$G^* = \frac{(i\omega\tau)^h}{a\Gamma(h+1)} \quad (3.62)$$

where  $J(t)$  is the creep function,  $h$  is the exponent such as  $0 < h < 1$  ( $h = 0$  (elastic) and  $h = 1$  (viscous)),  $a$  is the dimensionless constant ( $1/\lambda$ ),  $\lambda$  is a relaxation time,  $\Gamma$  is gamma function<sup>2</sup>,  $t$  is the loading time,  $\tau$  is the characteristic time (which value varies only with temperature),  $i$  is the complex number ( $i^2 = \sqrt{-1}$ ) and  $\omega$  is frequency. The linear dashpot can be written as:

$$G^* = \frac{i\omega\tau}{a} \quad (3.63)$$

where the parameters are as previously defined. A large number of the constitutive models to describe the viscoelastic behaviour of bituminous binders and asphalt mixtures were developed over the last six decades including the 2S2P1D Model (Fig. 3.19).

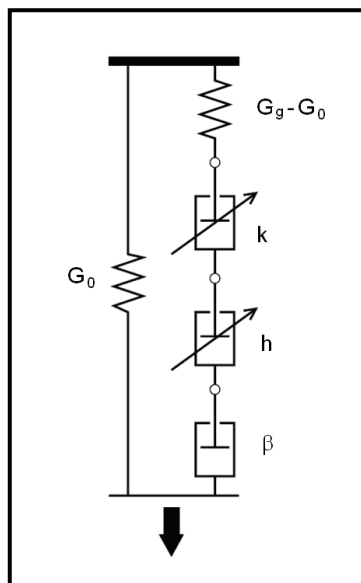


Fig. 3.19: The 2S2P1D Model [Olard and Di Benedetto, 2003]

The 2S2P1D Model, an abbreviation of combinations of two springs, two parabolic creep elements and one dashpot, is a unique rheological model to describe

<sup>2</sup> Gamma function is defined as  $\Gamma(n) = \int_0^{\infty} t^{n-1} e^{-t} dt$  [Olard and Di Benedetto, 2003]

the rheological properties for binders and asphalt mixtures [Olard and Di Benedetto, 2003; Olard *et al.*, 2003; Delaporte *et al.*, 2007; Pellinen *et al.*, 2007]. This model, based on the generalisation of the Huet-Sayegh Model, consists of seven parameters and the  $|G^*|$  equation is shown as:

$$G^*(\omega) = G_0 + \frac{G_g - G_0}{1 + \alpha(i\omega\tau)^k + (i\omega\tau)^{-h} + (i\omega\beta\tau)^{-1}} \quad (3.64)$$

where  $k$  and  $h$  are exponents with  $0 < k < h < 1$ ,  $\alpha$  is a constant,  $G_0$  is the static modulus when  $\omega \rightarrow 0$ ,  $G_g$  is the glassy modulus when  $\omega \rightarrow \infty$ . Meanwhile,  $\beta$  is a constant and is defined by:

$$\eta = (G_g - G_0)\beta\tau \quad (3.65)$$

where  $\eta$  is Newtonian viscosity and  $\tau$  is characteristic time and a function of temperature.  $\tau$  evolution can be approximated by a shift factor function such as the William, Landel and Ferry (WLF) and Arrhenius equations in the range of temperatures observed in the laboratory [Delaporte *et al.*, 2007]:

$$\tau = a_T(T) \times \tau_0 \quad (3.66)$$

or using the WLF equation;

$$\tau = \tau_0 \times 10^{\frac{-C_1(T-T_{ref})}{C_2+(T-T_{ref})}} \quad (3.68)$$

where  $a_T(T)$  is the shift factor at temperature,  $T_i$ , and  $\tau_0$  is  $\tau(T_{ref})$  determined at  $T_{ref}$ , and  $C_1$  and  $C_2$  are two constants to be determined (WLF equation). It is often sufficient to use a second order polynomial fitting function, shown as:

$$\ln \tau = a + bT + cT^2 \quad (3.69)$$

where  $a$ ,  $b$ , and  $c$  are parameters which need to be determined. The  $|G^*|$  equation can be separated into parts [Van Rompu, 2006]:

$$G^*(\omega) = \frac{G_g - G_0}{1 + A + iB} \quad (3.70)$$

where

$$A(\omega) = \alpha(\omega\tau)^{-k} \times \cos\left(\frac{k\pi}{2}\right) + (\omega\tau)^{-h} \times \cos\left(\frac{h\pi}{2}\right)$$

and

$$B(\omega) = -(\omega\beta\tau)^{-1} - \alpha(\omega\tau)^{-k} \times \sin\left(\frac{k\pi}{2}\right) - (\omega\tau)^{-h} \times \sin\left(\frac{h\pi}{2}\right)$$

The imaginary and real parts of  $|G^*|$  can be separated as the following:

$$\begin{aligned} G^*(\omega) &= \frac{G_g - G_0}{1 + A + iB} \\ &= G_0 + \frac{(G_g - G_0) \times (1 + A(\omega) - iB(\omega))}{(1 + A(\omega))^2 + B^2(\omega)} \end{aligned} \quad (3.71)$$

$$= \left[ G_0 + \frac{(G_g - G_0) \times (1 + A(\omega))}{(1 + A(\omega))^2 + B^2(\omega)} \right] + i \left[ \frac{(G_g - G_0) \times (-B(\omega))}{(1 + A(\omega))^2 + B^2(\omega)} \right] \quad (3.72)$$

$$= \left[ G_0 + \frac{G' \times (1 + A(\omega))}{DEN} \right] + i \left[ \frac{G' \times (-B(\omega))}{DEN} \right] \quad (3.73)$$

where  $G' = G_g - G_0$  and  $DEN = (1 + A(\omega))^2 + B^2(\omega)$ .

It has to be emphasised that this model only needs seven parameters to entirely determine the LVE rheological properties of the binders. However,  $G_0$  of bitumens is normally very close to zero and therefore, the parameters are reduced to six.  $G_0$ ,  $G_g$ ,  $k$ ,  $h$ ,  $\alpha$  and  $\beta$  are graphically illustrated in the Cole-Cole and Black diagrams, as depicted in Figs 3.20 and 3.21. Table 3.1 explains the functions of  $k$ ,  $h$ ,  $\alpha$  and  $\beta$  in greater detail.

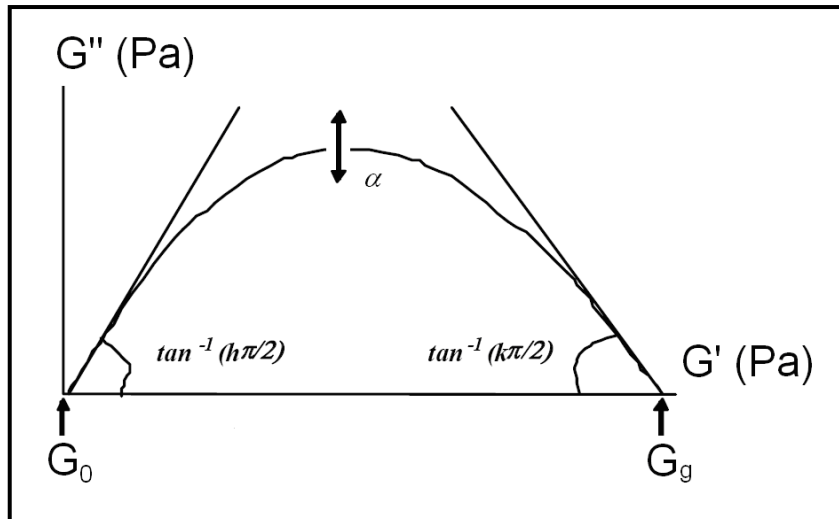


Fig. 3.20: Graphical representation of the model's parameters in terms of the Cole-Cole diagram

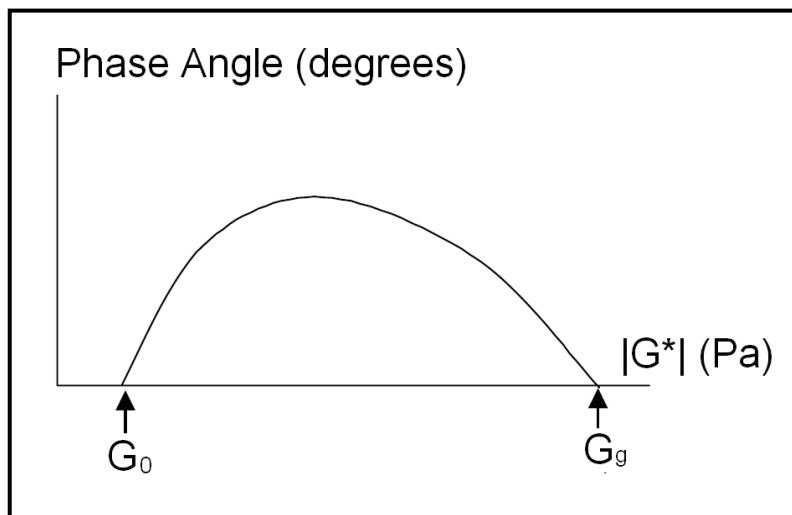


Fig. 3.21: Graphical representation of the model's parameters in terms of the Black diagram

Table 3.1: The 2S2P1D parameters functions

Parameter	Function(s)
$h$	controlled the slope at low values of $G''$ in the Cole-Cole diagram
$k$	controlled the slope at high values of $G''$ in the Cole-Cole diagram
$\delta$	controlled the slope at the low temperatures/high frequencies in the $ G^* $ master curve and the height of the pinnacle point of the Cole-Cole diagram
$\beta$	controlled the slope at the high temperatures/low frequencies of the $ G^* $ master curve where the higher the value of $\beta$ , the higher the values of $\eta$ and $ G^* $

Meanwhile the phase angle,  $\delta$ , is shown as:

$$\delta = \tan^{-1}\left(\frac{G''}{G'}\right) \quad (3.74)$$

where  $G'$  and  $G''$  are storage modulus and loss modulus respectively. Di Benedetto *et al.* carried out dynamic tests on nine binders and four asphalt mixtures (with one mixture design). They found that the 2S2P1D Model fitted the experimental data reasonably well even though anomalies had been seen particularly for the  $\delta$  values at 50 to 70° [Olard and Di Benedetto, 2003; Olard *et al.*, 2003].

This model was also used to fit the rheological properties of bitumen-filler mastics. It was observed that the parameters such as  $k$ ,  $h$ , and  $\alpha$  yielded similar values for all studied samples [Delaporte *et al.*, 2007]. Earlier, Pellinen *et al.* [2007] used the 2S2P1D Model and they found that the model showed a good agreement between measured and modelled data of asphalt mixtures.

### 3.5 Summary

Based on the literature review, several key observations can be drawn from this literature review study:

- The rheological properties of bitumen are generally and conveniently represented in terms of complex modulus magnitude and phase angle master curves. The use of models to describe these curves can be classified into three groups; nomographs, mathematical and mechanical models.
- In a mathematical model, the equation's parameters are adjusted to fit the experimental master curve. In the mechanical model, use is made of the fact that the linear viscoelastic properties of materials can be represented by a combination of simple spring and dashpot mechanical models, resulting in particular mathematical forms. The advantage of these approaches is that the elements might be relatable to structural features.
- Some models like the Sigmoidal Model, Generalised Logistic Sigmoidal Model, DBN Model and 2S2P1D Model are very unique because they can

be used for describing the rheological properties of both viscoelastic fluids (binders) and viscoelastic solids (asphalt mixtures).

- All the models are generally able to describe the rheological behaviour of bitumens satisfactorily if there are no major structural rearrangements with temperature and time, such as phase changes and, secondly, the tests are conducted within the linear viscoelastic region.
- The behaviour of bitumen becomes more complex with the presence of waxy elements, high asphaltene contents and crystalline structures, as well as polymer modification, all of which can render a breakdown of the time-temperature equivalency principle.

## Experimental Programs

---

### 4.1 Background

This chapter is divided into several sections. The first part describes various types of materials from the conducted experiments and also the Nottingham Transportation Engineering Centre (NTEC) DSR database that were used in this study. The second part discusses the use of a dynamic shear rheometer (DSR) in measuring the rheological properties of bituminous binders from low to high temperatures. The third part discusses the use of the Solver function and the final part covers the statistical analysis methods used to correlate between measured and modelled data.

### 4.2 Materials

Various types of materials from the conducted experiments and the NTEC DSR database were used in this study. These include unaged and aged unmodified bitumens, polymer-modified bitumens (PMBs) and bitumen-filler mastics. They are described as follows.

#### 4.2.1 Unaged unmodified bitumens

In general, a total of 12 penetration grade bitumens were used in this study and can be divided into three main groups. The first group consists of 10/20, 35/50, 40/60 100/150 and 160/220 penetration grade bitumens, covering from hard to soft bitumens. The second group of unmodified bitumens were taken from the previous

work done by Airey [1997]. Three bitumens from different crude sources namely a 80/100 penetration grade bitumen from a Middle East crude, a 80 penetration grade bitumen from a Russian crude and a 70/100 penetration grade bitumen from Venezuelan crude were selected as the base bitumens. Finally, the third group consists of three 15 penetration grade bitumens and a 50 penetration grade bitumen, taken from the work of Choi [2005]. The rheological and chemical properties of the unaged unmodified bitumens can be found in previous publications [Airey, 1997; Choi, 2005]. The complex modulus and phase angle data from the DSR tests of the unaged unmodified bitumens are shown in Appendix A.

#### **4.2.2 Aged unmodified bitumens**

A total of 14 aged unmodified bitumens were used and can be divided into two main groups. The first group consists of a 80/100 penetration grade bitumen from a Middle East crude, a 80 penetration grade bitumen from a Russian crude and a 70/100 penetration grade bitumen from Venezuelan crude that underwent ageing processes via the rolling thin film oven test (RTFOT) and the pressure ageing vessel (PAV). Details of the ageing procedures can be found in the previous work done by Airey [1997]. The rheological properties of the aged unmodified bitumens can be found in previous publication [Airey, 1997]. The complex modulus and phase angle data from the DSR tests of the aged unmodified bitumens are shown in Appendix B.

#### **4.2.3 Unaged polymer-modified bitumens**

The unaged polymer modified bitumens (PMBs) used in this study were taken from previous work done by Airey [1997]. All three unmodified bitumens (second group of unaged unmodified bitumens) were mixed with a plastomeric ethylene-vinyl acetate (EVA) polymer and an elastomeric styrene butadiene styrene (SBS) polymer to produce various PMBs. Three polymer contents (by mass) at 3, 5 and 7% were used to create 15 combinations of the EVA and SBS PMBs. However no Middle East–SBS PMBs were produced. The PMBs were all 100% miscible, homogeneous and storage stable, with no evidence of any phase separation. Details of the chemical and rheological properties of unaged PMBs can be found in

previous publication [Airey, 1997]. The complex modulus and phase angle data from the DSR tests of the unaged PMBs are shown in Appendix C.

#### **4.2.4 Aged polymer-modified bitumens**

All 15 unaged PMBs were subjected to laboratory short term and long term ageing using the RTFOT and PAV. Airey [1997] produced a total of 30 combinations of aged PMBs and subsequently a number of rheological and chemical tests were conducted to characterise their physical and chemical properties and investigate the effect of ageing on these properties. The fundamental and chemical properties of the binders can be found in a previous publication [Airey, 1997]. The complex modulus, and phase angle data from the DSR tests of the aged PMBs are shown in Appendix D.

#### **4.2.5 Unaged bitumen-filler mastics**

The unaged bitumen-filler mastics were taken from research conducted by Liao [2007] and Wu [2009]. The first group consists of three different fillers namely gritstone, limestone and cement, mixed with bitumen at 40% (by weight) [Wu, 2009]. The second group, originally from the work of Liao [2007], also consists of gritstone, limestone and cements mixed with bitumens. Two filler contents (by mass) at 35 and 65% were used to create six combinations of bitumen-filler mastics. Liao [2007] used a 50 penetration grade bitumen as the base bitumen. A total of 9 unaged bitumen-filler mastics were used in this study. The rheological properties of the binders can be found in previous publications [Liao, 2007; Wu, 2009]. The complex modulus and phase angle data from the DSR tests of the unaged bitumen-filler mastics are shown in Appendix E.

#### **4.2.6 Aged bitumen-filler mastics**

Wu [2009] used the thin film oven test (TFOT) to age the bitumen-filler mastics at 1, 3, 5, 10 and 20 hours of ageing times. Only gritstone and limestone were used to create 10 combinations of the aged bitumen-filler mastics. The fundamental and chemical properties of the aged bitumen-filler mastics can be

found in a previous publication by Wu [2009]. The complex modulus and phase angle from the DSR tests data of the aged bitumen-filler mastics are shown in Appendix F.

### 4.3 Dynamic Shear Rheometer

#### 4.3.1 Basic principle

The first attempt to do oscillatory experiments to measure the elasticity of a material was by Poynting in 1909 [Menard, 1999]. Later, the development of a commercial rheometer started with the invention of the Weissenberg Rheogoniometer (~1950) and the Rheovibron (~1958). According to Menard [1999], the technique remained fairly specialised until the late 1960s when commercial instruments became more user-friendly. At the beginning, instruments developed were difficult to use, slow and limited in processing the data. Later, a dynamic shear rheometer (DSR), with either strain or stress control was developed. The DSR is a tool to characterise the elastic, viscoelastic and viscous properties of materials including bitumens over a wide range of temperatures and frequencies (times of loading).

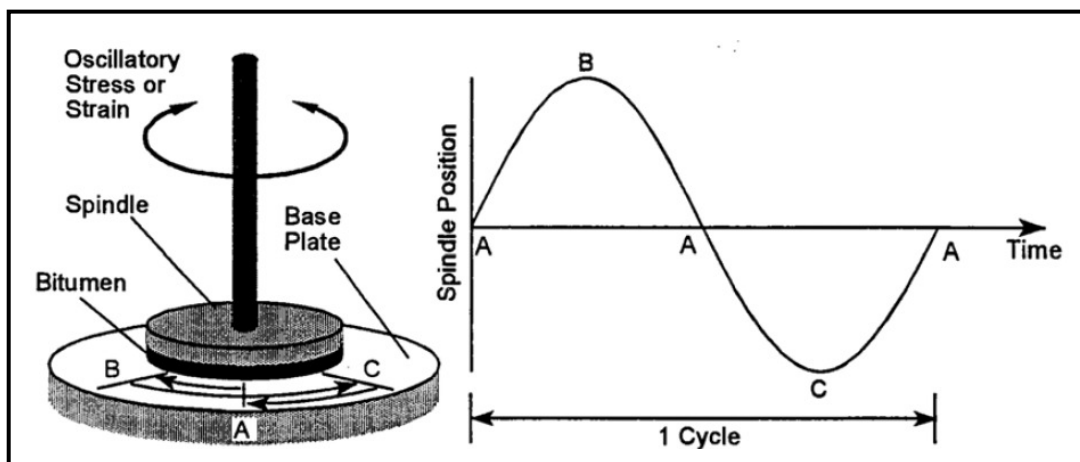


Fig. 4.1: Illustration of the DSR set-up [Airey, 1997]

The principles involved in DSR testing are illustrated in Fig. 4.1, where the bitumen is sandwiched between a spindle and a base plate. The base plate is fixed. A torque is applied to the top plate so that it oscillates back and forth. One cycle is

completed when the top plate goes from point A to point B, then reverses direction and moves past point A to Point C, followed by a further reversal and movement back to Point A. This oscillation comprises one smooth, continuous cycle which can be continuously repeated during the test. DSR tests can be carried out in either controlled stress or controlled strain testing modes. In the controlled stress mode, a specific magnitude of shear stress is applied to the bitumen by application of a torque to the spindle and the resultant spindle rotation is measured, from which the magnitude of shear strain is calculated. In the controlled strain mode, the magnitude of spindle rotation is specified and the required torque to achieve is measured, from which the magnitude of shear stress is calculated [Airey, 1997].

Various geometries, such as cone and plate, parallel plates, and cup and plate, can be used in dynamic mechanical testing. For many materials, cone and plate geometry is preferred, as shear stress and shear rate are constant over the entire area of the plate, thereby simplifying calculations and giving accurate fundamental rheological properties. However, for bitumen testing, parallel plate geometry is almost invariably used to avoid the very small gap present at the centre of the cone and plate geometry [Airey 2002a, 2002b].

In this study, two testing (plate) geometries are used with the DSR: an 8 mm diameter plate with a 2 mm testing gap and a 25 mm diameter plate with a 1 mm testing gap. The selection of the testing geometry is based on the operational conditions, with the 8 mm plate geometry generally being used at low temperatures (-5 to 20°C) and the 25 mm geometry at intermediate to high temperatures (20 to 80°C). It is also possible to use the same testing geometry over a wide temperature range, although the precision of the results may be limited as a result of compliance errors and reduction in the precision with which the torque can be measured at low stress levels [Airey 2002a, 2002b; Airey and Hunter, 2003].

#### **4.3.2 Strain limit**

To keep the rheological response of the bitumen within its linear viscoelastic (LVE) region, the DSR tests are conducted with a relatively small strain, which is commonly achieved by adopting strain or stress limit [Wu, 2009]. The LVE limit is

defined as the point where the complex modulus,  $|G^*|$  decreased to 95% of its initial value as prescribed during the SHRP study [Petersen *et al.*, 1994]. This point was determined by conducting a strain (or amplitude) sweep test, as shown in Fig. 4.2. In this procedure, the strain level to which a specimen was subjected was gradually increased until significant non-linearity appeared in the response. The strain limits vary, dependent on  $|G^*|$  of each material used. On the other hand, using the DSR conditions, the Strategic Highway Research Program (SHRP) research team found that the shear stress and strain LVE limits for penetration grade bitumens to be functions of  $|G^*|$  as defined by [Petersen *et al.*, 1994]:

$$\gamma = 12.0 / (|G^*|)^{0.29} \quad (4.1)$$

$$\tau = 0.12 / (|G^*|)^{0.71} \quad (4.2)$$

where  $\tau$  is the shear stress (calculated at the circumference of the spindle), Pa,  $\gamma$  is the shear strain (calculated at the circumference of the spindle) and  $|G^*|$  is the complex shear modulus, Pa. These functions were determined for a range of bituminous binders at different conditions by performing strain sweeps at selected temperatures at a frequency of 10 rad/s (1.59 Hz).

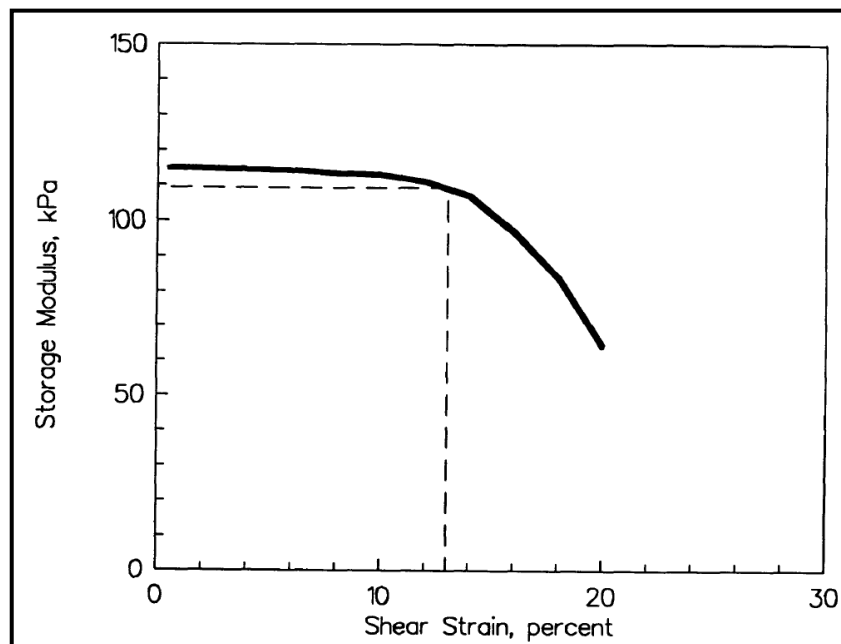


Fig. 4.2: Strain sweep used to determine the LVE region [Anderson *et al.*, 1994]

### 4.3.3 Testing procedure

The rheological properties of the unmodified bitumens, PMBs and bitumen-filler mastics blends, unaged and aged samples, were determined using dynamic mechanical methods consisting of temperature and frequency sweeps in an oscillatory-type testing mode performed within the linear viscoelastic region. The oscillatory tests were conducted on a Bohlin Gemini dynamic shear rheometer (DSR) using two parallel plate testing geometries consisting of 8 mm diameter plates with a 2 mm testing gap and 25 mm diameter plates with a 1 mm testing gap (Fig. 4.3). In this study, the samples were prepared using a hot pour method and a silicone mould method.

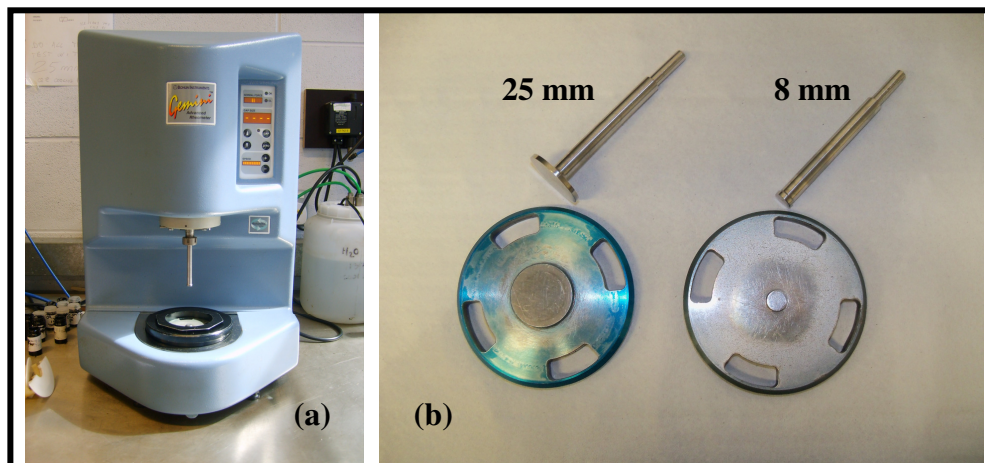


Fig. 4.3: (a) The DSR body and (b) 8 mm and 25 mm plates

In the hot pour method, the gap between the upper and lower plates was set to a desired height of 50  $\mu\text{m}$  plus the required testing gap, either at the proposed testing temperature or at the mid-point of an expected testing temperature range. Once the gap has been set, a sufficient quantity of hot bitumen (typically between 100–150°C) was poured onto the lower plate of the DSR to ensure a slight excess of material appropriate to the chosen testing geometry. The upper plate of the DSR was then gradually lowered to the required nominal testing gap plus 50  $\mu\text{m}$ . The bitumen that has been squeezed out between the plates was then trimmed flush to the edge of the plates using a hot spatula or blade. After trimming, the gap was closed by a further 50  $\mu\text{m}$  to achieve the required testing gap as well as a slight

bulge around the circumference of the testing geometry (periphery of the test specimen) [Airey and Hunter, 2003].

For the silicone mould method, the hot bitumen is poured into either an 8 mm or 25 mm diameter silicone mould of height approximately 1.5 times that of the recommended testing gap for the two geometries, namely 3 mm and 1.5 mm for the 8 mm and 25 mm geometries. The testing gap is set at a height of 50  $\mu\text{m}$  plus 1 mm or 2 mm. Once the bitumen has cooled, either by means of short-term refrigeration or by natural cooling, the bitumen disc (typically at ambient temperatures) is removed from the mould and centred on the lower plate of the DSR. The upper plate is then lowered to the required gap plus 50  $\mu\text{m}$ , the excess bitumen is trimmed with a hot spatula and the gap further closed to its final testing height [Airey and Hunter, 2003].

The DMA was performed using a Bohlin Gemini 200 DSR. First, amplitude sweep tests were conducted at 10 and 40  $^{\circ}\text{C}$  to determine the LVE region of the binders based on the point where  $|G^*|$  had decreased to 95% of its initial value [Anderson *et al.*, 1994]. After obtaining the limiting strain, frequency sweep tests were carried out under the following test conditions on each sample:

- Mode of loading : controlled-strain
- Temperature : 10 to 75 $^{\circ}\text{C}$  (with the interval of 5 $^{\circ}\text{C}$ )
- Frequencies : 0.01 Hz to 10 Hz
- Spindle geometries : 8 mm (diameter) and 2 mm gap (10 $^{\circ}\text{C}$  to 35 $^{\circ}\text{C}$ ) and 25 mm (diameter) and 1 mm gap (25 $^{\circ}\text{C}$  to 75 $^{\circ}\text{C}$ )
- Strain amplitude : within the LVE response, dependent on  $|G^*|$  of each materials used.

Table 4.1: Linear viscoelastic strain limits (%)

Penetration grade	10/20	35/50	40/60	100/150	160/220
8 mm at 10 $^{\circ}\text{C}$	0.6	0.8	1.3	1.4	1.5
25 mm at 40 $^{\circ}\text{C}$	0.8	1.0	2.0	3.0	4.0

Table 4.1 shows the linear viscoelastic strain limit obtained for several unaged unmodified bitumen samples using the 8 mm spindle at 10°C and 25 mm spindle at 40°C respectively. The data for each sample was then collected, analysed and, based on the time-temperature superposition principle (TTSP), presented in the form of master curves of complex modulus and phase angle at a reference temperature either of 10°C or 25°C.

#### **4.4 Solver Function**

Solver is a program tool that helps users to find the best way to allocate scarce resources. The Solver function can be found in the Microsoft Excel (MS Excel) add-in tool. This function is suited to fitting data with a non-linear function via an alternative algorithm. The Solver function finds parameters to optimise objective value with multiple constraints. Therefore, MS Excel can be considered as a good alternative even though there are various computer programs available for non-linear data fitting. The Solver function, together with initial seed values for the coefficients, is used to obtain the optimum values of the coefficients using a number of minimisation runs [Morrison, 2005]. When no further changes are observed, the iteration process is terminated and the final values quoted for the coefficients.

#### **4.5 Statistical Analysis**

The overall reliability of a model compared to the measurement can be evaluated by means of a graphical method and goodness-of-fit statistics. Several goodness-of-fit statistic methods namely the correlation of determination,  $R^2$ , standard error ratio,  $S_e/S_y$ , discrepancy ratio,  $r_i$ , mean normalised error (*MNE*) and average geometric deviation (*AGD*) were used in this study. However, it is worth mentioning that there are many possible solutions that have been used to find the goodness-of-fit statistical parameters. All of the rheological data will be assessed using both graphical method and goodness-of-fit statistics.

### 4.5.1 Graphical method

A graphical method is intended to visually and qualitatively show an agreement between model and measured values and to display the distribution error [Wu *et al.*, 2008]. A graph of measured ( $x$ -axis) and model ( $y$ -axis) is plotted and an observation is made to see data distribution from the equality line. It shows that the model is in good agreement with the measured data if the points are distributed nicely on the equality line. On the other hand, if the points are scattered from the equality line, the model is not in good agreement with the measurements.

### 4.5.2 Standard error ratio, $S_e/S_y$

The standard error of estimation,  $S_e$  and standard error of deviation,  $S_y$  can be defined as the following:

$$S_e = \sqrt{\frac{\sum(Y - \hat{Y})^2}{(n - k)}} \quad (4.3)$$

and

$$S_y = \sqrt{\frac{\sum(Y - \bar{Y})^2}{(n - 1)}} \quad (4.4)$$

where  $n$  is sample size,  $k$  is number of independent variables in the model,  $Y$  is tested dynamic function,  $\hat{Y}$  is modelled dynamic function and  $\bar{Y}$  is mean value of tested dynamic function. Therefore, the ratio  $S_e/S_y$  is a measure of the improvement in the accuracy of modelling due to the descriptive equation. When the ratio is small, e.g. near zero, more variation in the dynamic data about their mean can be explained by the equation. The small value indicates a better description [Tran and Hall, 2005].

### 4.5.3 Coefficient of determination, $R^2$

The coefficient of determination,  $R^2$ , is a measure of the model accuracy.  $R^2$  is expressed as follows:

$$R^2 = 1 - \frac{(n-k)}{(n-1)} \times \left( \frac{S_e}{S_y} \right)^2 \quad (4.5)$$

where the symbols are as previously defined. For the perfect fit,  $R^2=1$ . Subjective criteria, which were used in the NCHRP project 9-19 Task C, were used to evaluate the performance of the model in this study, as shown in Table 4.2 [Tran and Hall, 2005].

Table 4.2: Criteria of the goodness-of-fit statistics [Tran and Hall, 2005]

Criteria	$R^2$	$S_e/S_y$
Excellent	$\geq 0.90$	$\leq 0.35$
Good	0.70 – 0.89	0.36 – 0.55
Fair	0.40 – 0.69	0.56 – 0.75
Poor	0.20 – 0.39	0.76 – 0.89
Very Poor	$\leq 0.19$	$\geq 0.90$

### 4.5.4 The discrepancy ratio ( $r_i$ )

The discrepancy ratio,  $r_i$ , indicates the accuracy of the goodness-of-fit between the measured and modelled data. For example,  $r_i$  for the measured and descriptive dynamic function can be expressed as:

$$r_i = \frac{Y_{T_{pi}}}{Y_{T_{mi}}} \quad (4.6)$$

where  $Y_{T_{pi}}$  and  $Y_{T_{mi}}$  are the modelled and measured dynamic function, respectively.

The subscript  $i$  denotes the data set number. The discrepancy ratio,  $r_i$  is used to observe the model data's tabulation from the equality line with the perfect value of 1. When the  $r_i$  is larger or smaller than 1, it measures how much wider the description interval has to be to cover the observed number of cases [Wu *et al.*,

2008]. The  $r_i$  is being used for the data that are distributed on logarithmic scale and linear scale.

#### 4.5.5 The mean normalised error (*MNE*)

The mean normalised error (*MNE*) is related to the overall discrepancy between descriptions and observations:

$$MNE = \frac{100}{J} \sum_{i=1}^J \left| \frac{Y_{T_p} - Y_{T_m}}{Y_{T_m}} \right| \quad (4.7)$$

where  $J$  is the total number of the dataset. The other symbols are as previously defined. The *MNE* is being used for the data that are distributed on logarithmic scale. For a perfect fit,  $MNE = 0$  [Wu *et al.*, 2008].

#### 4.5.6 The average geometric deviation (*AGD*)

The Average Geometric Deviation (*AGD*) can be calculated as follows:

$$AGD = \left( \prod_{i=1}^J R_i \right)^{\frac{1}{J}}, \quad R_i = \begin{cases} Y_{T_p} / Y_{T_m} & \text{for } Y_{T_p} \geq Y_{T_m} \\ Y_{T_m} / Y_{T_p} & \text{for } Y_{T_p} < Y_{T_m} \end{cases} \quad (3.8)$$

For a perfect fit, *AGD* is equal to 1 [Wu *et al.*, 2008]. The *AGD* is being used for the data that are distributed on logarithmic scale. As defined in the equation, the  $R_i$  values are always greater or equal to unity.  $R_i$  is equal to 1 when the calculated and measured values are identical. Thus the lowest possible value for *AGD* is 1. *AGD* is a measure of the average ratio between measured and calculated values. For instance if it is 2 it means that the calculated will be 2 (or 0.5) times the measured value.

## Shift Factor Equations

---

### 5.1 Background

Studies into the viscoelastic behaviour of bitumen have received increased interest from various researchers since the early 1990s, following the activities and campaign of the Strategic Highway Research Program (SHRP) [Harrigan *et al.*, 1994; Rowe *et al.*, 2009]. The rheological properties of bitumens are normally presented in terms of the complex modulus ( $|G^*|$ ) and the phase angle ( $\delta$ ) master curves together with the determination of shift factors associated with temperature shifting of the rheological parameters. The temperature dependency of the viscoelastic behaviour of bitumens is indicated using shift factors and expressed as:

$$a_T = \frac{f_r}{f} \quad (5.1)$$

where  $a_T$  is the shift factor,  $f$  is the tested frequency and  $f_r$  is the reduced frequency at a reference temperature.

The construction of master curves can be done using an arbitrarily selected reference temperature to which all rheological data are shifted. At the reference temperature,  $T_{\text{ref}}$ , the value of  $a_T$  is equal to one ( $\log a_T$  is equal to zero). Through the use of the master curve and shift factor relationships it is possible to interpolate stiffness at an expanded range of frequencies and temperatures compared with those at which the data was collected. If functional forms are fitted to the shape of the master curve plot and to the  $a_T$  relationship this interpolation becomes rapid and easy to apply, for example, in computer software. In addition, if a functional form with some thermodynamic basis is used then the resulting equations can be

employed to extrapolate the data beyond the observed range of temperatures and frequencies [Rowe and Sharrock, 2011].

A considerable number of studies have been conducted using various shift factor equations in order to construct smooth and continuous  $|G^*|$  and  $\delta$  master curves [Goodrich, 1988; Airey and Brown, 1998; Pellinen *et al.*, 2002; Olard and Di Benedetto, 2003; Olard *et al.*, 2003; Shaw and MacKnight, 2005]. However, the different shift factor equations are usually used in isolation and no comparative study of the different shift factor functions or their applicability to different types of bituminous binders has been undertaken. The study is conducted to assess the validity of several different shifting functions for constructing  $|G^*|$  master curves of different bituminous binders by applying the time-temperature superposition principle (TTSP).

## **5.2 Results and Discussion**

### **5.2.1 Graphical comparisons**

In this study, only horizontal shift factor is used and do not involve with the vertical shift. Several different methods were used; namely (i) numerical, non-functional form shifting (ii) the William, Landel and Ferry (WLF), (iii) Arrhenius, (iv) Log-Linear, (v) viscosity temperature susceptibility Details of these methods can be found in Chapter 2. (VTS) and (vi) the Laboratoire Central des Ponts et Chaussées (LCPC) methods. Correlations between the numerical, non-functional form (non-linear least squares) shift approach and other functions are assessed by means of graphical and goodness-of-fit statistical analysis methods.

It also should be noted that this study only focuses on the comparison between measured and descriptive  $a_T$  values and does not consider anomalies that can be seen in the construction of some of the  $|G^*|$  master curves. This refers particularly to anomalies associated with the presence of highly crystalline bitumens (wax content  $> 7\%$ ), structured bitumen with high asphaltenes content and highly polymer-modified bitumens (PMBs) ( $> 5\%$  polymer content) [Airey, 2003].

Comparisons between descriptive (shift factor functions) and measured (numerical) shift factors are graphically shown in Figs 5.1 and 5.2. These plots are intended to visually and qualitatively show the agreement between model and experimental values and to display any errors associated with the model's equations and/or material combinations [Molinas and Wu, 2000]. The equations consist of the WLF, Arrhenius, Log-Linear, VTS and LCPC functions/procedures. The measured shift factor data consists of the numerical, non-functional form shift approach. This approach used non-linear least squares fitting with the aid of the Microsoft Excel Spreadsheet Solver function to simultaneously determine the coefficients associated with Equation 5.3. As discussed by Pellinen *et al.* [2002], the numerical shift approach produces the best results in terms of data shifting flexibility due to the fact that this method has the highest degree of freedom. This method, however, has no physical meaning (or functional form) and has simply been used as a comparison to the other shift factor methods.

The numerical shifts are always plotted on the  $x$ -axis (Figs 5.1 and 5.2). A combination of comparisons between measured and descriptive  $a_T$  for the unaged samples (i.e. unmodified bitumens, polymer-modified bitumens and bitumen-filler mastics) are shown in Fig. 5.1. Fig. 5.2 represents the combinations of these samples that have undergone various ageing processes. From Fig. 5.1, it can be seen that the WLF and Arrhenius equations show the best results with the descriptive  $a_T$  values being close to the equality line. Reasonable good correlations can also be seen for the VTS and LCPC methods. The WLF equation, originally derived from the empirical Doolittle equation relating fractional free volume theory to temperature, is clearly applicable for all bituminous materials. As mentioned by Dealy and Larson [2006], the WLF equation generally provides a better fit of the data at temperatures lower than the glass transition temperature,  $T_g$ . However, the results in Figs 5.1 and 5.2 also show that the WLF equation is applicable at higher temperatures for bituminous binders.

The Log-Linear equation showed the lowest correlation between measured and descriptive  $a_T$ . According to Pellinen *et al.* [2002], below about 0°C, the shift factor varies linearly with temperature for many binders and the same equation has been proposed suitable for asphalt mixture at low to intermediate temperatures.

However, it is found in this study that the  $a_T$  curve should be the same with temperature dependency of the binder since the binder is the only component in asphalt mixture which is temperature susceptible. Therefore, theoretically the shift factor curves for asphalt mixture should be in the same shape with the shift factor curves of bituminous binders. The VTS equation appears to be unsuitable for describing  $a_T$  of the unmodified bitumen at low frequencies and/or high temperatures. Finally, the LCPC method showed a dispersion of descriptive  $a_T$  data particularly for the unaged bitumen-filler mastics. Similar findings were observed by Chailleux *et al.* [2006] where anomalies had been seen particularly at higher frequencies. From their study, they found that the dispersion of  $a_T$  data normally occurs at the transition between the highest tested frequency for a particular temperature and the lowest tested frequency for the next (higher) temperature. It is observed that all the shift factor equations are unable to describe the rheological properties of highly unaged modified bitumen with EVA. This can be seen where the data scattered from the equality line. This EVA PMB does not behave as a thermo-rheological simple material.

Fig. 5.2 shows a comparison between measured and descriptive  $a_T$  of the different shift factor equations for the aged unmodified bitumens, PMBs and bitumen-filler mastics samples. The results show a larger discrepancy between the descriptive and measured  $a_T$  values, particularly at intermediate to high temperatures. The WLF, VTS, LCPC and Arrhenius methods produce almost identical results when comparing the measure and descriptive  $a_T$ . The Log-Linear equation slightly overestimates the measured  $a_T$ . In general, it is observed that all the models suffer from a similar drawback where they are unable to accurately describe the  $a_T$  data. This lack of agreement between measured and descriptive  $a_T$  for the aged mastics and PMBs can be attributed to the increased complexity of the rheological response of the materials following oxidation and increased structuring. An example of the Black diagram one of the PMBs is shown in Fig. 5.3. Moreover, most of the  $a_T$  equations (functions) are empirical and are therefore unable to account for changes in the physicochemical properties of the materials after ageing.

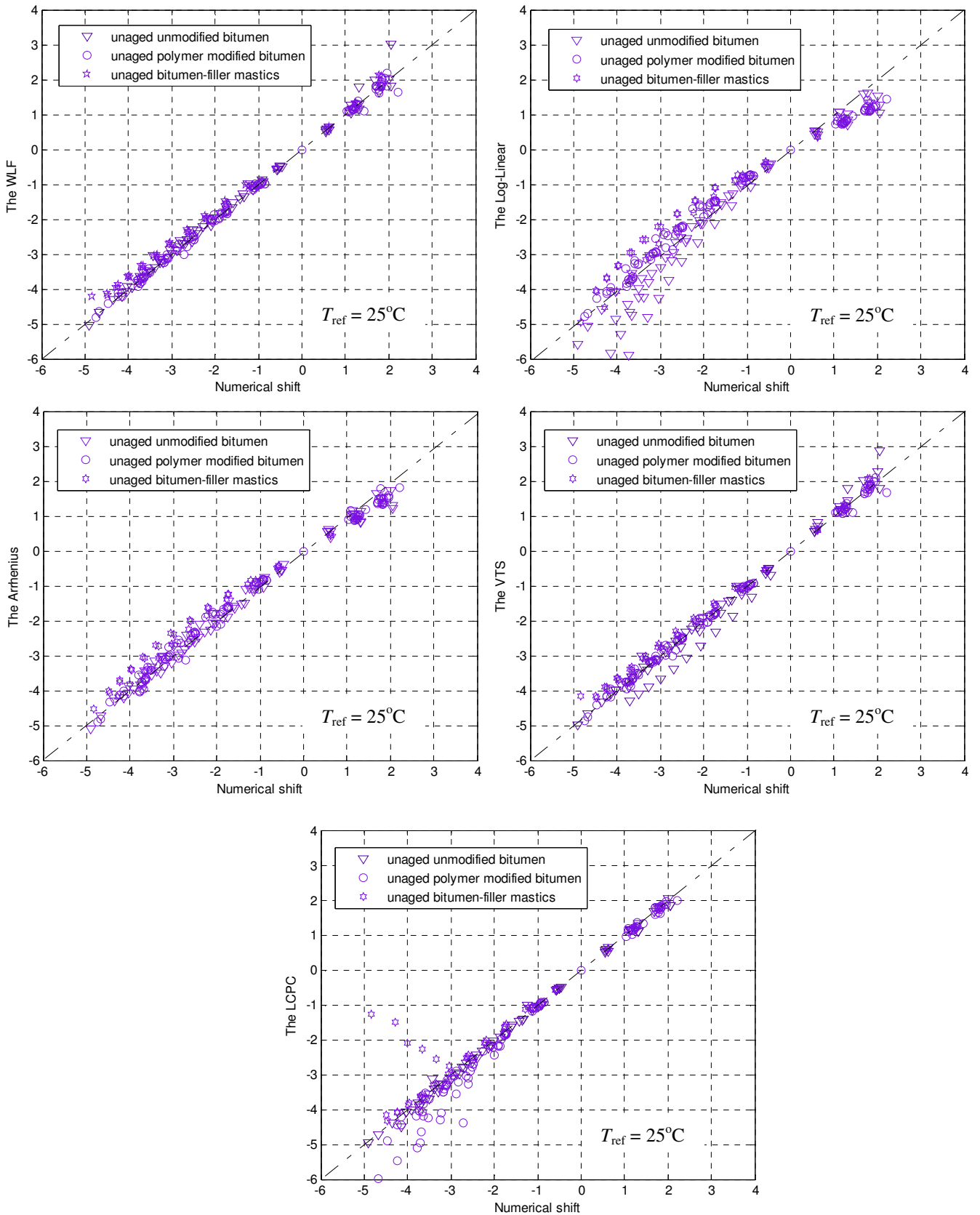


Fig. 5.1: Comparisons between  $a_T$  (numerical shift) and  $a_T$  (equation) of different shift factor equations of the unaged samples ( $T_{ref} = 25^{\circ}\text{C}$ )

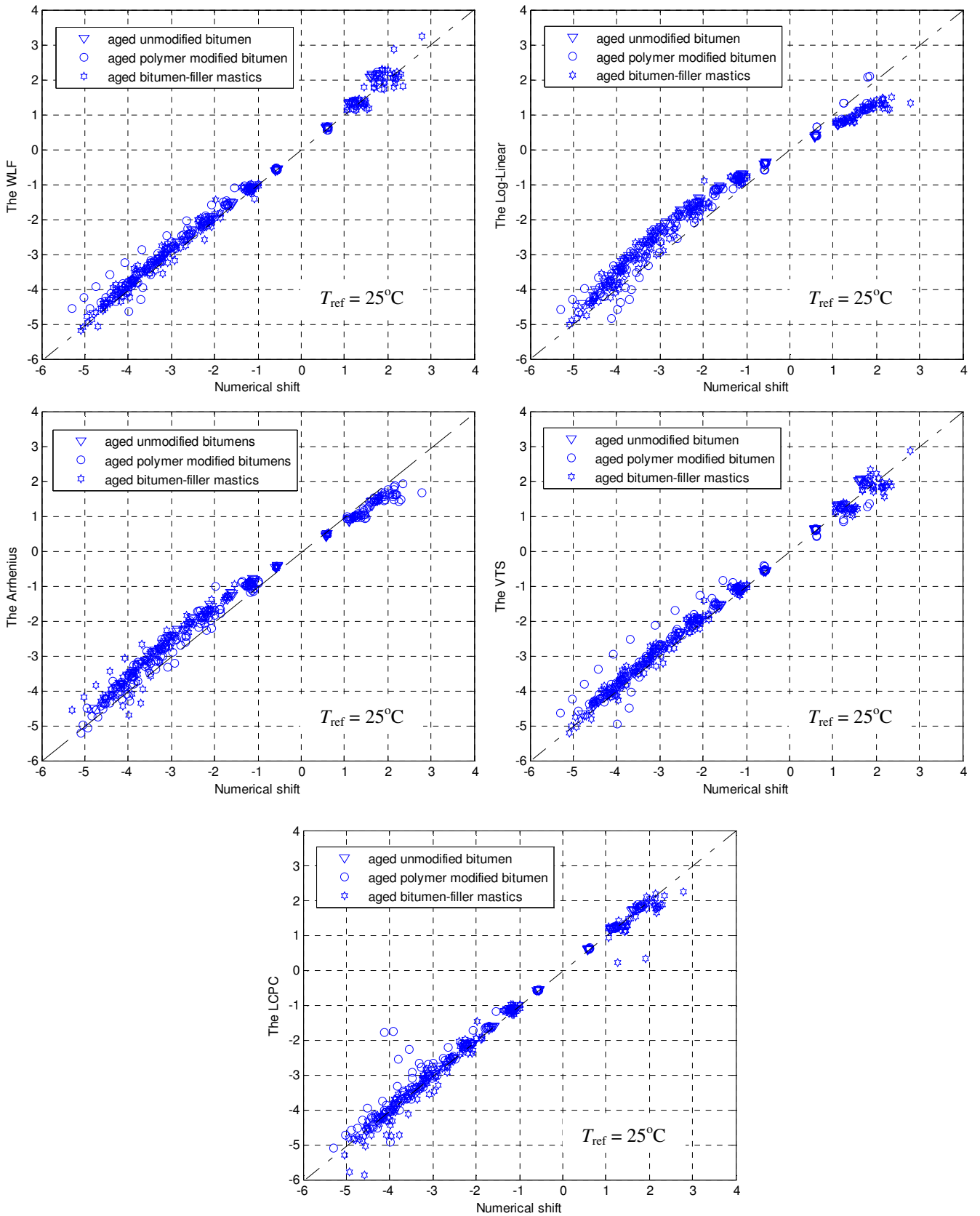


Fig. 5.2: Comparisons between  $a_T$  (numerical shift) and  $a_T$  (equation) of different shift factor equations of the aged samples ( $T_{ref} = 25^{\circ}\text{C}$ )

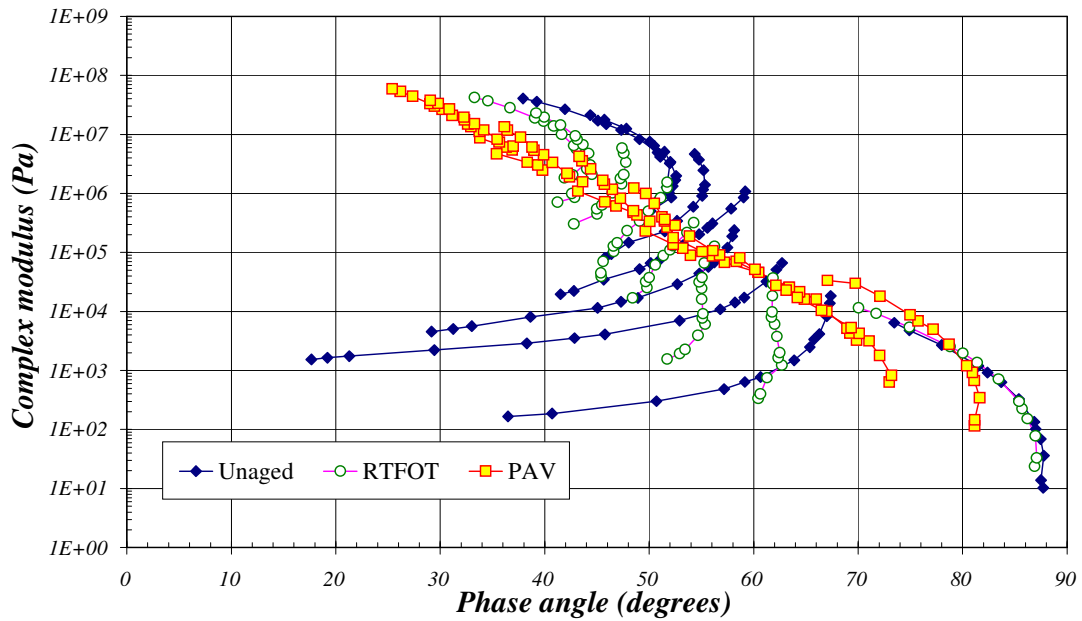


Fig. 5.3: Black diagram for unaged, RTFOT and PAV aged EVA PMB

### 5.2.2 Goodness-of-fit statistics

Tables 5.1 and 5.2 show the  $S_e/S_y$  and  $R^2$  goodness-of-fit statistics associated with the different  $a_T$  equations on unaged and aged samples. The unaged PMBs and bitumen-filler mastics shifted using the LCPC method show good correlation between measured and descriptive  $a_T$  data. The  $S_e/S_y$  and  $R^2$  parameters tend to indicate excellent correlation between measured and descriptive  $a_T$  data for all material and shift factor combinations. However, according to Tran and Hall [2005], the correlation coefficient,  $R^2$  is a better measure for linear models with a large sample size<sup>1</sup>.

In addition, it is questionable whether  $S_e/S_y$  is a good tool to perform a comparison between measured and descriptive data with. For example, in the case of complex modulus measurements over a large temperature range, the standard

<sup>1</sup> It is necessary to graph the data and, if the trend is somewhat linear, compute the correlation coefficient. Second, the correlation coefficient is a single-valued index that cannot reflect all circumstances such as clustering of points, extreme deviant points, nonlinearity, and random versus systematic scatter. Third, the correlation coefficient may not be adequate to suggest a model form [McCuen, 2003].

deviation ( $S_y$ ) has no meaning.  $S_y$  is only scientifically founded for multiple  $|G^*|$  measurements under the same experimental condition (i.e. at one temperature and one frequency). In this case,  $S_y$  corresponds to the average distance between the mean value and all the experimental data.

A more microscopic statistical analysis is needed and therefore, the discrepancy ratio ( $r_i$ ), the mean normalised error ( $MNE$ ) and the average geometric deviation ( $AGD$ ) are introduced, as shown in Tables 5.1 and 5.2. As discussed by Wu *et al.* [2008], it is not straightforward to determine which method performs best since different statistical methods lead to different rankings. The discrepancy ratio,  $r_i$ , is used to observe the descriptive data's tabulation from the equality line with a perfect value being one. When the  $r_i$  is larger or smaller than one, it measures how much wider the description interval has to be to cover the observed number of cases [Wu *et al.*, 2008]. A smaller range means a closer range to the perfect agreement. In this study, an interval of  $1 \pm (0.02, 0.04, 0.06, 0.08 \text{ and } 0.10)$  is used. An example is shown for the WLF equation of unmodified bitumens, with an understanding that the commentary applies to other equations, both on the unaged and aged samples.

A value of 0.98–1.02 represents an area where the ratio between descriptive and measured  $a_T$  data is taken 0.02 to each left and right side from the equality line. It is observed that the  $r_i$  is equal to 42.25%. When the region widens with 0.02 more on each right and left sides (now the range between 0.96–1.04), another 18.31% of data is included. In this range, the data's tabulation increased up to 60.56%. A similar process is repeated for the  $r_i$  in the range of 0.94–1.06, 0.92–1.08 and 0.90–1.10, resulting the data's tabulation up to 73.24, 81.69 and 87.32%. In general, the improvement in  $r_i$  happens in all ranges. The  $MNE$  is related to the overall discrepancy between measured and descriptive data. Meanwhile, the  $AGD$  is a measure of the average ratio between measured and descriptive  $a_T$  data. As defined in the equation, the  $\tilde{R}_i$  values are always greater or equal to unity.  $\tilde{R}_i$  is equal to one when the descriptive and measured  $a_T$  are identical. Thus the lowest possible value for  $AGD$  is 1.

Taking the range of  $r_i$  equal to 0.90–1.10 as an example, the LCPC method shows the best result, followed by the WLF, VTS, Arrhenius and Log-Linear equations. A similar finding is observed using the *MNE* goodness-of-fit parameter. No obvious difference in terms of the *AGD* values could be observed on the unaged samples. The Arrhenius equation might produce a better fit of  $|G^*|$  master curves for low temperatures [Zeng *et al.*, 2001; Pellinen *et al.*, 2002]. With one coefficient needing to be determined, the Arrhenius equation shows a low degree of freedom in its equation. At low temperatures, the activation energy,  $E_a$ , associated with the Arrhenius equation varies. However, at higher temperatures, the  $E_a$  values become more constant. Since the  $E_a$  values are relatively consistent, the Arrhenius equation is only reliant on the temperature and that therefore explains why this equation becomes invalid at high temperatures. The use of one  $E_a$  value is obviously unable to yield a complete behaviour of  $|G^*|$  and  $\delta$  master curves of bituminous binders.

In general, the LCPC equation shows the best correlation between measured and descriptive  $a_T$  of the  $r_i$  distribution in the range of 0.90–1.10 for the aged unmodified bitumens, as shown in Table 5.2. It was followed by the VTS, WLF, and Arrhenius equations. As expected, the Log-Linear shows the least correlation in term of goodness-of-fitting statistical analysis. It was proven that the ageing process results in an increase of asphaltenes content, rendering the breakdown in time-temperature equivalency principle. It is interesting to note that the LCPC method shows the most outstanding results in terms of  $r_i$ , *MNE* and *AGD*, respectively, followed by the WLF, VTS, Arrhenius and Log-Linear equations for the aged PMBs. The LCPC and WLF equations are well dispersed around the equality line for the aged bitumen-filler mastics. Meanwhile, the Arrhenius and Log-Linear equations show the largest scatter in descriptive results of  $r_i$  in the range of 0.90–1.10 for aged PMBs and bitumen-filler mastics. The  $|G^*|$  data of aged bitumen-filler mastics was dispersed randomly at high temperatures and implies greater influence of granular skeleton which renders the TTSP invalid [Delaporte *et al.*, 2007].

It can be inferred that all the equations described are fundamentally empirical and may not be applicable for some materials [Dealy and Larson, 2006]. The *AGD* parameter shows comparable results for most of the aged samples.

Table 5.1: Summary of the  $S_o/S_y$ ,  $R^2$ ,  $r_i$ ,  $MNE$  and  $AGD$  goodness-of-fit for unaged samples

Method	Binders	$n$	$S_o/S_y$	$R^2$	Data in range of discrepancy ratio, $r_i$ (%)					$MNE$	$AGD$
					0.98 - 1.02	0.96 - 1.04	0.94 - 1.06	0.92 - 1.08	0.90 - 1.10		
WLF	Unmodified bitumens	71	0.086	0.993	42.25	60.56	73.24	81.69	87.32	5.10	1.05
Arrhenius		71	0.110	0.988	23.94	38.03	50.70	60.56	69.01	8.58	1.10
Log-Linear		71	0.307	0.906	7.04	15.49	26.76	38.03	46.48	16.41	1.18
VTS		71	0.147	0.979	32.39	52.11	56.34	60.56	64.79	10.12	1.10
LCPC		71	0.057	0.997	40.85	54.93	78.87	84.51	90.14	4.29	1.04
WLF	PMBs	106	0.050	0.998	40.95	71.43	82.86	90.48	93.33	3.67	1.04
Arrhenius		106	0.106	0.989	11.43	28.57	38.10	52.38	58.10	10.09	1.12
Log-Linear		106	0.173	0.970	3.81	11.43	14.29	16.19	21.91	17.45	1.22
VTS		106	0.050	0.998	45.71	69.52	84.76	92.38	93.33	3.51	1.04
LCPC		106	0.410	0.831	13.33	31.43	49.52	58.10	69.52	11.36	1.10
WLF	Bitumen-filler mastics	42	0.138	0.981	4.76	14.29	16.67	30.95	61.91	9.27	1.11
Arrhenius		42	0.217	0.953	0.00	2.38	7.14	9.52	14.29	19.13	1.24
Log-Linear		42	0.262	0.932	4.76	7.14	11.91	11.91	16.67	24.09	1.33
VTS		42	0.133	0.983	11.91	14.29	21.43	45.24	71.43	8.47	1.09
LCPC		42	0.397	0.839	19.05	47.62	61.91	73.81	83.33	9.68	1.14

Table 5.2: Summary of the  $S_o/S_y$ ,  $R^2$ ,  $r_i$ ,  $MNE$  and  $AGD$  goodness-of-fit for aged samples

Method	Binders	$n$	$S_o/S_y$	$R^2$	Data in range of discrepancy ratio, $r_i$ (%)					$MNE$	$AGD$
					0.98 - 1.02	0.96 - 1.04	0.94 - 1.06	0.92 - 1.08	0.90 - 1.10		
WLF	Unmodified Bitumens	71	0.091	0.992	15.49	43.66	64.79	74.65	84.51	6.99	1.07
Arrhenius		71	0.200	0.960	0.00	0.00	0.00	5.63	15.49	17.20	1.21
Log-Linear		71	0.276	0.924	0.00	0.00	0.00	4.23	8.45	25.46	1.35
VTS		71	0.081	0.994	12.68	52.11	66.20	83.10	85.92	6.13	1.06
LCPC		71	0.022	0.999	70.42	85.92	94.37	100.00	100.00	1.84	1.02
WLF	PMBs	140	0.136	0.982	9.29	28.57	43.57	61.43	74.29	8.14	1.09
Arrhenius		140	0.155	0.976	6.70	16.76	22.35	30.73	39.67	13.94	1.17
Log-Linear		140	0.240	0.946	5.00	7.14	12.86	17.14	21.43	21.07	1.28
VTS		140	0.168	0.972	9.29	23.57	39.29	54.29	65.71	9.98	1.12
LCPC		140	0.180	0.968	37.14	57.86	75.00	84.29	86.43	5.48	1.06
WLF	Bitumen-filler mastics	179	0.085	0.993	26.26	45.25	62.01	74.30	79.33	6.57	1.07
Arrhenius		179	0.209	0.957	1.43	3.57	7.14	12.86	20.00	17.21	1.21
Log-Linear		179	0.222	0.951	3.91	10.06	15.64	18.99	22.91	21.57	1.29
VTS		179	0.097	0.991	18.99	37.43	49.72	59.22	64.25	8.05	1.09
LCPC		179	0.128	0.984	23.46	43.58	56.43	63.13	71.51	8.06	1.10

This finding concludes that the *AGD* method is not always reliable at detecting the goodness-of-fit between measured and descriptive  $a_T$  of bituminous binders, unaged and aged samples. Finally, it is worth mentioning that there are many possible solutions that have been used to find the goodness-of-fit statistical parameters.

### 5.2.3 WLF coefficients

For the WLF equation, two constants  $C_1$  and  $C_2$  are needed. Table 5.3 shows of  $C_1$  and  $C_2$  obtained from the study. It is shown that the values of  $C_1$  and  $C_2$  are inconsistent from one sample to the next. Similar results were obtained by Olard and Di Benedetto [2003] and Olard *et al.* [2003] with the values for  $C_1$  being more consistent than those for  $C_2$ .

Table 5.3: Shifting coefficients of the WLF equation

Sample		unmodified bitumen		bitumen-filler mastics		PMBs	
		$C_1$	$C_2$	$C_1$	$C_2$	$C_1$	$C_2$
Unaged	Average	22	126	12	107	17	158
	Minimum	12	109	11	93	11	104
	Maximum	46	162	14	130	51	479
Aged	Average	15	131	13	114	17	136
	Minimum	14	124	11	90	11	67
	Maximum	16	150	21	191	39	304

The  $C_1$  and  $C_2$  firstly thought to be universal constants where Williams *et al.* [1954] proposed if reference temperature is suitably chosen for each material then these constants could be allotted universal values of 8.86 and 101.6 respectively Brodynan *et al.* [1961] found the universal constants fitted well with the bitumen data for  $T - T_{ref} > -20^\circ\text{C}$  but at lower temperatures, the descriptive shift factors were too great. The study done by Christensen and Anderson [1992] indicates that at  $T_{ref}$  equal to glassy temperature,  $T_g$ , the shift factors for the unaged and aged binders showed that the constants essentially had the same values: 19 for  $C_1$  and 92 for  $C_2$ . Olard *et al.* [2003] used the WLF coefficients on various and the mean values obtained for  $C_1$  and  $C_2$  parameters are 19 and 143 respectively. The constants should be obtained by optimisation process from the experimental data. No universal values can, a priori, be applied.

### 5.3 Summary

Based on this study, several key observations can be drawn;

- For the range of temperatures from 10–75°C, the Generalised Logistic Sigmoidal Model is able to describe or model the complex modulus data obtained from frequency sweep tests undertaken with a DSR. With the exception of the LCPC method, all the factor equations can be used together with this model to construct complex modulus master curves at an arbitrary selected reference temperature.
- The numerical, non-functional form shift function produces the most consistent set of results due to the high degree of freedom and overall flexibility of this non-linear least squares fitting approach.
- In terms of functional form approaches, the LCPC and WLF equations generally produced the best results compared to the numerical shift approach (model versus measured shift factor data) for all the material combinations studied, followed by the VTS and Arrhenius equations. The Log-Linear equation showed the lowest correlation with measured shift factor data.
- The Log-Linear equation is not suitable to be used for binders and asphalt mixtures. The  $a_T$  curve of Log-Linear equation should be the same with temperature dependency of the binder since the binder is the only component in asphalt mixture which is temperature susceptible. Therefore, the shift factor curves for asphalt mixture should be in the same shape with the shift factor curves of the binders.
- All of the shift factor equations are unable to satisfactorily describe the rheological properties of highly modified binder.
- In terms of comparing the different shift factor function and methods, both a graphical and a number of goodness-of-fit statistics were used. The graphical plots are intended to visually observe the agreement between descriptive values and measurements; however, this method is unreliable to detect small changes.
- It is found that the  $R^2$  and  $S_e/S_y$  are not really good enough to be used for describing the mismatch. The  $R^2$  is more applicable for linear models and subsequently both  $R^2$  and  $S_e/S_y$  are not really independent. The average

geometric deviation (*AGD*) is also not always reliable to check the goodness-of-fit even though it was meant for data scattered over a logarithmic scale. Therefore, it is suggested to use the other goodness-of-fit statistics such as the discrepancy ratio ( $r_i$ ) and the mean normalised error (*MNE*) since both of them provide better observation between measured and descriptive data.

### 6.1 Background

In principle, the complete modulus versus frequency (or time of loading) behaviour of any polymer at any temperature can be measured [Shaw and MacKnight, 2005]. This principle also can be applied for bituminous binders. Data can be shifted relative to the reduced frequency ( $\omega_r$ ), so that the various curves can be aligned to form a single curve. This curve is called as a master curve. A master curve represents a binder's behaviour at a given temperature for a large range of frequencies. The rheological behaviour of bituminous binder is bounded by two main transitions. At high frequencies and/or low temperatures, the elastic modulus approaches a limiting value, called a glassy modulus,  $G_g$ . At low frequencies and/or high temperatures, a material behaves as a Newtonian (viscous) fluid [Herh *et al.*, 1999].

Once the master curve is established, it is possible to derive interpolated values of property for any combination of temperature or frequency inside the range covered by the measurements [Pellinen *et al.*, 2002]. All of these methods, however, only involve the horizontal shifting. A good rheological model should be able to describe as completely as possible the linear viscoelastic functions of the studied materials. Complex modulus magnitude,  $|G^*|$  and phase angle,  $\delta$  functions are needed to yield complete information about materials in a rheological study [Stastna *et al.*, 1997].

This study investigates the use of four mathematical models; namely the Sigmoidal Model, the Generalised Logistic Sigmoidal Model, the Christensen and Anderson (CA) Model and the Christensen, Anderson and Marasteanu (CAM)

Model to describe the rheological properties of bituminous binders. Details of these models can be found in Chapter 3. The rheological data of unaged and aged unmodified and polymer-modified bitumens (PMBs) are measured using a dynamic shear rheometer (DSR) in the linear viscoelastic region. A correlation between measured and descriptive  $|G^*|$  data is assessed using graphical and goodness-of-fit statistical methods.

## 6.2 Detailed Procedure

The construction of the  $|G^*|$  master curve was done with the aid of the Solver function in MS Excel. This function is used for performing optimisation of data with non-linear least squares regression techniques. The procedure consisted of minimising the sum of square error (SSE) between measured  $|G^*|$  (hereafter called measured) and modelled (hereafter called descriptive) as shown in Equation 6.1:

$$\text{SSE} = \sum \frac{\left( \log |G_{\text{exp}}^*(f, T)| - \log |G_{\text{pre}}^*(a_T(T, T_{\text{ref}}) \cdot f, T_{\text{ref}})| \right)^2}{\left( \log |G_{\text{exp}}^*(f, T)| \right)^2} \quad (6.1)$$

where  $|G_{\text{exp}}^*(f, T)|$  is measured complex modulus,  $|G_{\text{pre}}^*(f, T)|$  is descriptive complex modulus,  $T$  is temperature ( $^{\circ}\text{C}$ ),  $T_{\text{ref}}$  is the reference temperature,  $f$  is frequency (Hz) and  $a_T(T, T_{\text{ref}})$  is shift factor. In this study, the  $T_{\text{ref}}$  was arbitrarily taken as  $10^{\circ}\text{C}$ . For example (in the case of the Generalised Logistic Sigmoidal Model), by combining the model and Equation 6.1, the following equation is obtained:

$$\text{SSE} = \sum \frac{\left( \log |G_{\text{exp}}^*(f, T)| - \left( \delta + \frac{\text{Max} - \delta}{[1 + \lambda e^{\beta + \gamma \log(a_T(T, T_{\text{ref}}) \cdot f)]^{1/\lambda}} \right) \right)^2}{\left( \log |G_{\text{exp}}^*(f, T)| \right)^2} \quad (6.2)$$

The coefficients  $\alpha$ ,  $\delta$ ,  $\beta$ ,  $\lambda$ , and  $a_T(T, T_{\text{ref}})$  are fitted in the minimisation procedure between measured and modelled data. The shift factor functions were used together with the master curve model. For example, when the lines are shifted manually, Equation 6.2 becomes:

$$SSE = \sum \frac{\left( \log|G_{\text{exp}}^*(f, T)| - \left( \delta + \frac{Max - \delta}{\left[ 1 + \lambda e^{\beta + \gamma \log a_T + \log f} \right]^{1/\lambda}} \right) \right)^2}{\left( \log|G_{\text{exp}}^*(f, T)| \right)^2} \quad (6.3)$$

The coefficients that need to be determined are now  $\alpha$ ,  $\delta$ ,  $\beta$ ,  $\lambda$ , and  $\log a_T$ . The Solver function, together with initial seed values for the coefficients, is used to obtain the optimum values of the coefficients using a number of minimisation runs [Morrison, 2005]. When no further changes are observed, the iteration process is terminated and the final values quoted for the coefficients.

## 6.3 Results and Discussion

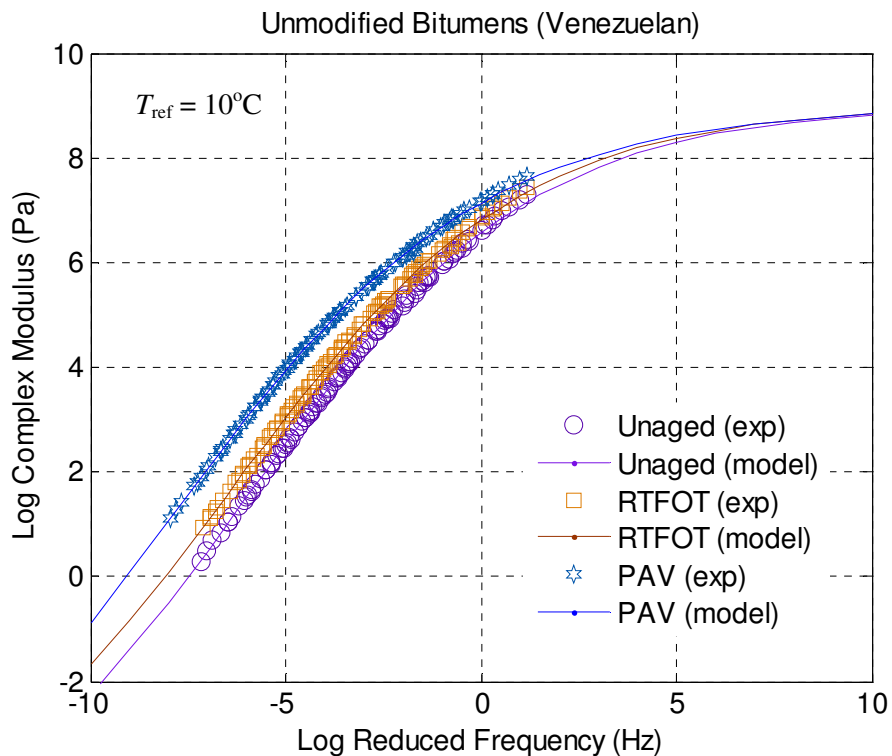
### 6.3.1 The Sigmoidal Model

The Sigmoidal Model is originally sought to be used for fitting the complex modulus of asphalt mixtures [Pellinen and Witczak, 2002]. However, this model has been modified to be used for bituminous binders (unmodified and polymer-modified bitumens) data. Three fitting parameters;  $\beta$ ,  $\delta$ , and  $\gamma$  are estimated using a numerical optimisation technique. The optimisation process is done with the aid of the Solver function in MS Excel. Data at high frequencies and/or low temperatures are no longer needed since  $G_g$  can be taken as  $1 \times 10^9$  Pa. For modelling purposes, the following initial values are used;  $\beta = -1$ ,  $\delta = 1$  and  $\gamma = 1$ . The selected initial values must be reasonable

Table 6.1: The Sigmoidal parameters for unmodified bitumens

Source	Condition	Parameters		
		$\delta$	$B$	$\gamma$
Middle East	Unaged	-4.75	-1.74	0.29
	RTFOT	-5.35	-1.87	0.28
	PAV	-5.91	-2.09	0.27
Russian	Unaged	-3.98	-1.64	0.31
	RTFOT	-4.50	-1.76	0.30
	PAV	-5.17	-2.04	0.28
Venezuelan	Unaged	-6.08	-1.65	0.27
	RTFOT	-5.68	-1.74	0.27
	PAV	-6.95	-2.02	0.25

The Solver function replaces the initial guesses with optimised values for the unaged and aged unmodified bitumens, as shown in Table 6.1. The rheological data used in this section can be found in Appendices A and B. It is observed that the  $\delta$  values are negative. The negative value indicates  $|G^*|$  of bitumens is really small at high temperatures and/or low frequencies. This finding is in good agreement with previous research done by Olard and Di Benedetto [2003]. The  $\delta$  in the analysis will be small since most of these materials will behave like a viscoelastic liquid, only the part of the sigmoid above the inflection point will be fitted – resulting in small values of  $\delta$ . Therefore, the inflection point will be to the left of all data.  $\beta$ , which controls the horizontal position of the turning point, decreases from unaged to aged unmodified bitumens regardless of the crude source. This can be attributed to the fact that ageing increases the asphaltenes content and subsequently produces harder bitumens. The  $\gamma$  values are observed to be consistent for all samples, showing that the ageing did not play a significant role in influencing master curve's slope from intermediate to high temperatures. At high frequencies and/or low temperatures,  $|G^*|$  approaches a limiting value of  $1 \times 10^9$  Pa. Examples of  $|G^*|$  master curves for the unaged and aged Venezuelan 70/100, Middle East 80/100 and Russian 80 penetration grade bitumens are shown in Fig. 6.1.



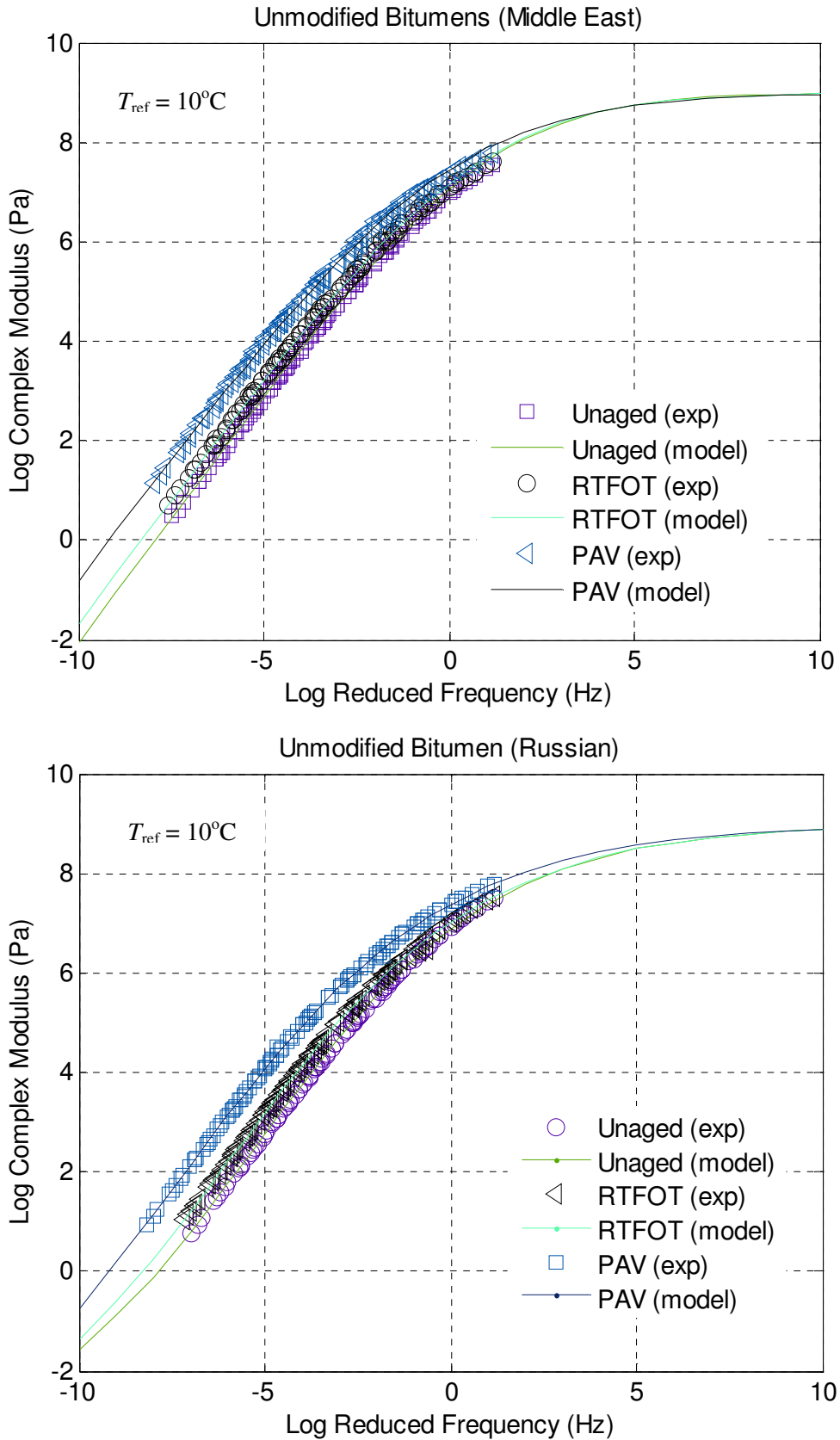


Fig. 6.1: Comparisons between measured and model of unaged and aged unmodified bitumen data using the Sigmoidal Model

Table 6.2: The Sigmoidal parameters for the EVA PMBs

Source	Condition	Modifier	%	Parameters		
				$\delta$	$B$	$\gamma$
Middle East	Unaged	EVA	3	-6.99	-1.93	0.25
			5	-8.85	-2.06	0.23
			7	-12.81	-2.32	0.20
	RTFOT		3	-7.14	-2.03	0.25
			5	-10.48	-2.28	0.22
			7	-13.10	-2.40	0.20
	PAV		3	-9.42	-2.30	0.23
			5	-7.75	-2.33	0.23
			7	-10.24	-2.48	0.21
Russian	Unaged	3	-5.73	-1.82	0.26	
		5	-13.91	-2.27	0.21	
		7	-14.88	-2.28	0.17	
	RTFOT	5	-11.32	-2.23	0.21	
		7	-15.16	-2.43	0.19	
	PAV	5	-8.18	-2.26	0.23	
7		-16.11	-2.66	0.19		
Venezuelan	Unaged	3	-6.58	-1.76	0.25	
		5	-15.08	-2.27	0.19	
		7	-21.92	-2.52	0.18	
	RTFOT	5	-14.74	-2.58	0.17	
		7	-26.98	-3.73	0.14	
	PAV	5	-9.75	-2.27	0.20	
7		-21.26	-2.77	0.16		

Table 6.3: The Sigmoidal parameters for the SBS PMBs

Source	Condition	Modifier	%	Parameters		
				$\delta$	$B$	$\gamma$
Russian	Unaged	SBS	3	-2.70	-1.53	0.30
			5	-2.08	-1.45	0.29
			7	-0.53	-1.20	0.31
	RTFOT		3	-4.18	-1.78	0.28
			5	-4.18	-1.78	0.28
			7	-10.28	-2.11	0.21
	PAV		3	-7.32	-2.15	0.24
			5	-8.20	-2.18	0.23
			7	-7.83	-2.22	0.23
Venezuelan	Unaged	3	-6.15	-1.71	0.26	
		5	-6.77	-1.77	0.24	
		7	-5.91	-1.75	0.24	
	RTFOT	3	-7.93	-1.91	0.23	
		5	-7.99	-1.89	0.22	
		7	-11.68	-2.16	0.20	
	PAV	3	-7.83	-2.09	0.23	
		5	-6.19	-1.91	0.25	
		7	-7.36	-2.06	0.21	

The model parameters of the EVA and SBS PMBs, unaged and aged samples, are shown in Tables 6.2 and 6.3 respectively. Figs 6.2 to 6.5 show an example of  $|G^*|$  master curves for the unaged and aged EVA and SBS PMBs, using the 70/100 penetration grade bitumens from a Venezuelan crude as base bitumens. Like the unaged and aged unmodified bitumens, the  $\delta$  values obtained for the unaged and aged PMBs are small. The  $\delta$  in the analysis will be small since most of these materials will behave like a viscoelastic liquid and only the part of the sigmoid above the inflection point will be fitted – resulting in small values of  $\delta$ . Therefore, the inflection point will be to the left of all data. This indicates that  $|G^*|$  at low frequencies and high temperatures is very small. It is also observed that the presence of both EVA and SBS polymers in unaged samples decreases the  $\beta$  values. The presence of semi-crystalline EVA (different crystalline structures at different temperatures) and elastomeric SBS (enhanced high temperature and/or low frequency elastic response due to the polymer network) may attribute to the difference in the coefficient values.

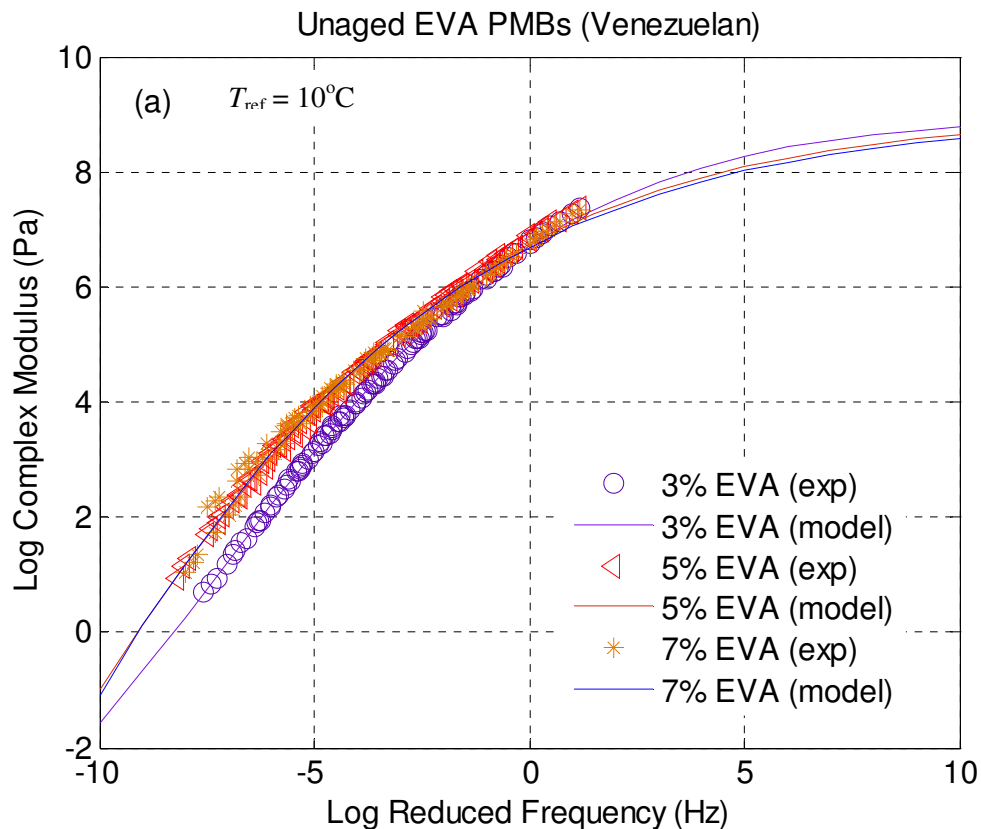


Fig. 6.2: Comparisons between measured and model of the unaged EVA PMBs data using the Sigmoidal Model

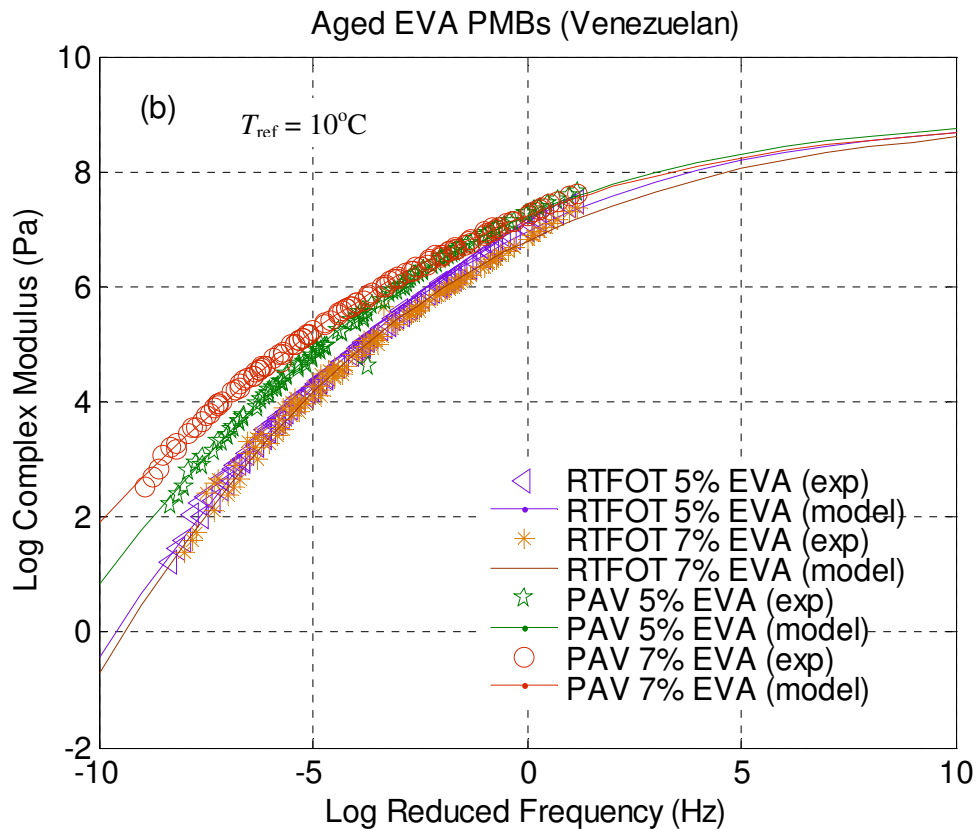


Fig. 6.3: Comparisons between measured and model of the RTFOT and PAV EVA PMBs data using the Sigmoidal Model

In general, the values for most tested PMBs are similar to the unmodified bitumens except for several samples. For instance, the difference observed between the Venezuelan RTFOT 5% and 7% EVA PMBs are quite significant where the values for certain parameters deviate significantly compared to the other samples. Previous findings suggested the critical network forms around 5% of modification and this may lead to the suggestions that the partial breakdown of a polymer network occurs in the PMB [Chen *et al.*, 2002]. Moreover, the presence of "waves" in certain  $|G^*|$  curves cannot be described by the Sigmoidal Model. This observation indicates that the Sigmoidal Model is unable to fit the rheological properties of highly modified binders. The anomalies are shown in Figs 6.2 to 6.3. No critical observations, however, can be observed for the unaged and aged Venezuelan SBS PMBs (Figs 6.4 to 6.5).

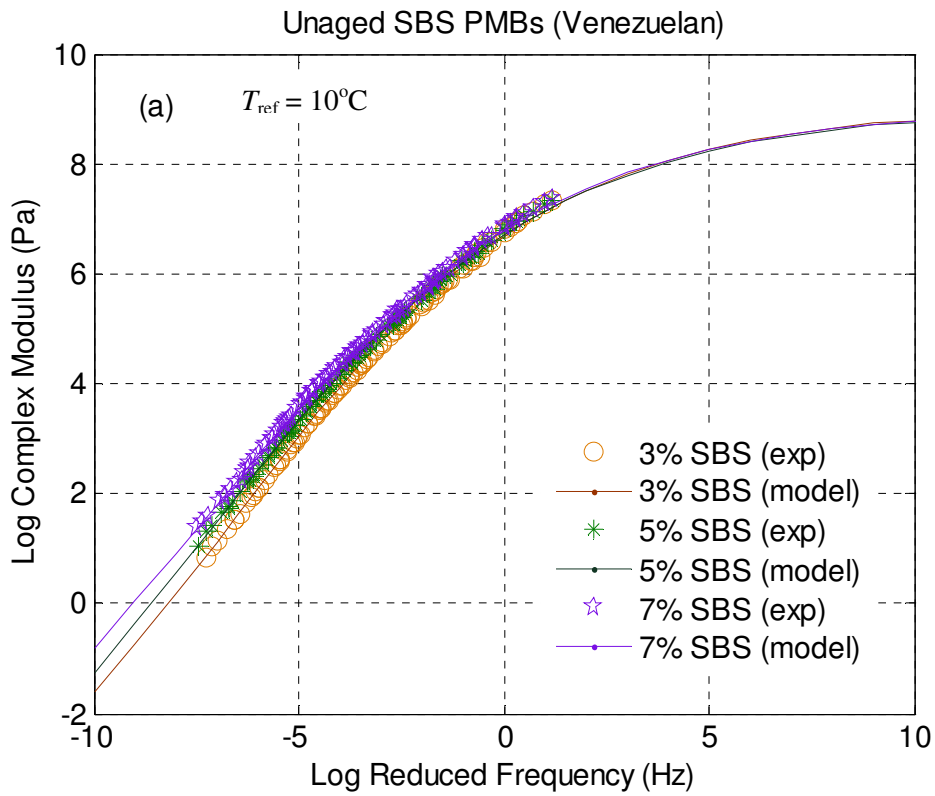


Fig. 6.4: Comparisons between measured and model of the unaged SBS PMBs data using the Sigmoidal Model

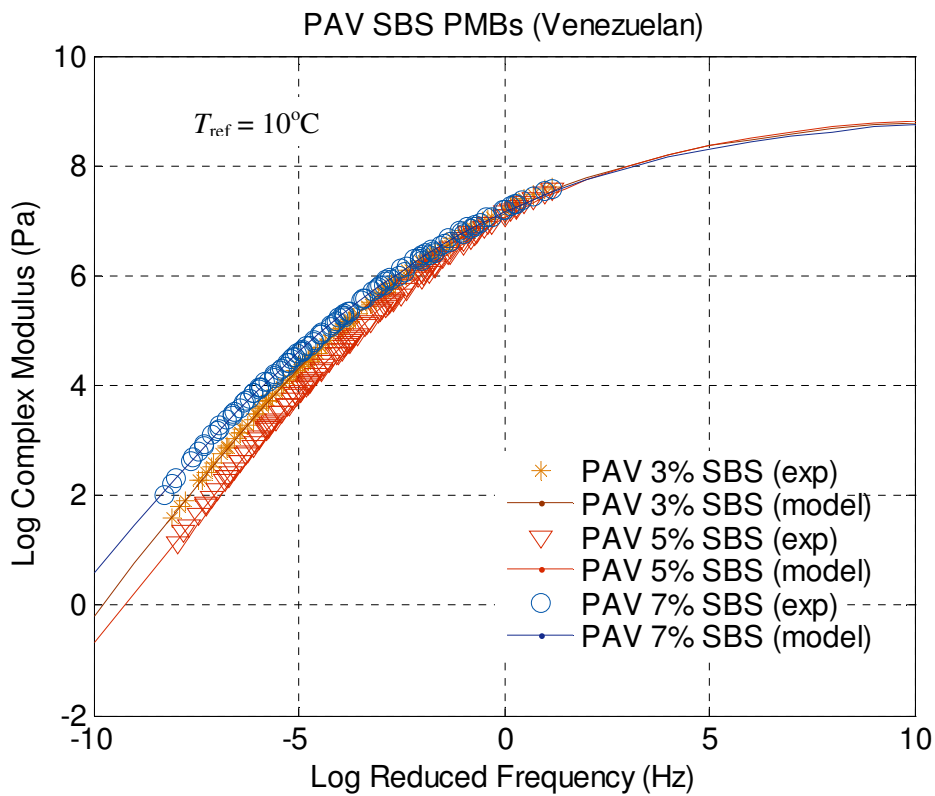


Fig. 6.5: Comparisons between measured and model of PAV SBS PMBs data using the Sigmoidal Model

### 6.3.2 The Generalised Logistic Sigmoidal Model

The Generalised Logistic Sigmoidal Model (or Richards Model) introduces the addition of  $\lambda$  parameter that allows a curve to take a non-symmetrical shape. This means – as a minimum when the additional parameter = 1, the generalised version will have the same error as the normal Sigmoidal Model. It is expected that if the Sigmoidal Model has any non-symmetric behaviour, the Generalised Logistic Sigmoidal Model will have a better fit. The following initial values are used for the modelling program;  $\delta = 0$ ,  $\beta = 1$ ,  $\gamma = 1$  and  $\lambda = 1$ . The Solver function is used with this model to minimise the sum of square errors (SSE) between measured and modelled  $|G^*|$ . The results are shown in Table 6.4. The glassy modulus is fixed equal to  $1 \times 10^9$  Pa (or equal to 9 in log scale).

Table 6.4: The Generalised Logistic Sigmoidal parameters for unmodified bitumens

Source	Condition	Parameters			
		$\delta$	$\beta$	$\gamma$	$\lambda$
Middle East	Unaged	-6.08	-1.55	0.26	0.96
	RTFOT	-7.38	-1.70	0.24	0.96
	PAV	-6.56	-2.05	0.26	0.99
Russian	Unaged	-6.58	-1.35	0.24	0.93
	RTFOT	-4.64	-1.74	0.29	1.00
	PAV	-5.04	-2.06	0.29	1.00
Venezuelan	Unaged	-11.33	-1.35	0.19	0.92
	RTFOT	-7.58	-1.63	0.24	0.97
	PAV	-9.00	-1.96	0.22	0.98

Like the Sigmoidal Model, the  $\delta$  values are observed to be negative values. The  $\delta$  in the analysis will be small since most of these materials will behave like a viscoelastic liquid only, if part of the sigmoid above the inflection point will be fitted – resulting in small values of  $\delta$ . The  $\beta$  and  $\lambda$  values are slightly decreased and increased from unaged to aged samples. This indicates that the ageing influences bitumen microstructure, where the changes in bitumen rheology will reflect the changes in structure. A slight change of  $\lambda$  values can be observed particularly from unaged to PAV samples. This indicates that the presence of  $\lambda$  plays a significant role in the shape of master curve. This parameter is also useful for fitting the viscoelastic properties of asphalt mixtures [Rowe *et al.*, 2009]. An example of the  $|G^*|$  master

curves for the unmodified bitumens (Middle East), unaged and aged samples, is shown in Fig. 6.6.

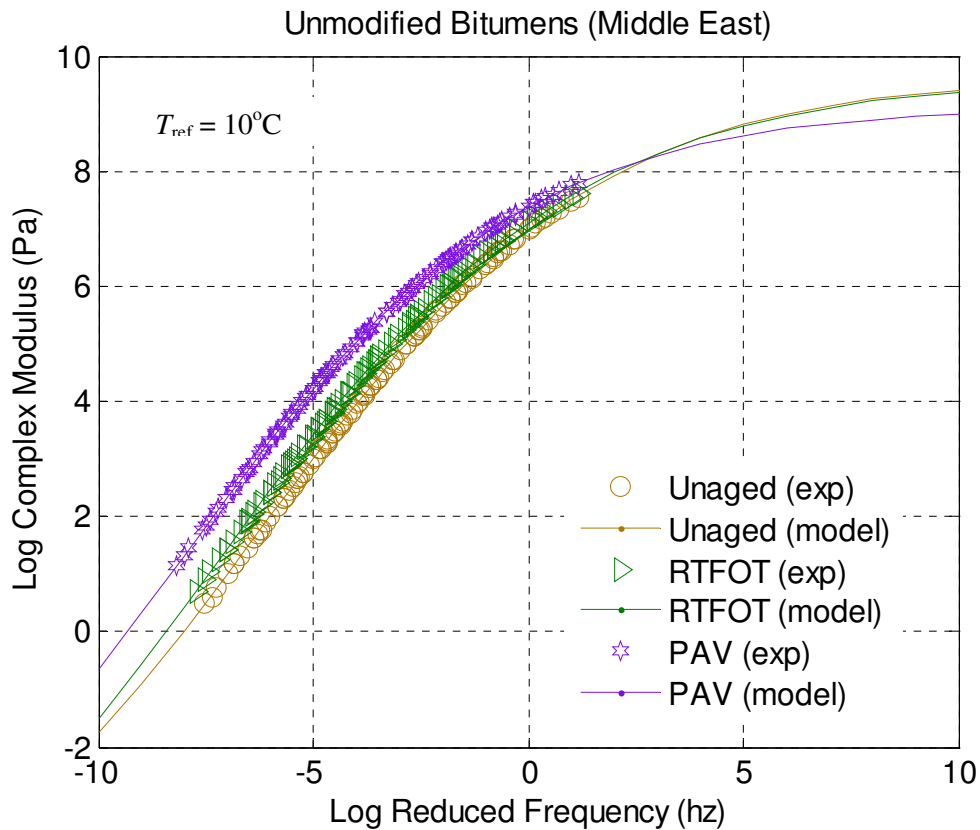


Fig. 6.6: Comparisons between measured and model of the unaged and aged unmodified bitumen data using the Generalised Logistic Sigmoidal Model

Table 6.5 shows the Generalised Logistic Sigmoidal Model parameters for the EVA PMBs. Similar discussion is made with the unmodified bitumens, where the  $\delta$  values are found to be negative. The anomaly is detected since this model is not able to describe the presence of the "waves" in the EVA  $|G^*|$  master curve particularly at intermediate to high temperatures, as shown in Fig. 6.7. This affects the inconsistency of  $\gamma$  and  $\lambda$  values. This EVA PMB does not behave not as a thermorheologically simple material. However, as the temperature increases, the curve reverts back to a unit slope associated with the Newtonian asymptote found for unmodified bitumens. The  $\beta$  values are observed to decrease from the unaged to the aged samples due to ageing.

Table 6.5: The Generalised Logistic Sigmoidal parameters for EVA PMBs

Source	Condition	Modifier	%	Parameters			
				$\delta$	$\beta$	$\gamma$	$\lambda$
Middle East	Unaged	EVA	3	-12.45	-1.78	0.19	0.95
			5	-15.34	-2.03	0.18	0.97
			7	-33.67	-2.63	0.15	0.98
	RTFOT		3	-8.60	-1.97	0.23	0.98
			5	-12.26	-2.24	0.21	0.99
			7	-111.55	-3.85	0.14	0.99
	PAV		3	-8.85	-2.31	0.23	1.00
			5	-21.18	-2.69	0.18	0.99
			7	-117.77	-4.08	0.14	1.00
Russian	Unaged	3	-14.15	-1.40	0.15	0.89	
		5	-53.70	-2.31	0.10	0.94	
		7	-77.83	-3.16	0.11	0.98	
	RTFOT	5	-26.56	-2.29	0.15	0.96	
		7	-177.11	-4.14	0.12	0.99	
	PAV	5	-21.16	-2.52	0.17	0.98	
7		-90.97	-3.71	0.14	0.99		
Venezuelan	Unaged	3	-11.19	-1.60	0.19	0.95	
		5	-73.75	-2.94	0.12	0.98	
		7	-84.62	-3.28	0.12	0.99	
	RTFOT	5	-129.12	-3.73	0.13	0.99	
		7	-126.06	-3.83	0.12	1.00	
	PAV	5	-28.65	-2.56	0.14	0.98	
7		-77.66	-3.50	0.13	0.99		

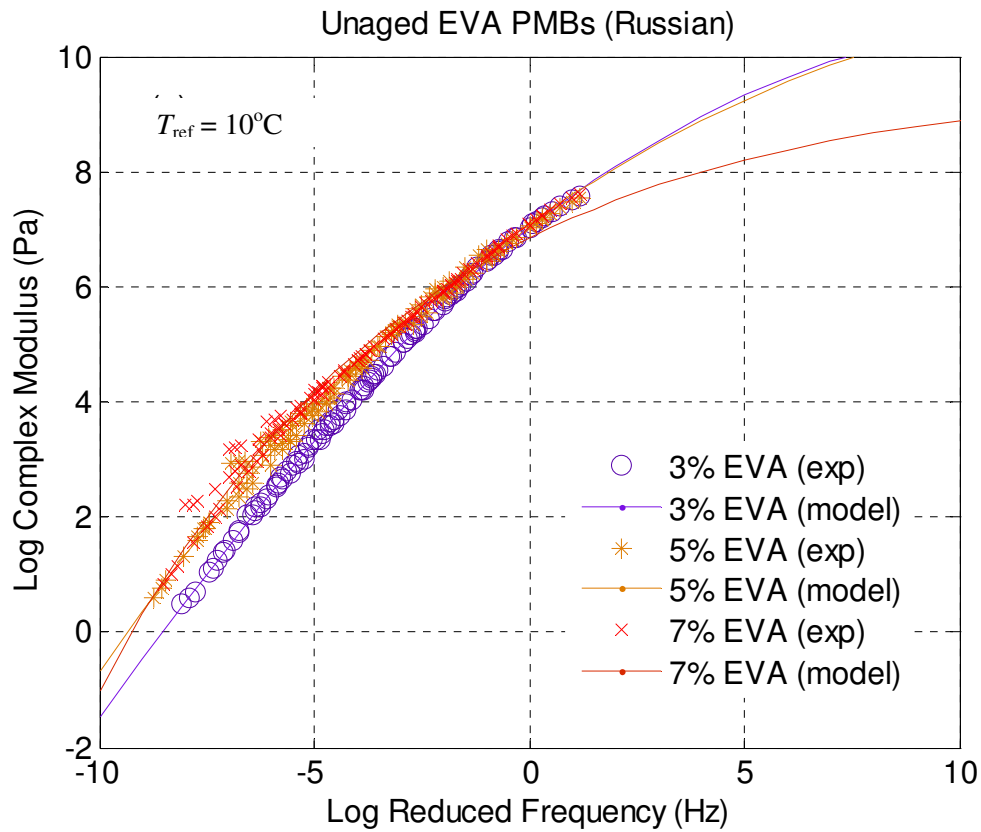


Fig. 6.7: Comparisons between measured and model of the unaged EVA PMBs data using the Generalised Logistic Sigmoidal Model

Like the EVA PMBs, the  $\delta$ ,  $\beta$ ,  $\gamma$  and  $\lambda$  values are inconsistent for the SBS PMBs, as shown in Table 6.6. This could be explained by the presence of the elastomeric behaviour of SBS. As discussed by Airey [1997, 2002a], the effect of ageing on the polymer dominant regions of behaviour for the SBS PMBs relate to a shifting of the rheological properties towards greater viscous response as a result of the thermo-oxidative degradation of the SBS polymer (Fig. 6.8).

Table 6.6: The Generalised Logistic Sigmoidal parameters for SBS PMBs

Source	Condition	Modifier	%	Parameters			
				$\delta$	$\beta$	$\gamma$	$\lambda$
Russian	Unaged	SBS	3	-2.86	-1.49	0.30	0.99
			5	-3.23	-1.20	0.25	0.94
			7	-0.22	-1.36	0.34	1.04
	RTFOT		3	-6.02	-1.59	0.24	0.95
			5	-6.03	-1.59	0.24	0.95
			7	-60.68	-2.79	0.12	0.97
	PAV		3	-11.30	-2.09	0.20	0.97
			5	-17.91	-2.25	0.17	0.97
			7	-46.64	-2.78	0.13	0.97
Venezuela	Unaged	3	-12.85	-1.55	0.18	0.93	
		5	-18.65	-1.75	0.15	0.94	
		7	-12.07	-1.66	0.18	0.95	
	RTFOT	3	-29.43	-2.11	0.14	0.95	
		5	-37.67	-2.33	0.13	0.96	
		7	-81.69	-3.07	0.12	0.98	
	PAV	3	-21.18	-2.18	0.16	0.96	
		5	-15.21	-1.79	0.17	0.94	
		7	-60.06	-2.84	0.11	0.97	

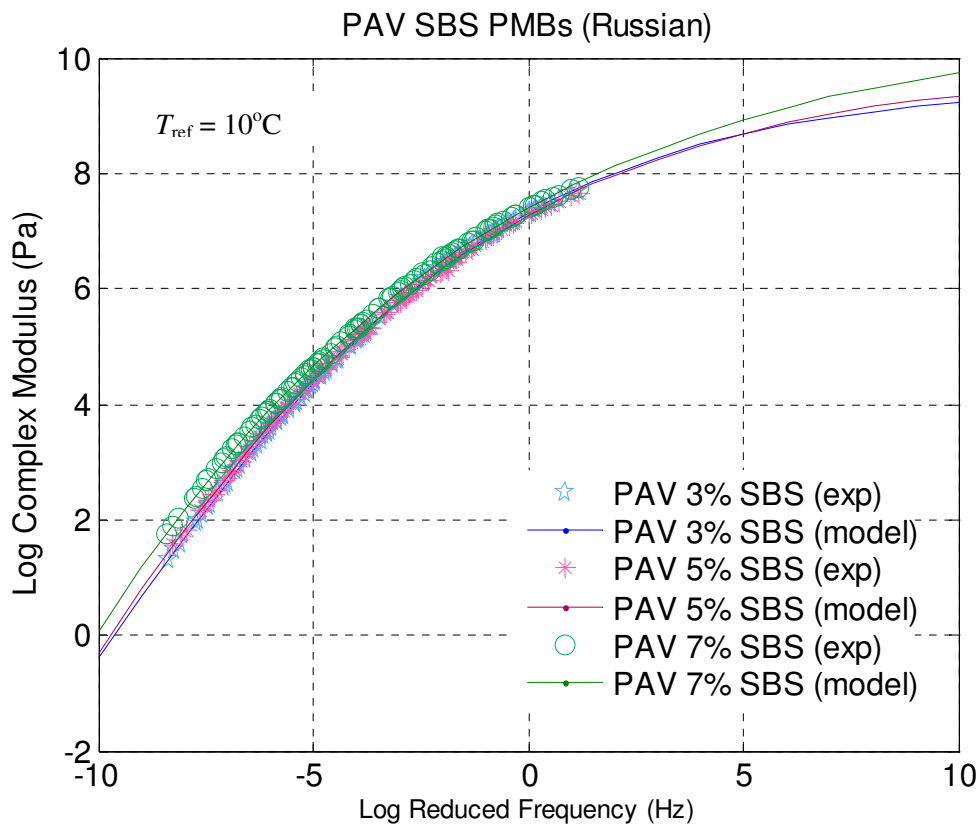


Fig. 6.8: Comparisons between measured and model of PAV SBS PMBs data using the Generalised Logistic Sigmoidal Model

### 6.3.3 Christensen and Anderson (CA) Model

Stastna *et al.* [1997] used the CA Model in their study and fixed  $G_g$  value at  $1.1 \times 10^9$  Pa and left  $\omega_c$  and  $R$  as free parameters. However, they found that the model overestimated  $|G^*|$  at high frequencies and/or low temperatures. Later, they allowed  $G_g$  to be a free parameter and observed that the overall fits were better than the one with fixed  $G_g$ , with the new  $G_g$  value being approximately  $0.4 \times 10^9$  Pa. In the initial work, the  $G_g$  values are set by the Solver function. However,  $|G^*|$  values at low temperatures and/or high frequencies underestimate  $G_g$ . Therefore the  $G_g$  value in this study is taken as  $1 \times 10^9$  Pa to avoid the underestimation of its value during the optimisation process. The model parameter values for unaged and aged unmodified bitumens are shown in Table 6.7. Meanwhile, Fig. 6.9 shows an example of modelling the complex modulus master curve using the CA Model.

Table 6.7: The CA Model parameters for unmodified bitumens

Source	Condition	Parameters			
		$G_g (\times 10^9)$	Log 2	$\omega_c$	$R$
Middle East	Unaged	1.00	0.30	1.36	10.79
	RTFOT	1.00	0.30	1.48	4.47
	PAV	1.00	0.30	1.67	0.58
Russian	Unaged	1.00	0.30	1.29	18.55
	RTFOT	1.00	0.30	1.43	7.19
	PAV	1.00	0.30	1.55	0.98
Venezuelan	Unaged	1.00	0.30	1.33	43.28
	RTFOT	1.00	0.30	1.55	10.05
	PAV	1.00	0.30	1.79	0.98

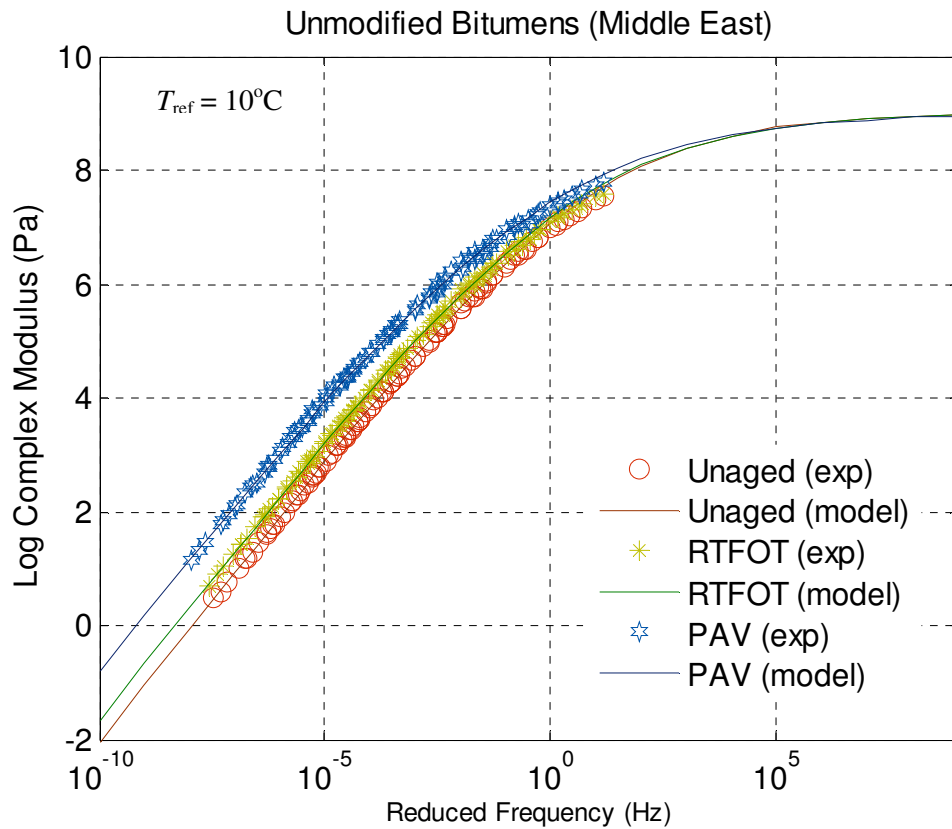


Fig. 6.9: Comparisons between measured and descriptive unmodified bitumens (unaged and aged) data using the CA Model

Table 6.8 shows the CA Model parameter values for the unaged and aged EVA PMBs. Similar observations have also been made on the SBS PMBs (Table 6.9). The  $\omega_c$  values are increased from unaged to aged samples, from 3–7% modification. This indicates that the samples become harder as the modification increases. On the other hand, the width of the relaxation spectrum becomes smaller. This behaviour supports some authors who relate  $R$  to the binder asphaltene content, finding that it reduces as those polar molecules increase [Silva *et al.*, 2004]. However, like the previous models, the CA Model is not able to describe the presence of special elements such as the semi-crystalline structure in the EVA PMBs. This is shown in Fig. 6.10.

Table 6.8: The CA Model parameters for the EVA PMBs

Source	Condition	Modifier	%	Parameter(s)			
				$G_g (\times 10^9)$	Log 2	$\omega_c$	R
Middle East	Unaged	EVA	3	1.00	0.30	1.66	3.40
			5	1.00	0.30	2.00	0.80
			7	1.00	0.30	2.00	0.80
	RTFOT		3	1.00	0.30	1.78	1.05
			5	1.00	0.30	2.00	0.27
			7	1.00	0.30	2.36	0.07
	PAV		3	1.00	0.30	2.01	0.13
			5	1.00	0.30	2.22	0.02
			7	1.00	0.30	2.56	0.00
Russian	Unaged	3	1.00	0.30	1.78	2.51	
		5	1.00	0.30	2.42	0.18	
		7	1.00	0.30	2.80	0.02	
	RTFOT	5	1.00	0.30	2.21	0.22	
		7	1.00	0.30	2.74	0.01	
	PAV	5	1.00	0.30	2.28	0.03	
7		1.00	0.30	2.57	0.00		
Venezuela n	Unaged	3	1.00	0.30	1.80	6.25	
		5	1.00	0.30	2.24	0.74	
		7	1.00	0.30	2.74	0.11	
	RTFOT	5	1.00	0.30	2.40	0.14	
		7	1.00	0.30	2.99	0.02	
	PAV	5	1.00	0.30	2.70	0.01	
7		1.00	0.30	3.20	0.00		

Table 6.9: The CA Model parameters for the SBS PMBs

Source	Condition	Modifier	%	Parameter			
				$G_g (\times 10^9)$	Log 2	$\omega_c$	R
Russian	Unaged	SBS	3	1.00	0.30	2.02	1.51
			5	1.00	0.30	2.45	0.25
			7	1.00	0.30	3.08	0.02
	RTFOT		3	1.00	0.30	1.82	1.18
			5	1.00	0.30	1.82	1.18
			7	1.00	0.30	2.14	0.57
	PAV		3	1.00	0.30	1.97	0.20
			5	1.00	0.30	2.14	0.11
			7	1.00	0.30	2.25	0.03
Venezuelan	Unaged	3	1.00	0.30	1.78	7.53	
		5	1.00	0.30	2.03	2.45	
		7	1.00	0.30	2.21	0.83	
	RTFOT	3	1.00	0.30	1.94	2.20	
		5	1.00	0.30	2.25	0.74	
		7	1.00	0.30	2.36	0.25	
	PAV	3	1.00	0.30	2.22	0.13	
		5	1.00	0.30	1.98	0.70	
		7	1.00	0.30	2.70	0.01	

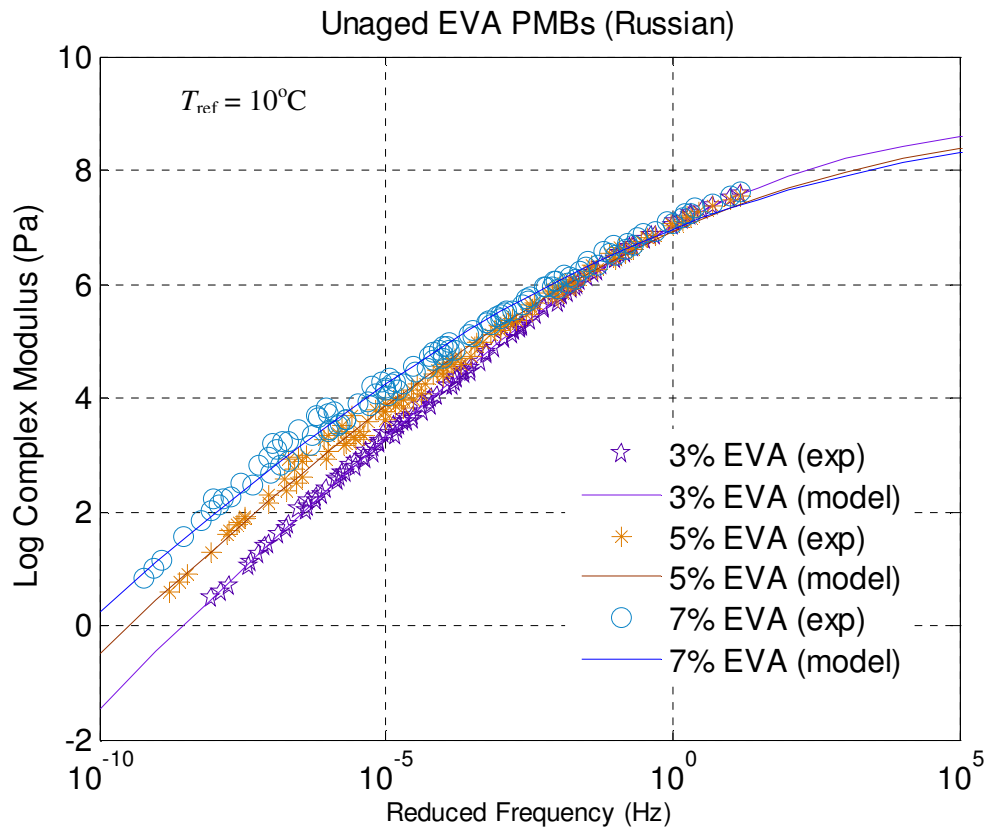


Fig. 6.10: Comparisons between measured and model of RTFOT and PAV EVA PMBs data using the CA Model

### 6.3.4 Christensen Anderson and Marasteanu (CAM) Model

The CAM Model is proposed to improve the CA Model and by comparing these, it can be noted that  $\log 2/R$  is equivalent to the  $\nu$  of the CAM Model [Silva *et al.*, 2004]. In this study, the  $G_g$  value is taken as  $1 \times 10^9$  Pa for all materials. The CAM model parameter values are shown in Table 6.10. It is observed that the  $\nu$  values decrease from unaged to aged samples. As frequency approaches zero, the PAV samples reach the  $45^\circ$  asymptote faster than unaged bitumens. Silva *et al.* [2004] observed that the  $\nu$  values for two AC-20<sup>1</sup> bitumens (low and high asphaltene contents) were 0.2568 and 0.2068. This result is expected because the unmodified bitumens used in these two studies are different.  $R$  increases from unaged to aged unmodified bitumens, suggesting that the asphaltene content increases. In the CAM Model, the  $R$  values are opposite compared to the CA Model

<sup>1</sup> AC-20 is a bitumen grade which is specified by the original viscosity at 60°C (140°F) poise for use in pavement construction.

where higher values of  $R$  indicate a smaller width of the relaxation spectrum. Meanwhile, the  $\omega_c$  values decrease from unaged to aged unmodified bitumens. This could be attributed to the ageing influence on the values of  $\omega_c$ . As mentioned before, ageing relatively increased the asphaltenes content. This finding is in good agreement with the work of Silva *et al.* [2004] where they found that  $\omega_c$  values for their two bitumens were 1.034 and 0.994 respectively.

Table 6.10: The CAM Model parameters for unmodified bitumens

Source	Condition	Parameters			
		$\nu$	$w$	$\omega_c$	$R$
Middle East	Unaged	0.17	1.09	1.26	1.78
	RTFOT	0.16	1.11	0.40	1.89
	PAV	0.14	1.20	0.01	2.20
Russian	Unaged	0.18	1.08	3.63	1.63
	RTFOT	0.17	1.10	0.96	1.79
	PAV	0.15	1.14	0.05	1.98
Venezuelan	Unaged	0.17	1.10	4.40	1.81
	RTFOT	0.15	1.14	0.55	2.03
	PAV	0.13	1.23	0.01	2.39

Fig. 6.10 shows an example of  $|G^*|$  master curves of a Middle East 80/100 penetration grade bitumen, unaged and aged samples. It is observed that the CAM Model is able to satisfactorily describe the rheological properties of unaged and aged unmodified bitumens.

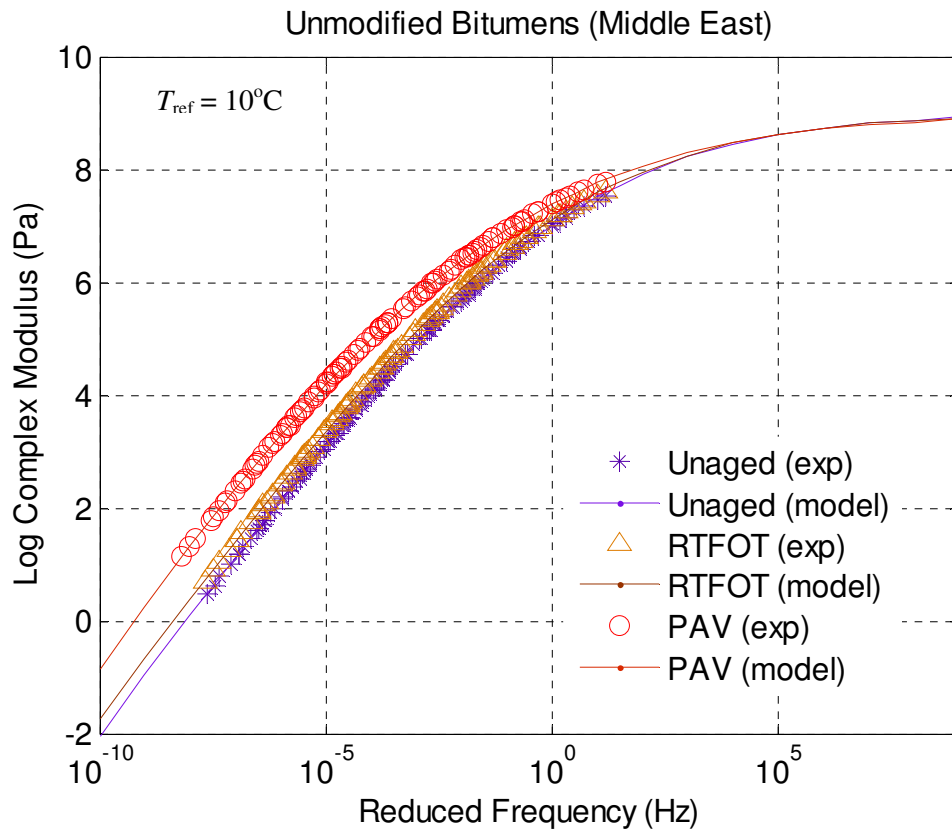


Fig. 6.11: Comparisons between measured and model of the unaged and aged unmodified bitumen data using the CAM Model

Table 6.11 shows the CAM Models parameters for unaged and aged EVA PMBs. The parameters for unaged and aged SBS PMBs are shown in Table 6.12. Except for the PAV Middle East EVA PMBs, the  $\nu$  values for all samples generally depict constant values. The  $R$  values increase as the asphaltenes content increases. In contrast,  $w$  decreases from 3–7% modification, showing that the 3% PMB reaches the 45° asymptote faster than the 7% PMB. However, the CAM Model is also not capable of describing the inconsistencies of PMBs data, as shown in Fig. 6.12.

Table 6.11: The CAM Model parameters for the EVA PMBs

Source	Condition	Modifier	%	Parameters			
				$\nu$	$w$	$\omega_c$	$R$
Middle East	Unaged	EVA	3	0.16	1.07	0.94	1.85
			5	0.16	1.00	0.96	1.92
			7	0.16	0.95	0.95	1.91
	RTFOT		3	0.17	1.02	0.94	1.76
			5	0.17	0.96	0.94	1.75
			7	0.15	0.91	0.94	1.98
	PAV		3	0.20	0.93	0.94	1.68
			5	0.14	0.97	0.94	2.10
			7	0.15	0.84	0.45	1.98
Russian	Unaged	3	0.16	1.01	1.75	1.85	
		5	0.14	0.93	0.96	2.10	
		7	0.13	0.83	0.97	2.31	
	RTFOT	5	0.15	0.95	0.94	1.96	
		7	0.14	0.84	0.96	2.12	
	PAV	5	0.17	0.86	0.90	1.82	
7		0.16	0.81	0.94	1.87		
Venezuelan	Unaged	3	0.14	1.12	0.42	2.22	
		5	0.14	0.97	0.97	2.15	
		7	0.12	0.91	0.96	2.47	
	RTFOT	5	0.14	0.92	0.97	2.10	
		7	0.12	0.84	0.97	2.54	
	PAV	5	0.15	0.82	0.95	2.07	
		7	0.13	0.74	0.95	2.33	

Table 6.12: The CAM Model parameters for the SBS PMBs

Source	Condition	Modifier	%	Parameters			
				$\nu$	$w$	$\omega_c$	$R$
Russian	Unaged	SBS	3	0.14	1.00	1.09	2.10
			5	0.14	0.92	1.50	2.20
			7	0.12	0.84	1.39	2.60
	RTFOT		3	0.17	1.00	1.17	1.82
			5	0.17	1.00	1.17	1.82
			7	0.15	0.99	0.96	2.04
	PAV		3	0.17	0.95	0.93	1.70
			5	0.17	0.91	0.95	1.82
			7	0.17	0.88	0.93	1.77
Venezuelan	Unaged	3	0.13	1.16	0.22	2.31	
		5	0.13	1.11	0.19	2.38	
		7	0.13	1.06	0.19	2.40	
	RTFOT	3	0.15	1.04	0.97	2.04	
		5	0.14	0.99	0.97	2.20	
		7	0.14	0.93	0.97	2.16	
	PAV	3	0.16	0.93	0.95	1.92	
		5	0.16	1.00	0.89	1.94	
		7	0.14	0.84	0.97	2.12	

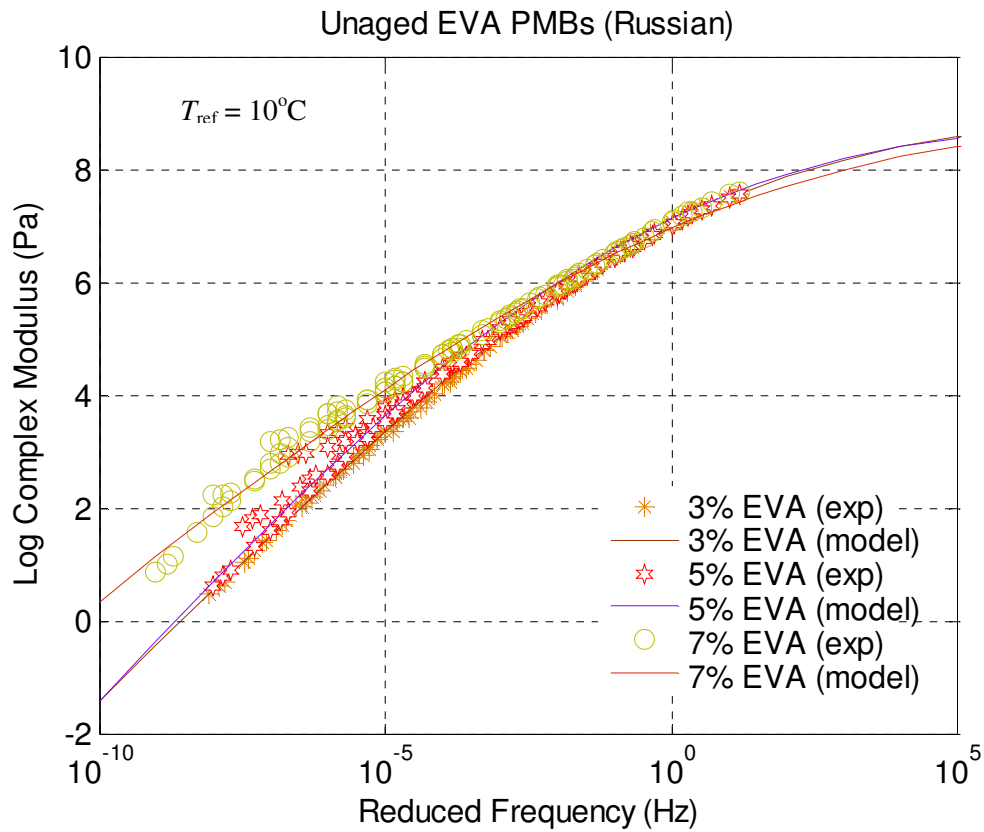


Fig. 6.12: Comparisons between measured and model of unaged EVA PMBs data using the CAM Model

It is worth mentioning that Marasteanu [1999] found the CAM Model improves the curve fitting particularly at higher and lower temperatures. This phenomenon is shown in Fig. 6.13 where the descriptive data at low temperatures and/or high frequencies are improved using the CAM Model compared to the CA Model. Silva *et al.* [2004] observed that this model did not fit  $|G^*|$  master curves really well at both extreme temperatures. It is believed that the use of different sources of binders plays a significant role in modelling work since different materials yield different chemical compositions and different rheological properties [Silva *et al.*, 2004].

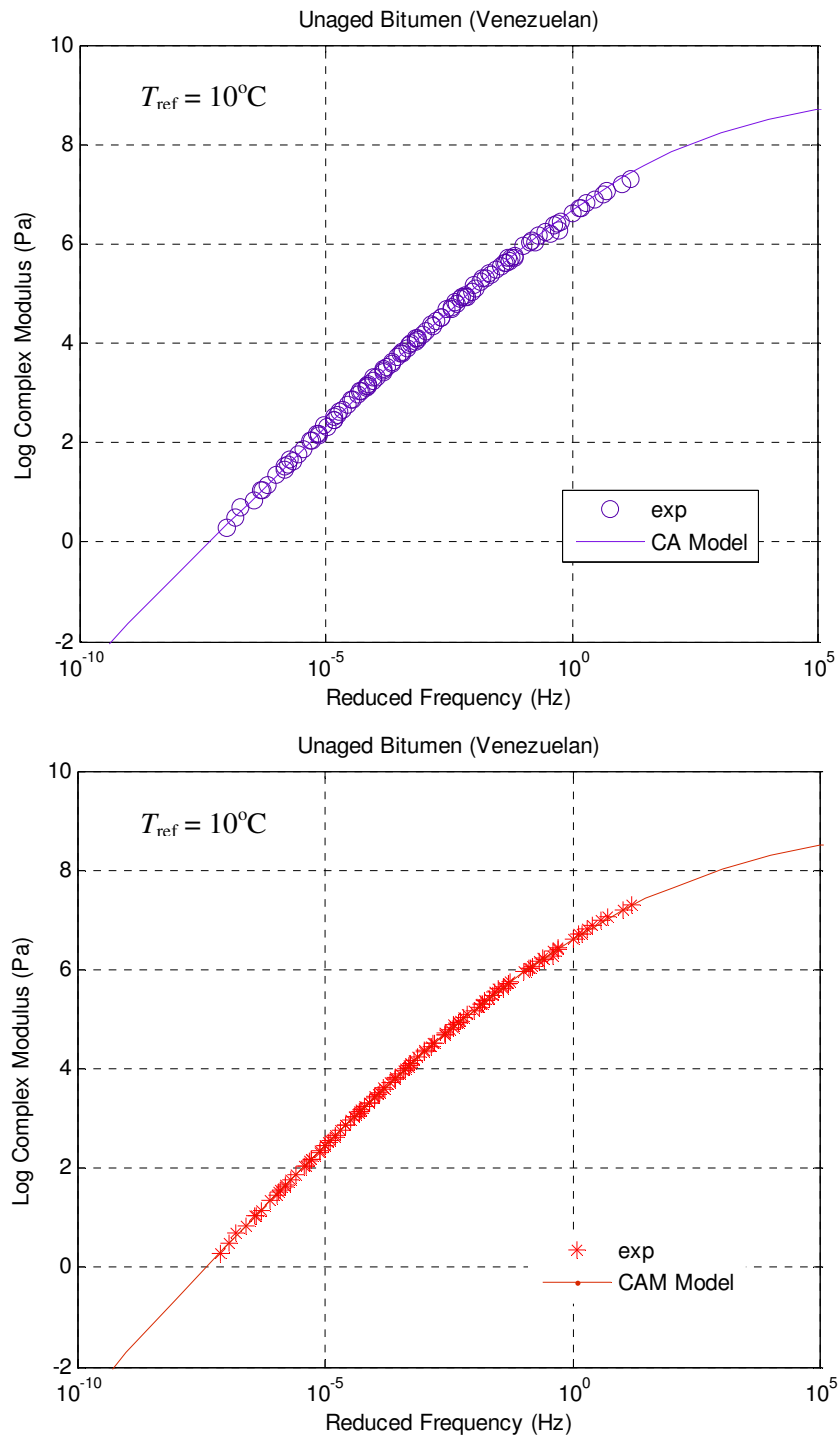


Fig. 6.13: Comparisons between measured and model of unaged unmodified bitumen data using the CA and CAM Models

An example of  $|G^*|$  master curves for the unaged and PAV Venezuelan SBS PMBs are shown in Figs 6.14 and 6.15 respectively. No unusual results can be observed from these samples. Therefore, these are thermo-rheological simple materials.

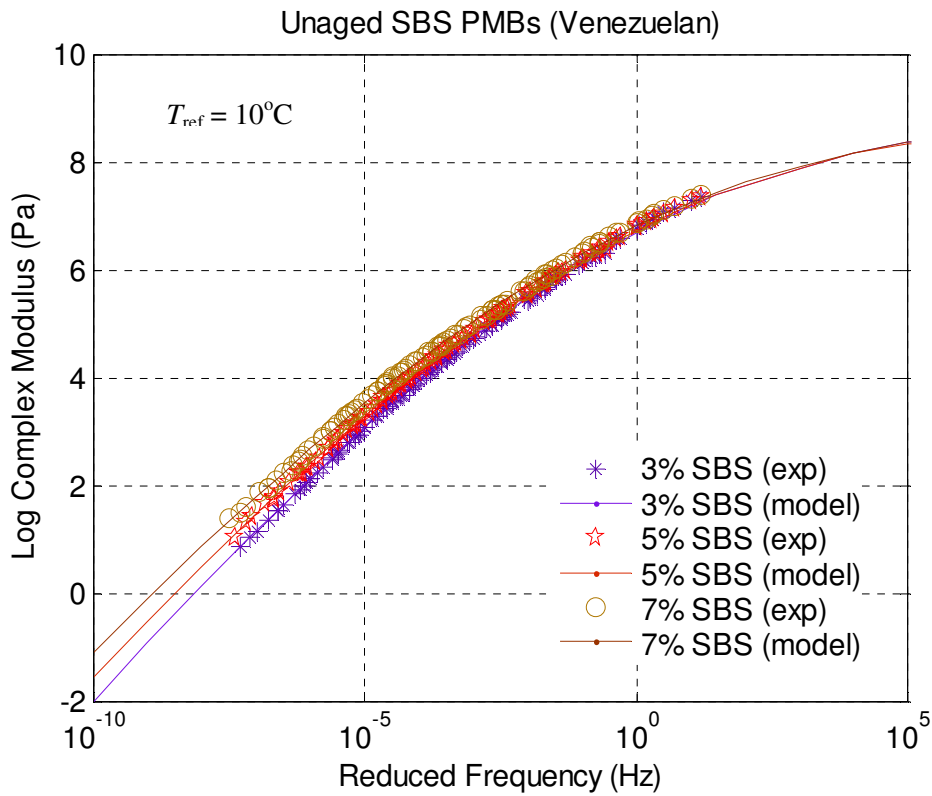


Fig. 6.14: Comparisons between measured and model of unaged SBS PMBs data using the CAM Model

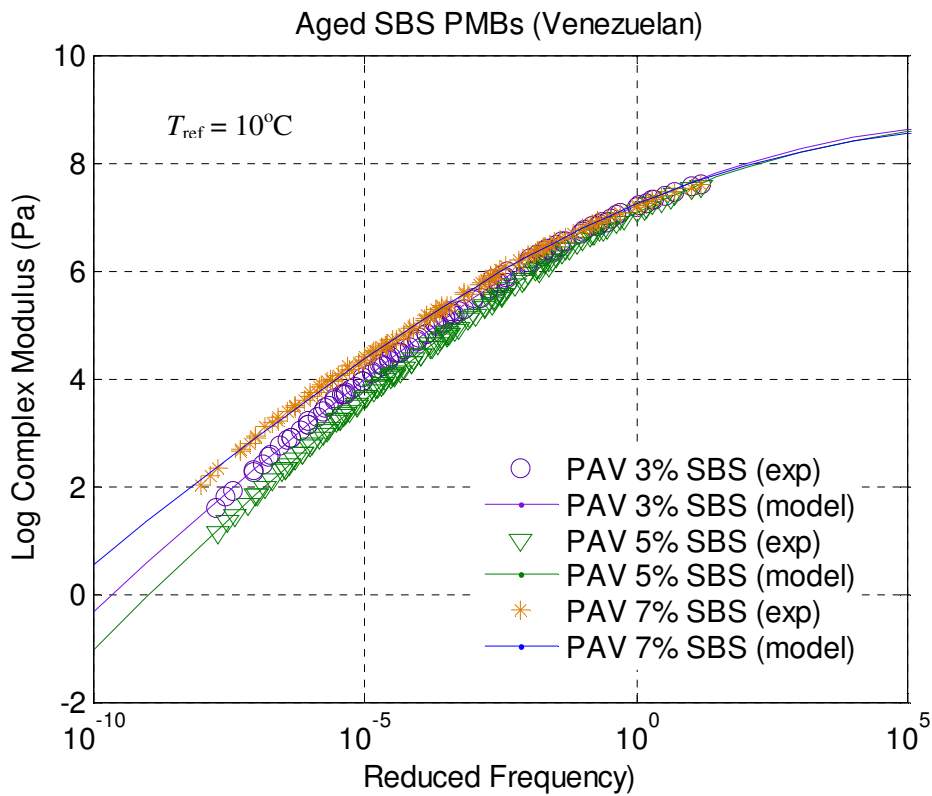


Fig. 6.15: Comparisons between measured and model of PAV SBS PMBs data using the CAM Model

### 6.5.5 Statistical analysis

Comparisons between measured and model  $|G^*|$  for unmodified bitumens and PMBs, unaged and aged samples, are graphically shown in Figs 6.16 and 6.17. These plots are intended to visually and qualitatively show the agreement between measured and descriptive values and to display any errors associated with the models and/or materials combinations [Molinas and Wu, 2000]. No obvious differences can be observed graphically for the unaged and aged bitumens, where all the samples show similar consistencies (Fig. 6.16). In Fig. 6.17, the Sigmoidal Model, the Generalised Logistic Sigmoidal Model and the CAM Model show outstanding correlations between measured and descriptive data. The CA Model slightly over-estimated the measured  $|G^*|$  at high temperatures. For the aged PMBs, all the results are graphically consistent.

Tables 6.13 to 6.19 show the SSE values for the unaged and aged unmodified and PMBs. It is observed that the Generalised Logistic Sigmoidal Model shows the most consistent results for all the studied unaged and aged samples. Meanwhile on the other hand, the CA Model shows the least SSE correlation between measured and model data. The SSE values for the Sigmoidal Model and CAM Model are inconsistent. In general, the Sigmoidal Model shows the lower SSE values of unaged and aged EVA PMBs compared to the CAM Model. However, for the unaged and RTFOT SBS PMBs, both of these models show a comparable result. And for the PAV SBS PMBs, the Sigmoidal Model shows a smaller SSE values compared to the CAM Model.

To evaluate the performance of the models studied, a correlation between measured and descriptive  $|G^*|$  is further assessed using the goodness-of-fit statistics. The ratio of standard error of estimation and standard error of deviation ( $S_e/S_y$ ) and coefficient of correlations ( $R^2$ ) goodness-of-fit statistics showed that all the models used in this study showed excellent correlations. An analysis is also done by means of the discrepancy ratio ( $r_i$ ), average geometric deviation ( $AGD$ ) and mean normalised error ( $MNE$ ) goodness-of-fit statistics. The  $r_i$  is used to observe the calculated data dispersion from the equality line. In this study, the interval of 0.99–1.01 from the equality line was used until  $r_i$  reaches an interval of 0.95–1.05. Table

6.20 shows the goodness-of-fit statistics for unaged and aged unmodified bitumens in general. It is observed that all of the models studied show good correlations with  $r_i$  equal to 0.95–1.05. This observation inferred that all models used in this study are able to satisfactorily describe the rheological properties of the unaged and aged unmodified bitumens.

For the unaged unmodified bitumens, the Generalised Logistic Sigmoidal Model shows the most outstanding correlation between measured and calculated  $|G^*|$  with the smallest and highest values of  $AGD$  and  $MNE$ , respectively. It is followed by the Sigmoidal Model, CAM Model and CA Model. For the aged unmodified bitumens, the Sigmoidal, Generalised Logistic Sigmoidal Model and CAM Model show the most outstanding correlation with 0.95–1.05 of  $r_i$ . However, it also can be seen that the CA Model data dispersed closely to the equality line. The Generalised Logistic Sigmoidal Model shows the most outstanding correlation with low  $AGD$  and high  $MNE$  values indicating that the presence of  $\lambda$  plays an important role for the aged samples. Meanwhile the Sigmoidal Model and CAM Model also described the measured data really well.

Table 6.21 shows the goodness-of-fit statistics for unaged and aged PMBs in general. It is observed that for the unaged PMB, the Generalised Logistic Sigmoidal Model and Sigmoidal Model show comparable result at the  $r_i$  of 0.95–1.05, followed by the CAM Model and CA Model. The Sigmoidal Model describes satisfactorily the properties of the PMBs with the lowest  $AGD$  and the highest  $MNE$  values. The CA Model, originally developed for unmodified bitumens was observed not to be suitable for the unaged PMBs, particularly of highly modified binders. The Generalised Logistic Sigmoidal Model shows the most outstanding correlation in terms of  $MNE$  for the aged PMBs, even though it shows comparable results for the  $r_i$  of 0.95–1.05 and  $AGD$  with the Sigmoidal Model. The CA Model also shows a good correlation with the lower and higher values of  $AGD$  and  $MNE$ , respectively. The CAM Model with five unknown parameters was unable to describe the complex behaviour of the aged PMBs. In general, it can be inferred that all the models used in this study suffer from similar drawbacks where they were unable to precisely describe the rheological properties of unaged and aged PMBs.

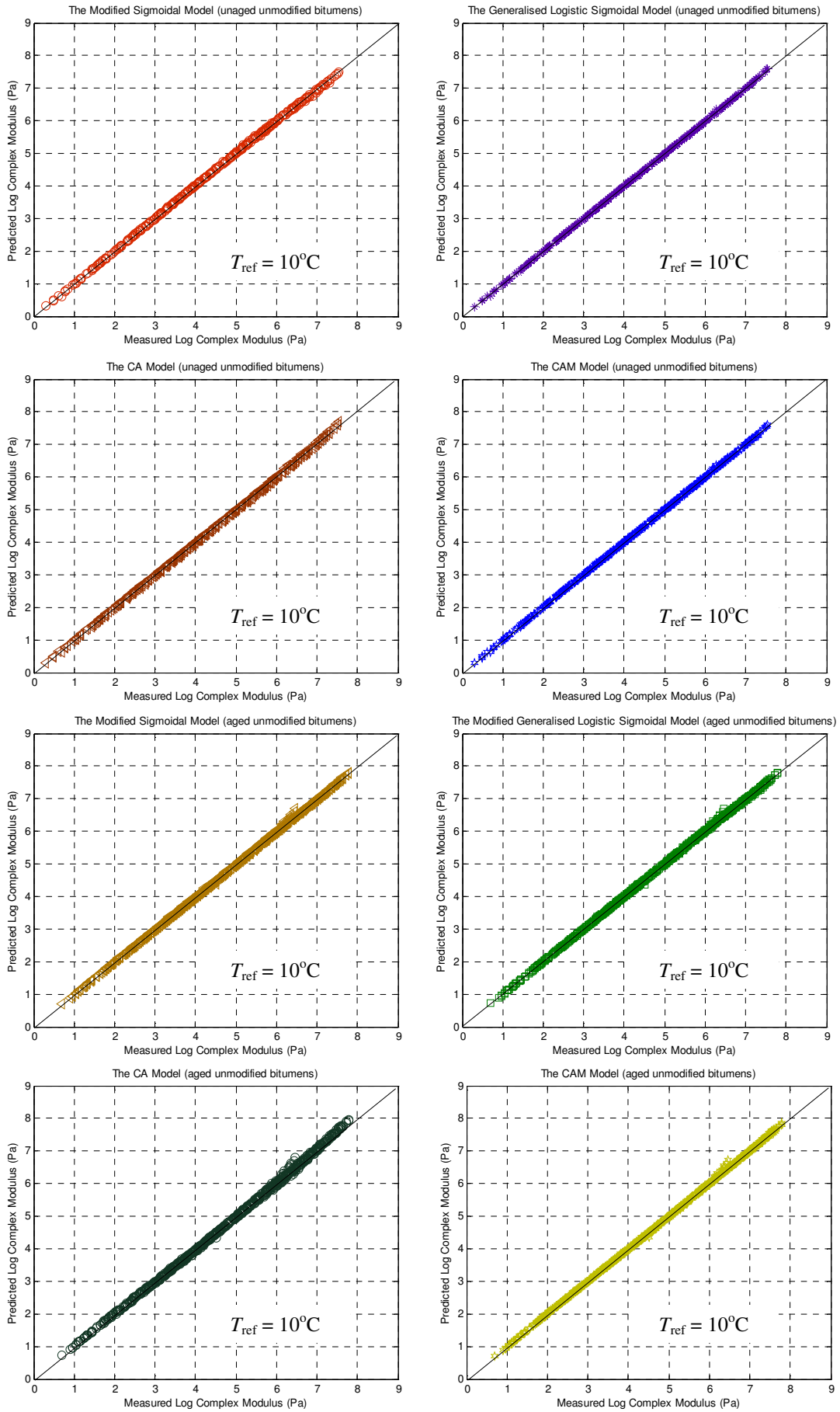


Fig. 6.16: Comparisons between measured and modelled of unmodified bitumens

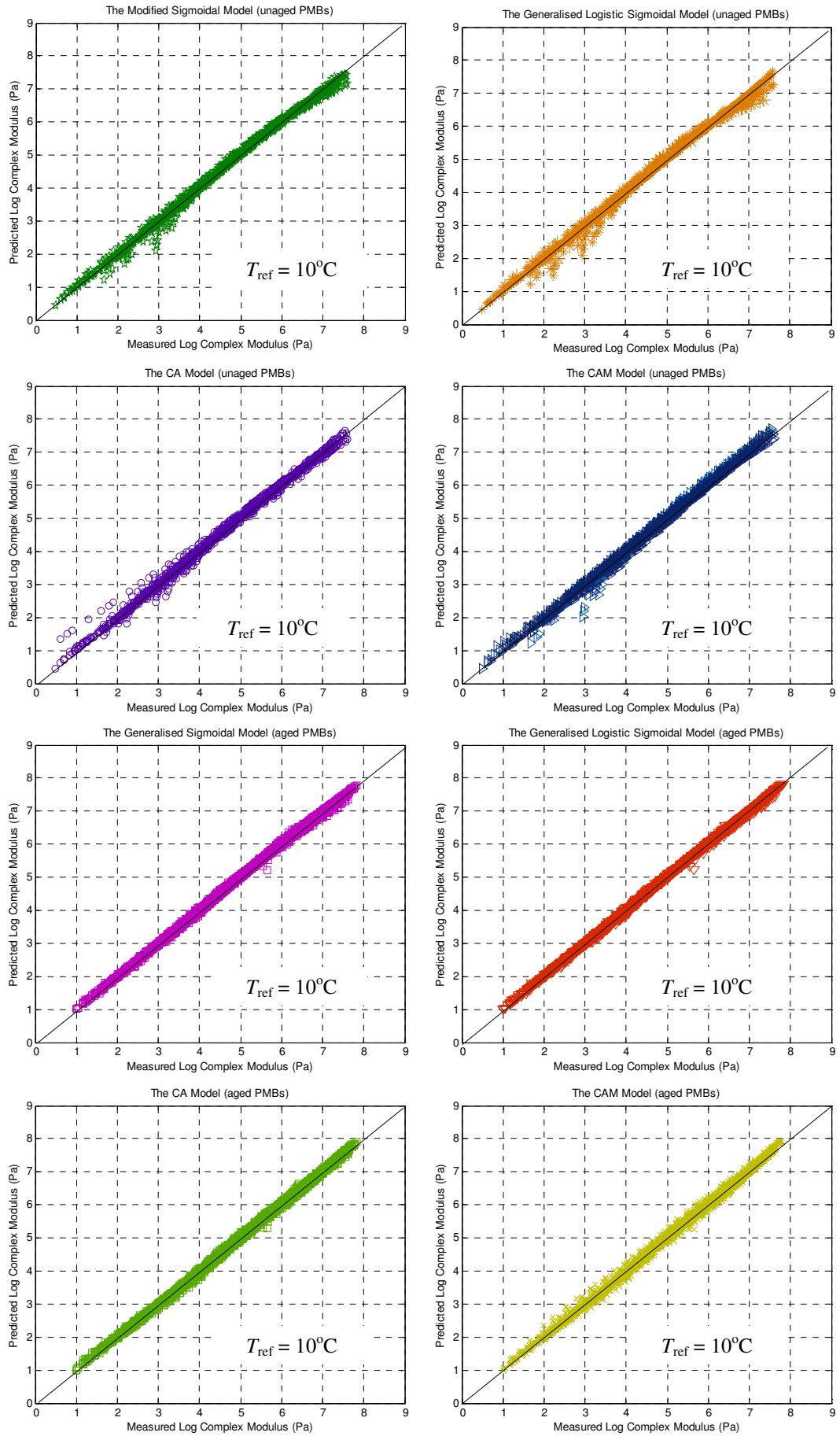


Fig. 6.17: Comparisons between measured and modelled of PMBs

Table 6.13: SSE for the unaged and aged unmodified bitumens

Model	Unaged bitumen			RTFOT Aged bitumen			PAV Aged bitumen		
	Middle East	Russian	Venezuelan	Middle East	Russian	Venezuelan	Middle East	Russian	Venezuelan
Generalised Logistic	0.0054	0.0015	0.0157	0.0020	0.0034	0.0022	0.0004	0.0021	0.0014
Sigmoidal	0.0074	0.0045	0.0221	0.0034	0.0034	0.0031	0.0005	0.0021	0.0018
CA	0.0147	0.0053	0.0358	0.0142	0.0164	0.0151	0.0144	0.0194	0.0154
CAM	0.0083	0.0019	0.0151	0.0018	0.0056	0.0027	0.0010	0.0047	0.0018

Table 6.14: SSE for the unaged EVA PMBs

Model	Unaged EVA PMBs (3%)			Unaged EVA PMBs (5%)			Unaged EVA PMBs (7%)		
	Middle East	Russian	Venezuelan	Middle East	Russian	Venezuelan	Middle East	Russian	Venezuelan
Generalised Logistic	0.0028	0.0307	0.0075	0.0032	0.1855	0.0177	0.0027	0.4819	0.0522
Sigmoidal	0.0058	0.0441	0.0100	0.0048	0.1539	0.0372	0.0043	0.1495	0.3065
CA	0.0196	0.0335	0.0157	0.0178	0.1663	0.0432	0.0178	0.1776	0.0848
CAM	0.0087	0.0333	0.0084	0.0201	0.6340	0.0520	0.0363	0.3784	0.1008

Table 6.15: SSE for the RTFOT Aged EVA PMBs

Model	RTFOT Aged EVA PMBs (3%)			RTFOT Aged EVA PMBs (5%)			RTFOT Aged EVA PMBs (7%)		
	Middle East	Russian	Venezuelan	Middle East	Russian	Venezuelan	Middle East	Russian	Venezuelan
Generalised Logistic	0.0010	-	-	0.0019	0.0134	0.0164	0.0044	0.1063	0.0438
Sigmoidal	0.0015	-	-	0.0025	0.0201	0.0607	0.0059	0.0443	0.1730
CA	0.0160	-	-	0.0205	0.0299	0.0456	0.0360	0.0741	0.0689
CAM	0.0144	-	-	0.0330	0.0393	0.0614	0.0540	0.1083	0.0908

Table 6.16: SSE for the PAV Aged EVA PMBs

Model	PAV Aged EVA PMBs (3%)			PAV Aged EVA PMBs (5%)			PAV Aged EVA PMBs (7%)		
	Middle East	Russian	Venezuelan	Middle East	Russian	Venezuelan	Middle East	Russian	Venezuelan
Generalised Logistic	0.0012	-	-	0.0009	0.0007	0.0455	0.0020	0.0029	0.0062
Sigmoidal	0.0012	-	-	0.0013	0.0014	0.0748	0.0028	0.0054	0.0176
CA	0.0151	-	-	0.0127	0.0056	0.0485	0.0147	0.0160	0.0104
CAM	0.0300	-	-	0.0164	0.0177	0.0578	0.0326	0.0434	0.0222

Table 6.17: SSE for the unaged SBS PMBs

Model	Unaged SBS PMBs (3%)		Unaged SBS PMBs (5%)		Unaged SBS PMBs (7%)	
	Russian	Venezuelan	Russian	Venezuelan	Russian	Venezuelan
Generalised Logistic Sigmoidal	0.0149	0.0040	0.0365	0.0085	0.0097	0.0120
Sigmoidal	0.0149	0.0074	0.0379	0.0128	0.0101	0.0140
CA	0.0355	0.0103	0.0623	0.0132	0.0737	0.0137
CAM	0.0372	0.0058	0.0379	0.0101	0.0533	0.0130

Table 6.18: SSE for the RTFOT aged SBS PMBs

Model	RTFOT Aged SBS PMBs (3%)		RTFOT Aged SBS PMBs (5%)		RTFOT Aged SBS PMBs (7%)	
	Russian	Venezuelan	Russian	Venezuelan	Russian	Venezuelan
Generalised Logistic Sigmoidal	0.0010	0.0027	0.0010	0.0054	0.0226	0.0056
Sigmoidal	0.0027	0.0066	0.0027	0.0079	0.0283	0.0117
CA	0.0013	0.0145	0.0013	0.0109	0.0357	0.0169
CAM	0.0013	0.0105	0.0013	0.0117	0.0382	0.0249

Table 6.19: SSE for the PAV aged SBS PMBs

Model	PAV Aged SBS PMBs (3%)		PAV Aged SBS PMBs (5%)		PAV Aged SBS PMBs (7%)	
	Russian	Venezuelan	Russian	Venezuelan	Russian	Venezuelan
Generalised Logistic Sigmoidal	0.0012	0.0020	0.0017	0.0021	0.0028	0.0040
Sigmoidal	0.0021	0.0051	0.0030	0.0071	0.0063	0.0082
CA	0.0094	0.0071	0.0090	0.0059	0.0079	0.0068
CAM	0.0194	0.0136	0.0210	0.0063	0.0199	0.0124

Table 6.20: The goodness-of-fit statistics for unmodified bitumens

Models	Condition	Discrepancy ratio, $r_i$ (%)					$S_e/S_y$	$R^2$	AGD	MNE
		0.99-1.01	0.98-1.02	0.97-1.03	0.96-1.04	0.95-1.05				
Sigmoidal	Unaged	89.13	97.52	99.07	99.38	99.38	0.0180	0.9997	1.0059	0.5819
Generalised Logistic Sigmoidal		95.65	97.83	99.07	99.38	99.38	0.0092	0.9999	1.0035	0.3446
CA		84.78	98.45	99.07	99.38	99.38	0.0170	0.9997	1.0053	0.5269
CAM		96.27	98.14	98.76	99.07	99.38	0.0102	0.9999	1.0041	0.4111
Sigmoidal	Aged	96.43	98.96	99.55	100.00	100.00	0.0139	0.9998	1.0029	0.2892
Generalised Logistic Sigmoidal		97.32	98.96	99.70	100.00	100.00	0.0119	0.9999	1.0025	0.2487
CA		59.67	92.11	98.81	99.41	99.70	0.0342	0.9988	1.0095	0.9412
CAM		95.83	99.11	99.70	99.85	100.00	0.0145	0.9998	1.0033	0.3300

Table 6.21: The goodness-of-fit statistics for PMBs

Models	Condition	Discrepancy ratio, $r_i$ (%)					$S_e/S_y$	$R^2$	AGD	MNE
		0.99-1.01	0.98-1.02	0.97-1.03	0.96-1.04	0.95-1.05				
Sigmoidal	Unaged	65.42	83.51	90.83	94.76	97.32	0.0476	0.9977	1.0115	1.1388
Generalised Logistic		74.23	86.96	92.50	95.66	97.50	0.0376	0.9986	1.0097	0.9595
Sigmoidal		50.95	75.00	85.24	90.24	92.86	0.0572	0.9967	1.0171	1.6771
CA		56.43	79.94	89.52	93.75	95.71	0.0479	0.9977	1.0141	1.3889
CAM	Aged	80.36	95.36	98.56	99.52	99.79	0.0315	0.9990	1.0067	0.6692
Modified Sigmoidal		88.61	96.29	98.62	99.42	99.76	0.0242	0.9994	1.0051	0.5071
Generalised Logistic		70.83	90.95	96.63	97.87	99.00	0.0345	0.9988	1.0087	0.8659
Sigmoidal		54.52	80.01	89.75	93.57	95.73	0.1463	0.9786	1.0173	1.6316
CA										
CAM										

### 6.3.6 Measurement Error

The DSR is often known as a useful tool to determine the elastic, viscoelastic and viscous properties of bitumen. The rheometer, however, has its limitation where it is unable to reach extreme temperatures and frequencies. In the SHRP A-369 Report, Anderson *et al.* [1994] recommended using the following guidelines although the ranges of moduli that can be successfully measured with different size plates vary according to the design (resolution and compliance) of each rheometer.

- if a complex modulus,  $|G^*|$  value is greater than  $1 \times 10^7$  Pa, it is suggested that measurements are done using either the bending beam rheometer (BBR) or torsion bar geometry.
- use the 8 mm parallel plate with a 2 mm gap when  $1 \times 10^5$  Pa  $< |G^*| < 1 \times 10^7$  Pa
- use 25 mm parallel plate with a 1 mm gap when  $1 \times 10^3 < |G^*| < 1 \times 10^5$  Pa
- use 50 mm parallel plate when  $|G^*| < 1 \times 10^3$  Pa

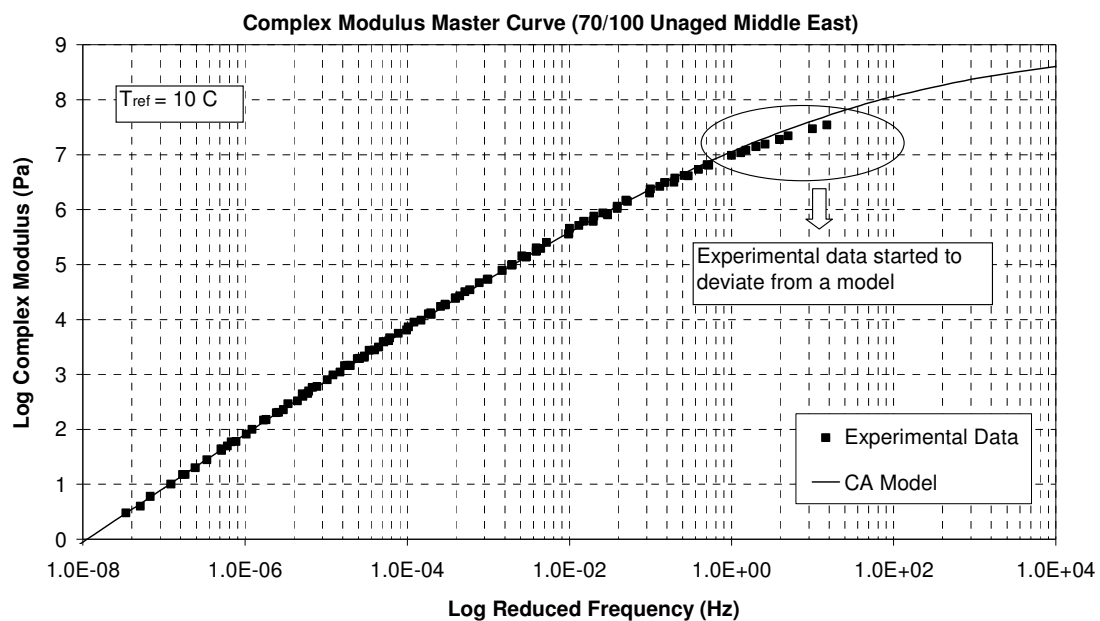


Fig. 6.18: Error from DSR measurements

Fig. 6.18 shows an example of a comparison between the CA Model and experimental data of complex modulus master curve. As can be seen from this figure, the log  $|G^*|$  measurements started to deviate from the model from  $1 \times 10^7$  Pa. The

deviation can be associated with the measurement error from the DSR. To calculate the measurement error, the following approach is taken. As previously shown in Table 6.13, the SSE of the 70/100 Middle East penetration grade bitumen is 0.01467. The experimental value of  $1 \times 10^7$  Pa and higher is deleted and the SSE value is re-calculated. By deleting these values, the new SSE value obtained is 0.01259. Therefore, the error (in percent) is calculated as the following;

$$\begin{aligned} \text{Measurement error} &= \frac{0.01467 - 0.01259}{0.01467} \\ &= 0.14208 \times 100 = 14.21\% \end{aligned}$$

The measurement error can be taken as 14.21% for the 70/100 Middle East penetration grade bitumen. The same process is done for other samples. Tables 6.22 to 6. 28 show the measurement error values for all the studied samples. It is observed that the measurement error values are affected by the selection of a model. The Generalised Logistic Sigmoidal Model shows the most consistent results for all samples, followed by the CAM Model, CA Model and Sigmoidal Model. In general, the Generalised Logistic Sigmoidal Model, the CAM Model and the CA Model satisfactorily fit the complex modulus master curves for a temperature range from 10 to 75°C. It is found that the Sigmoidal Model satisfactorily fit for a temperature range from 15 to 75°C.

Table 6.22: Measurement error (%) of the unaged and aged unmodified bitumens

Model	Unaged bitumen			RTFOT Aged bitumen			PAV Aged bitumen		
	Middle East	Russian	Venezuelan	Middle East	Russian	Venezuelan	Middle East	Russian	Venezuelan
Generalised Logistic	1.1643	13.6041	0.3590	5.6153	1.6671	6.4460	2.9920	1.6902	4.3783
Sigmoidal	7.8229	14.1125	4.3332	7.5162	2.5661	27.9123	12.2133	1.3729	23.5618
CA	14.2084	27.4090	2.2264	17.9791	16.1015	4.6118	16.7918	18.4327	6.7335
CAM	1.3244	3.3598	0.1500	12.7476	5.4561	4.0260	6.3628	7.5351	4.4823

Table 6.23: Measurement error (%) of the unaged EVA PMBs

Model	Unaged EVA PMBs (3%)			Unaged EVA PMBs (5%)			Unaged EVA PMBs (7%)		
	Middle East	Russian	Venezuelan	Middle East	Russian	Venezuelan	Middle East	Russian	Venezuelan
Generalised Logistic	0.6161	1.0934	0.7934	1.0344	0.8599	3.5093	0.60017	3.0987	6.2993
Sigmoidal	20.2007	8.6179	11.5767	16.9180	8.9834	10.0067	16.5142	12.7961	0.9720
CA	5.2633	3.3509	0.3646	3.6056	1.7057	0.2195	3.6044	3.0313	1.5928
CAM	2.0420	1.3752	1.5323	6.7428	0.2821	0.3643	8.5288	1.0144	0.6051

Table 6.24: Measurement error (%) of the RTFOT aged EVA PMBs

Model	RTFOT Aged EVA PMBs (3%)			RTFOT Aged EVA PMBs (5%)			RTFOT Aged EVA PMBs (7%)		
	Middle East	Russian	Venezuelan	Middle East	Russian	Venezuelan	Middle East	Russian	Venezuelan
Generalised Logistic	6.0644	-	-	8.1856	2.0463	5.7366	3.8670	11.2224	6.7023
Sigmoidal	27.2660	-	-	23.3747	14.8665	2.4800	16.3145	19.1773	0.9847
CA	8.7360	-	-	5.7232	0.0344	0.0530	2.8282	0.4293	1.1606
CAM	9.0959	-	-	11.5552	0.5615	1.5862	4.2228	1.4013	0.0559

Table 6.25: Measurement error (%) of the PAV aged EVA PMBs

Model	PAV Aged EVA PMBs (3%)			PAV Aged EVA PMBs (5%)			PAV Aged EVA PMBs (7%)		
	Middle East	Russian	Venezuelan	Middle East	Russian	Venezuelan	Middle East	Russian	Venezuelan
Generalised Logistic	2.0967	-	-	1.3446	2.1769	0.1079	1.1106	1.3988	2.9134
Sigmoidal	1.4782	-	-	14.1468	13.6101	0.3250	12.0261	18.6612	1.2973
CA	15.5284	-	-	7.6402	4.8671	0.2396	5.0821	2.5552	0.5263
CAM	19.6074	-	-	6.2222	10.7362	2.2669	9.1243	6.1338	2.5465

Table 6.26: Measurement error (%) of the unaged SBS PMBs

Model	Unaged SBS PMBs (3%)		Unaged SBS PMBs (5%)		Unaged SBS PMBs (7%)	
	Russian	Venezuelan	Russian	Venezuelan	Russian	Venezuelan
Generalised Logistic Sigmoidal	1.4122	1.1085	0.2466	0.3309	0.0156	0.6350
Sigmoidal	2.4307	17.8594	0.8857	9.4601	1.5334	5.4671
CA	3.2374	0.1013	3.9492	0.1281	3.1469	0.6897
CAM	2.5613	12.3963	0.9910	4.4117	1.5735	2.8477

Table 6.27: Measurement error (%) of the RTFOT aged SBS PMBs

Model	RTFOT Aged SBS PMBs (3%)		RTFOT Aged SBS PMBs (5%)		RTFOT Aged SBS PMBs (7%)	
	Russian	Venezuelan	Russian	Venezuelan	Russian	Venezuelan
Generalised Logistic Sigmoidal	8.3619	1.5553	8.4387	0.9220	0.3622	1.3771
Sigmoidal	17.7663	24.5888	17.7718	13.9019	4.0616	14.9067
CA	6.3125	0.3251	6.2948	0.0835	0.7558	0.0249
CAM	6.2005	0.1472	6.1724	0.1469	1.5552	2.3348

Table 6.28: Measurement error (%) of the PAV aged SBS PMBs

Model	PAV Aged SBS PMBs (3%)		PAV Aged SBS PMBs (5%)		PAV Aged SBS PMBs (7%)	
	Russian	Venezuelan	Russian	Venezuelan	Russian	Venezuelan
Generalised Logistic	11.2295	1.9801	5.4757	6.6165	8.5935	1.9235
Sigmoidal	6.9131	15.4206	11.6605	16.9758	10.8843	9.6364
CA	14.3978	1.0410	6.6169	0.8681	1.3608	2.3758
CAM	14.4622	4.9871	11.6903	1.1773	6.9107	4.1954

## 6.4 Summary

Based on this study, several observations can be drawn:

- In general it is observed that all the rheological models can satisfactorily describe the rheological properties of unaged and aged unmodified bitumens.
- However, the models suffer from the drawback where they are unable to describe the rheological properties of the unaged PMBs due to the presence of semi-crystalline EVA and SBS modifiers, rendering a breakdown in the time-temperature superposition principle (TTSP).
- The glassy modulus,  $G_g$ , for unaged and aged unmodified bitumens and PMBs can be taken as  $1 \times 10^9$  Pa for modelling purposes. On the other end, the elastic modulus is too small and can be neglected for bituminous binders.
- In terms of SSE, the Generalised Logistic Sigmoidal Model generally shows the best correlation between measured and modelled data, followed by the Sigmoidal Model, CAM Model and CA Model.
- When the measurement errors are taken into account, the Generalised Logistic Sigmoidal Model, the CAM and CA Model can be used for a temperature range from 10 to 75°C. A temperature range from 15 to 75°C is found suitable for the Sigmoidal Model.
- It is observed that for the unaged and aged unmodified bitumens, the Modified Generalised Logistic Sigmoidal Model shows the most outstanding correlations between measured and modelled  $|G^*|$  data, followed by the Sigmoidal, CA and CAM Models.
- For the unaged and aged polymer-modified bitumens, the Generalised Logistic Sigmoidal and Sigmoidal Models show the outstanding correlation between measured and modelled  $|G^*|$  data.
- The use of different types of bitumens plays a crucial role in modelling work, as different binders bring different chemical compositions and different rheological properties in the linear viscoelastic region. However, most of the models are basically empirical and cannot be used universally.

## 7.1 Background

In general, the rheological properties of binders can be fitted using a model [Ferry, 1980]. The models are used to describe complex modulus,  $|G^*|$ , and phase angle,  $\delta$ , master curves. The technique of the determination of the master curve is based on the time-temperature superposition principle (TTSP). A standard reference temperature ( $T_{ref}$ ) is normally selected in the range of the tested temperatures. The amount of shifting required at each temperature to form the master curve is termed the shift factor,  $a_T$  [Airey, 2002a]. Through the use of the master curve and shift factor relationships, it is possible to interpolate stiffness at an expanded range of frequencies and temperatures compared with those at which the data was collected. If functional forms are fitted to the shape of the master curve plot and to the shift factor relationship this interpolation becomes rapid and easy to apply in computer software. In addition, if a functional form with some thermodynamic basis is used then the resulting equations can be employed to extrapolate the data beyond the observed range of temperatures and frequencies [Rowe and Sharrock, 2011].

Among them, the 2S2P1D Model is found to be a unique model which it is used to fitting the rheological properties of bituminous binders and asphalt mixtures. The model was originally developed and calibrated at the *Ecole Nationale des Travaux Publics de l'Etat* (ENTPE), France using an annular shear rheometer (ASR) [Olard and Di Benedetto, 2003; Olard *et al.*, 2003; Delaporte *et al.*, 2007]. This model, based on the generalisation of the Huet-Sayegh Model, consists of seven parameters and the  $|G^*|$  equation is shown as:

$$G^*(\omega) = G_0 + \frac{G_g - G_0}{1 + \alpha(i\omega\tau)^k + (i\omega\tau)^{-h} + (i\omega\beta\tau)^{-1}} \quad (7.4)$$

where  $k$  and  $h$  are exponents with  $0 < k < h < 1$ ,  $\alpha$  is a constant,  $G_0$  is the static modulus when  $\omega \rightarrow 0$ ,  $G_g$  is the glassy modulus when  $\omega \rightarrow \infty$ . Details of the model can be found in Chapter 3.

However, the validity of this model has yet to be assessed by other types of rheometers. This study attempts to evaluate the suitability of the model to describe the rheological properties of a large dynamic shear rheometer (DSR) database. This consists of unaged and aged unmodified bitumens, polymer-modified bitumens (PMBs) and bitumen-filler mastics. Correlations between measured and modelled data are evaluated using graphical and goodness-of-fit statistical analysis methods. In this study, the model's parameters are changed using a trial-and-error method until a good master curve is obtained. The Solver function is not used in this section. Meanwhile, the model's parameters are fitted manually where the initial values of those parameters were selected based on the works done by Di Benedetto *et al.* The trial-and-error process is done using the Excel spreadsheet until the most suitable parameters are obtained. The reference temperature,  $T_{\text{ref}}$  is arbitrarily chosen in this study at a temperature of 10°C. A selective result obtained is then compared with the work of Di Benedetto *et al.*

## 7.2 Results and Discussion

### 7.2.1 Unaged unmodified bitumens

Table 7.1 shows the model parameters for different types of penetration grade of unaged unmodified bitumens used in this study. As previously mentioned, the parameters are fitted manually using a trial-and-error method until a good curve is obtained. The same parameters are used for plotting the complex modulus and phase angle master curves, a Black diagram and a Cole-Cole diagram. However, the Cole-Cole diagram is not shown here because this study did not involve measurements at very low temperatures. The unaged bitumens tend to show Newtonian behaviour at low frequencies (high temperatures).  $G_0$  is too small and

can be neglected and only six parameters of the 2S2P1D Model need to be determined. Interestingly, five of the model's parameters;  $G_g$ ,  $G_0$ ,  $k$ ,  $h$  and  $\alpha$  are the same for all samples, regardless of the penetration grade of bitumens. It is found that the  $\beta$  values for 10/20, 40/60 and 70/100 penetration grade bitumens are the same due to the fact that they have the same slope at low frequencies and high temperatures. As expected a 160/220 penetration grade bitumen with the lowest viscosity value has the smallest value of  $\beta$ . The presence of higher asphaltene contents plays a significant role to determine the  $\beta$  value. The value of  $\beta$  increases as the asphaltene content increases.

Table 7.1: The model parameters for unaged unmodified bitumens

Pen Grade	$G_0$ (Pa)	$G_g$ (Pa)	$k$	$h$	$\alpha$	$\tau$	$\beta$
10/20	0	1.00E+09	0.22	0.64	4.00	6.00E-03	90
35/50	0	1.00E+09	0.22	0.64	4.00	1.50E-03	90
40/60	0	1.00E+09	0.22	0.64	4.00	3.00E-04	90
70/100	0	1.00E+09	0.22	0.64	4.00	6.00E-05	90
160/220	0	1.00E+09	0.22	0.64	4.00	3.50E-05	45

Table 7.2 shows a comparison between the NTEC dataset and the works of Di Benedetto *et al.* [Olard and Di Benedetto, 2003; Olard *et al.*, 2003; Delaporte *et al.*, 2007]. Several values are noticeably different when examining the NTEC dataset and Di Benedetto *et al.*'s.

Table 7.2: Comparisons between NTEC and Di Benedetto *et al.*'s model parameters

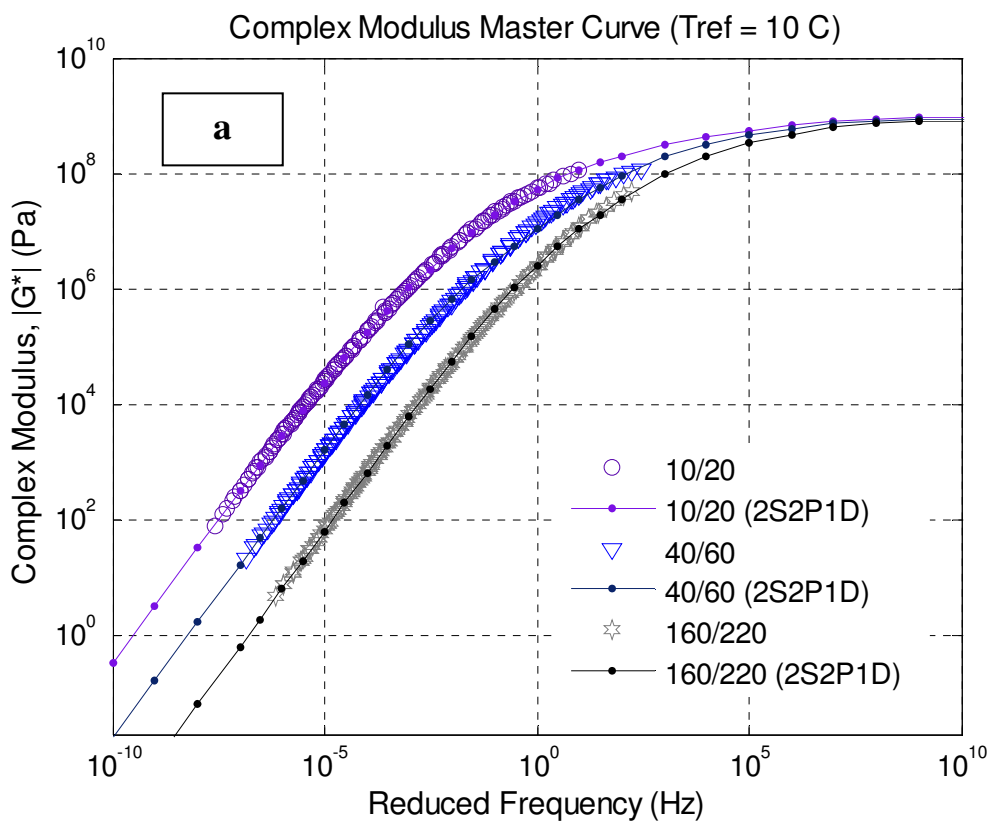
Source*	PG	$G_0$ (Pa)	$G_g$ (Pa)	$k$	$h$	$\alpha$	$\tau$	$\beta$
1	10/20	0	1.00E+09	0.22	0.64	4.00	6.00E-03	90
2		0	2.00E+09	0.19	0.52	2.20	2.50E-03	800
1	40/60	0	1.00E+09	0.22	0.64	4.00	1.00E-04	200
2	50/70	0	2.00E+09	0.18	0.55	2.00	1.90E-03	320
3	50/70	0	9.00E+08	0.21	0.55	2.30	8.00E-05	400

\*1 – NTEC, 2 – Olard *et al.* [2003], 3 – Delaporte *et al.* [2007]

For instance, the  $G_g$  values obtained by Di Benedetto *et al.* vary from  $0.9 \times 10^9$  to  $2 \times 10^9$  Pa, whilst the value of  $1 \times 10^9$  Pa had been used in this study. The  $k$  and  $h$  values are almost the same, even though a slightly higher value of  $h$  is observed. Di Benedetto *et al.* show higher and lower values of  $\beta$  and  $\delta$  compared to the NTEC dataset. These findings might be attributed to several factors. First, different crude

sources used by the respective studies might play a significant rule in influencing viscosities of the unaged unmodified bitumens. Secondly, the use of different types of rheometers may affect the precision of rheological data. Di Benedetto *et al.* used the annular shear rheometer (ASR) while the dynamic shear rheometer (DSR) is used in this study. Delaporte *et al.* [2009] showed that the use of ASR allows continuous measurements of  $|G^*|$  over 7 decades (in norm), from about  $1 \times 10^3$  to  $1 \times 10^{10}$  Pa.

It is worth mentioning that  $\alpha$  can be thought as an appropriate parameter to assess the occurrence of measurement errors of  $|G^*|$ . A higher value of  $\alpha$  indicates that  $|G^*|$  is exposed to measurement errors and vice versa. Finally, an example of the 2S2P1D Model of  $|G^*|$  and  $\delta$  master curves and the Black diagram for some of the tested unaged unmodified bitumens (10/20, 40/60 and 160/220) are presented in Fig. 7.1. From these figures, it is observed that the 2S2P1D Model satisfactorily fits the experimental results.



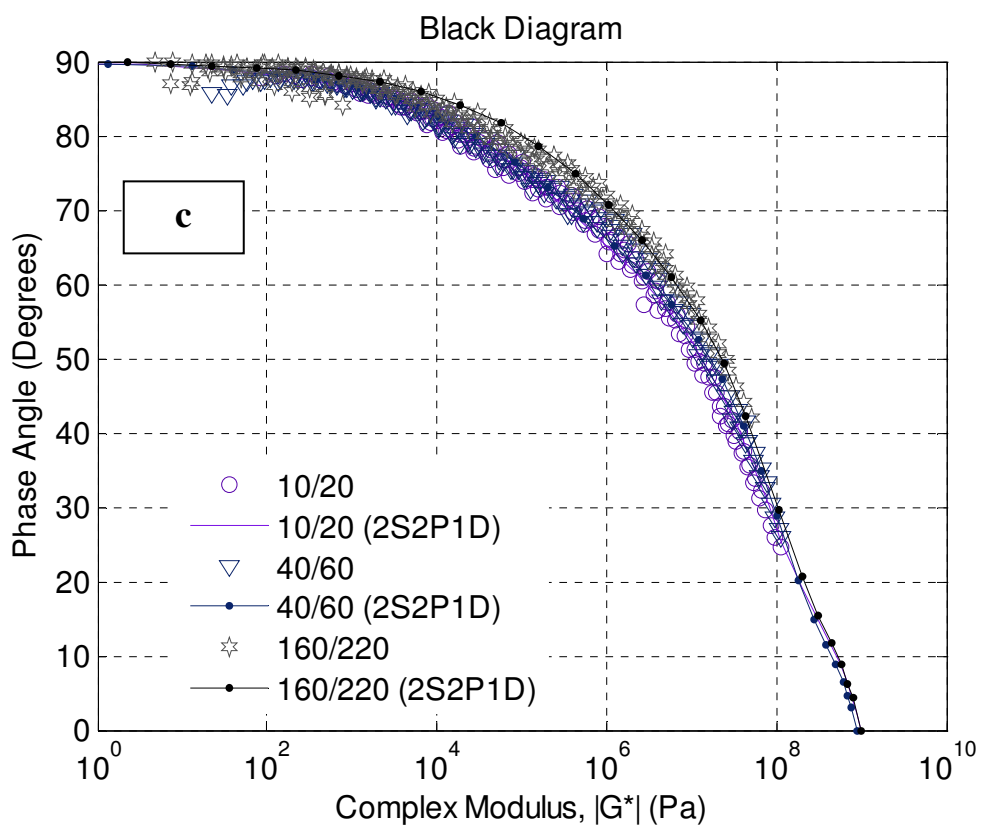
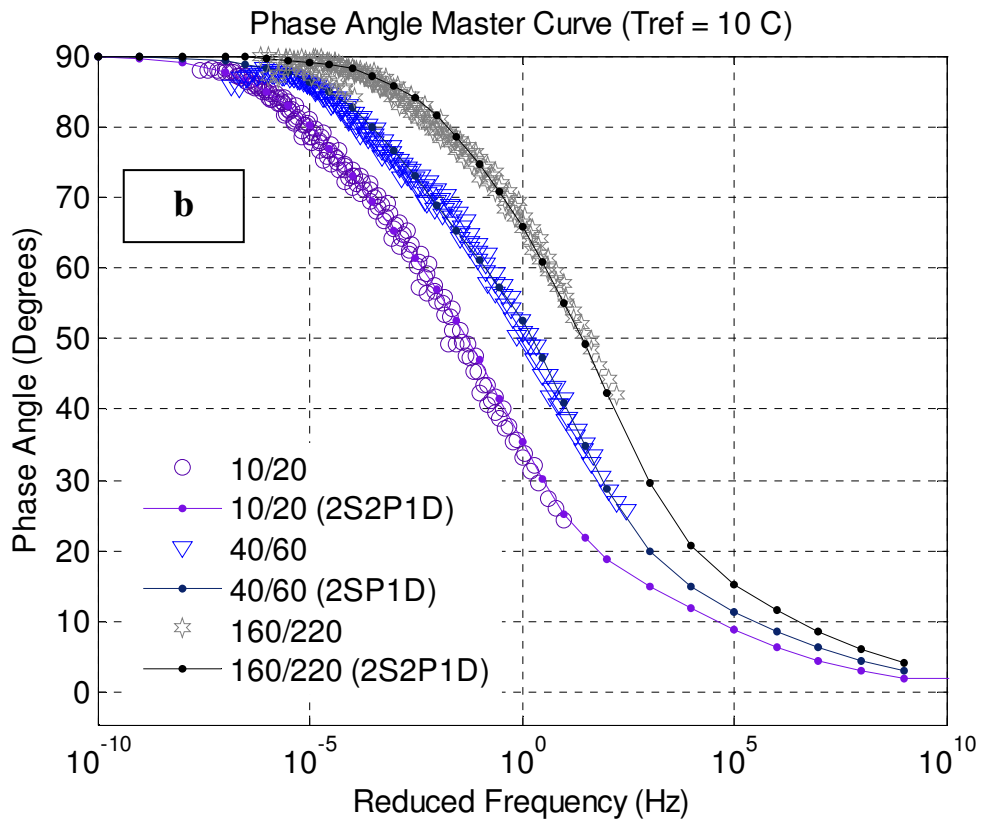


Fig. 7.1: (a) Complex modulus, (b) phase angle and (c) Black diagrams of unaged unmodified bitumens

## 7.2.2 Unaged bitumen-filler mastics

Mastics, composed of bitumen and filler, is an intermediate material between bitumen and asphalt mixture [Delaporte *et al.*, 2007]. The presence of mineral filler cannot be neglected as it brings important effects such as improved strength, plasticity, amount of voids, resistance to water action and resistance to weathering [Liao, 2007]. Three types of fillers; cement, gritstone and limestone are used in this study [Liao, 2007; Wu, 2009]. The model parameters for each sample are shown in Tables 7.3 (by volume) and 7.4 (by weight). Meanwhile, Fig. 7.2 shows the plot of  $|G^*|$  and  $\delta$  master curves and the Black diagram of measured and modelled data of the unaged bitumen-filler mastics (by volume).

Table 7.3: The model parameters for bitumen filler mastics (40% by volume)

Material*	$G_0$ (Pa)	$G_g$ (Pa)	$k$	$h$	$\alpha$	$\tau$	$\beta$
Gritstone	6000	4.00E+09	0.21	0.55	4.00	1.10E-04	250
Limestone	10	2.00E+09	0.21	0.55	2.30	4.00E-04	250
Cement	120	2.00E+09	0.21	0.55	2.30	3.00E-04	250

\*fillers were mixed with a 100/150 penetration grade bitumen

Table 7.4: The model parameters for bitumen-filler mastics (by weight)

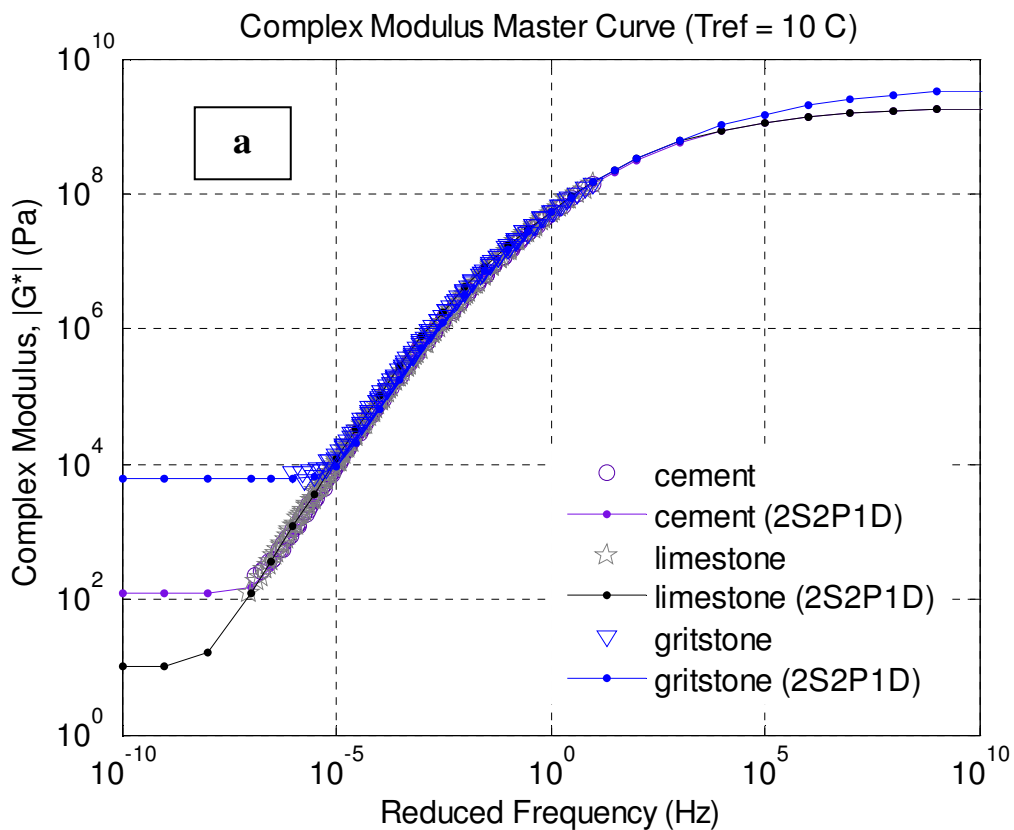
Filler*	(%)	$G_0$ (Pa)	$G_g$ (Pa)	$k$	$h$	$\alpha$	$\tau$	$\beta$
Gritstone	35	0	1.00E+09	0.21	0.59	2.30	7.00E-04	100
	65	8	1.00E+09	0.21	0.59	2.30	5.20E-03	100
Limestone	35	0	1.20E+09	0.21	0.59	2.30	7.00E-04	150
	65	5	1.50E+09	0.21	0.59	2.30	2.00E-03	150
Cement	35	0	1.30E+09	0.21	0.55	2.30	1.50E-04	250
	65	5	1.40E+09	0.21	0.55	2.30	1.50E-03	250

\*fillers were mixed with a 50 penetration grade bitumen

In general, the  $k$ ,  $h$  and  $\beta$  values are found to be the same for all samples used in this study. This indicates that the samples have the same slope at low frequencies and high temperatures. The presence of mineral filler is clearly observed where the  $G_0$  values are higher than those of the unaged unmodified bitumens. Results show that the  $G_0$  values are double for limestone and cement bitumen-filler mastics, whereas the  $G_0$  values for gritstone bitumen-filler mastics are four times higher compared to the unaged unmodified bitumens. The  $G_0$  values for bitumen-filler mastics cannot be neglected anymore. Delaporte *et al.* [2007]

found that the  $G_0$  values are higher due to the existence of solid contacts between particles.

Further investigation is done to fit the 2S2P1D Model using the bitumen-filler mastics at different percentages of 35 and 65% (by weight). The results are shown in Table 7.5. At 35%, all samples tend to behave in a Newtonian behaviour at very low frequencies where the  $G_g$  values are equal to zero. However, as the percentage increases up to 65%, the presence of mineral filler slowly appears at low frequencies even though these values are apparently small. This indicates that the considerably higher  $|G^*|$  for the 65% bitumen-filler mastics might be caused by the filler skeleton being present in the bitumen-filler system. Like the unaged unmodified bitumens, the 2S2P1D Model is also able to satisfactorily describe the rheological properties of the bitumen-filler mastics (Fig. 7.2).



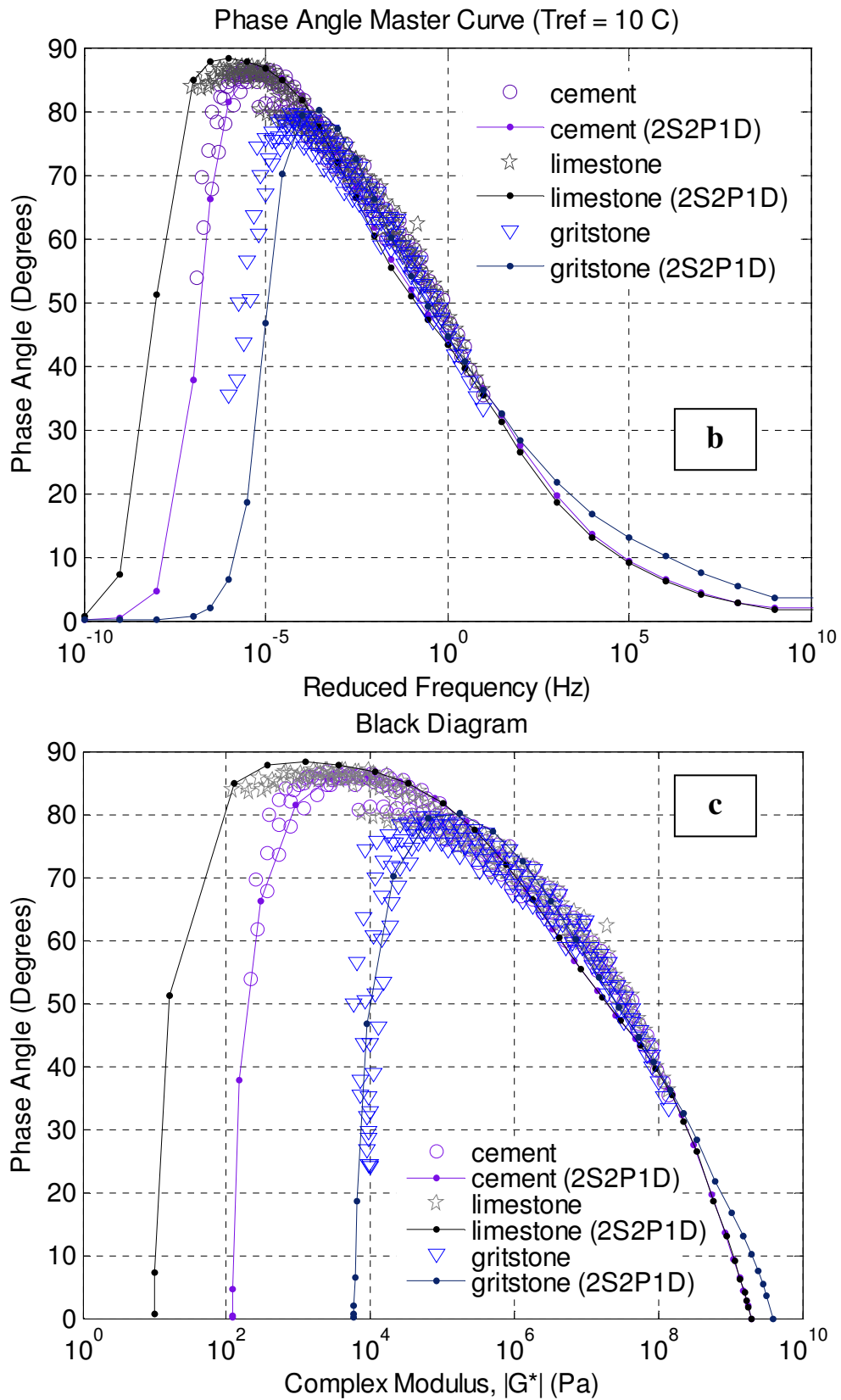


Fig. 7.2: (a) Complex modulus, (b) phase angle and (c) Black diagram of unaged bitumen-filler mastics

Delaporte *et al.* [2009] used different types of bitumen-filler mastics to evaluate the influence of different fillers on the 2S2P1D Model parameters. Fillers such as limestone (noted as LS), a mixture of limestone and ultrafine particles (noted as LSS) and a new type of filler composed of ultrafine particles (noted as S) mixed with a 50/70 penetration grade bitumen effect the model parameters as shown in Table 7.5.

Table 7.5: The model parameters for bitumen filler mastics obtained by Delaporte *et al.* [2009] (40% by volume)

Material	$G_0$ (Pa)	$G_g$ (Pa)	$k$	$h$	$\alpha$	$\tau$	$\beta$
B5070	0	9.00E+08	0.21	0.55	2.30	1.00E-04	400
B5070LS40	150	6.00E+09	0.21	0.55	2.30	6.00E-05	400
B5070LSS40	200	7.00E+09	0.21	0.55	2.30	6.00E-05	1200
B5070S40	500	9.00E+09	0.21	0.55	2.30	5.00E-04	30000

It was observed that  $\alpha$ ,  $k$  and  $h$  are the same regardless of the selected filler mastics when a comparison between the NTEC (Table 7.3) and Delaporte *et al.* [2009] (Table 7.5) dynamic data was made. These three parameters were not dependent on the filler content and they were fixed by the binder. The  $G_0$  values are different, depending on the type of filler and binder used. Delaporte *et al.* [2009] observed higher  $G_g$  compared to the values obtained in Table 7.4. This result is expected since Delaporte *et al.* [2009] used a harder bitumen (50/70 penetration grade) compared to the softer 100/150 penetration grade bitumen used in this study. The  $\beta$  values reported by Delaporte *et al.* [2009] were also higher compared to the NTEC data.

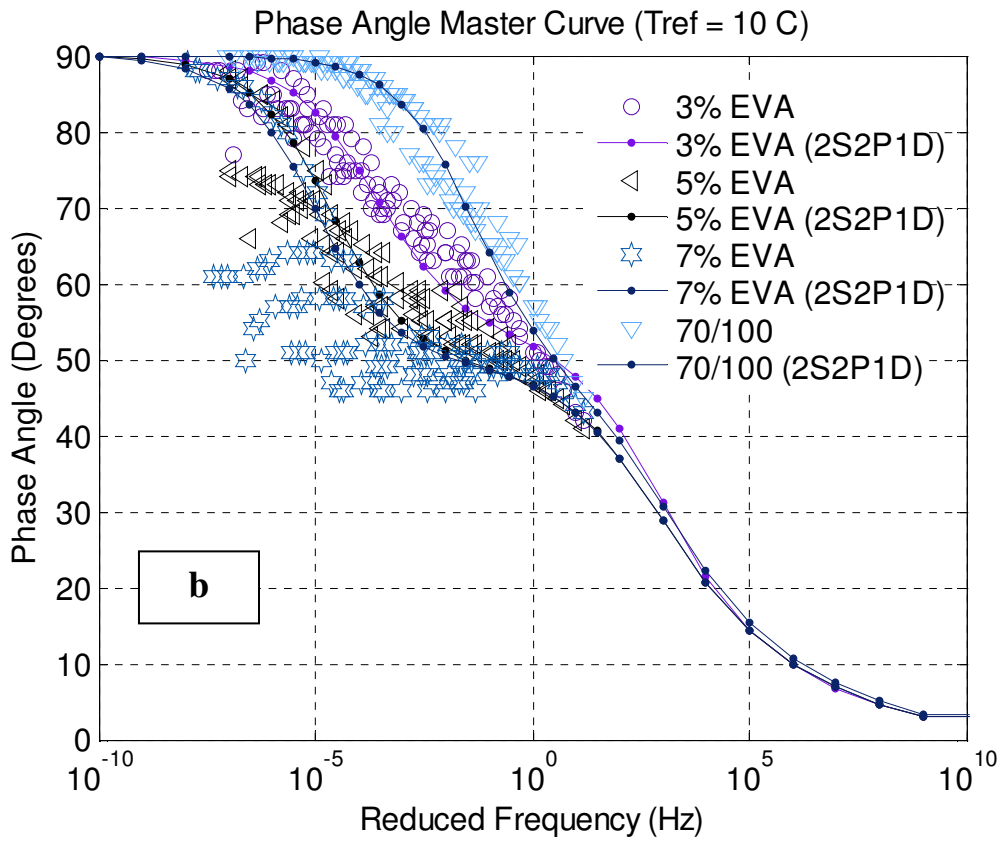
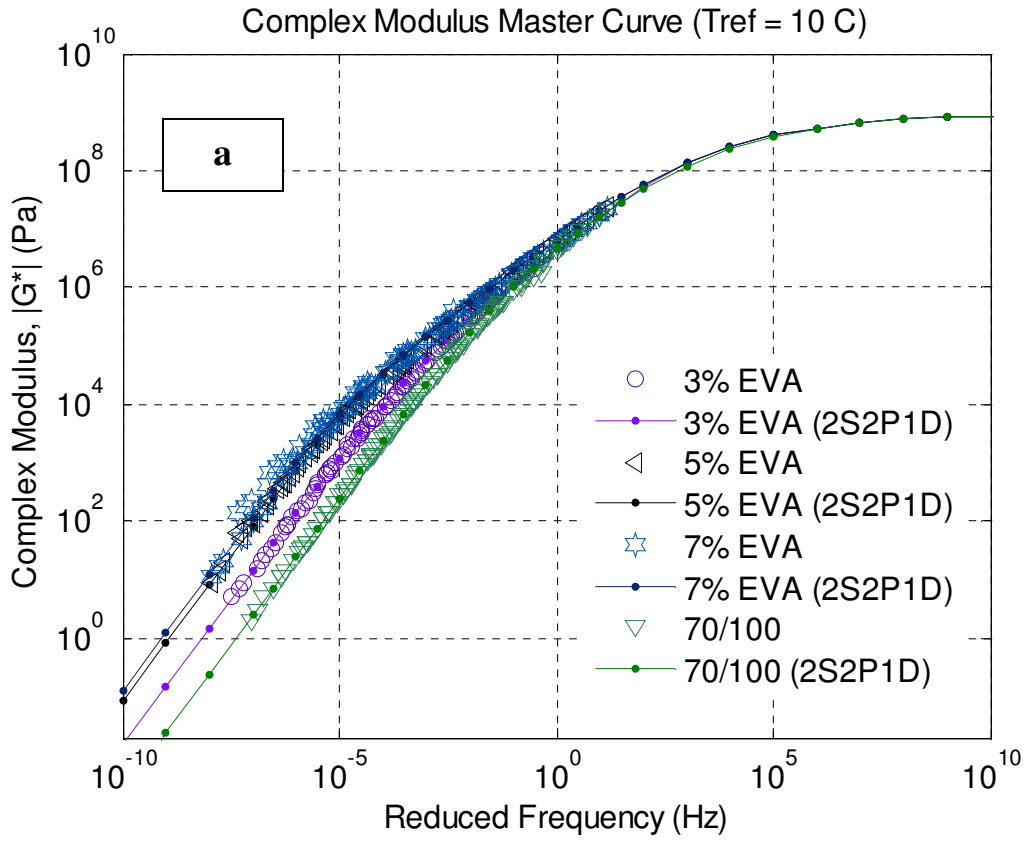
### 7.2.3 Unaged polymer-modified bitumens

Table 7.6 shows the 2S2P1D Model's parameters of the EVA and SBS PMBs. For simplification,  $G_g$  is taken as  $1 \times 10^9$  Pa. The results show that the  $G_g$ ,  $G_0$ ,  $k$  and  $h$  values are the same for all unaged PMBs but  $\alpha$ ,  $\tau$  and  $\beta$  vary. The  $\alpha$  value is more consistent for the SBS PMBs than those of the EVA PMBs. This is probably due to the presence of semi-crystalline structure at different temperatures which increases the complexity of a mixture. A thorough discussion on the rheological characteristics of the EVA and SBS PMBs can be found in previous publications

[Airey, 2002a, 2002b, 2003]. Results show that the 2S2P1D Model is able to simulate the effect of polymer modification as the  $\beta$  value increases when the percentage of a modifier is increased. The presence of polymer modification increases the viscosity of the mixture.

Table 7.6: The model parameters for unaged polymer-modified bitumens

Percent	Modifier	Source	$G_0$ (Pa)	$G_g$ (Pa)	$k$	$h$	$\alpha$	$\tau$	$\beta$
0	Control	Middle East	0	1.00E+09	0.21	0.55	2.30	5.00E-05	300
		Russian	0	1.00E+09	0.21	0.55	3.50	5.00E-05	150
		Venezuelan	0	1.00E+09	0.21	0.55	2.30	1.50E-05	200
3 5 7	EVA	Middle East	0	1.00E+09	0.21	0.55	3.50	7.00E-05	900
			0	1.00E+09	0.21	0.55	5.00	7.00E-05	2500
			0	1.00E+09	0.21	0.55	5.00	1.00E-04	6000
3 5 7	EVA	Russian	0	1.00E+09	0.21	0.55	3.50	5.00E-05	600
			0	1.00E+09	0.21	0.55	3.00	6.00E-05	1000
			0	1.00E+09	0.21	0.55	2.30	6.00E-05	6000
3 5 7	EVA	Venezuelan	0	1.00E+09	0.21	0.55	2.30	2.00E-05	1200
			0	1.00E+09	0.21	0.55	2.30	2.00E-05	7000
			0	1.00E+09	0.21	0.55	2.30	2.00E-05	10000
3 5 7	SBS	Russian	0	1.00E+09	0.21	0.55	2.30	3.00E-05	1500
			0	1.00E+09	0.21	0.55	2.30	3.00E-05	3000
			0	1.00E+09	0.21	0.55	2.30	5.00E-06	20000
3 5 7	SBS	VE	0	1.00E+09	0.21	0.55	2.30	2.00E-05	700
			0	1.00E+09	0.21	0.55	2.30	2.00E-05	1300
			0	1.00E+09	0.21	0.55	2.30	2.00E-05	2500



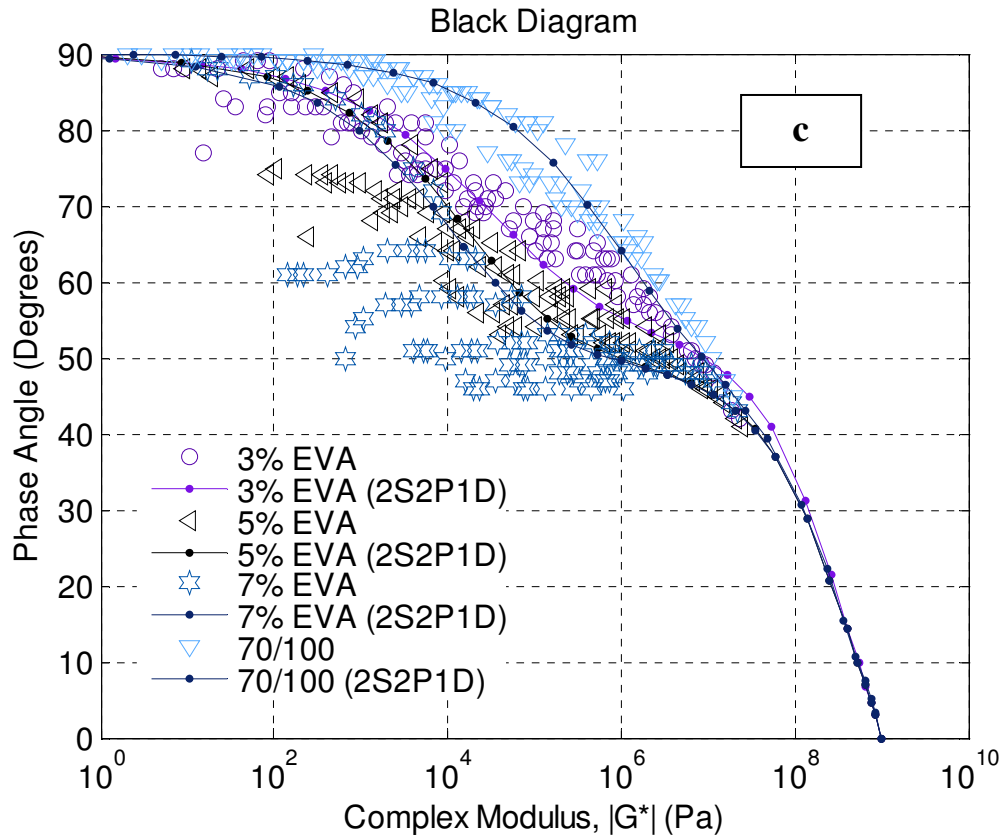


Fig 7.3: (a) Complex modulus, (b) phase angle and (c) Black diagrams of unaged PMBs

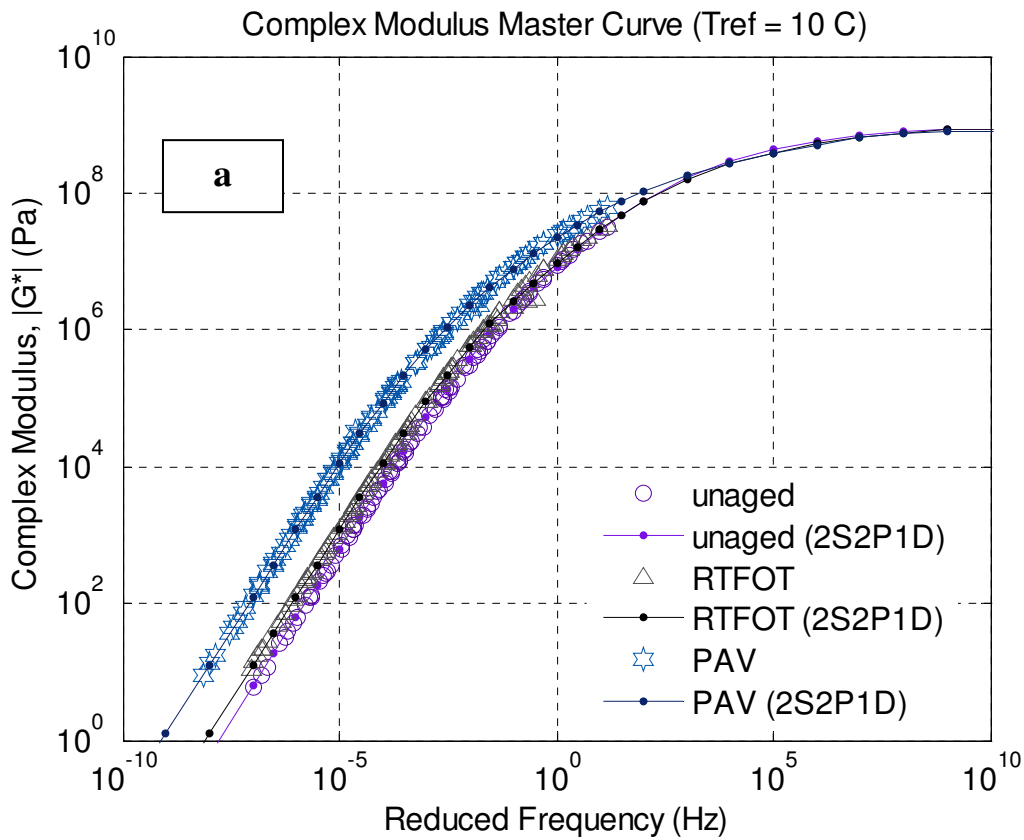
The plot of  $|G^*|$  and  $\delta$  master curves and of the Black diagram one of the unaged PMB (EVA) used in this study are shown in Fig. 7.3. It is observed that the 2S2P1D Model is only capable to satisfactorily describe  $|G^*|$  master curves but not for  $\delta$  master curves. This finding is expected as other constitutive models are also not able to describe the viscoelastic properties of highly modified bitumens. The quality of data is normally further evaluated using the Black diagram.

#### 7.2.4 Aged unmodified bitumens

It is experimentally observed that there is an important change in behaviour due to the binder's ageing mainly at high temperatures and low frequencies (Table 7.8). Fig. 7.8 shows  $|G^*|$  and  $\delta$  angle master curves and the Black diagram of aged unmodified bitumens. The parameters such as  $G_g$ ,  $G_0$ ,  $k$  and  $h$  are consistent for all materials. This indicates that these parameters are independent of the ageing process. Moreover, the  $\beta$  value that is linked to the Newtonian viscosity,  $\eta$ , of the 2S2P1D Model has a large

influence in this domain. The influence of the binder ageing on the model's parameters mainly affected the  $\beta$  value. The values of  $\beta$  increase from unaged to aged unmodified bitumens.

The  $\alpha$  value is increased as a material becomes harder. Delaporte *et al.* [2007] disclosed the same findings where the  $\alpha$  values increased from 2.3 to 3.0 when the curve is plotted using an aged 50/70 penetration grade bitumen. Therefore, it can be inferred that the  $\alpha$  value can be used as an ageing indicator, where the aged samples show a higher  $\alpha$  value compared to the unaged samples.



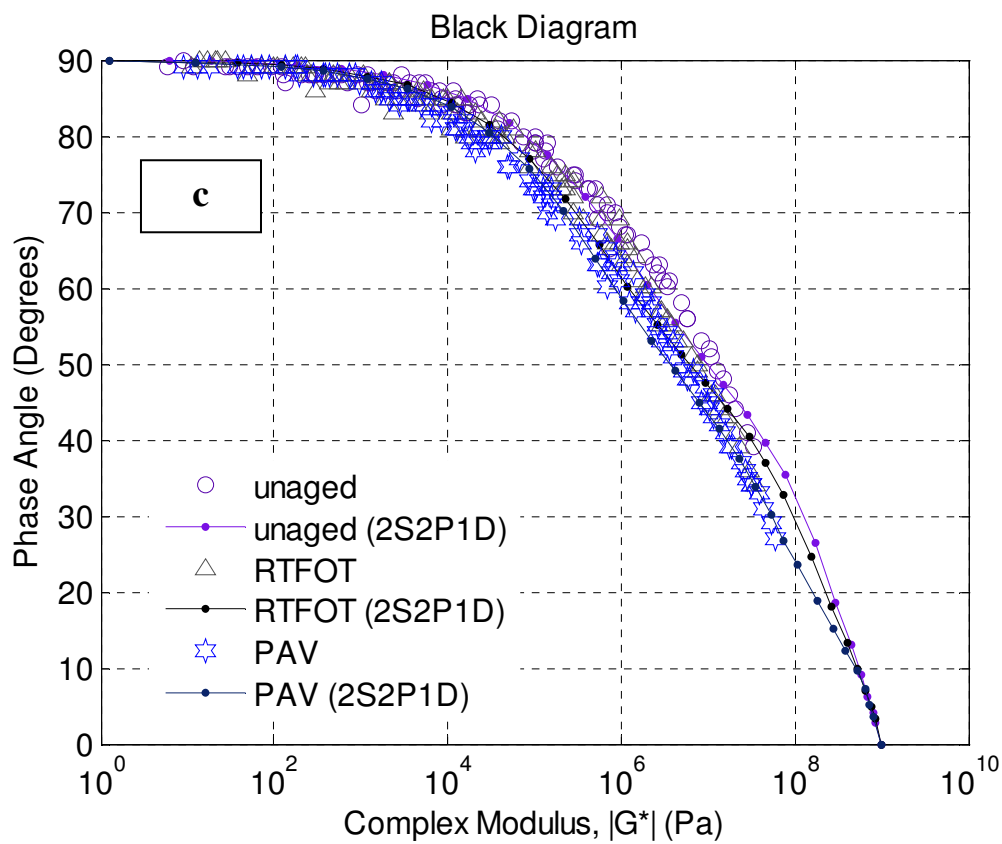
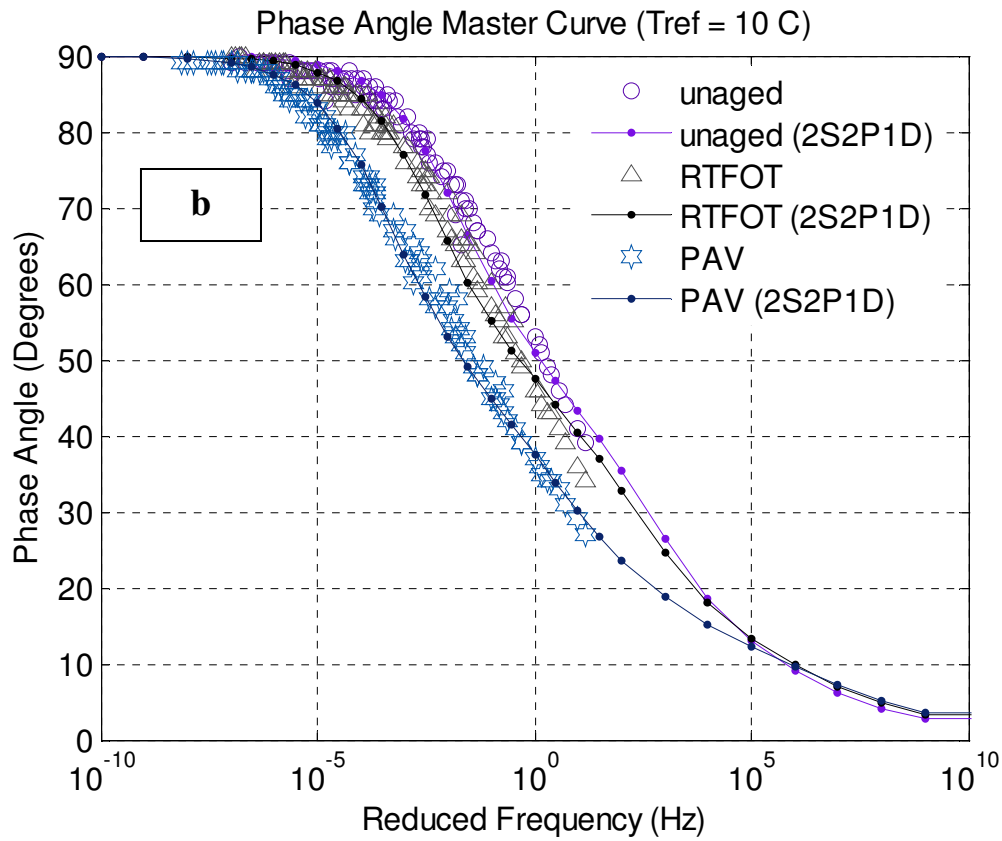


Fig. 7.4: (a) Complex modulus, (b) phase angle and (c) Black diagrams of aged unmodified bitumen

### 7.2.5 Aged bitumen-filler mastics

An attempt is also made to fit the aged bitumen-filler mastics using the 2S2P1D Model (Table 7.9). Only two filler mastics (gritstone and limestone) are used in this ageing study as cement bitumen-filler mastics did not produce good data. It is found that the 2S2P1D Model is able to describe the aged bitumen-filler mastics with the same quality of the aged unmodified bitumens. The gritstone and limestone bitumen-filler mastics show the same values of  $k$ ,  $h$ ,  $\alpha$  and  $\beta$  with ageing times from 1 to 10 hours. However, as the ageing time is increased to 20 hours, the  $\beta$  values increase to 600 (gritstone) and 800 (limestone). Like the unaged bitumen-filler mastics, the values of  $G_g$  are also taken into account due to the existence of solid contacts between particles in a mixture. The acidic gritstone bitumen-filler mastic shows a slight difference of  $G_g$  with ageing time compared to the limestone bitumen-filler mastic.

As expected,  $|G^*|$  of the gritstone bitumen-filler mastic increases as the ageing time increases. However, an initial reduction is observed for the limestone bitumen-filler mastic  $|G^*|$ , with the lowest value after an hour of ageing time. This phenomenon is believed to be caused by the adsorption of heavier fractions from bitumen to the mineral surface of the limestone bitumen-filler mastics [Wu, 2009]. Fig. 7.5 shows an example of the dynamic data ( $|G^*|$  and  $\delta$ ) and the Black diagram of the aged cement bitumen-filler mastic. It is observed that the 2S2P1D Model satisfactorily describes the measurements.

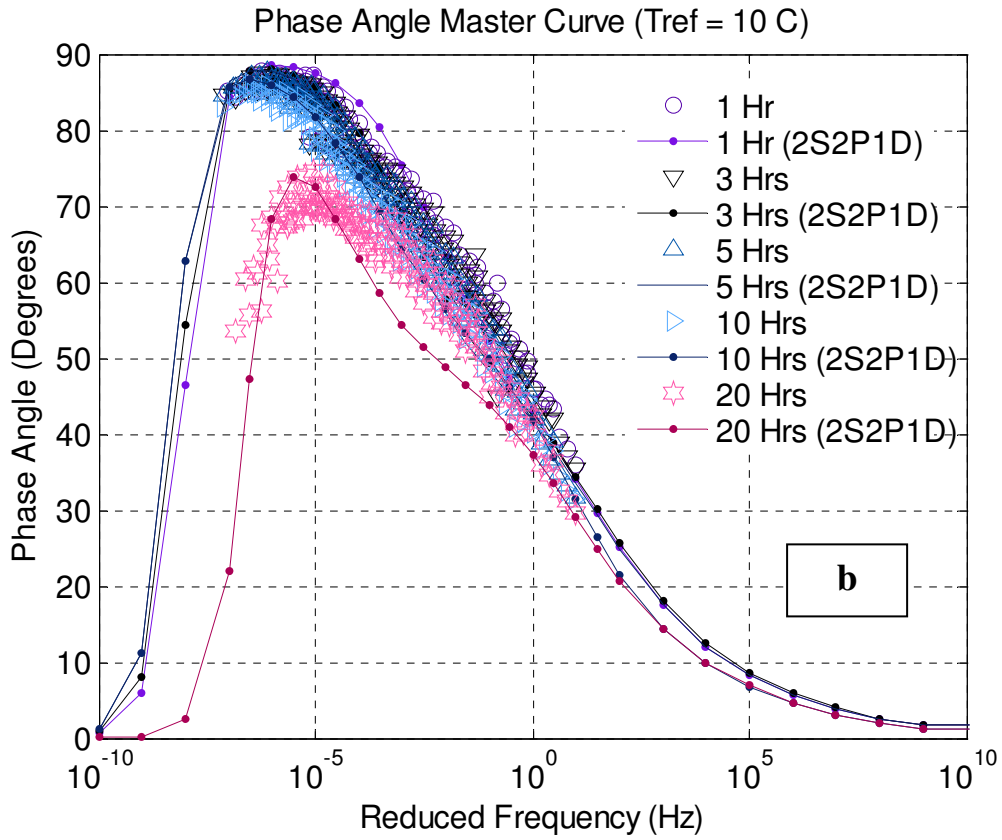
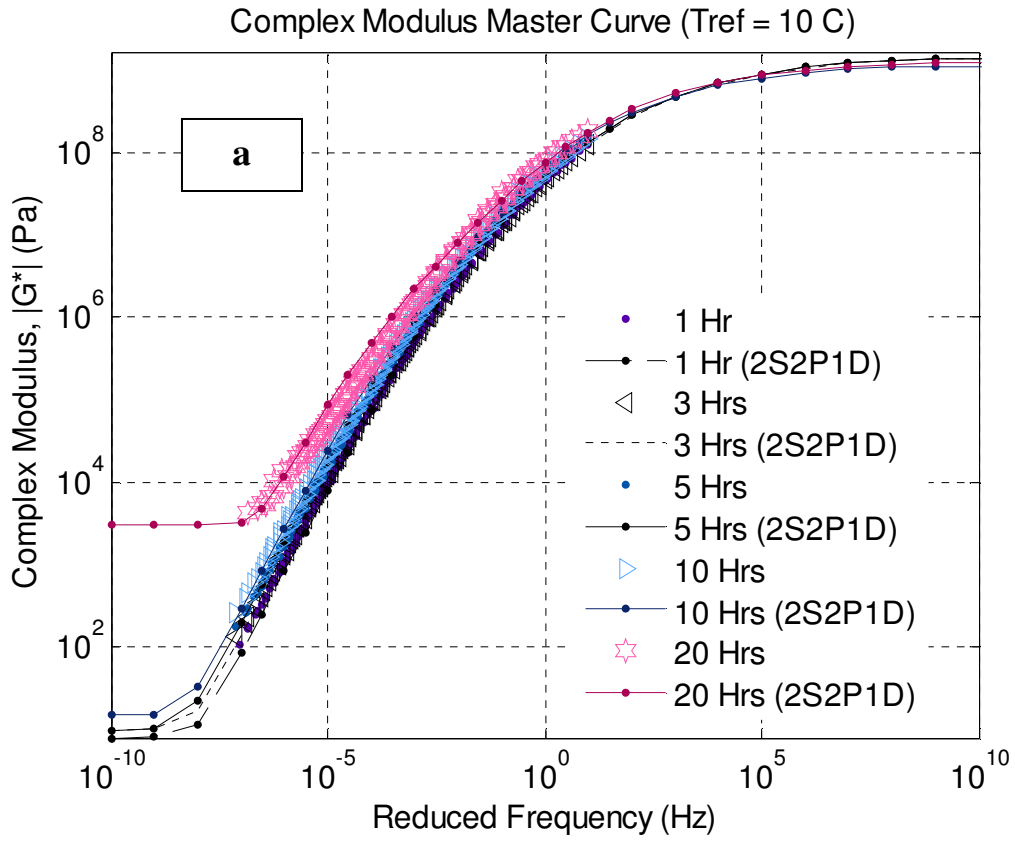
Table 7.8: The model parameters for the aged unmodified bitumens

Method*	Source	$G_0$ (Pa)	$G_g$ (Pa)	$k$	$h$	$\alpha$	$\tau$	$\beta$
Unaged	Middle East	0	1.00E+09	0.21	0.55	2.30	5.00E-05	300
RTFOT		0	1.00E+09	0.21	0.55	4.00	7.00E-05	700
PAV		0	1.00E+09	0.21	0.55	5.00	4.00E-04	1000
Unaged	Russian	0	1.00E+09	0.21	0.55	3.50	5.00E-05	150
RTFOT		0	1.00E+09	0.21	0.55	5.00	5.00E-05	400
PAV		0	1.00E+09	0.21	0.55	5.00	4.00E-04	1500
Unaged	Venezuelan	0	1.00E+09	0.21	0.55	2.30	1.50E-05	200
RTFOT		0	1.00E+09	0.21	0.55	3.50	3.20E-05	500
PAV		0	1.00E+09	0.21	0.55	4.50	1.00E-04	1500

\*RTFOT – Rolling Thin Film Oven test, PAV – Pressure Ageing Vessel

Table 7.9: The model parameters for the aged bitumen-filler mastics (40% by volume)

Material	Time (h)	$G_0$ (Pa)	$G_g$ (Pa)	$k$	$h$	$\alpha$	$\tau$	$\beta$
Gritstone	1	200	1.40E+09	0.21	0.55	2.30	9.50E-04	150
	3	12000	1.60E+09	0.21	0.55	2.30	6.00E-04	150
	5	8000	1.70E+09	0.21	0.55	2.30	8.00E-04	150
	10	600	1.40E+09	0.21	0.55	2.30	2.00E-03	150
	20	600	1.00E+09	0.21	0.55	2.30	1.00E-02	600
Limestone	1	8	1.50E+09	0.21	0.55	2.30	5.50E-04	150
	3	10	1.50E+09	0.21	0.55	2.30	8.00E-04	150
	5	10	1.50E+09	0.21	0.55	2.30	1.00E-03	150
	10	10	1.20E+09	0.21	0.55	2.30	2.00E-03	150
	20	3000	1.30E+09	0.21	0.55	2.30	2.00E-03	800



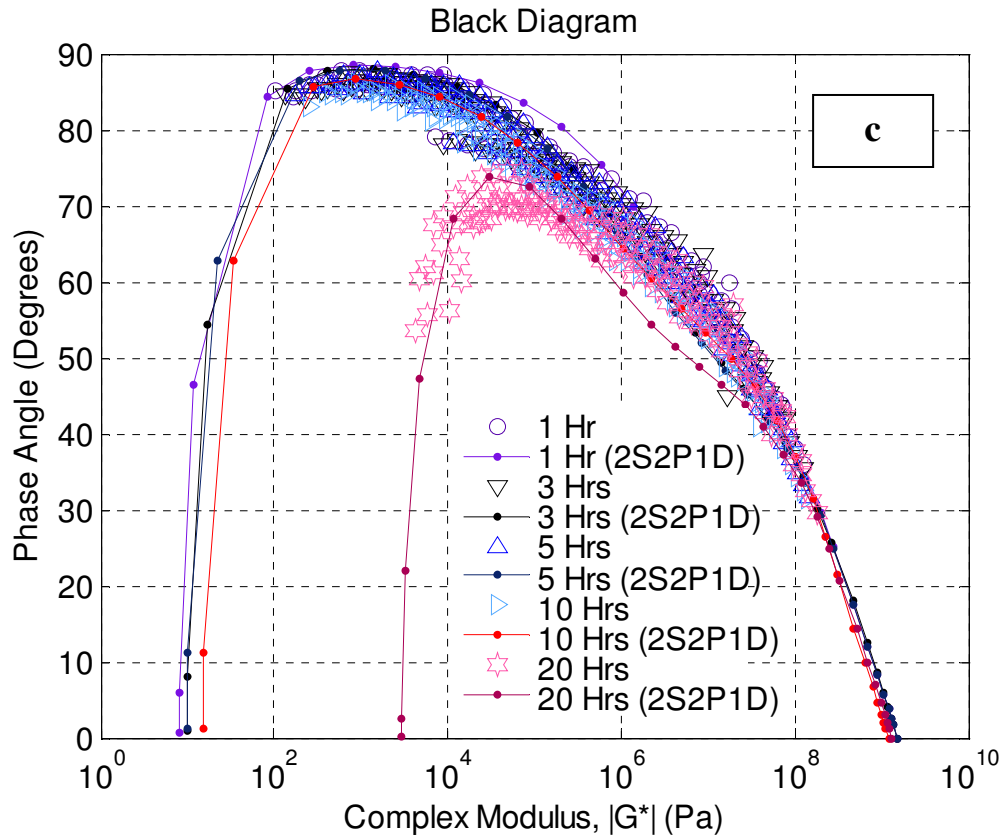


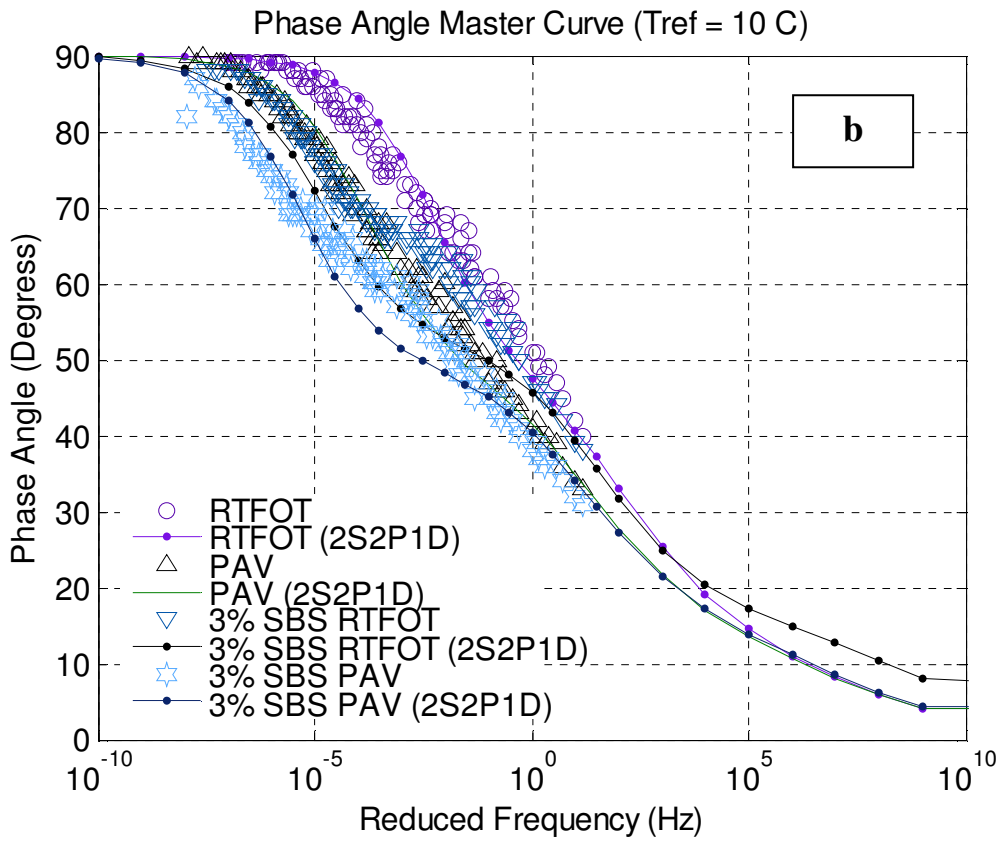
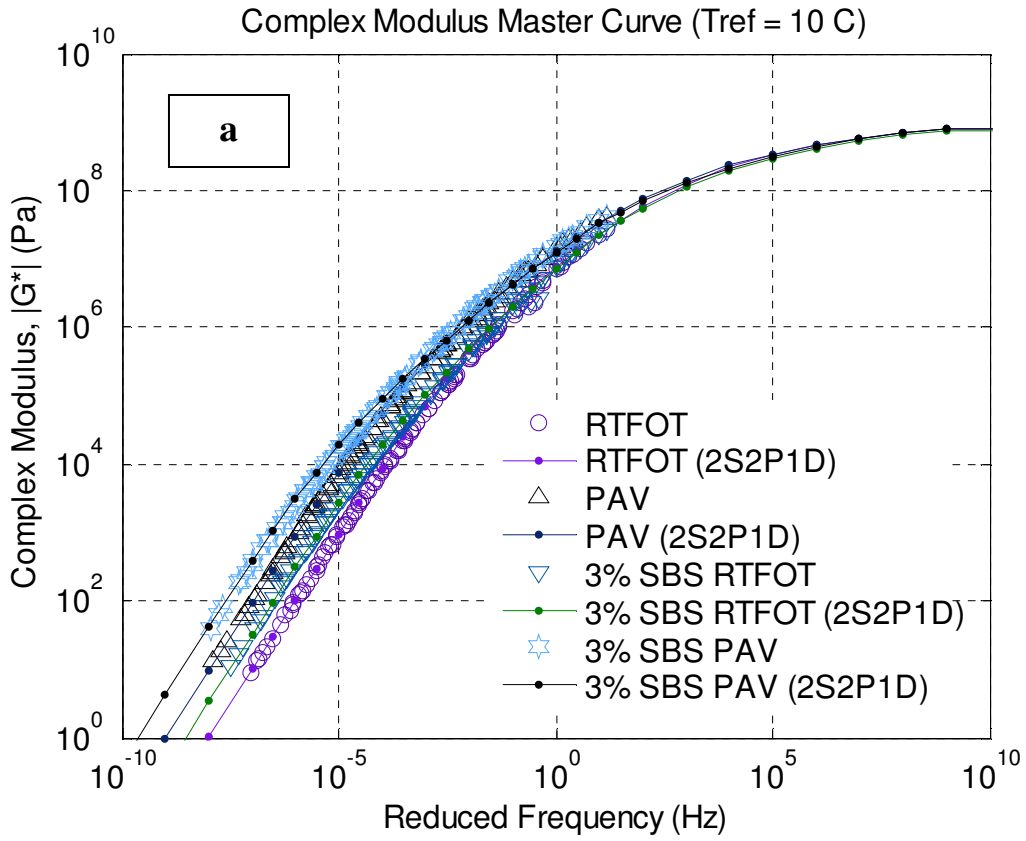
Fig. 7.5: (a) Complex modulus, (b) phase angle and (c) Black diagrams of aged bitumen-filler mastic

### 7.2.6 Aged polymer-modified bitumens

The model parameters for all the aged PMBs are shown in Table 7.10. Meanwhile, Fig. 7.6 shows the simulations of  $|G^*|$  and  $\delta$  master curves and the Black diagram of one of the aged SBS PMB used in this study. The  $G_g$ ,  $G_0$ ,  $k$  and  $h$  values are the same for all samples. The  $\beta$  value which is linked to the Newtonian viscosity  $\eta$  of the 2S2P1D Model has a large influence in this domain of behaviour, where  $\beta$  increases as polymer modification is increased. For some samples, the changes of the  $\alpha$  value depends on the percentage of modification and the crudes source. As the temperature increases, the polymer-rich phase plays a more dominant role in determination of the LVE rheological properties of bitumens. The effect of ageing can be seen as an alteration of the Black diagram waves associated with the different EVA crystalline structures and a general reduction in polymer modification [Airey, 2002a].

Table 7.10: The model parameters for the aged polymer-modified bitumens

Method	%	Modifier	Source	$G_0$ (Pa)	$G_g$ (Pa)	$k$	$H$	$\alpha$	$\tau$	$\beta$	
RTFOT	3	EVA	ME	0	1.00E+09	0.21	0.55	4.50	1.00E-04	1500	
	5			0	1.00E+09	0.21	0.55	5.00	3.00E-04	2000	
	7			0	1.00E+09	0.21	0.55	5.00	2.00E-04	10000	
PAV	3			0	1.00E+09	0.21	0.55	7.00	5.00E-04	2500	
	5			0	1.00E+09	0.21	0.55	7.00	2.00E-03	3000	
	7			0	1.00E+09	0.21	0.55	7.00	2.00E-03	10000	
RTFOT	5		RU	0	1.00E+09	0.21	0.55	5.00	8.00E-05	8000	
	7			0	1.00E+09	0.21	0.55	5.00	2.00E-04	20000	
	PAV			5	0	1.00E+09	0.21	0.55	5.00	8.00E-04	3000
7				0	1.00E+09	0.21	0.55	7.00	9.00E-04	25000	
RTFOT				5	VE	0	1.00E+09	0.21	0.55	5.00	1.00E-04
	7			0		1.00E+09	0.21	0.55	3.00	3.00E-05	60000
	PAV	5	0	1.00E+09		0.21	0.55	7.00	5.00E-04	10000	
7		0	1.00E+09	0.21		0.55	7.00	4.00E-04	60000		
RTFOT		3	SBS	RU		0	1.00E+09	0.21	0.55	5.00	8.00E-05
	5	0				1.00E+09	0.21	0.55	5.00	9.00E-05	1000
	7	0			1.00E+09	0.21	0.55	5.00	3.00E-05	5000	
PAV	3	0			1.00E+09	0.21	0.55	7.00	4.50E-04	1500	
	5	0			1.00E+09	0.21	0.55	7.00	2.00E-04	3000	
	7	0			1.00E+09	0.21	0.55	5.00	3.00E-04	5000	
RTFOT	3	VE		0	1.00E+09	0.21	0.55	4.00	3.00E-05	1800	
	5			0	1.00E+09	0.21	0.55	5.00	1.50E-05	8000	
	7			0	1.00E+09	0.21	0.55	5.00	3.00E-05	8000	
PAV	3			0	1.00E+09	0.21	0.55	5.00	1.00E-04	6000	
	5			0	1.00E+09	0.21	0.55	5.00	3.00E-05	5000	
	7			0	1.00E+09	0.21	0.55	5.00	3.00E-04	8000	



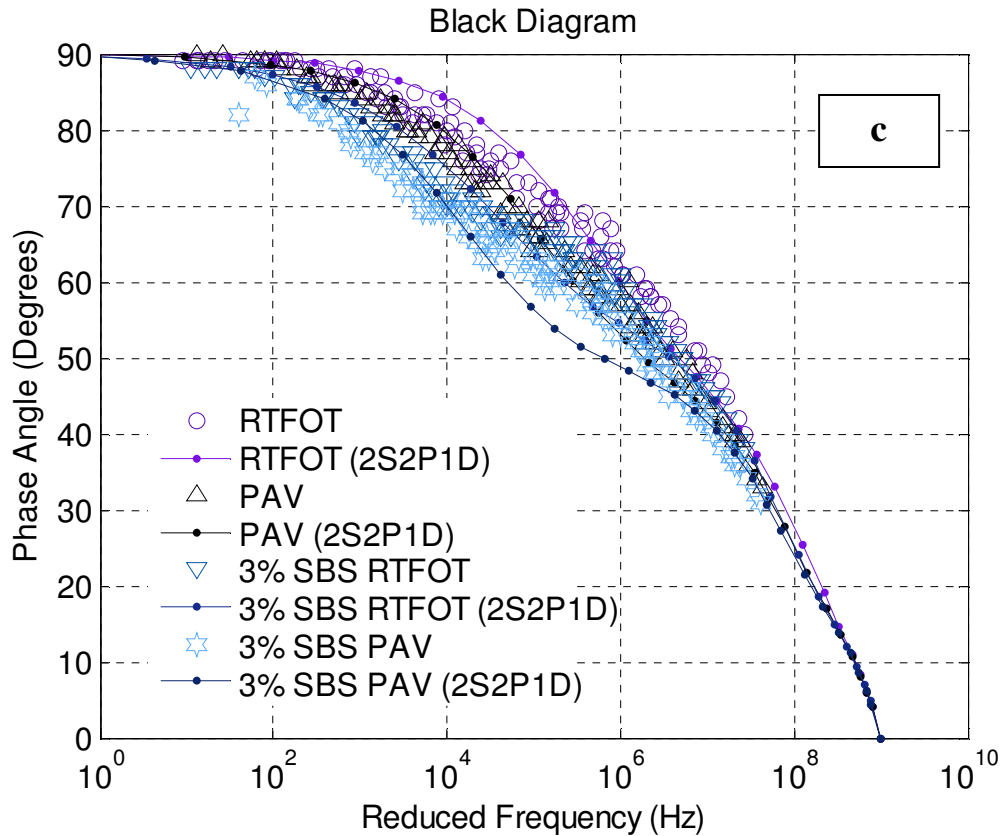


Fig. 7.6 (a) Complex modulus, (b) phase angle and (c) Black diagrams of aged PMBs

Olard and Di Benedetto [2003] found an identical problem for the PMBs and they called this property the partial time-temperature superposition principle (PTTSP) as shifting procedures give only a unique and continuous  $|G^*|$  master curves. However, it is found that the PTTSP might be or not be applicable for certain conditions (or percentage) of polymer modifications and not suitable to be used on highly polymer-modified bitumens. Airey [2002a, 2002b] showed that both the TTSP and PTTSP are unable to describe the branching and discontinuous waves in the master curves that show the presence of highly semi-crystalline EVA copolymer.

### 7.3 Statistical Analysis

#### 7.3.1 Graphical comparisons

Comparisons between measured and modelled  $|G^*|$  and  $\delta$  of all samples are shown in Figs 7.7 and 7.8. The measured and modelled values are equated by matching two values in a normal scale graph. If the matching points are fairly distributed around

the equality line, then the model should have a good correlation to the measured data [Tran and Hall, 2005]. Graphically, it is observed that the 2S2P1D Model is able to describe  $|G^*|$  values for the unaged and aged unmodified bitumens and bitumen-filler mastics well (Fig. 7.6). However, the modelled  $|G^*|$  of the unaged PMBs are slightly scattered from the equality line particularly for samples of high modification.

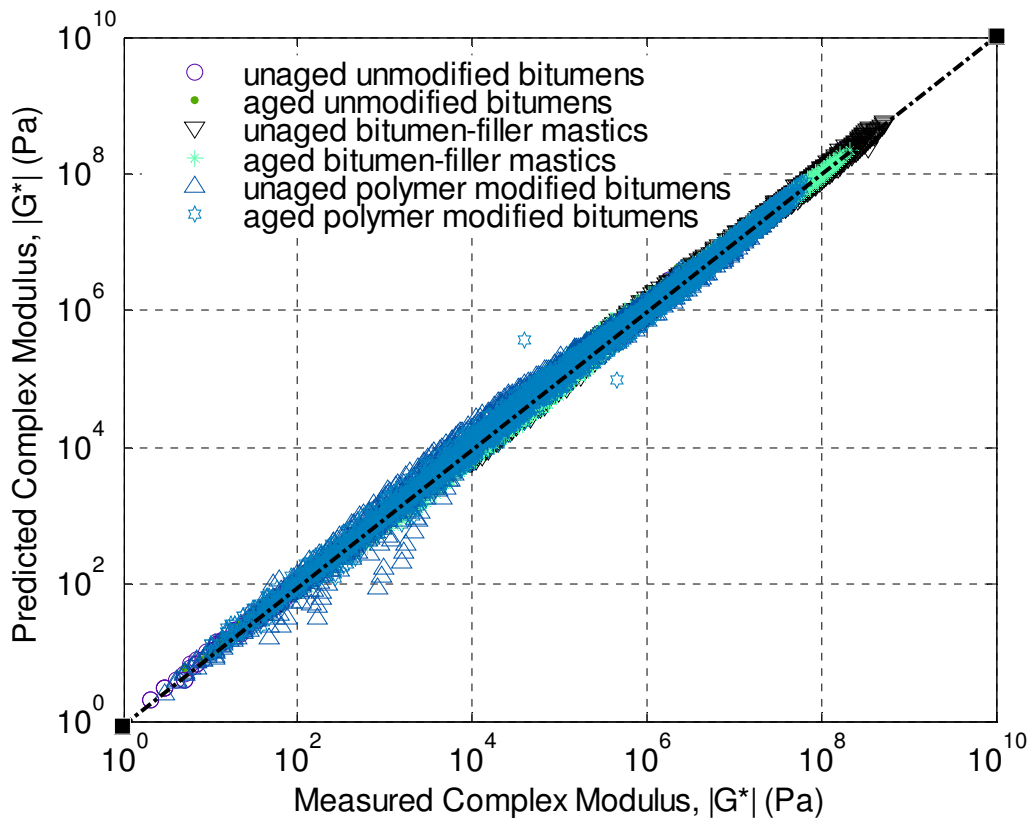


Fig. 7.6: Graphical comparison between measured and modelled  $|G^*|$

Meanwhile Fig. 7.7 shows a comparison between measured and modelled  $\delta$ . It is found that the unaged and aged unmodified bitumens show good correlation between measured and model data. However, the modelled unaged and aged PMBs, and aged bitumen-filler mastics are slightly scattered from the equality line. Di Benedetto *et al.* also found the same problem where this model was partially satisfied in fitting  $|G^*|$  and  $\delta$  master curves of PMBs [Olard and Di Benedetto, 2003; Olard *et al.*, 2003].

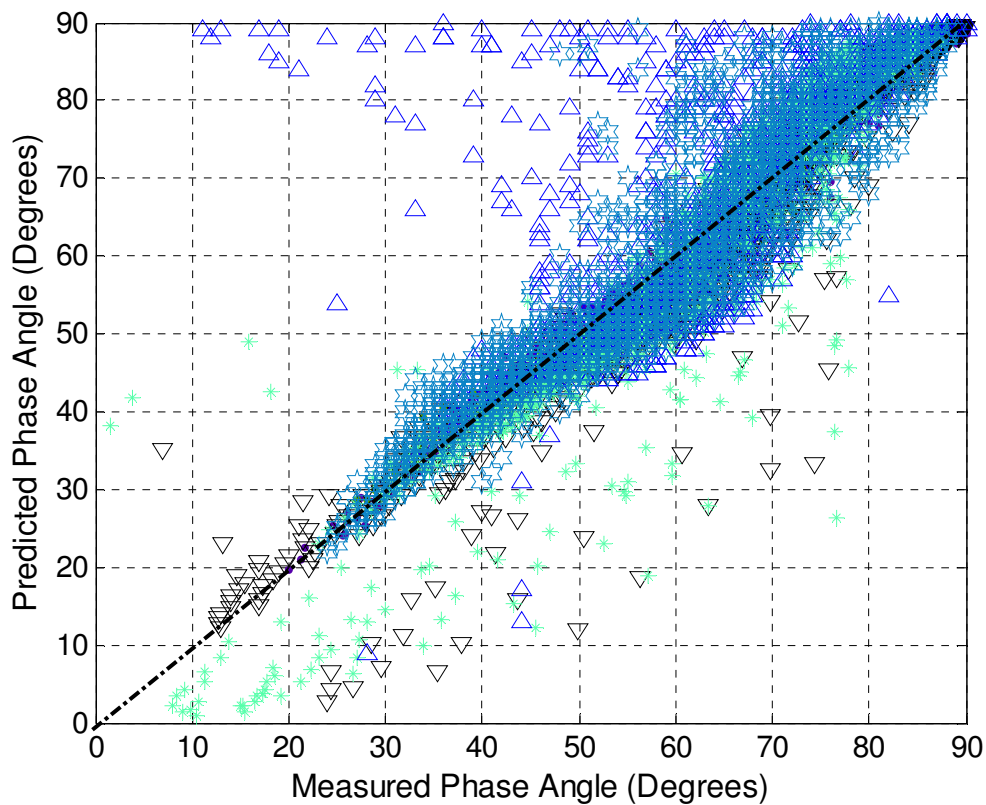


Fig. 7.7: Graphical comparison between measured and modelled  $\delta$

### 7.3.2 Goodness-of-fit statistics

The goodness-of-fit statistics between measured and modelled  $|G^*|$  and  $\delta$  are shown in Tables 7.10 and 7.11, respectively. In summary, the  $S_e/S_y$  for all samples are in "excellent" correlations between measured and modelled  $|G^*|$  data. Similarly, the  $S_e/S_y$  for  $\delta$  of unaged and aged unmodified bitumens and unaged bitumen-filler mastics show "excellent" correlations. Conversely, the  $S_e/S_y$  for aged bitumen-filler mastics and PMBs are in "good" correlations, whereas the  $S_e/S_y$  for unaged PMBs shows "poor" correlation between measured and modelled data. All samples show "excellent" correlations of  $R^2$  for  $|G^*|$  data. However for  $\delta$ , it is found that the  $R^2$  is in "good" correlations of unaged and aged PMBs. As expected, the unaged PMBs show "poor" correlations. However, it is observed that the use of  $R^2$  and  $S_e/S_y$  is not really suitable for describing mismatches between measured and modelled data.

The discrepancy ratio,  $r_i$  is used to observe the model data's tabulation from the equality line. A perfect value is equal to 1. When the discrepancy ratio is larger or

smaller than 1, it measures how much wider the model interval had to be to cover the observed number of cases [Wu *et al.*, 2009]. With the interval of  $1 \pm 0.04$  used in this study, the unaged unmodified bitumen data dispersed close to the equality line, followed by the aged unmodified bitumens, unaged bitumen-filler mastics, aged filler mastics and aged PMBs. As expected, the unaged PMBs showed the worst correlation between measured and modelled  $|G^*|$ . As discussed earlier, the 2S2P1D Model is unable to satisfactorily fit the rheological properties of highly modified polymers.

Like the  $r_i$ , the *MNE* and *AGD* are also used to observe the difference between measured and modelled data. The unaged unmodified bitumens show the most outstanding correlation for both  $|G^*|$  and  $\delta$ , followed by the aged unmodified bitumens, unaged bitumen-filler mastics, aged PMBs, aged bitumen-filler mastics and unaged PMBs. An observation is made where the ageing process renders the aged PMBs more stable compared to the unaged samples. The ageing process may also possibly affect the breakdown in polymer structures, therefore decreasing the effect of polymer-rich phase network in the mixtures. Based on Tables 7.10 and 7.11, it is found that the *AGD* is not always reliable at detecting the goodness-of-fit as only small differences between measurements and model are observed. It is therefore recommended that the  $r_i$  and *MNE* provide the best means of identifying the goodness-of-fit statistics for model and experiment associated with the rheological data over a wide range of temperatures and frequencies.

Table 7.10: Statistical analysis for the complex modulus magnitude master curves

Sample	Condition	Discrepancy ratio, $r_i$ (%)					$S_e/S_y$	$R^2$	AGD	MNE
		0.96 – 1.04	0.92 – 1.08	0.88 – 1.12	0.84 – 1.16	0.80 – 1.20				
unmodified bitumen	unaged	26.43	48.87	72.10	87.78	96.27	0.171	0.971	1.090	8.733
	aged	39.29	64.88	75.00	80.51	82.89	0.069	0.995	1.092	9.421
bitumen-filler mastics	unaged	25.30	47.82	65.55	76.31	84.93	0.145	0.979	1.116	11.318
	aged	12.62	25.00	35.27	45.55	57.30	0.114	0.987	1.212	19.197
PMBs	unaged	13.69	29.46	41.43	51.13	59.05	0.102	0.990	1.253	25.631
	aged	17.37	35.19	50.19	62.75	71.96	0.171	0.971	1.161	16.034

Table 7.11: Statistical analysis for the phase angle master curve

Sample	Condition	Discrepancy ratio, $r_i$ (%)					$S_e/S_y$	$R^2$	AGD	MNE
		0.96 – 1.04	0.92 – 1.08	0.88 – 1.12	0.84 – 1.16	0.80 – 1.20				
unmodified bitumen	unaged	88.81	98.96	99.91	100.00	100.00	0.107	0.989	1.018	1.787
	aged	71.28	90.63	98.96	100.00	100.00	0.163	0.974	1.032	3.064
bitumen-filler mastics	unaged	61.06	81.79	91.05	96.03	97.48	0.294	0.914	1.063	5.500
	aged	40.10	69.31	87.50	92.39	93.94	0.405	0.837	1.107	10.395
PMBs	unaged	36.81	65.16	76.47	83.80	89.10	0.808	0.345	1.110	12.893
	aged	40.57	67.69	85.03	93.60	96.73	0.357	0.873	1.069	6.736

## 7.4 Summary

Based on this study, several key observations can be drawn;

- The 2S2P1D Model is quite simple in its formulation, as a combination of springs, dashpot and parabolic elements. The calibration of this model is not a very difficult task and is good for bituminous binders over a wide range of frequencies and/or temperatures. The model can be thought of as a unique model as its parameters are relatable to the construction of complex modulus and phase angle master curves, the Black diagram and the Cole-Cole diagram. It also takes into account the presence of polymers, mastics and ageing.
- It is observed that this model is able to fit the rheological properties of unmodified bitumens (unaged and aged), bitumen-filler mastics (unaged and aged) and polymer-modified bitumens (aged). However, the model failed to fit the rheological properties of unaged polymer-modified bitumens particularly with high modifications. The fit is even worse when a comparison is made for measured and modelled  $\delta$ .
- For modelling purposes, the  $G_g$  values can be taken as  $1 \times 10^9$  Pa (in shear) and  $3 \times 10^9$  Pa (in extension or flexure) for unmodified and PMBs, for both unaged and aged samples. They approach a limiting maximum modulus at very low temperatures. However, for the unaged and aged bitumen-filler mastics, the  $G_g$  values vary. The  $G_g$  values depend on the percentage and a type of mineral fillers used. This phenomenon occurs due to the existence of physical interaction in the mixture.

## Phase Angle Equations

---

### 8.1 Background

The principal viscoelastic parameters that are obtained from the DSR are the magnitude of the complex modulus ( $|G^*|$ ) and the phase angle ( $\delta$ ).  $|G^*|$  consists of two components namely the storage modulus ( $G'$ ) and loss modulus ( $G''$ ). Meanwhile  $\delta$  is the phase, or time difference between stress and strain in harmonic oscillation [Eurobitume, 1995]. The  $\delta$  is also known as phase angle (or loss tangent) and shown as the following:

$$\delta = \tan^{-1} \frac{G''}{G'} \quad (8.1)$$

Tan  $\delta$  is the ratio of loss energy to stored energy. An elastic behaviour is defined as in-phase strain response to an applied load and  $\delta$  is  $0^\circ$  and marks the coordinated long chain molecular mobilisation. Viscous behaviour is a strain response that is  $90^\circ$  out-of-phase from the applied load and indicates full molecular mobilisation [Gardiner, 1996]. Viscoelastic behaviour of material including bitumen occurs when  $\delta$  is greater than  $0^\circ$  but less than  $90^\circ$ . It is worth mentioning that  $\delta$  can be thought of as the second part of  $|G^*|$  to yield complete information about the linear viscoelastic function of the binders.

Complex modulus test procedures and models developed in the early 1950s. Contrarily, the development of  $\delta$  models to describe the viscoelastic behaviour of the binders is rarely seen. To obtain  $\delta$  information from an experimental data set using a simple method would be advantageous and increase the utility of the data [Rowe, 2009]. A reasonable number of studies had been done to evaluate various  $\delta$

equations covering a wide range of temperatures and frequencies [Dickinson and Witt, 1974; Stastna *et al.* 1997; Chailleux *et al.*, 2006]. However, none of those studies were devoted to evaluate the applicability of different  $\delta$  equations on different types of binders.

This study attempts to evaluate the validity of several  $\delta$  equations based on the data set that is held at the Nottingham Transportation Engineering Centre (NTEC). This data set included different combinations of the dynamic shear rheometer data of unmodified bitumens and PMBs [Airey, 1997]. Correlations between equations and measurements are evaluated using a graphical method and goodness-of-fit statistical analysis.

## 8.2 Phase Angle Equations

### 8.2.1 Kramers-Kronig relationship

Booij and Thoone [1982] carried out experimental work on polyvinyl-acetate (PVA) samples using oscillatory type measurements, on a mechanical spectrometer at 5 different frequencies and temperatures between 22–120°C. Using the Kramers-Kronig relationship, they showed that  $\delta$  can be determined as follows:

$$\delta(\omega) \cong \frac{\pi}{2} \left( \frac{d \log |G^*|}{d \log \omega} \right) \quad (8.2)$$

where the symbols are as previously defined. However, Booij and Thoone suggested the above equation needed to be supported by the experimental data. Eq. 8.2 can be re-written as [Chailleux *et al.*, 2006]:

$$\frac{\delta(\omega)}{90} = \left( \frac{d \log |G^*|}{d \log \omega} \right) \quad (8.3)$$

### 8.2.2 Christensen and Anderson (CA) Model

During the Strategic Highway Research Program (SHRP) A-002A campaign, Christensen and Anderson [1992] developed the  $|G^*|$  and  $\delta$  equations that describe the viscoelastic behaviour of bitumen. The  $|G^*|$  equation is shown in Chapter 3. For  $\delta$ , the following equation applies:

$$\delta(\omega) = \frac{90}{\left(1 + (\omega/\omega_0)^{\log 2/R}\right)} \quad (8.4)$$

where  $\delta$  is the phase angle,  $\omega$  is the reduced frequency,  $\omega_0$  is the crossover frequency and  $R$  is the rheological index. Equation 8.4 is followed the form of Equation 8.3.

### 8.2.3 Fractional Model

Stastna *et al.* [1997] developed the Fractional Model to describe the LVE behaviour of unmodified bitumens and PMBs. The phase angle equation,  $\delta$  is given as:

$$\delta(\omega) = \frac{\pi}{2} + \left(\frac{1}{n-m}\right) \left[ \sum_1^m \arctan(\mu_k \omega) - \sum_1^n \arctan(\lambda_k \omega) \right] \quad (8.5)$$

where  $\mu_k$  and  $\lambda_k$  is the relaxation time ( $\mu_k > 0$ ,  $\lambda_k > 0$ ),  $m$  and  $n$  are the numbers of relaxation time ( $n > m$ ).

### 8.2.4 Christensen, Anderson and Marasteanu (CAM) Model

In 1999, Marasteanu and Anderson developed a new model with the modification of the CA Model to improve the curve fitting particularly at lower and higher frequencies. The  $\delta$  equation can be shown as [Marasteanu and Anderson, 1999a]:

$$\delta(\omega) = \frac{90w}{\left(1 + (\omega_0/\omega)^v\right)} \quad (8.6)$$

where the symbols are as previously defined. The new parameter in the CAM Model,  $w$  addresses the issue of how fast or slow  $\delta$  converged to the two asymptotes (90 or zero degrees, respectively), as the frequency goes to zero or infinity. The  $v$  has resemblance to  $\log 2/R$  in the CA Model. Equation 8.6 is followed the form of Equation 8.3.

### 8.2.5 Al-Qadi and Co-workers Model

Elseifi *et al.* [2002] proposed the  $|G^*|$  and  $\delta$  equations to describe the LVE behaviour of unmodified bitumens and PMBs, called the Al-Qadi and Co-workers Model. Like the CAM Model, they used the Havriliak and Negami function form to develop the  $|G^*|$  equation and the details of this function can be found in Chapter 3. The  $\delta$  equation proposed is as follows:

$$\delta(\omega) = \frac{90}{\left(1 + (\omega/\omega_0)^v\right)^w} \quad (8.7)$$

where  $\omega$  is the reduced frequency,  $\omega_0$  is the reduced frequency value that defines the location along the  $x$ -axis,  $v$  and  $w$  are the fitting parameters. This equation was found to adequately describe the unmodified bitumens and PMBs with error less than 5 and 10%, respectively [Elseifi *et al.*, 2002]. Equation 8.7 is also followed the form of Equation 8.3.

## 8.2 Construction of the Phase Angle Master Curves

The  $\delta$  data collected at different temperatures can be shifted relative to the frequency (or time of loading), so that the various curves can be aligned to form a single line called a master curve [Pellinen *et al.*, 2002]. The amount of shifting required at each temperature to form the master curve is termed the shift factor,  $a_T$ . The master curve can be constructed using an arbitrarily selected reference temperature,  $T_{\text{ref}}$  to which all data are shifted. In this study, the  $\delta$  curves were shifted randomly (highest degree of freedom), without assuming any function for the shift factors.  $T_{\text{ref}}$  was arbitrarily chosen at 10°C. The construction of  $\delta$  master curves was done with the aid of the Solver function in Microsoft Excel, a function for

performing optimisation with a non-linear least squares regression technique. This process was done by minimising the sum of square errors (SSE) between measured and modelled  $\delta$ :

$$\text{Sum of square error (SSE)} = \sum \frac{(\delta_{\text{measured}_i} - \delta_{\text{model}_i})^2}{(\delta_{\text{measured}_i})^2} \quad (8.8)$$

where  $\delta_{\text{measured}_i}$  and  $\delta_{\text{model}_i}$  are the measured and modelled phase angles and the subscript  $i$  denotes the data set number. The Solver function replaced the initial guesses with optimised values. In order to check the best possible solution, this Solver solution can be kept and the Solver function run again; this runs another minimisation using the values from the last search to produce values for the new search. When no more changes can be observed, the iteration process was terminated.

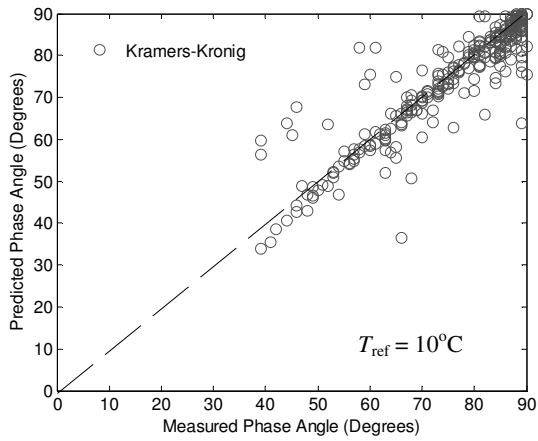
## 8.4 Results and Discussion

### 8.5.1 Graphical comparisons

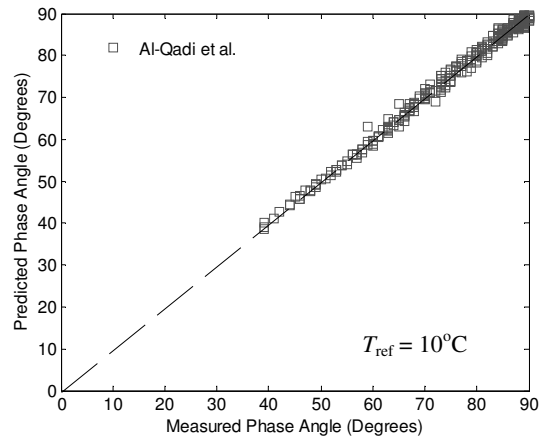
Comparisons between measured and descriptive  $\delta$  for the unaged and aged unmodified bitumens and PMBs are graphically displayed in Figs 8.1 to 8.4. These plots are intended to visually and qualitatively show an agreement between measured and descriptive values and to display the distribution error [Wu *et al.*, 2008]. It is observed that in Fig. 8.1, the Al-Qadi and Co-workers, CA, CAM and Fractional and Models are able to describe the viscoelastic behaviour of unaged unmodified bitumen satisfactorily. However, the Kramers-Kronig relationship shows some dispersion of descriptive  $\delta$  data from the equality line particularly at high frequencies and at the changes between the end of one temperature and next. Chailleux *et al.* [2006] also found a similar problem for asphalt mixtures where the Kramers-Kronig relationship cannot precisely describe  $\delta$  at high frequencies.

A similar observation is made for the aged unmodified bitumens (Fig. 8.2). The Al-Qadi and Co-workers, CAM and Fractional equations describe  $\delta$  satisfactorily. In contrast,  $\delta$  is found to be bit dispersed from the measurement data

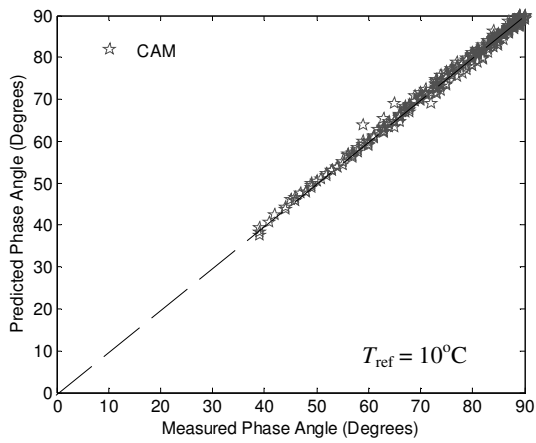
when comparing with the CA Model, showing that the ageing effect plays a significant role in the model's precision. As samples undergo ageing, the asphaltene content increases and  $\delta$  becomes more elastic. In a previous study, Christensen and Anderson [1992] found that the CA Model can be used over a wide range of temperatures and frequencies extended well into the glassy region. However, this model does not generate consistent results as viscous flow is approached. Therefore, they recommended using two sets of parameter values for primary (glassy to transition) and secondary (viscous) regions. A comparison between measured and modelled  $\delta$  for the unaged unmodified bitumen and aged PMB are shown graphically in Figs 8.3 and 8.4. It is observed that most of the  $\delta$  equations are unable to describe the viscoelastic behaviour of unaged and aged PMBs, particularly with the polymer modification exceeds 5%.



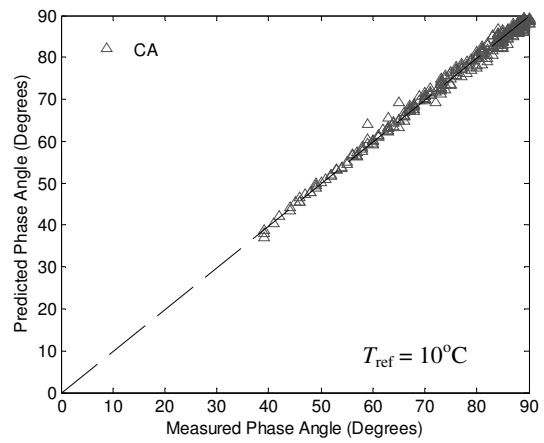
(a) The Kramers-Kronig Relationship



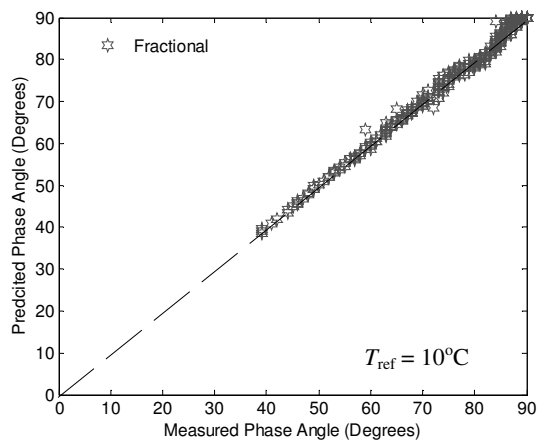
(b) The Al-Qadi and Co-workers Model



(c) The CAM Model

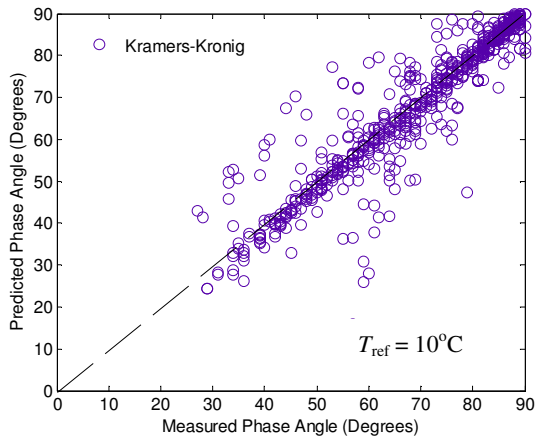


(d) The CA Model

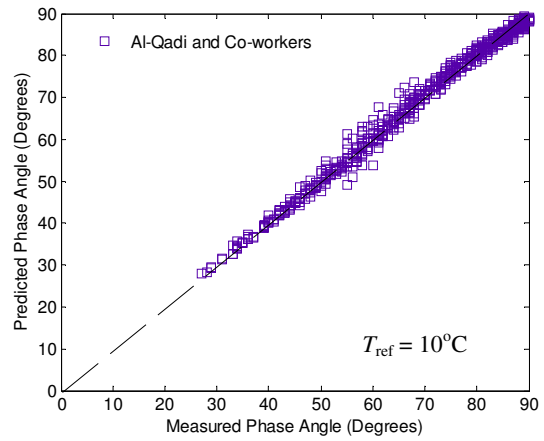


(e) The Fractional Model

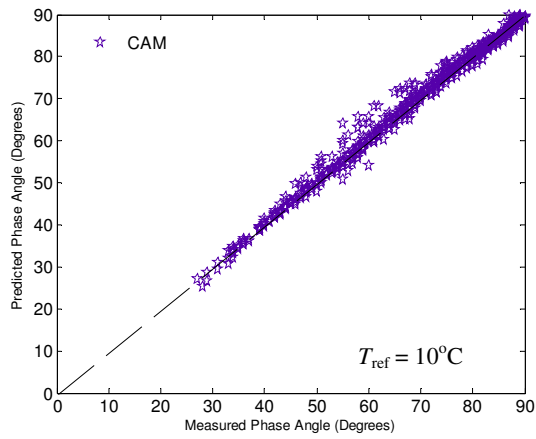
Fig. 8.1: Measured versus descriptive of  $\delta$  data of the unaged unmodified bitumens



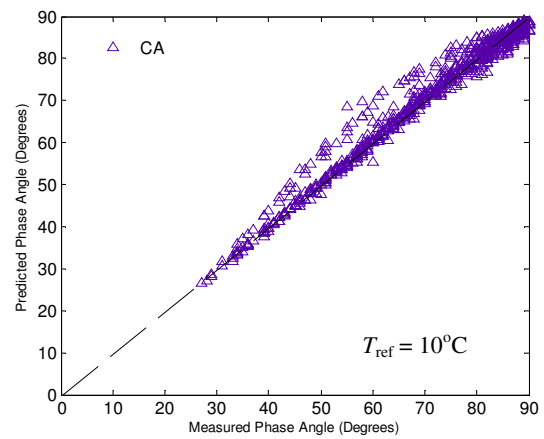
(a) The Kramers-Kronig Relationship



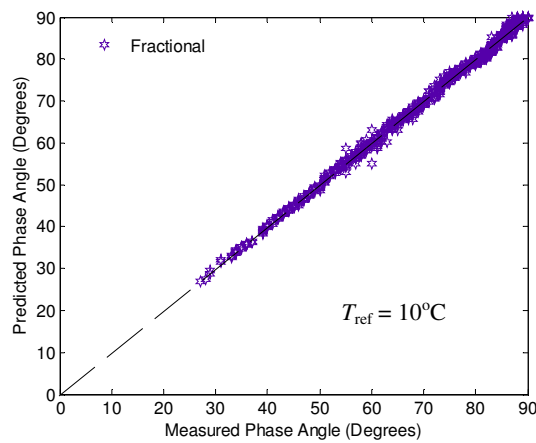
(b) The Al-Qadi and Co-workers Model



(c) The CAM Model

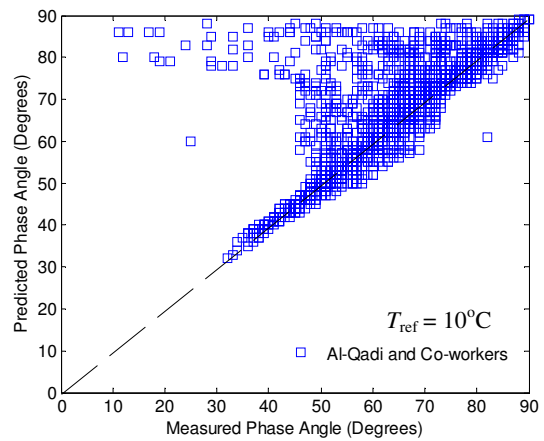
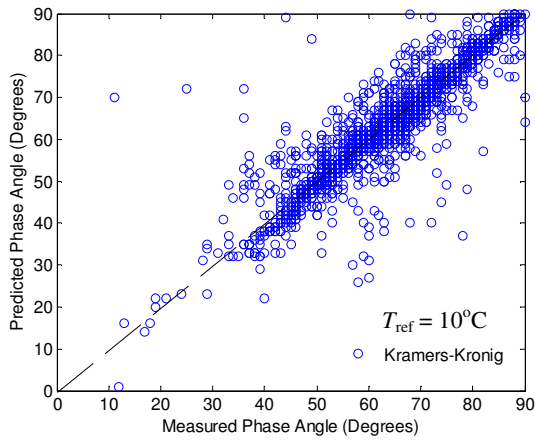


(d) The CA Model

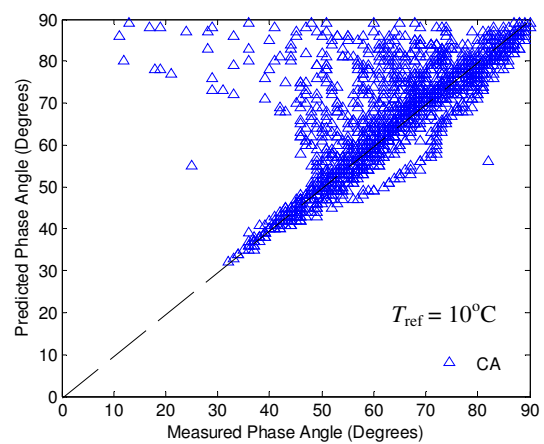
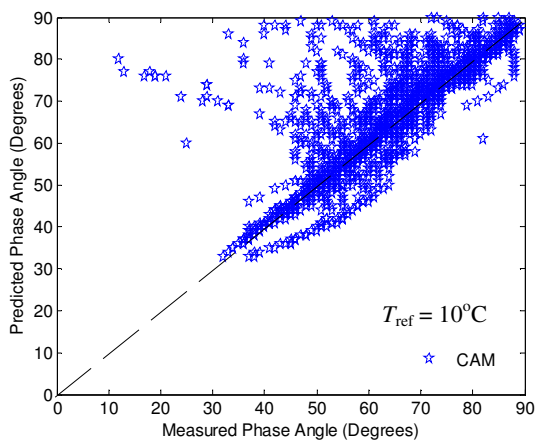


(e) The Fractional Model

Fig. 8.2: Measured versus descriptive of  $\delta$  data of the aged unmodified bitumens

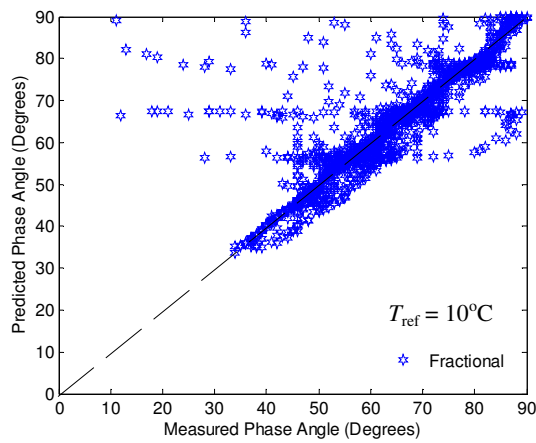


(a) The Kramers-Kronig Relationship (b) The Al-Qadi and Co-workers Model



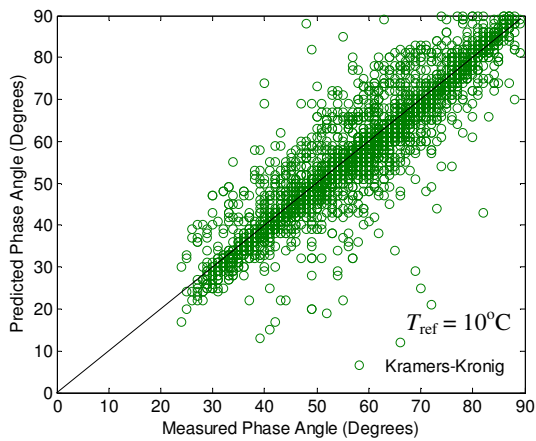
(c) The CAM Model

(d) The CA Model

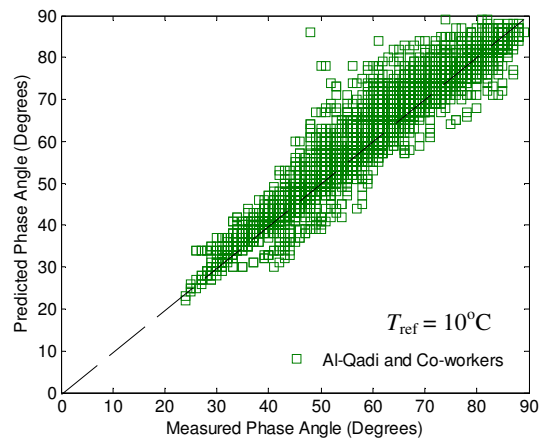


(e) The Fractional Model

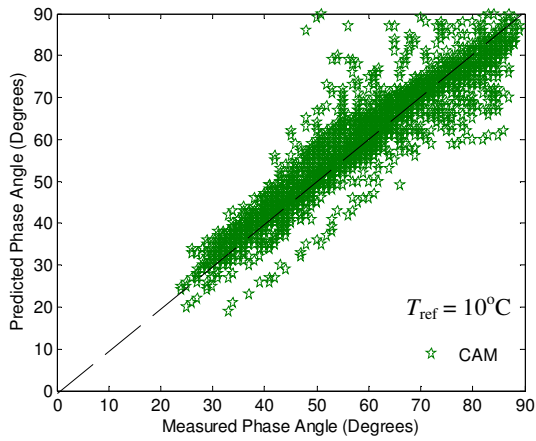
Fig. 8.3: Measured versus descriptive of  $\delta$  data of the unaged PMBs



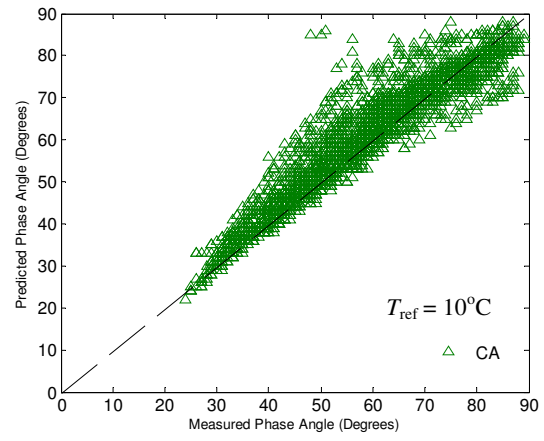
(a) The Kramers-Kronig Relationship



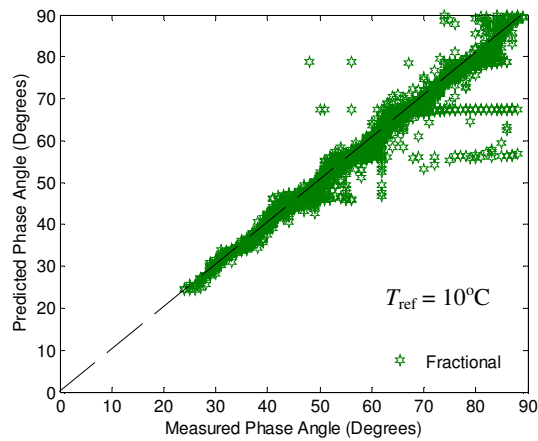
(b) The Al-Qadi and Co-workers Model



(c) The CAM Model



(d) The CA Model



(e) The Fractional Model

Fig. 8.4: Measured versus descriptive of  $\delta$  data of the aged PMBs

A significant observation has been made for the unaged unmodified bitumen, where the models are capable of fitting the  $\delta$  values pretty well with the  $\delta$  values decreasing from  $90^\circ$  to approximately around  $40^\circ$  as the frequency increases. The  $\delta$  values keep decreasing to a low value (Fig. 8.5). This phenomenon describes a thermorheological simple material obeying the TTSP.

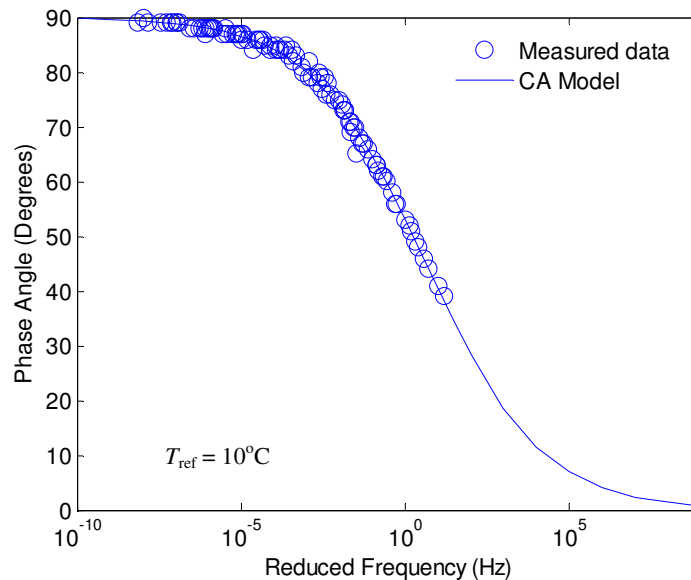


Fig. 8.5: A comparison between measured and the CA Model  $\delta$  of the unaged unmodified bitumen

Figs 8.6 and 8.7 shows a comparison of the  $\delta$  master curves between measured and modelled (Fractional Model and Al-Qadi and Co-workers Model) values of an aged PMB. There is a significant change observed in the shape of the  $\delta$  master curve of PMB with the appearance of a plateau in the master curve. The appearance of a plateau is believed to be associated with the polymer modification of the binders. According to Silva *et al.* [2004], this plateau means that in this region the elastic ( $G'$ ) and viscous ( $G''$ ) complex modulus components vary in the same proportion, in such a way that the phase angle does not change ( $\tan \delta = G''/G'$ ). Then, this plateau indicates that the polymer addition decreases the asphalt thermal susceptibility. This does not mean that the PMB complex modulus does not decrease when temperature is increased, but that the elastic component is constant in a broader range of temperature than that of the pure binder. Besides, plateau rheological curves are a characteristic of the viscoelastic response of rubbers. Thus this plateau indicates that in this range of frequency the modified binder presents a

rubber-like behaviour, which indicates a more effective contribution of the elastomeric modifier to the binder mechanical response. So, the appearance of this plateau in phase angle curves can be taken as an indicative of a better interaction between the polymeric modifiers and the binders, leading to an effective modification of the asphalt relaxation mechanisms. The width of this plateau could be related to the compatibility between polymer and asphalt phases [Silva *et al.*, 2004].

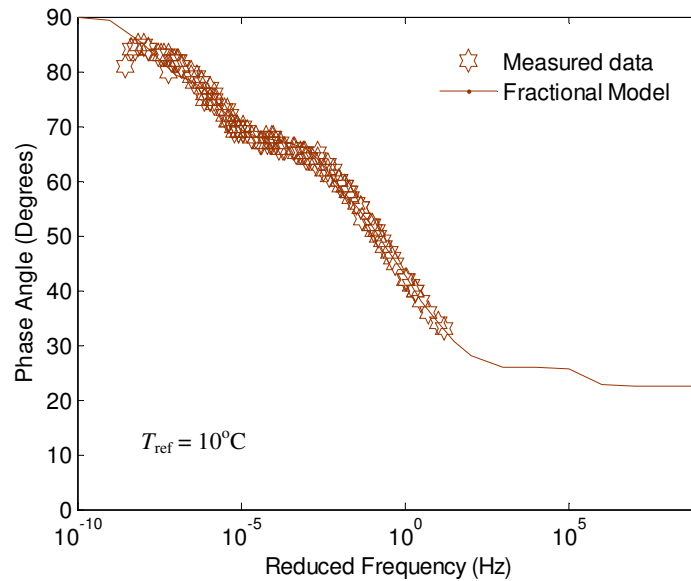


Fig. 8.6: A comparison between measured and the Fractional Model  $\delta$  of the aged PMB

In this study, the values of  $m = 2$  and  $n = 10$  were used for the Fractional Model, similar to the values used in Stastna *et al.* [1997]. As discussed by Marasteanu and Anderson [1999a], the degree of flexibility offered by this model is really useful when simulating a plateau or other irregularities in the master curves. When a high number of parameters are being used, this is actually conceptually close to fitting a discrete spectrum to the data. Similar findings were observed in this study and shown in Fig. 9.8. Marasteanu and Anderson [1999a], in addition, reported that the model lacked statistical robustness because the number of unknown coefficients approached the degree of freedom in the data. This can lead to the fitting of anomalous portions of the master curve that are the result of testing error, rather than real rheological behaviour [Marasteanu and Anderson, 1999a]. In

addition, this model is not really suitable for practical purposes due to the high number of coefficients that need to be solved simultaneously.

Fig. 9.8 shows a comparison between the experimental data of  $\delta$  and the Al-Qadi and Co-workers Model. It is observed that this model suffers from the drawback of being unable to describe  $\delta$  values with the appearance of a plateau in the  $\delta$  master curve. The same observations can be expected for the CA and CAM Models because they use the same form of equation, based on the Havriliak and Negami function. This can be explained where the Havriliak and Negami function takes the form of a sigmoidal shape. However, the  $\delta$  curve of modified binders was not in the sigmoidal shape. Therefore, it can be inferred that these models (CA, CAM and Al-Qadi and Co-workers) are unable to describe the presence of more than one transition curve in the  $\delta$  master curves.

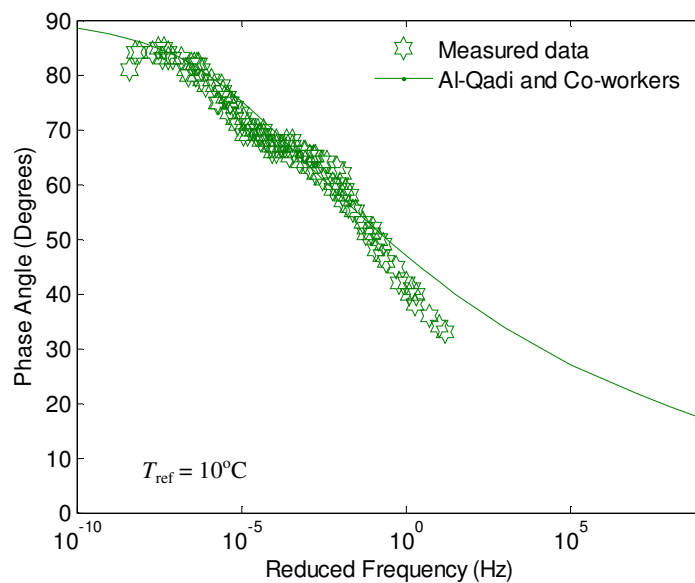


Fig. 9.8: A comparison between measured and the Al-Qadi and Co-workers Model  $\delta$  of the aged PMB

### 8.5.2 Statistical Analysis

Table 8.1 to 8.7 shows the SSE values for the unaged and aged unmodified and PMBs. For the unaged and aged unmodified bitumens, the Fractional Model, the Al-Qadi and Co-workers Model, the CA and the CAM Model show almost comparable results. The Kramers-Kronig relationship shows the least correlation

between measured and model data. For the unaged EVA PMBs, the Fractional Model shows the best correlation, followed by the Kramers-Kronig relationship. The Al-Qadi and Co-workers Model, CA Model and CAM Model show comparable results for all the unaged samples. However, as the EVA PMBs undergone the short-term (RTFOT) and long term (PAV) ageing, the SSE values become smaller and are generally comparable for every model. Similar observation also can be made for the unaged and aged SBS PMBs, as shown in Tables 8.5 to 8.7.

The goodness-of-fit statistics between measured and model  $\delta$  overall data for all samples are shown in Tables 8.8 and 8.9. The discrepancy ratio,  $r_i$  is used to observe the modelled data's tabulation from the equality line with the perfect value of 1. When the  $r_i$  is larger or smaller than 1, it measures how much wider the prediction interval has to be to cover the observed number of cases. With the interval of  $1 \pm 0.01$  used in this study, it is observed that all of the models except the Kramers-Kronig relationship show a good correlation with  $r_i$  more than 90% in the range of 0.95–1.05. Moreover, their  $S_e/S_y$  and  $R^2$  also show an 'excellent' correlation. The  $S_e/S_y$  and  $R^2$  goodness-of-fit for the Kramers-Kronig relationship are shown to be 'good' and 'fair', respectively. For the aged unmodified bitumens, the Fractional Model shows the most outstanding correlation between measured and modelled data, followed by the Al-Qadi and Co-workers, CAM, CA and the Kramers-Kronig relationship.

As shown in Table 8.9, the Fractional Model is found to be the most outstanding model with  $r_i$  more than 70% in the range of 0.95–1.05 of the unaged PMBs. However, in terms of  $S_e/S_y$  and  $R^2$ , the models' correlations vary from 'fair' to 'poor' and from 'good' to 'poor'. This finding indicates that most of them are unable to satisfactorily describe the viscoelastic properties of unaged PMBs. The Al-Qadi and Co-workers, CA and CAM Models show comparable results of  $r_i$  in the range of 0.95–1.05. This, as discussed earlier, could relate to the reason why these models cannot support the appearance of a plateau in the  $\delta$  master curves. Similarly, the Fractional Model correlates well between measured and  $\delta$  data of the aged PMBs with  $r_i$  in the range of 0.95–1.05. For  $S_e/S_y$ , the Fractional, Al-Qadi and Co-workers and CAM Models show 'excellent' correlations, followed by the CA and Kramers-

Kronig relationship (good). Except for the Fractional Models which show an 'excellent' correlation, all other models show 'good' correlations in terms of  $R^2$  (Table 9.9).

Traditionally phase angle of binder and mixtures has presented a complex verification of properties. Only recently an article in the Society of Rheology commented on the difficulty that occurs due to a lack of calibration standards for phase angle measurement [Velankar and Giles, 2007]. However, accepting the relationships that exist and using these to verify and check the adequacy of phase angle measurements will assist in this aspect [Rowe, 2009].

Table 8.1: SSE values for the unaged and aged unmodified bitumens

Model	Unaged bitumen			RTFOT Aged bitumen			PAV Aged bitumen		
	Middle East	Russian	Venezuelan	Middle East	Russian	Venezuelan	Middle East	Russian	Venezuelan
Kramers-Kronig	6.5629	3.4428	36.6203	7.9943	7.6777	7.7410	11.6734	10.4890	10.9048
Al-Qadi and Co-workers	0.0233	0.0102	0.0203	0.0176	0.0074	0.0342	0.1803	0.0271	0.0552
CAM	0.0268	0.0131	0.0120	0.0136	0.0064	0.0227	0.3098	0.0255	0.0371
CA	0.0372	0.0137	0.0214	0.0289	0.0138	0.0383	0.9351	0.0503	0.0897
Fractional	0.0285	0.0291	0.0137	0.0169	0.0078	0.0102	0.0219	0.0206	0.0232

Table 8.2: SSE values for the unaged EVA PMBs

Model	Unaged EVA PMBs (3%)			Unaged EVA PMBs (5%)			Unaged EVA PMBs (7%)		
	Middle East	Russian	Venezuelan	Middle East	Russian	Venezuelan	Middle East	Russian	Venezuelan
Kramers-Kronig	0.0054	10.6185	0.0081	0.0032	3.5125	0.0234	0.0033	0.9046	0.0530
Al-Qadi and Co-workers	0.0522	48.2519	0.0519	0.0778	85.6407	3.1779	0.1240	84.9081	12.0482
CAM	0.0394	62.0445	0.0489	0.0686	60.8253	3.3506	0.1006	73.5512	12.0501
CA	0.0592	48.2920	0.0495	0.0904	95.3341	3.6068	0.1721	77.4921	12.0110
Fractional	0.0248	52.2994	0.0559	0.0325	72.8857	0.9741	0.1287	51.6524	0.6915

Table 8.3: SSE values for the RTFOT aged EVA PMBs

Model	RTFOT Aged EVA PMBs (3%)			RTFOT Aged EVA PMBs (5%)			RTFOT Aged EVA PMBs (7%)		
	Middle East	Russian	Venezuelan	Middle East	Russian	Venezuelan	Middle East	Russian	Venezuelan
Kramers-Kronig	0.8207	-	-	2.1610	1.0441	1.9520	3.2868	2.6873	3.1462
Al-Qadi and Co-workers	0.6596	-	-	0.9575	2.5052	1.8166	0.1025	3.2435	3.9225
CAM	0.1055	-	-	0.9049	5.8784	0.6458	0.9375	3.2567	1.5590
CA	0.3424	-	-	1.4520	4.5138	0.5399	6.6103	2.6955	2.4808
Fractional	0.1609	-	-	0.5295	0.9830	0.5562	0.6385	2.1834	1.1133

Table 8.4: SSE values for the PAV aged EVA PMBs

Model	PAV Aged EVA PMBs (3%)			PAV Aged EVA PMBs (5%)			PAV Aged EVA PMBs (7%)		
	Middle East	Russian	Venezuelan	Middle East	Russian	Venezuelan	Middle East	Russian	Venezuelan
Kramers-Kronig	1.7502	-	-	5.9655	8.8326	6.2326	7.5738	5.9943	7.7519
Al-Qadi and Co-workers	0.4864	-	-	0.1077	0.1060	0.3951	1.9839	1.0165	0.1548
CAM	1.0483	-	-	0.6123	1.2331	0.1492	1.7240	1.2121	0.3450
CA	0.6424	-	-	1.9294	0.2305	0.9260	0.4198	1.4215	0.8337
Fractional	0.2212	-	-	0.0934	0.0770	0.1069	0.0805	0.0838	0.1483

Table 8.5: SSE values for the unaged SBS PMBs

Model	Unaged SBS PMBs (3%)		Unaged SBS PMBs (5%)		Unaged SBS PMBs (7%)	
	Russian	Venezuelan	Russian	Venezuelan	Russian	Venezuelan
Kramers-Kronig	0.3485	0.2850	0.9135	0.6208	1.9126	1.2750
Al-Qadi and Co-workers	4.0984	0.0956	7.0305	0.2783	18.4378	0.4696
CAM	4.3088	0.0843	7.5797	0.2754	19.7091	0.5194
CA	4.1706	0.0954	6.8121	0.2852	13.6127	0.4270
Fractional	3.9231	0.0300	0.5529	0.1445	2.1756	0.1385

Table 8.6: SSE values for the RTFOT aged SBS PMBs

Model	RTFOT Aged SBS PMBs (3%)		RTFOT Aged SBS PMBs (5%)		RTFOT Aged SBS PMBs (7%)	
	Russian	Venezuelan	Russian	Venezuelan	Russian	Venezuelan
Kramers-Kronig	0.2952	0.5729	0.2952	1.7851	1.3862	2.3778
Al-Qadi and Co-workers	0.4594	0.1092	0.4445	0.5920	0.2810	0.2207
CAM	2.8061	0.4113	0.4615	0.2162	0.5542	0.2810
CA	0.1593	0.1233	0.3989	0.2289	0.3212	0.2810
Fractional	0.1514	0.0240	0.0366	0.0926	0.2689	0.0862

Table 8.7: SSE values for the PAV aged SBS PMBs

Model	PAV Aged SBS PMBs (3%)		PAV Aged SBS PMBs (5%)		PAV Aged SBS PMBs (7%)	
	Russian	Venezuelan	Russian	Venezuelan	Russian	Venezuelan
Kramers-Kronig	2.2858	3.3551	3.3447	0.8760	4.4642	4.9864
Al-Qadi and Co-workers	0.4244	0.2977	0.4974	1.1782	1.0025	2.0310
CAM	0.3811	0.1171	0.5232	0.1629	0.7117	0.3469
CA	0.0736	0.1060	0.4379	0.6318	0.8031	0.5674
Fractional	0.0210	0.0456	0.0389	0.0661	0.1026	0.0551

Table 8.8: The goodness-of-fit statistics for the unaged and aged unmodified bitumens

Model	Condition	Discrepancy ratio ( $r_i$ ) (%)					$S_e/S_y$	$R^2$
		0.99 – 1.01	0.98 – 1.02	0.97 – 1.03	0.96 – 1.04	0.95 – 1.05		
Kramers-Kronig	unaged	26.65	46.40	57.68	69.28	74.30	0.552	0.694
Al-Qadi and Co-workers		63.67	88.20	97.83	99.07	99.38	0.074	0.995
CAM		68.63	89.13	98.45	98.76	99.38	0.071	0.995
CA		55.28	84.16	95.96	98.76	99.07	0.087	0.992
Fractional		50.60	84.23	96.73	98.81	99.41	0.090	0.992
Kramers-Kronig	aged	24.21	42.56	53.53	62.26	69.62	0.423	0.821
Al-Qadi and Co-workers		48.07	77.98	88.84	94.20	95.98	0.087	0.992
CAM		54.32	80.21	89.14	92.41	94.05	0.094	0.991
CA		36.76	63.10	78.57	85.71	88.10	0.159	0.975
Fractional		61.46	92.41	98.07	99.41	99.55	0.054	0.997

Table 8.9: The goodness-of-fit statistics for the unaged and aged PMBs

Model	Condition	Discrepancy ratio ( $r_i$ ) (%)					$S_e/S_y$	$R^2$
		0.99 – 1.01	0.98 – 1.02	0.97 – 1.03	0.96 – 1.04	0.95 – 1.05		
Kramers-Kronig	unaged	21.74	37.78	49.61	59.10	66.19	0.719	0.482
Al-Qadi and Co-workers		15.44	32.72	46.19	53.64	59.30	0.841	0.294
CAM		16.51	32.54	43.80	50.95	56.14	0.807	0.349
CA		13.65	27.53	39.09	47.20	53.40	0.831	0.310
Fractional		29.07	48.30	60.81	67.66	71.77	0.584	0.660
Kramers-Kronig	aged	14.50	29.70	41.57	50.16	57.57	0.501	0.749
Al-Qadi and Co-workers		14.87	28.02	39.94	50.21	58.41	0.336	0.887
CAM		13.19	26.25	38.51	49.26	57.13	0.352	0.876
CA		11.92	25.09	36.53	46.12	53.81	0.362	0.869
Fractional		33.22	56.65	71.83	81.21	86.53	0.247	0.939

## 8.4 Summary

Several key observations can be drawn from this study:

- In general, the phase angle,  $\delta$  can be thought of as the second part of the complex modulus in order to yield complete information about the linear viscoelastic function of bituminous binders.
- The Al-Qadi and co-workers, CA and CAM Models follow the form of the Kramers-Kronig relationship -  $\frac{\delta(\omega)}{90} = \left( \frac{d \log |G^*|}{d \log \omega} \right)$ .
- For the unaged and aged unmodified bitumens, the Fractional Model, the Al-Qadi and Co-workers Model, the CA and the CAM Model show almost comparable SSE results. The Kramers-Kronig relationship shows the least SSE correlation between measured and model data.
- For the unaged EVA PMBs, the Fractional Model shows the best SSE correlation, followed by the Kramers-Kronig relationship. The Al-Qadi and Co-workers Model, CA Model and CAM Model show comparable results for all the unaged samples. However, as the EVA PMBs that undergone the short-term (RTFOT) and long term (PAV) ageing, the SSE values become smaller and generally comparable for every model. Similar observation also can be made for the unaged and aged SBS PMBs
- From this study, it is observed that most of the tested models; the Fractional, Al-Qadi and Co-workers, Christensen and Anderson (CA) and Christensen, Anderson and Marasteanu (CAM) Models are able to fit or describe the linear viscoelastic region of unmodified bitumen satisfactorily. Except for the Fractional Model, most of the models are unable to describe the appearance of a plateau in the  $\delta$  master curves of unaged PMBs.
- The Fractional Model is resemblance to the discrete spectrum method and fit the viscoelastic properties of many materials really well.

## Conclusions and Recommendations

---

### 9.1 Conclusions

This chapter summarises the principal conclusions that can be drawn from the study and makes recommendations for future work. They are discussed as follows:

#### Shift Factor Equations

- It is observed that the random, non-functional form shift function produces the most consistent set of results due to the high degree of freedom and overall flexibility of this non-linear least squares fitting approach.
- In the shift factor equations study, in a temperature range from 10–75°C, the LCPC and WLF equations generally produced the best results compared to the random shift approach (measured versus model) for all the material combinations studied, followed by the VTS and Arrhenius equations. The Log-Linear equation showed the lowest correlation with measured shift factor data.
- However, most of the equations are unable to describe the master curves of highly modified bitumen – in this case, the unaged EVA polymer-modified bitumens.

#### Mathematical Models

- In a range of temperature from 10–75°C, It is observed that the Sigmoidal, Generalised Logistic Sigmoidal, Christensen and Anderson (CA), and

Christensen, Anderson and Marasteanu (CAM) Models are able to satisfactorily describe the rheological properties of unaged and aged unmodified bitumens.

- From this study, it is found that the Generalised Logistic Sigmoidal and Sigmoidal Models which are generally used for asphalt mixtures also can be used for describing the complex modulus master curves of bituminous binders.
- The glassy modulus for unaged and aged unmodified bitumens and polymer-modified bitumens can be taken as  $1 \times 10^9$  Pa. On the other hand, the elastic modulus tends to be too small and can be neglected.
- All the models suffer from the drawback that they are unable to describe the rheological properties of the unaged polymer-modified bitumens due to the presence of highly semi-crystalline EVA substances. This EVA PMB does not behave as a thermo-rheological simple material.
- For the unaged and aged unmodified bitumens, the Generalised Logistic Sigmoidal Model shows the best correlation between measured and modelled data, followed by the Sigmoidal, CA and CAM Models. Meanwhile, for the unaged and aged PMBs, the Generalised Logistic Sigmoidal Model and Sigmoidal Model show the best correlation between measured and modelled data.

### **A Mechanical Model**

- The 2S2P1D Model can satisfactorily describe the rheological properties of unmodified bitumens (unaged and aged), bitumen-filler mastics (unaged and aged) and polymer-modified bitumens (aged).
- The model can be thought of as a unique model as its parameters are relatable to the construction of complex modulus and phase angle master curves, the Black diagram and the Cole-Cole diagram.
- However, like mathematical models, the 2S2P1D Model failed to describe the rheological properties of highly modified of unaged polymer-modified bitumens.

## Phase Angle Equations

- It is observed that most of the tested models; the Fractional, Al-Qadi and co-workers, Christensen and Anderson (CA) and Christensen, Anderson and Marasteanu (CAM) Models are able to fit the response of unmodified bitumen satisfactorily for the temperature range from 10 to 75°C.
- It is worth mentioning that the Al-Qadi and co-workers, CA and CAM Models follow the form of the Kramers-Kronig relationship -
$$\frac{\delta(\omega)}{90} = \left( \frac{d \log |G^*|}{d \log \omega} \right).$$
- Except for the Fractional Model, most of the models are unable to describe the appearance of a plateau in the  $\delta$  master curves of unaged PMBs. This can be attributed to the fact that these models are unable to describe the presence of more than one transition of the  $\delta$  master curve.
- The Fractional Model is resemblance to the discrete spectrum model which has been found to work well with different types of materials.

## 9.2 Recommendations for Future Work

- Chapter 3 discusses various models used to describe the rheological properties of bituminous binders. Similarly, a reasonable number of studies found from literature have been conducted to develop rheological models for asphalt mixtures. Like the binder's model, most of the asphalt mixture models are presented in terms of dynamic (complex) modulus,  $|E^*|$  and phase angle,  $\varphi$ , master curves. They also can be classified into three main groups; nomographs, mathematical and mechanical models. Therefore, it is recommended that asphalt mixture models be reviewed as well.
- It is accepted that the use of polymer-modified bitumens in road paving provides many advantages compared to unmodified bitumens. However, despite real achievements, many challenges and opportunities remain. It is therefore important to review the challenges and solutions taken to improve polymer-modified bitumens characteristics and its storage stability problem.

- Chapter 5 discusses various shift factor equations used to construct master curves for bituminous binders. These methods are also can be used for asphalt mixtures. It is recommended to assess the suitability of different shifting methods on the construction of master curves of asphalt mixtures.
- From literature, it was found that the 2S2P1D Model (Chapter 6) is applicable for both binders and asphalt mixtures. Therefore, this model is recommended to be used to describe the rheological properties of NTEC asphalt mixture database.
- Different phase angle equations are available for asphalt mixtures and it is also recommended to conduct a comparison study of phase angle equations of asphalt mixtures.
- The research in this thesis has concentrated on moderate to high temperature testing of binders. To obtain a broader understanding of the rheological properties of unmodified and modified binders, low temperature rheological testing using testing equipments such as the bending beam rheometer (BBR) and the direct tension tester (DTT) are recommended.

## References

- Adams, Y.E., Zeghal, M. and Mohamed, E.H. Complex Modulus Test Protocol and Procedure for Determining Huet-Sayegh Model Parameters. IRC-IR-871, National Research Council Canada, 2006.
- Airey, G.D. Rheological Characteristics of Polymer Modified and Aged Bitumens. PhD Thesis, the University of Nottingham, 1997.
- Airey, G.D. Use of Black Diagrams to Identify Inconsistencies in Rheological Data. *Road Materials and Pavement Design*, Vol. 3 (4), pp. 403–424, 2002a.
- Airey, G.D. Rheological Evaluation of Ethylene Vinyl Acetate Polymer Modified Bitumens. *Construction and Building Materials*, Vol. 16, pp. 473–487, 2002b.
- Airey, G.D. Rheological Properties of Styrene Butadiene Styrene Polymer Modified Road Bitumens. *Fuel*, Vol. 82, pp. 1709–1719, 2003.
- Airey, G.D. Styrene Butadiene Styrene Polymer Modification of Road Bitumens. *Journal of Materials Science*, Vol. 39, pp. 951–959, 2004.
- Airey, G.D. Chapter 23: Bitumen Properties and Test Methods. ICE Manual of Construction Materials, Institution of Civil Engineers, UK, 2009.
- Airey, G.D. and Brown, S.F. Rheological Performance of Aged Polymer Modified Bitumens. *Journal of the Association of Asphalt Paving Technologists*, Vol. 67, pp. 66–100, 1998.
- Airey, G.D. and Hunter, E. Dynamic Mechanical Testing of Bitumen: Sample Preparation Methods. *Proceedings of the Institution of Civil Engineers: Transport* 156. Issue TR 2, pp 85–92, 2003.
- Ait-Kadi, A., Brahim, B., and Bousmina, M. Polymer Blends for Enhanced Asphalt Binders". *Polymer Engineering and Science*, Vol. 36 (12), pp. 1724–1733, 1996.
- Anderson, D.A., Christensen, D.W. and Bahia, H. Physical Properties of Asphalt Cement and the Development of Performance-Related Specifications. *Journal of the Association of Asphalt Paving Technologists*. Vol. 60; pp. 437–532, 1991.
- Anderson D.A., Christensen D.W., Bahia H.U, Dongré, R., Sharma M.G, Antle C.E and Button, J. Binder Characterization and Evaluation. Volume 3: Physical Characterization. SHRP-A-369. National Research Council, Washington D.C., 1994.

- Anderson, D.A., Christensen, D.W., Roque, R. and Roybak, R.A. Rheological Properties of Polymer Modified Emulsion Residue, Polymer Modified Asphalt Binders, ASTM STP 1108, Kenneth R. Wardlaw and Scott Shuler, Eds., American Society for Testing and Materials, Philadelphia, 1992.
- Asphalt Academy. Technical Guideline: The Use of Modified Bituminous Binders in Road Construction (TG 1) Second Edition. South Africa, 2007.
- Bahia, H.U., Hanson, D.I., Zeng, M., Zhai, H., Khatri, M.A. and Anderson, R.M. Characterisation of Modified Asphalt Binders in Superpave Mix Design. NCHRP Report 459. Transportation Research Board – National Research Council. 2001.
- Bari, J. and Witzak, M.W. New Predictive Models for Viscosity and Complex Shear Modulus of Asphalt Binders: for use with Mechanistic-Empirical Pavement Design Guide. *Transportation Research Record*, No. 2001, pp. 9–19, 2007.
- Barnes, H.A., Hutton, J.F. and Walters, K. An Introduction to Rheology, Volume 3. Netherland; Elsevier Science Publishers, B.V., 1989.
- Blab, R., Kappl, K., Lackner, R. and Aiger, L. Sustainable and Advance Materials for Road InfraStructure (SAMARIS) Report. Permanent Deformation of Bituminous Bound Materials in Flexible Pavements: Evaluation of Test Methods and Prediction Models. SAM-05-D28, 2006.
- Biswas, K.G., and Pellinen, T.K. Practical Methodology of Determining the In Situ Dynamic (Complex) Moduli for Engineering Analysis. *Journal of Materials in Civil Engineering*, Vol. 19 (6), pp. 508–513, 2007.
- Bonaquist, R., and Christensen, D.W. Practical Procedure for Developing Dynamic Modulus Master Curves for Pavement Structural Design. Transportation Research Record No. 1929, pp. 208–217, 2005.
- Bonnaure, F., Gest, G., Gravois, A. and Uge, P. A New Method of Predicting the Stiffness of Asphalt Paving Mixtures. *Proceedings of the Association of Asphalt Paving Technologists*, Vol. 46, pp. 64–104, 1977.
- Booij, H.C. and Thoone, G.P.J.M. Generalization of Kramers-Kronig Transforms and Some Approximations of Relations between Viscoelastic Quantities. *Rheologica Acta*, Vol. 21, pp. 15–24, 1982.
- Bouldin, M.G., Dongre, R., Rowe, G.M., Sharrock, M.J. and Anderson, D.A. Predicting Thermal Cracking of Pavements from Binder Properties: Theoretical

- Basis and Field Validation. *Journal of the Association of Asphalt Paving Technologists*, Vol. 69, pp. 455-496, 2000.
- Brodynan J.G., Gaskins, F.H., Philippoff, W. and Thelen E. The Rheology of Asphalt III. Dynamic Mechanical Properties of Asphalt. *Transactions of the Society of Rheology*, Vol. 4, pp. 279–296, 1960.
- Brown, S.F., Rowlett, R.D. and Boucher, J.L. Asphalt Modification. *Proceedings of the Conference on US SHRP Highway Research Program: Sharing the Benefits*, ICE; pp. 191–203, 1990.
- Chailleux, E., Ramond, G., and de la Roche, C. A Mathematical-based Master Curve Construction Method Applied to Complex Modulus of Bituminous Materials. *Journal of Road Materials and Pavement Design*, Vol 7, pp. 75–92, 2006.
- Chen, J.S., Liao, M.C. and Tsai, H.H. Evaluation and Optimization of the Engineering Characteristics of Polymer-Modified Asphalt. *Practical Failure Analysis*, Vol. 2 (3), pp. 75–83, 2002.
- Choi, K.Y. Development of the Saturation Ageing Tensile Stiffness (SATS) Test for High Modulus Base Materials. PhD Thesis, the University of Nottingham, 2005.
- Christensen D.W. and Anderson D.A. Interpretation of Dynamic Mechanical Test Data for Paving Grade Asphalt. *Journal of the Association of Asphalt Paving Technologists*, Vol. 61, pp. 67–116, 1992.
- Cong, Y., Huang, W. and Liao, K. Compatibility between SBS and Asphalt. *Petroleum Science and Technology*, Vol. 26 (3), pp. 346–352, 2008.
- Corbett, L.C. Relationship Between Composition and Physical Properties of Asphalts. *Proceedings of the Association of Asphalt Paving Technologists*, Vol. 39, pp. 481–498, 1970.
- Dealy, J.M. and Larson, R.G. Structure and Rheology of Molten Polymers from Structure to Flow Behavior and Back Again. Munich; Hanser Publisher, 2006.
- Delaporte, B., Di Benedetto, H., Chaverot, P. and Gauthier, G. Linear Viscoelastic Properties of Bituminous Materials; from Binders to Mastics. *Journal of Association of Asphalt Paving Technologists* Vol. 76, pp. 455–494, 2007.
- Delaporte, B., Di Benedetto, H., Chaverot, P. and Gauthier, G. Linear Viscoelastic Properties of Bituminous Materials Including New Products Made with Ultrafine Particles. *Road Materials and Pavement Design*, Vol. 10 (1), pp. 7–38, 2009.

- Di Benedetto, H., Mondher, N., Sauzeat, C. and Olard, F. Three-dimensional Thermo-viscoplastic Behaviour of Bituminous Materials: The DBN Model. *Road Materials and Pavement Design*, Vol. 8, pp. 285–315, 2007.
- Dickinson E.J., and Witt, H.P. The Dynamic Shear Modulus of Paving Asphalts as Function of Frequency. *Transactions of the Society of Rheology*, Vol. 18 (4), pp. 591–606, 1974.
- Dobson, G.R. The Dynamic Mechanical Properties of Bitumen. *Proceedings of the Association of Asphalt Paving Technologists*, Vol. 38, pp. 123–135, 1969.
- Dobson G.R. On the Development of Rational Specifications for the Rheological Properties of Bitumen. *Journal of the Institute of Petroleum*, Vol. 58, pp. 14–24, 1972.
- Dukatz, E.L. and Anderson, D.A. The Effect of Various Fillers on the Mechanical Behaviour of Asphalt and Asphalt Concrete. *Proceedings of the Association of Asphalt Paving Technologists*. Vol. 49, pp. 530 – 549, 1980.
- Edwards, Y., Tasdemir, Y. Isacson, U. Rheological Effects of Commercial Waxes and Polyphosphoric Acid in Bitumen 160/220-Low Temperature Performance. *Fuel*, 85, pp. 989–997, 2006.
- Elseifi, M.A., Al-Qadi, I., Flinch, G.W. and Masson, J.F. Viscoelastic Modeling of Straight Run and Modified Binders using the Matching Function Approach. *The International Journal of Pavement Engineering*, Vol. 3 (1), pp. 53–61, 2002.
- Eurobitume. First European Workshop on the Rheology of Bituminous Binders, Brussels, April 5<sup>th</sup> to 7<sup>th</sup>, European Bitumen Association, 1995.
- Eurobitume. Rheology of Bituminous Binders Glossary of Rheological Terms: A Practical Summary of the Most Common Concepts, European Bitumen Association, 1996.
- Garcia, G. and Thompson, M.R. HMA Dynamic Modulus Predictive Models: A Review. Research Report FHWA-ICT-07-2005. Illinois Centre for Transportation, 2007.
- Gardiner, M.S. The Significance of Phase Angle Measurements for Asphalt Cement. *Journal of the Associations of Asphalt Paving Technologists*, Vol. 65, pp. 321–356, 1996.
- Gershoff, D.R., Carswell, J. and Nicholls J.C. Rheological Properties of Polymer-Modified Binders for use in Rolled Asphalt Wearing Course Transport Research Laboratory 157, Thomas Telford Ltd, 1999.

- Goodrich, J.L. Asphalt and Polymer Modified Asphalt Properties Related to the Performance of Asphalt Concrete Mixes. *Proceedings of the Association of Asphalt Paving Technologists*, Vol. 57, pp. 116 – 175, 1988.
- Halstead, J.C. Relation of Asphalt Chemistry to Physical Properties and Specifications. *Proceedings of the Association of Asphalt Paving Technologists*, Vol. 54, pp. 91–117, 1985.
- Harrigan, E.T., Leahy, R.B. and Youtcheff, J.S. The SUPERPAVE Mix Design System Manual of Specifications, Test Methods and Practices, SHRP-A-379, Strategic Highways Research Program, National Research Council, Washington D.C., 1994.
- Herh, P.K.W., Colo, S.M. and Rudolph, B.K.S. Dynamic Shear Rheometers Pave the Way for Quality Asphalt Binders. Application Note. Rheo Logica Instruments, 1999.
- Heukelom, W. Observations on the Rheology and Fracture of Bitumens and Asphalt Mixes. *Proceedings of the Association of Asphalt Paving Technologists*, Vol. 36, pp. 359–397, 1966.
- Heukolem, W. An Improved Method of Characterizing Asphaltic Bitumens with the Aid of Their Mechanical Properties. *Proceedings of the Association of Asphalt Paving Technologists*, Vol. 42, pp. 67–98, 1973.
- Heukolem, W. and Klomp, J.G. Road Design and Dynamic Loading. *Proceedings of the Association of Asphalt Paving Technologists*, Vol. 33, pp. 92–125, 1964.
- Ho, S. and Zanzotto, L. The Low Temperature Characteristics of Unmodified and Modified Asphalt Binders Evaluated by the Failure Energy and Secant Modulus from Direct Tension Tests. *Materials and Structures*, Vol. 38, pp. 137–143, 2005.
- Hopkins, I.L. and Hamming, R.W. On Creep and Relaxation. *Journal of Applied Physics*, Vol. 28 (8), pp. 906 – 909, 1957.
- Huet, C. Étude Par Une Methods D'impédance Du Comportement Viscoélastique Des Matériaux Hydrocarbons. These de Docteur-Ingenieur, Faculté des Science de Paris, 1963 (In French).
- Isacsson, U. and Lu, X. Testing and Appraisal of Polymer Modified Road Bitumens – State of the Art. *Materials and Structures*, Vol. 28, pp. 139–159, 1995.

- Jongepier, R. and Kuilman, B. Characteristics of the Rheology of Bitumens. *Proceedings of the Association of Asphalt Paving Technologists*, Vol 38, pp. 98–122, 1969.
- Jongepier, R. and Kuilman, B. The Dynamic Shear Modulus of Bitumens as a Function of Frequency and Temperature. *Rheologica Acta*, Vol. 9, pp. 102–111, 1970.
- Khong, T.D., Malhotra, S.L. and Blanchard, L.P. Rheological Behaviour of Asphalts, *Rheologica Acta*, Vol. 18 (3), pp. 382–391, 1979.
- Lenoble, C. and Nahas, N.C. Dynamic Rheology and Hot Mix Performance of Polymer Modified Asphalt. *Journal of the Association of Asphalt Paving Technologists*, Vol. 63, pp. 450–480, 1994.
- Lesueur, D. Letter to the Editor: On the Thermo-rheological Complexity and Relaxation of Asphalt Cements. *Journal of Rheology*, Vol. 43, pp. 1701–1704, 1999.
- Lesueur, D. The Colloidal Structure of Bitumen: Consequences on the Rheology and on the Mechanisms of Bitumen Modification. *Advances in Colloid and Interface Science*, Vol. 145, pp. 42–82, 2009.
- Lesueur, D., Gerard, J.F., Claudy, P., Letoffe, J.M., Plance, J.P. and Martin, D. A Structure Related Model to Describe Asphalt Linear Viscoelasticity. *Journal of Rheology*. Vol. 40 (5), pp. 813–836, 1996.
- Levenberg, E. and Shah, A. Interpretation of Complex Modulus Test Results for Asphalt Aggregate Mixes. *ASTM Journal of Testing and Evaluation*, Vol. 36 (4), pp. 326–334, 2008.
- Li, X., Zofka, A., Marasteanu, M., and Clyne, T.R. Evaluation of Field Aging Effects on Asphalt Binder Properties. *Road Materials and Pavement Design*, Vol. 7, pp. 57–73, 2006.
- Liao, M.C. Small and Large Strain Rheological and Fatigue Characterisation of Bitumen-Filler Mastics. PhD Thesis, The University of Nottingham, 2007.
- Lu, X. and Isacsson, U. Artificial Aging of Polymer Modified Bitumens. *Journal of Applied Polymer Science*, Vol. 76, pp. 1811–1824, 1999a.
- Lu, X. and Isacsson, U. Chemical and Rheological Characteristics of Styrene Butadiene Styrene Polymer Modified Bitumens. *Transportation Research Record*, Vol. 1661, pp 83–92, 1999b.

- Lu, X., Isacsson, U. and Ekblad, J. Low Temperature Characteristics of Styrene Butadiene Styrene Polymer Modified Bitumens. *Construction and Building Materials*, Vol. 12, pp. 405–414, 1998.
- Maccarrone, S. Rheological Properties of Weathered Asphalts Extracted from Sprayed Seals Nearing Distress Conditions. *Proceedings of the Associations of Asphalt Paving Technologists*, Vol. 56, pp. 654–687, 1987.
- Marasteanu, M.O. Inter-conversions of the Linear Viscoelastic Functions Used for the Rheological Characterization of Asphalt Binders. PhD Thesis, Pennsylvania State University, Pennsylvania, 1999.
- Marasteanu, M. and Anderson, D. Time Temperature Dependency of Asphalt Binders- An Improved Model. *Journal of the Association of Asphalt Paving Technologists*, Vol. 65, pp 407–448, 1996.
- Marasteanu, O. and Anderson, D.A. Improved Model for Bitumen Rheological Characterization. *Eurobitume Workshop on Performance Related Properties for Bitumens Binder*, Luxembourg, paper no. 133, 1999a.
- Marasteanu, M.O. and Anderson, D.A. Booij and Thoone Approximation and Bitumen Relaxation Spectrum Generation. *Eurobitume Workshop for Performance Related Properties for Bituminous Binders*, Luxembourg, paper no. 134, 1999b.
- McCuen, R.H. Modeling Hydrologic Change: Statistical Methods. Lewis Publishers, CRC Press Company, Boca Raton, Florida, 2003.
- McLeod, N.W. A 4 Year Survey of Low Temperature Transverse Pavement Cracking on Three Ontario Test Roads. *Proceedings of the Association of Asphalt Paving Technologists*, Vol. 41, pp. 424–493, 1972.
- McLeod, N.W. Asphalt Cements: Pen-Vis Number and Its Application to Moduli of Stiffness. *Journal of Testing and Evaluation*, Vol. 4 (4), pp. 275–282, 1976.
- McLeod, N.W. Using Paving Asphalt Rheology to Impair or Improve Asphalt Pavement Design Performance. *Asphalt Rheology: Relationship to Mixture*, ASTM STP 941, O.E. Briscoe Ed., American Society for Testing and Materials, Philadelphia, pp. 51–57, 1987.
- Medani, T.O. and Huurman, M. Constructing the Stiffness Master Curves for Asphaltic Mixes. Report 7-01-127-3. Delft University and Technology, 2003.

- Medani, T.O., Huurman, M. and Molenaar, A.A.A. On the Computation of Master Curves for Bituminous Mixes. *Proceedings 3<sup>rd</sup> Eurobitume Congress*, Vienna, Austria, Vol. 2, pp. 1909–1917, 2004.
- Menard, K.P. *Dynamic Mechanical Analysis: A Practical Introduction*. Boca Raton; CRC Press, 1999.
- Mezger, T.G. *Rheology Handbook Second Edition*. Hannover; William Andrew Publisher, 2006.
- Minnesota Asphalt Pavement Association. *Asphalt Paving Design Guide*. New Brighton, MN. 2003
- Mirza, M.W. and Witczak, M.W. Development of a Global Aging System for Short and Long Term Aging of Asphalt Cements. *Journal of the Association of Asphalt Paving Technologists*, Vol. 64, pp. 393–430, 1995.
- Mohammad, L.N., Wu, Z., Myres, L., Cooper, S. and Abadie, C. A Practical Look at Simple Performance Tests: Louisiana's Experience. *Journal of the Association of Asphalt Paving Technologists*, Vol. 74, pp. 557–600, 2005.
- Molinas, A. and Wu, B. Comparison of Fractional Bed-Material Load Computation Methods in Sand-Bed Channels. *Earth Surface Processes and Landforms*, Vol. 25, pp. 1045–1068, 2000.
- Monismith, C.L., Alexander, R.L. and Secor, K.E. Rheological Behaviour of Asphalt Concrete. *Proceedings of the Association of Asphalt Paving Technologists*, Vol. 35, pp. 400–450, 1966.
- Morrison, F.A. Using the Solver Add-in in Microsoft Excel, 2005  
[www.chem.mtu.edu/~fmorriso/cm4650/Using\\_Solver\\_in\\_Excel.pdf](http://www.chem.mtu.edu/~fmorriso/cm4650/Using_Solver_in_Excel.pdf) (online).
- Nellenstyen, F.J. The Constitution of Asphalt. *Journal of the Institute of Petroleum Technologists*, Vol. 10, pp. 311–325, 1924.
- Nielsen, E. Complex Modulus for Original and Hardened Binder. *Proceedings of the Rheology of Bituminous Binders European Workshop, Eurobitume*. Paper No. 28, Brussels, 1995.
- Olard, F., Di Benedetto, H., Eckmann, B. and Triquigneaux, J.P. Linear Viscoelastic Properties of Bituminous Binders and Mixtures at Low and Intermediate Temperatures. *Road Materials and Pavement Design*, Vol. 4 (1), pp. 77–107, 2003.

- Olard, F. and Di Benedetto, H. General "2S2P1D" Model and Relation between the Linear Viscoelastic Behaviours of Bituminous Binders and Mixes. *Road Materials and Pavement Design*, Vol. 4 (2), pp. 185–224, 2003.
- Olard, F. and Di Benedetto, H. The "DBN" Model: A Thermo-Visco-Elasto Plastic Approach for Pavement Behavior Modeling. *Journal of the Association of Asphalt Paving Technologists*, Vol. 74, pp. 791–828, 2005a.
- Olard, F. and Di Benedetto, H. Thermo-Visco-Elasto-Plastic Law for Bituminous Mixes: Simulation of Direct Tensile Tests and Restrained Thermal Shrinkage. *Bulletin Des Laboratoires Des Ponts et. Chaussées*–254, Ref. 4531, pp. 15–39, 2005b.
- Panda, M. and Mazumdar, M. Utilization of Reclaimed Polyethylene in Bituminous Paving Mixes. *Journal of Materials in Civil Engineering*, Vol. 14 (6), pp. 527–530, 2002.
- Pellinen, T.K., and Witzak, M.W. Stress Dependent Master Curve Construction for Dynamic (Complex) Modulus. *Journal of the Association of Asphalt Paving Technologists*, Vol. 71, pp. 281–309, 2002.
- Pellinen, T.K, Witzak, M.W. and Bonaquist, R.F. Asphalt Mix Master Curve Construction using Sigmoidal Fitting Function with Non-Linear Least Squares Optimization Technique. *Proceedings of 15th ASCE Engineering Mechanics Conference June 2-5, 2002*, Columbia University, New York, 2002.
- Pellinen, T. K., Zofka, A., Marasteanu, M. and Funk, N. Asphalt Mixture Stiffness Predictive Models. *Journal of the Association of Asphalt Paving Technologists*, Vol. 76, pp. 575–626, 2007.
- Petersen, J.C. Chemical Composition of Asphalt as Related to Asphalt Durability: State of the Art. *Transportation Research Record*, No. 999, pp. 13–30, 1984.
- Petersen, J.C., Robertson, R.E., Branhaver, J.F., Harnsberger, P.M., Duvall, J.J., Kim, S.S., Anderson, D.A., Christiansen, D.W. and Bahia, H.U. Binder Characterization and Evaluation-:Volume 1. SHRP-A-367. Strategic Highway Research Program, National Research Council, Washington D.C., 1994.
- Pfeiffer, J.P. and Saal, R.N.J. Asphaltic Bitumen as Colloidal System. *Physical Chemistry*, Vol. 44, pp. 139–149, 1940.
- Pink, H.S., Merz, R.E. and Bosniack, D.S. Asphalt Rheology: Experimental Determination of Dynamic Moduli at Low Temperatures. *Proceedings of the Association of Asphalt Paving Technologists*. Vol. 49; pp. 64–94, 1980.

- Polacco, G., Vacin, O.J., Biondi, D., Stastna, J. and Zanzotto, L. Dynamic Curve of Polymer Modified Asphalt from Three Different Geometries. *Applied Rheology*. Vol 13. No. 3, pp. 118–124, 2003.
- Polacco, G., Stastna, J., Vlachovicova, Z., Biondi, D., and Zanzotto, L. Temporary Networks in Polymer Modified Asphalts. *Polymer Engineering and Science*, Vol. 44 (12), pp. 2185–2193, 2004.
- Pronk, A.C. Revival of the Huet-Sayegh Response Model- Notes on the Huet-Sayegh Rheological Model. DWW-2003-029, RHED, Delft, 2003a.
- Pronk, A.C. The Variable Dashpot. DWW-2003-030, RHED, Delft, 2003b.
- Pronk, A.C. The Huet-Sayegh Model: A Simple and Excellent Rheological Model for Master Curves of Asphaltic Mixes. *Asphalt Concrete Simulations, Modeling and Experimental Characterization: Proceedings of the R. Lytton Symposium on Mechanics of Flexible Pavements*, Baton Rouge, Louisiana, American Society of Civil Engineers, Eds Masad, E., Panoskaltsis, V.P., and Wang, L, pp. 73–82, 2005.
- Read, J. and Whiteoak, D. The Shell Bitumen Handbook Fifth Edition. Thomas Telford Ltd, London, 2003.
- Redelius, P. The Structure of Asphaltenes in Bitumen. *Road Materials and Pavement Design*, Vol. 7, pp. 143–162, 2006.
- Roberts, F.L., Kandhal, P.S., Brown, E.R., Lee, D.Y., Kennedy, T.W. Hot Mix Asphalt Materials, Mixture Design, and Construction Second Edition. Lanham Maryland; NAPA Education Foundation, 1996.
- Rouse, Jr, P.E. A Theory of the Linear Viscoelastic Properties of Dilute Solutions of Coiling Polymers. *The Journal of Chemical Physics*. Vol. 21 (7); pp. 1272–1280, 1953.
- Rowe, G. Phase Angle Determination and Interrelationship within Bituminous Materials. *Proceedings of 7th International RILEM Symposium ATCBM09 on Advanced Testing and Characterization of Bituminous Materials*, Rhodes, Greece, 2009.
- Rowe, G.M. A Generalized Logistic Function to describe the Master Curve Stiffness Properties of Binder Mastics and Mixtures. *45th Petersen Asphalt Research Conference*, Laramie, Wyoming, July "14-16, 2008.
- Rowe, G., Baumgardner, G. and Sharrock, M. Functional Forms for Master Curve Analysis of Bituminous Materials. *Proceedings of 7th International RILEM*

- Symposium ATCBM09 on Advanced Testing and Characterization of Bituminous Materials*, Rhodes, Greece, Vol. 1, pp. 81–91, 2009.
- Rowe, G.M. and Sharrock, M.J. The Measurement and Analysis System to Accurately Determine Asphalt Concrete Properties Using the Indirect Tensile Mode. *The 1<sup>st</sup> International Symposium on Binder Rheology and Pavement Performance*, the University of Calgary, August 14-15, Alberta, Canada, 2000.
- Rowe, G.M. and Sharrock, M.J. Alternate Shift Factor Relationship for Describing the Temperature Dependency of the Visco-elastic Behaviour of Asphalt Materials. *Transportation Research Board Annual Meeting*, Washington, DC, 2011.
- Rowe, G.M., Sharrock, M.J., Bouldin, M.G. and Bouldin, R.N. Advanced Techniques to Develop Asphalt Master Curve from the Bending Beam Rheometer. *Petroleum and Coal*, Vol. 43 (1): pp. 54–59, 2001.
- Saleh, F.M. Effect of Rheology on the Bitumen Foam-ability and Mechanical Properties of Foam Bitumen Stabilised Mixes. *International Journal of Pavement Engineering*, Vol. 8 (2), pp. 99–110, 2007.
- Sayegh, G. Viscoelastic Properties of Bituminous Mixtures. *Proceedings of the Second International Conference on Structural design of Asphalt Pavement*, Held at Rackham Lecture Hall, University of Michigan, Ann Arbor, USA, pp. 743–755, 1967.
- Scholz, T.V. Durability of Bituminous Paving Mixtures. PhD Thesis, the University of Nottingham, 1995.
- Sengoz, B., Topal, A. and Isikyakar, G. Morphology and Image Analysis of Polymer Modified Bitumens. *Construction and Building Materials*, Vol. 23, pp. 1986–1992, 2009.
- Shaw, M.T. and MacKnight, W.J. Introduction to Polymer Viscoelasticity. New Jersey; John Wiley and Sons Inc, 2005.
- Silva, L.S.D., Forte, M.M.D.C., Vignol, L.D.A. and Cardozo, N.S.M. Study of Rheological Properties of Pure and Polymer-Modified Brazilian Asphalt Binders. *Journal of Materials Science*, Vol. 39 (8), pp. 539–546, 2004.
- Soleymani, H.R, Bahia, H.U. and Bergan, A.T. Time-Temperature Dependency of Blended and Rejuvenated Asphalt Binders. *Journal of the Association of Asphalt Paving Technologists*, Vol. 68, pp. 129–152, 1999.

- SpecialChem. Ethylene Vinyl Acetate. 2012. <http://www.specialchem4adhesives.com/tc/ethylene-copolymers/index.aspx?id=eva> (online).
- Stastna, J, De Kee, D. and Powley M.B. Complex Viscosity as a Generalized Response Function. *Journal of Rheology*, Vol. 29 (41), pp 457–469, 1985.
- Stastna, J., Zanzotto, L. and Ho, K. Fractional Complex Modulus Manifest in Asphalt. *Rheologica Acta*, Vol. 33, pp. 344–354, 1994.
- Stastna, J. Zanzotto, L. and Kennepohl, G. Dynamic Material Functions and the Structure of Asphalts. *Transportation Research Record*, No. 1535, pp. 3–9, 1996.
- Stastna, J, Zanzotto, L. and Berti, J. How Good are Some Rheological Models of Dynamic Material Functions of Asphalt?. *Journal of the Association of Asphalt Paving Technologists*, Vol. 66, pp. 458–479, 1997.
- Stastna, J. and Zanzotto, L. Linear Response of Regular Asphalts to External Harmonic Fields. *Journal of Rheology*, Vol. 43 (3), pp. 719–734, 1999a.
- Stastna, J. and Zanzotto, L. Response to "letter to the Editor: On the Thermo-rheological Complexity and Relaxation of Asphalt Cements" [J. Rheol. 43 1701 (1999)]. *Journal of Rheology*, Vol. 43 (6), pp. 1705–1708, 1999b.
- Sui, C., Farrar, M.J., Tuminello, W.H. and Turner, T.F. A New Technique for Measuring Low-Temperature Properties of Asphalt Binders with Small Amounts of Materials. *Transportation Research Board 89th Annual Meeting 2010*, Washington, D.C. Paper 10-1681, 2010.
- Taylor, R. and Airey, G.D. Polymer Modified Bitumens Part One: Background and History. *Asphalt Professional*, Issue 34, September 2008, pp. 11–16, 2008a.
- Taylor, R. and Airey, G.D. Polymer Modified Bitumens Part Two: Rheological Characteristics and Asphalt Mixture Performance. *Asphalt Professional*, Issue 35, November 2008, pp. 11–18, 2008b.
- Thom, N. Principle of Pavement Engineering. London; Thomas Telford Publishing, 2008.
- Tran, N.H. and Hall, K.D. Evaluating the Predictive Equation in Determining Dynamic Moduli of Typical Asphalt Mixtures Used in Arkansas. *Electronic Journal of the Association of Asphalt Paving Technologists*, Vol. 74E, 2005.
- Traxler, R.N. Durability of Asphalt Cements. *Proceedings of the Association of Asphalt Paving Technologists*, Vol. 32; pp. 44 – 58.

- Ullidtz, P. A Fundamental Method for the Prediction of Roughness, Rutting and Cracking in Asphalt Pavements. *Proceedings of the Associations of Asphalt Paving Technologists*, Vol. 48, pp. 557–586, 1979.
- Ullidtz, P. and Larsen, B.K. Mathematical Model for Predicting Pavement Performance. *Transportation Research Record*, No. 949, pp. 45–55, 1983.
- Valenkar, S.S. and Giles, D. How do I Know if My Phase Angles Are Correct?. *Rheology Bulletin*, 76 (2), pp. 8–20, 2007.
- Vallerga, B.A., Monismith, C.L. and Granthem, K. A Study of Some Factors Influencing the Weathering of Paving Asphalts. *Proceedings of the Association of Asphalt Paving Technologists*. Vol. 26, pp. 126 – 150.
- Van der Poel, C. A General System Describing the Viscoelastic Properties of Bitumens and its Relation to Routine Test Data. *Journal of Applied Chemistry*, Vol. 4, pp. 231–236, 1954.
- Van der Poel, C. Time and Temperature Effects on the Deformation of Asphaltic Bitumens and Bitumen Mineral Mixtures. *Society of Plastic Engineers Journal*, Vol. 11, pp. 47–53, 1955.
- Van Rompu, J. Etude du Comportement Mécanique des Mastics Bitumineux à L'aide D'un Rhéomètre à Cisaillement Annulaire. MSc Dissertation, Ecole Nationale des TPE, France, 2006 (In French).
- Vlachovicova, Z., Stastna, J., MacLeod, D. and Zanzotto, L. Shear Deformation and Material Characteristics of Polymer-Modified Asphalt. *Petroleum & Coal*, Vol. 47 (3), pp. 38–78, 2005.
- Williams, M.L., Landel, R.F. and Ferry, J.D. The Temperature Dependence of Relaxation Mechanisms in Amorphous Polymers and Other Glass-Forming Liquids. *Journal Americans Chemical Society*, Vol. 77, pp. 3701–3707, 1955.
- Wojciech, G. and Mieczyslaw, S. Changes of Functional Characteristics of the Four Road Bitumens used in Poland, Modified with Polymer SBS. *Euroasphalt & Eurobitume Congress 1996*. E & E. 5. 140. Luxembourg (CD-ROM), 1996.
- Wu, B., Maren, D.S.V. and Li, L. Predictability of Sediment Transport in the Yellow River using Selected Transport Formulas. *International Journal of Sediment Research*, Vol. 23, pp. 283–298, 2008.
- Wu, J. The Influence of Mineral Aggregates and Binder Volumetrics on Bitumen Ageing. PhD Thesis, the University of Nottingham, 2009.

- Yeh, P.H., Nien, Y.H., Chen, W.C., and Liu, W.T. Modifying Asphalt with Varying Levels of Polyethylene Additives. *Plastics Research Online* (Polymer Modifiers). Society of Plastic Engineers, 10.1002/spepro.002911, 2010.
- Yildirim, Y. Polymer Modified Asphalt Binders. *Construction and Building Materials*, Vol. 21, pp. 66–72, 2007.
- Yoder, E.J. and Witczak, M.W. Principle of Pavement Design Second Edition. New York; John Wiley & Sons Inc, 1975.
- Zeng, M., Bahia, H.U., Zhai, H., Anderson, M.R. and Turner P. Rheological Modeling of Modified Asphalt Binders and Mixtures. *Journal of the Association of Asphalt Paving Technologists*, Vol. 70, pp. 403–441, 2001.

# Appendix A

Dynamic Shear Rheometer Data for the Unaged  
Unmodified Bitumens

Table A1: complex modulus and phase angle data of a 10/20 penetration grade bitumen

Freq/Temp	10°C	15°C	25°C	35°C	45°C	55°C	65°C	75°C	80°C
0.1 Hz	24677000	9502300	1164600	148800	20999	3567.6	715.95	161.54	82.764
0.15849 Hz	30225000	12170000	1619100	216290	30995	5382.5	1126.7	255.38	131.38
0.25119 Hz	36793000	15678000	2232500	313060	46149	8355.3	1757	404.08	211.93
0.39811 Hz	44066000	19814000	3071500	451010	67815	12667	2752.2	642.85	334.19
0.63096 Hz	52149000	24770000	4176200	647100	99283	19035	4259.9	1004.6	525.56
1 Hz	61024000	30644000	5621400	921640	146030	28777	6542.4	1566.5	830.14
1.5849 Hz	68679000	37016000	7500500	1304000	213110	43058	9963.8	2435.3	1297.8
2.5119 Hz	80152000	44553000	9869100	1831200	307010	64579	15211	3766.5	2035.4
3.9811 Hz	86105000	52284000	12869000	2547500	438870	94931	22978	5820.5	3157.4
6.3096 Hz	100320000	62064000	16581000	3519900	620880	140060	34538	8965.6	4872.4
10 Hz	109040000	71838000	21121000	4804100	855740	205020	51626	13714	7452.7

Freq/Temp	10°C	15°C	25°C	35°C	45°C	55°C	65°C	75°C	80°C
0.1 Hz	41.29	50.61	65.71	73.19	78.82	84.13	87.09	88.16	87.89
0.15849 Hz	40.29	49.42	63.84	72.33	77.7	83.3	86.25	87.57	88.06
0.25119 Hz	38.02	47.39	62.29	71.4	76.41	81.77	85.7	87.57	87.92
0.39811 Hz	35.86	45.4	60.68	70.23	75.02	80.67	85.21	87.2	87.67
0.63096 Hz	33.75	43.01	58.79	69.09	74.35	80.1	83.79	87.08	87.98
1 Hz	31.77	40.47	56.93	67.88	72.45	78.56	83.38	86.11	87.29
1.5849 Hz	30.67	38.73	54.93	66.61	70.78	78.04	82.01	85.4	86.44
2.5119 Hz	28.08	36.72	53.01	65.1	68.98	76.68	81.24	84.61	85.89
3.9811 Hz	27.93	35.33	51.01	63.67	66.53	75.55	80.44	83.98	85.18
6.3096 Hz	24.87	32.76	49.05	62.1	63.52	74.52	79.62	83.45	84.49
10 Hz	23.66	31.28	47.09	60.59	60.12	73.12	78.95	82.93	83.97

Table A2: Complex modulus and phase angle data of a 35/50 penetration grade bitumen

Freq/Temp	10°C	15°C	25°C	35°C	45°C	55°C	65°C	75°C	80°C
0.1 Hz	7923400	2904300	346250	44575	5890.8	1038.6	217.82	56.726	29.88
0.15849 Hz	10230000	3906500	491430	66194	8909.2	1625.3	343.35	91.756	51.921
0.25119 Hz	13327000	5269700	700500	97370	13426	2509.8	543.14	143.34	78.91
0.39811 Hz	17155000	7064900	994460	143080	20326	3890.6	848.78	228.05	125.79
0.63096 Hz	21819000	9319900	1393700	210010	30318	5967.3	1317.6	361.47	198.59
1 Hz	27466000	12181000	1945500	304940	45110	9165	2062.3	566.51	310.84
1.5849 Hz	33867000	15746000	2701400	443120	66622	13901	3201.4	888.46	490.92
2.5119 Hz	42047000	20221000	3708800	639400	98865	21051	4940.4	1399	775.54
3.9811 Hz	51205000	25644000	5056600	917570	144800	31578	7557.1	2187.2	1216
6.3096 Hz	61005000	32071000	6832000	1306200	211570	47444	11577	3397.4	1896.8
10 Hz	72345000	39668000	9115500	1841500	304930	70745	17653	5220.8	2944.1

Freq/Temp	10°C	15°C	25°C	35°C	45°C	55°C	65°C	75°C	80°C
0.1 Hz	53.15	59.96	69.93	77.02	82.59	86.6	88.7	88.46	88.88
0.15849 Hz	52.29	58.9	69.25	76	81.43	85.46	88.09	88.05	87.83
0.25119 Hz	50.24	57.15	68.15	74.98	80.66	84.91	87.36	88.91	88.75
0.39811 Hz	48.1	55.44	66.97	74.1	79.81	83.83	86.95	88.18	88.06
0.63096 Hz	46.16	53.49	65.62	73.22	78.31	82.91	86.13	87.54	87.98
1 Hz	43.9	51.66	64.17	72.37	77.57	81.98	85.6	87.44	88.16
1.5849 Hz	42.28	49.57	62.69	71.3	76.07	81.12	84.93	87.12	87.67
2.5119 Hz	40.07	47.46	61.18	70.32	75.05	80.32	84.19	86.43	87.03
3.9811 Hz	38.07	45.9	59.61	69.29	73.91	79.43	83.34	85.8	86.59
6.3096 Hz	36.41	43.94	57.97	68.21	72.46	78.67	82.57	85.21	86.04
10 Hz	34.71	41.95	56.41	67.15	70.94	77.82	81.99	84.67	85.25

Table A3: Complex modulus and phase angle data of a 40/60 penetration grade bitumen

Freq/Temp	10°C	15°C	25°C	35°C	45°C	55°C	65°C	75°C	80°C
0.1 Hz	1540000	1240000	127000	18900	2450.6	556.42	134.68	37.533	21.774
0.15849 Hz	4490000	1570000	182000	28000	4429.8	867.56	212.47	58.009	33.969
0.25119 Hz	6000000	2170000	264000	41600	6785.2	1347.3	336.09	91.459	52.747
0.39811 Hz	7960000	2980000	381000	61700	10335	2091.2	530.96	145.11	83.448
0.63096 Hz	10500000	4080000	547000	91200	15612	3228.1	830.07	229.26	132.22
1 Hz	13600000	5500000	782000	135000	23537	4979.5	1295.6	359.09	208.33
1.5849 Hz	17600000	7360000	1110000	197000	35342	7632	2013.4	564.92	327.33
2.5119 Hz	22400000	9770000	1570000	287000	52572	11647	3104.1	887.55	516.33
3.9811 Hz	28100000	12800000	2200000	416000	78178	17614	4786.5	1391.7	807.39
6.3096 Hz	34900000	16500000	3060000	602000	115350	26612	7376.6	2163.5	1256.9
10 Hz	42400000	21000000	4210000	861000	169110	39979	11250	3333	1941.4

Freq/Temp	10°C	15°C	25°C	35°C	45°C	55°C	65°C	75°C	80°C
0.1 Hz	46.05	68.6	72.78	78.9	76.94	87.12	88.2	86.69	85.72
0.15849 Hz	57.86	64.14	72.33	78.22	82.89	86.41	88	87.15	85.49
0.25119 Hz	56.48	62.7	71.48	77.26	82.1	85.89	87.75	87.41	86.84
0.39811 Hz	54.69	61.16	70.52	76.38	81.08	85.04	87.28	87.57	87.18
0.63096 Hz	52.75	59.53	69.5	75.5	80.13	84.16	86.69	87.41	87.26
1 Hz	50.83	57.81	68.38	74.63	79.08	83.32	86.15	87.22	87.37
1.5849 Hz	48.9	56.13	67.19	73.79	78.13	82.52	85.41	87.02	87.12
2.5119 Hz	47	54.26	65.94	72.92	77.19	81.73	84.72	86.59	86.89
3.9811 Hz	44.89	52.48	64.62	72.06	76.21	80.9	84.1	86.13	86.5
6.3096 Hz	43.04	50.74	63.33	71.12	75.22	80.22	83.52	85.64	85.94
10 Hz	41.52	49.07	62.02	70.13	74.1	79.6	82.97	85.1	85.23

Table A4: Complex modulus and phase angle data of a 70/100 penetration grade bitumen

Freq/Temp	10°C	15°C	25°C	35°C	45°C	55°C	65°C	75°C	80°C
0.1 Hz	2808600	1129300	148340	20463	2884.4	541.27	116.54	33.689	19.832
0.15849 Hz	3614100	1495600	205100	29489	4308	834.49	183.45	53.922	30.837
0.25119 Hz	4684400	2001400	285740	44256	6436.9	1280.1	288.72	85.16	48.05
0.39811 Hz	5990700	2658500	397440	64082	9586	1951.9	452.56	133.26	76.079
0.63096 Hz	7614200	3487800	549810	91267	14166	2951.9	707.09	209.59	121.96
1 Hz	9585800	4537800	757000	128700	20814	4455.7	1091.8	331.26	193.42
1.5849 Hz	11946000	5791800	1035500	181240	30372	6705.3	1680.6	515.53	299.95
2.5119 Hz	14627000	7342100	1403400	253430	44263	10012	2576.8	803.01	472.68
3.9811 Hz	17755000	9041000	1893600	355290	64001	14865	3923.1	1245.5	737.73
6.3096 Hz	21637000	11021000	2540900	493210	92178	21899	5936.1	1910.4	1140
10 Hz	25942000	13692000	3357000	681420	132350	32104	8916.2	2901.9	1741.6

Freq/Temp	10°C	15°C	25°C	35°C	45°C	55°C	65°C	75°C	80°C
0.1 Hz	53.37	58.35	65.98	73.85	79.83	84.74	87.55	89.12	89.71
0.15849 Hz	52.86	58.01	65.62	72.73	78.8	83.73	87.13	87.77	89.05
0.25119 Hz	51.47	56.64	64.83	70.99	77.62	82.82	86.51	87.22	89.33
0.39811 Hz	49.84	55.25	63.98	69.96	76.89	81.71	85.45	87.86	87.38
0.63096 Hz	48.19	53.93	63.1	69.34	75.52	80.79	84.72	87.39	88.17
1 Hz	46.52	52.38	62.17	68.89	74.55	79.67	83.87	86.28	87.26
1.5849 Hz	45.04	50.95	61.17	67.85	73.53	78.58	82.79	85.85	86.95
2.5119 Hz	43.45	49.48	60.06	67.25	72.62	77.74	81.92	84.94	85.69
3.9811 Hz	42.03	47.92	58.97	66.36	71.86	76.96	80.99	84.03	84.87
6.3096 Hz	40.73	46.55	57.81	65.41	71	76.14	80.24	83.18	83.86
10 Hz	39.43	45.27	56.7	64.59	70.28	75.48	79.49	82.18	82.65

Table A5: Complex modulus and phase angle data of a 100/150 penetration grade bitumen

Freq/Temp	10°C	20°C	25°C	35°C	45°C	55°C	65°C	75°C	80°C
0.1 Hz	749880	76716	25742	3449.3	10298	1545	283.71	56.742	33.346
0.15849 Hz	1052600	112510	38172	5330.6	15381	2355.6	424.91	89.128	50.691
0.25119 Hz	1464200	164750	56671	7982.7	22762	3597.8	659.55	145.28	87.444
0.39811 Hz	2008000	239180	83847	12190	33714	5479	1035	229.69	139.04
0.63096 Hz	2733000	343480	123560	18227	49772	8264.1	1611.6	363.69	214.72
1 Hz	3686600	493560	180750	27287	72968	12424	2449	563.94	336.18
1.5849 Hz	4944200	702860	263900	40714	106940	18665	3774.4	893.35	529.36
2.5119 Hz	6543400	991510	382540	60848	155420	28023	5754	1372	815.21
3.9811 Hz	8580800	1390600	547130	90760	224560	41693	8753.8	2146	1261
6.3096 Hz	11126000	1936900	782450	135140	322930	62271	13392	3355.8	1951.7
10 Hz	14058000	2621800	1087500	194370	454410	90703	19901	5096.2	2985.9

Freq/Temp	10°C	20°C	25°C	35°C	45°C	55°C	65°C	75°C	80°C
0.1 Hz	65.6	74.4	77.9	83.2	78.3	82.2	83.4	85.2	87.3
0.15849 Hz	64.0	73.5	77.0	82.1	77.3	81.9	84.9	86.2	84.7
0.25119 Hz	62.4	72.3	76.0	81.7	76.6	81	84.6	87.6	85.3
0.39811 Hz	60.8	71.4	74.9	80.8	75.8	80.8	84	86.4	86.9
0.63096 Hz	59.0	70.2	74.0	79.9	74.8	80	83.7	86.8	87.7
1 Hz	57.3	69.0	73.1	78.7	74	79.5	83.5	86.3	87.5
1.5849 Hz	55.5	67.8	71.9	77.4	72.8	78.7	83	86	86.5
2.5119 Hz	53.6	66.4	70.9	76.2	71.4	78	82.5	86	86.6
3.9811 Hz	51.9	65.0	69.8	74.7	70	77.3	82	85.5	86.3
6.3096 Hz	50.2	63.7	68.7	72.9	68.2	76.7	81.6	84.9	85.6
10 Hz	48.9	62.5	67.5	69.7	66.4	76.1	81.2	84.4	84.8

Table A6: Complex modulus and phase angle data of a 160/220 penetration grade bitumen

Freq/Temp	10°C	15°C	25°C	35°C	45°C	55°C	65°C	75°C	80°C
0.1 Hz	401150	131250	15144	2153.1	365.69	87.68	22.709	7.5377	4.8519
0.15849 Hz	577270	194250	23107	3358.3	579.65	138.88	37.217	12.794	7.4724
0.25119 Hz	834390	286560	34970	5201.9	914.55	221.96	58.244	19.558	12.29
0.39811 Hz	1199600	420370	52664	8013.6	1440	350.45	92.756	30.642	19.482
0.63096 Hz	1706800	612790	79254	12330	2246.1	556.01	147.67	49.706	31.206
1 Hz	2413900	887490	118770	18975	3506.5	876.94	233.12	77.08	49.499
1.5849 Hz	3388600	1279200	177270	28979	5438	1380.2	371.91	124.4	78.297
2.5119 Hz	4703300	1826900	263420	43878	8405.3	2161.8	590.8	197.7	124.06
3.9811 Hz	6445400	2587800	389340	66566	12941	3368.4	938.99	312.77	196.74
6.3096 Hz	8728500	3629900	570570	99854	19856	5223.4	1481.4	491.35	308.9
10 Hz	11658000	5028500	831640	148250	30316	8072.2	2314.9	761.86	477.34

Freq/Temp	10°C	15°C	25°C	35°C	45°C	55°C	65°C	75°C	80°C
0.1 Hz	72.86	76.55	81.77	85.59	88.61	89.57	89.69	89.97	89.84
0.15849 Hz	72.07	75.56	80.91	84.93	88.03	89.54	89.3	87.35	87.02
0.25119 Hz	70.82	74.6	80.13	84.29	87.55	89.01	89.18	89.19	86.84
0.39811 Hz	69.54	73.68	79.44	83.64	87.1	88.84	89.58	89.33	89.49
0.63096 Hz	68.09	72.54	78.66	82.82	86.31	88.26	88.91	88.26	89.08
1 Hz	66.5	71.33	77.86	82.01	85.74	87.9	88.78	88.33	87.81
1.5849 Hz	64.81	70.04	77.1	81.14	85.12	87.44	88.6	87.92	87.15
2.5119 Hz	63.08	68.65	76.25	80.23	84.51	86.94	88.13	87.25	86.6
3.9811 Hz	61.3	67.19	75.37	79.36	83.91	86.46	87.95	86.52	85.93
6.3096 Hz	59.54	65.68	74.46	78.27	83.37	86.02	87.66	85.53	85.26
10 Hz	57.79	64.2	73.45	78.21	82.92	85.69	87.56	84.05	85.28

Table A7: Complex modulus and phase angle of a 15 penetration grade bitumen I [Choi, 2005]

Fre/Temp	10°C	15°C	25°C	35°C	45°C	55°C	65°C	75°C	80°C
0.10 Hz	15375000	6414100	652560	222035	33812	8705.475	1899.7	379.52	195.84
0.14 Hz	18028000	8521600	1441150	283555	53306	11799.53	2649.763	548.2	281.71
0.20 Hz	20982500	10244750	1806000	361815	69210	15766.5	3635.375	770.45	398.14
0.29 Hz	24728500	12258500	2241350	456250	89263	20980	4973.863	1070.45	560.145
0.41 Hz	29082000	14536500	2768100	578135	116575	27909.13	6760.9	1482.45	786.545
0.59 Hz	33937000	17148000	3410350	733400	152610	36964	9118.525	2045.9	1098.75
0.84 Hz	39057500	20413500	4209950	930130	197685	48865.63	12371.13	2805.9	1530.1
1.20 Hz	45371500	24009500	5168450	1180050	255085	64393.5	16638.75	3847.85	2126.3
1.70 Hz	51881500	28110000	6315850	1493550	327310	84701.25	22371.5	5270.8	2937.25
2.44 Hz	59505500	32956000	7679050	1878700	422230	111218.9	29654.63	7204.95	4048.05
3.49 Hz	67555500	38398500	9315750	2360000	544850	145892.5	39530.75	9809.85	5547.6
5.00 Hz	76618500	44518000	11178500	2936000	699795	190410	51863	13294	7570
7.14 Hz	86625500	51341000	13391000	3664450	892445	247415	68468.5	17905	10246
10.00 Hz	96064000	58336500	15727500	4463600	1114100	313868.8	87994.25	23391.5	13513

Fre/Temp	10°C	15°C	25°C	35°C	45°C	55°C	65°C	75°C	80°C
0.10 Hz	43	50.4	61.8	53	75.2	76.9875	81.7125	84.5	86.65
0.14 Hz	42.2	47.55	56.6	62.15	67.9	74.5125	80.2375	83.9	85.1
0.20 Hz	41.05	45.5	55.55	61.7	67.35	73.45	79.0875	83.2	84.45
0.29 Hz	40.2	45.25	54.7	60.85	66.25	72.2625	78.1875	82.3	83.85
0.41 Hz	39.1	43.9	53.65	60.4	65.65	71.3625	77.0125	81.55	83.2
0.59 Hz	38.5	42.75	52.7	59.55	65.05	70.35	76.1125	80.8	82.5
0.84 Hz	37.25	42.05	51.85	59.15	64.45	69.55	75.1125	79.9	81.85
1.20 Hz	35.8	41.05	50.8	58.4	63.85	68.575	74.125	79	81
1.70 Hz	34.95	39.8	49.85	57.7	63.35	67.7875	73.225	78.1	80.3
2.44 Hz	33.55	38.85	48.8	57	62.9	66.9875	72.4125	77.2	79.3
3.49 Hz	32.65	37.9	47.8	56.3	62.5	66.3	71.625	76.4	78.6
5.00 Hz	31.4	37	46.85	55.5	62.05	65.6	70.925	75.65	77.9
7.14 Hz	30.5	35.95	45.85	54.95	61.75	64.9125	70.4875	75	77.25
10.00 Hz	30.05	35.3	45	54.45	61.6	64.4	70.2	74.65	76.85

Table A8: Complex modulus and phase angle of a 15 penetration grade bitumen II [Choi, 2005]

Fre/Temp	10°C	15°C	25°C	35°C	45°C	55°C	65°C	75°C	80°C
0.10 Hz	21958500	10806750	2596600	527880	99155	12624	3927	1008	505
0.14 Hz	25546625	13265250	3195500	654520	134010	28019	5513	1422	742
0.20 Hz	28979875	15848750	3876200	817010	166580	37122	7369	1937	1042
0.29 Hz	33280625	18382375	4674800	1024600	210270	48272	9998	2674	1451
0.41 Hz	38349625	21258500	5664800	1276300	268850	62960	13373	3649	2012
0.59 Hz	44206000	24566000	6854900	1585500	342880	81709	17830	4959	2782
0.84 Hz	50249625	28216250	8249100	1970700	423930	105670	23667	6719	3794
1.20 Hz	56841875	32425500	9893200	2447600	535130	136225	31235	9047	5183
1.70 Hz	63892125	37659875	11815000	3022700	683690	175080	41052	12098	7014
2.44 Hz	70811875	43900375	14095000	3694300	869810	223675	53965	16180	9476
3.49 Hz	78749125	50778000	16652000	4538500	1104700	286460	70406	21470	12719
5.00 Hz	87187500	57339750	19544000	5548600	1385400	362955	91925	28488	16990
7.14 Hz	96106000	64013250	22779000	6730500	1727100	459405	118625	37376	22440
10.00 Hz	104712500	70239000	26109000	7994400	2083500	564675	150240	48205	29118

Fre/Temp	10°C	15°C	25°C	35°C	45°C	55°C	65°C	75°C	80°C
0.10 Hz	39.63	43.83	51.10	58.40	63.60	78.15	79.70	82.95	83.65
0.14 Hz	38.20	42.58	50.50	57.10	63.20	69.25	76.35	81.05	82.00
0.20 Hz	37.43	41.55	49.50	56.50	62.60	68.25	75.05	79.85	81.05
0.29 Hz	36.20	40.48	48.60	55.80	61.70	67.15	73.70	78.85	80.25
0.41 Hz	35.00	39.50	47.60	55.20	61.10	66.20	72.75	78.00	79.25
0.59 Hz	34.15	38.83	46.70	54.40	60.50	65.20	71.55	76.90	78.20
0.84 Hz	33.05	37.73	45.70	53.80	59.90	64.25	70.55	75.80	77.10
1.20 Hz	32.15	36.93	44.70	53.00	59.20	63.25	69.55	74.70	76.05
1.70 Hz	31.15	35.70	43.70	52.20	58.70	62.30	68.50	73.70	74.95
2.44 Hz	30.13	34.80	42.30	51.50	58.10	61.40	67.55	72.65	73.85
3.49 Hz	29.10	33.85	41.70	50.70	57.60	60.45	66.70	71.70	72.95
5.00 Hz	28.13	32.95	40.70	50.00	57.10	59.50	66.00	70.85	72.10
7.14 Hz	27.23	32.15	39.90	49.30	56.70	58.60	65.25	70.10	71.50
10.00 Hz	26.68	31.53	39.20	48.80	56.50	57.55	64.75	69.65	71.10

Table A9: Complex modulus and phase angle of a 15 penetration grade bitumen III [Choi, 2005]

Fre/Temp	10°C	15°C	25°C	35°C	45°C	55°C	65°C	75°C	80°C
0.10 Hz	20573750	8197175	706335	95640	21967	3392	778	196	94
0.14 Hz	24210750	10834375	1638550	217150	30789	5041	1145	283	133
0.20 Hz	28295000	13086000	2180800	284805	42214	7052	1615	403	188
0.29 Hz	33021500	15760500	2766450	380255	57180	9824	2261	577	268
0.41 Hz	38432250	18826000	3544950	499780	77103	13583	3151	818	377
0.59 Hz	44656250	22482250	4502650	663350	103840	18748	4380	1155	532
0.84 Hz	51372250	26587750	5718500	871750	139745	25691	6154	1636	756
1.20 Hz	58514750	31297250	7241300	1141350	187758	35152	8602	2312	1060
1.70 Hz	66609500	36558000	9114100	1491650	251335	47896	12014	3250	1494
2.44 Hz	75366000	42484750	11411500	1943750	336118	65186	16739	4608	2098
3.49 Hz	84497250	49071500	14168000	2515150	447598	88543	23218	6469	2945
5.00 Hz	93974250	56233000	17513000	3245350	592363	119960	31977	9073	4118
7.14 Hz	103901500	63868500	21377000	4134400	777575	161455	43846	12567	5729
10.00 Hz	113040000	71347750	25501000	5158800	995600	212010	58688	17056	7768

Fre/Temp	10°C	15°C	25°C	35°C	45°C	55°C	65°C	75°C	80°C
0.10 Hz	46.60	57.90	69.55	84.90	78.65	85.30	80.30	88.55	89.10
0.14 Hz	44.45	52.45	65.80	72.50	77.95	83.35	86.70	88.30	88.40
0.20 Hz	42.80	50.65	63.10	71.35	76.90	82.40	86.05	88.10	88.55
0.29 Hz	41.35	48.80	61.85	70.55	76.35	81.70	85.55	87.80	88.35
0.41 Hz	39.70	47.40	60.65	69.60	75.65	80.80	84.90	87.35	88.15
0.59 Hz	38.10	45.40	59.20	68.65	74.95	80.10	84.30	86.85	87.80
0.84 Hz	36.50	43.95	57.70	67.95	74.35	79.30	83.65	86.45	87.30
1.20 Hz	34.85	42.45	56.00	66.95	73.65	78.50	82.95	86.05	87.00
1.70 Hz	33.25	40.85	54.40	65.80	73.10	77.75	82.20	85.60	86.55
2.44 Hz	31.85	39.10	52.65	64.70	72.30	77.00	81.65	85.10	86.15
3.49 Hz	30.35	37.65	50.90	63.50	71.60	76.25	81.00	84.80	85.60
5.00 Hz	28.90	36.20	49.10	62.25	70.90	75.40	80.40	84.40	85.20
7.14 Hz	27.60	34.80	47.45	61.10	70.25	74.60	80.00	84.25	84.80
10.00 Hz	26.55	33.55	45.95	60.05	69.50	73.85	79.70	84.25	84.45

Table A10: Complex modulus and phase angle of a 50 penetration grade bitumen [Choi, 2005]

Fre/Temp	10°C	15°C	25°C	35°C	40°C	45°C	50°C	55°C	60°C
0.10 Hz	2737875	811003	83012	15114	5182	2234	929	429	216
0.14 Hz	3638325	1316775	147355	20268	7604	3204	1311	601	310
0.20 Hz	4602275	1712250	196990	27861	10878	4456	1838	858	438
0.29 Hz	5827475	2234000	263195	38528	15659	6194	2586	1206	603
0.41 Hz	7380600	2894100	350700	52572	21887	8528	3630	1707	837
0.59 Hz	9286325	3729800	467075	71580	30385	11730	5077	2400	1167
0.84 Hz	11523750	4786200	622165	97084	41778	16257	7078	3380	1640
1.20 Hz	14275250	6087875	825375	131878	57158	22433	9868	4749	2305
1.70 Hz	17494250	7725550	1092000	177983	77590	30909	13708	6650	3229
2.44 Hz	21333000	9709100	1443400	239295	104542	42440	19037	9290	4504
3.49 Hz	25901500	12131750	1892850	322735	140628	58419	26355	12967	6321
5.00 Hz	31096750	14998000	2471050	432318	187900	80018	36410	18035	8808
7.14 Hz	36874250	18461000	3188000	574588	250108	109205	50015	24842	12307
10.00 Hz	42956750	22220750	4019450	743410	324368	145300	66811	33598	16704

Fre/Temp	10°C	15°C	25°C	35°C	40°C	45°C	50°C	55°C	60°C
0.10 Hz	71.55	69.00	75.05	82.25	88.40	85.70	87.25	84.95	78.40
0.14 Hz	63.10	67.25	75.15	80.00	82.65	84.70	86.00	87.10	87.85
0.20 Hz	60.85	66.35	73.80	79.25	81.75	83.90	85.50	86.55	87.35
0.29 Hz	59.40	64.70	73.25	78.50	81.05	83.30	84.85	86.25	87.05
0.41 Hz	58.05	63.85	72.30	77.85	80.25	82.50	84.35	85.75	86.85
0.59 Hz	56.35	62.80	71.70	77.30	79.55	81.90	83.85	85.40	86.40
0.84 Hz	55.05	61.20	70.85	76.60	78.85	81.25	83.25	84.75	86.10
1.20 Hz	53.40	60.10	69.95	76.15	78.10	80.55	82.60	84.20	85.60
1.70 Hz	51.85	58.75	69.00	75.50	77.35	79.85	82.00	83.65	85.15
2.44 Hz	50.25	57.05	67.95	74.80	76.60	79.25	81.35	83.10	84.65
3.49 Hz	48.55	55.55	66.90	74.40	75.75	78.60	80.85	82.65	84.25
5.00 Hz	47.05	54.45	65.80	73.85	74.85	77.95	80.35	82.25	83.80
7.14 Hz	45.50	52.50	64.70	73.35	73.90	77.35	79.85	81.85	83.55
10.00 Hz	44.10	51.40	63.70	72.90	72.85	76.80	79.65	81.50	83.20

Table A11: Complex modulus and phase angle of aMiddle East 80/100 penetration grade bitumen [Airey, 1997]

Freq\Temp	10°C	15°C	25°C	35°C	45°C	55°C	65°C	75°C
0.01 Hz	459500	142500	13200	1455	227	41	10	3
0.015 Hz	613500	200500	19000	2050	331	60	15	4
0.02 Hz	760000	252000	24800	2790	447	82	20	6
0.05 Hz	1490000	515000	54350	6455	1100	203	50	15
0.1 Hz	2360000	863500	97800	12300	2150	398	100	28
0.15 Hz	3110000	1150000	136000	18400	3135	599	150	44
0.2 Hz	3740000	1405000	173000	24000	4110	797	201	59
0.5 Hz	6565000	2650000	360000	54450	9720	1945	496	148
1 Hz	9725000	4155000	617500	99050	18500	3780	982	293
1.5 Hz	12100000	5385000	843500	139500	26800	5560	1455	439
2 Hz	14050000	6415000	1040000	177500	34750	7295	1935	583
5 Hz	22050000	10900000	1995000	368000	78300	17200	4665	1440
10 Hz	29700000	15600000	3170000	614000	140500	32000	8885	2760
15 Hz	34600000	18900000	4105000	804000	194500	46350	12600	3940

Freq\Temp	10°C	15°C	25°C	35°C	45°C	55°C	65°C	75°C
0.01 Hz	72	73	82	86	89	89	90	89
0.015 Hz	67	71	81	85	88	89	90	89
0.02 Hz	66	70	79	85	88	89	89	89
0.05 Hz	63	67	77	83	87	89	89	89
0.1 Hz	59	66	75	82	86	88	89	89
0.15 Hz	58	64	73	81	85	88	89	90
0.2 Hz	57	63	73	80	85	87	89	90
0.5 Hz	53	59	70	77	83	86	88	89
1 Hz	49	57	68	75	81	85	88	89
1.5 Hz	48	55	67	74	80	85	87	89
2 Hz	46	53	66	73	80	84	87	89
5 Hz	42	49	63	68	77	82	86	88
10 Hz	39	46	60	63	75	81	85	87
15 Hz	38	44	58	59	74	80	84	84

Table A12: Complex modulus and phase angle of a Russian 80 penetration grade bitumen [Airey, 1997]

Freq\Temp	10°C	15°C	25°C	35°C	45°C	55°C	65°C
0.01 Hz	294000	100850	8530	1004	136	27	6
0.015 Hz	420500	147500	12400	1435	209	38	9
0.02 Hz	545500	186500	16050	1890	278	50	12
0.05 Hz	1120000	405000	37400	4450	686	127	31
0.1 Hz	1890000	700500	69350	8570	1355	250	63
0.15 Hz	2545000	957000	99300	12700	1990	372	93
0.2 Hz	3095000	1185000	127500	16650	2625	496	123
0.5 Hz	5645000	2330000	277500	38850	6365	1215	305
1 Hz	8575000	3745000	492500	73150	12350	2400	601
1.5 Hz	10850000	4880000	685000	105000	18150	3555	899
2 Hz	12700000	5855000	857000	136000	23750	4705	1190
5 Hz	20300000	10150000	1725000	301000	55500	11400	2915
10 Hz	27750000	14800000	2810000	527500	102500	21900	5655
15 Hz	32550000	17950000	3640000	713000	141500	31500	8190

Freq\Temp	10°C	15°C	25°C	35°C	45°C	55°C	65°C
0.01 Hz	75	79	84	84	87	89	89
0.015 Hz	73	76	84	86	88	89	90
0.02 Hz	71	76	83	86	88	89	89
0.05 Hz	67	73	81	85	87	88	89
0.1 Hz	64	70	79	85	87	88	89
0.15 Hz	62	68	78	84	87	88	89
0.2 Hz	61	67	77	83	86	88	89
0.5 Hz	56	63	75	82	86	87	88
1 Hz	53	60	73	80	85	87	88
1.5 Hz	51	58	71	79	84	87	88
2 Hz	49	56	70	78	84	87	88
5 Hz	44	52	66	74	82	86	88
10 Hz	41	48	63	69	80	85	87
15 Hz	39	46	61	65	79	84	86

Table A13: Complex modulus and phase angle of a Venezuelan 70/100 penetration grade bitumen [Airey, 1997]

Freq\Temp	10°C	15°C	25°C	35°C	45°C	55°C	65°C	75°C
0.01 Hz	150500	48500	6720	901	143	29	7	2
0.015 Hz	207500	67800	9680	1290	213	42	11	3
0.02 Hz	265000	87000	12600	1730	286	58	14	5
0.05 Hz	536000	179000	28300	3970	708	146	36	11
0.1 Hz	918500	310000	53250	7655	1385	291	73	22
0.15 Hz	1180000	419000	75350	11000	2040	439	110	33
0.2 Hz	1415000	525000	95300	14350	2680	588	146	45
0.5 Hz	2650000	1050000	199500	32750	6300	1440	363	108
1 Hz	4165000	1740000	343000	59950	11850	2810	720	215
1.5 Hz	5370000	2290000	463500	85100	17200	4115	1070	323
2 Hz	6445000	2790000	572500	109000	22200	5395	1410	430
5 Hz	11100000	5060000	1060000	232500	49900	12600	3375	1070
10 Hz	16050000	7710000	1565000	401500	89200	23400	6465	2060
15 Hz	20000000	9520000	1845000	532500	124000	32550	9055	2980

Freq\Temp	10°C	15°C	25°C	35°C	45°C	55°C	65°C	75°C
0.01 Hz	73	76	81	85	89	89	90	90
0.015 Hz	70	73	80	86	89	89	90	90
0.02 Hz	70	73	80	85	88	89	90	89
0.05 Hz	67	71	77	83	87	89	89	89
0.1 Hz	65	69	76	82	86	89	90	89
0.15 Hz	64	68	75	81	85	88	89	89
0.2 Hz	63	68	74	80	85	88	89	89
0.5 Hz	60	65	73	78	83	86	89	89
1 Hz	57	63	72	77	81	85	88	89
1.5 Hz	55	61	70	75	81	85	87	88
2 Hz	54	60	70	74	80	84	87	88
5 Hz	50	57	68	71	78	82	85	87
10 Hz	47	54	66	67	76	81	84	86
15 Hz	45	52	65	65	76	81	83	85

# Appendix B

Dynamic Shear Rheometer Data for the Aged  
Unmodified Bitumens

Table B1: Complex modulus and phase angle of the RTFOT aged Middle East 80/100 penetration grade bitumen [Airey, 1997]

Freq\Temp	10°C	15°C	25°C	35°C	45°C	55°C	65°C
0.01 Hz	833000	283000	30200	3270	471	82	18
0.015 Hz	1035000	395500	43550	4690	708	121	26
0.02 Hz	1335000	509500	56150	6105	932	162	35
0.05 Hz	2405000	958500	116000	14200	2250	404	87
0.1 Hz	3650000	1555000	202500	26300	4305	801	174
0.15 Hz	4675000	2010000	275500	37450	6365	1185	261
0.2 Hz	5425000	2410000	340500	47850	8300	1570	347
0.5 Hz	8885000	4225000	672000	101650	18850	3735	852
1 Hz	12600000	6310000	1100000	177500	34600	7155	1660
1.5 Hz	15300000	7890000	1450000	244500	49050	10350	2450
2 Hz	17350000	9215000	1770000	303500	62500	13500	3215
5 Hz	26050000	14700000	3175000	608000	133000	30500	7540
10 Hz	34150000	20250000	4820000	997500	225000	55100	14150
15 Hz	39450000	23900000	5985000	1315000	293500	74750	20250

Freq\Temp	10°C	15°C	25°C	35°C	45°C	55°C	65°C
0.01 Hz	65	69	78	83	87	88	90
0.015 Hz	62	66	75	82	87	89	89
0.02 Hz	60	65	75	82	86	89	89
0.05 Hz	56	62	71	79	85	88	89
0.1 Hz	54	60	69	77	83	87	89
0.15 Hz	52	58	68	76	82	86	88
0.2 Hz	51	57	67	75	82	86	88
0.5 Hz	48	54	65	73	79	84	87
1 Hz	45	51	63	71	77	83	86
1.5 Hz	43	49	61	70	76	82	85
2 Hz	42	48	60	70	75	81	85
5 Hz	39	44	57	67	72	79	83
10 Hz	36	42	55	65	70	77	82
15 Hz	35	40	53	64	68	76	81

Table B2: Complex modulus and phase angle of the PAV aged Middle East 80/100 penetration grade bitumen [Airey, 1997]

Freq\Temp	10°C	15°C	25°C	35°C	45°C	55°C	65°C	75°C
0.01 Hz	2575000	1065000	135000	17000	2040	320	59	14
0.015 Hz	3030000	1335000	189500	25050	2970	468	89	21
0.02 Hz	3635000	1620000	230500	30350	3895	627	118	28
0.05 Hz	5995000	2760000	447500	64500	8845	1525	294	70
0.1 Hz	8370000	4095000	710000	111500	16350	2930	583	136
0.15 Hz	10400000	5155000	941500	156500	23050	4275	866	206
0.2 Hz	11800000	6010000	1135000	190000	29350	5545	1135	274
0.5 Hz	17700000	9570000	2020000	364000	61650	12650	2720	677
1 Hz	23600000	13250000	3050000	588000	106000	23150	5195	1330
1.5 Hz	27950000	15950000	3860000	778000	144000	32500	7520	1960
2 Hz	31150000	18100000	4530000	942000	178000	41250	9745	2575
5 Hz	43500000	26400000	7365000	1720000	342500	85900	21650	6060
10 Hz	54100000	34200000	10300000	2650000	543000	144500	38650	11350
15 Hz	60400000	38950000	11950000	3320000	687000	190500	51400	15850

Freq\Temp	10°C	15°C	25°C	35°C	45°C	55°C	65°C	75°C
0.01 Hz	55	58	68	77	84	88	88	90
0.015 Hz	51	56	66	76	83	87	89	90
0.02 Hz	50	55	65	74	82	87	89	90
0.05 Hz	46	51	61	71	79	85	88	89
0.1 Hz	44	50	60	69	77	83	87	89
0.15 Hz	43	48	59	68	75	82	87	89
0.2 Hz	42	47	58	67	75	82	86	88
0.5 Hz	39	44	55	64	72	79	84	87
1 Hz	37	42	53	62	69	77	82	86
1.5 Hz	35	40	51	61	67	75	81	85
2 Hz	34	39	51	61	66	74	80	85
5 Hz	31	36	47	58	62	72	78	83
10 Hz	29	34	45	56	58	69	76	81
15 Hz	28	33	44	55	55	68	75	80

Table B3: Complex modulus and phase angle of the RTFOT aged Russian 80 penetration grade bitumen [Airey, 1997]

Freq\Temp	10°C	15°C	25°C	35°C	45°C	55°C	65°C
0.01 Hz	580000	203000	21800	2335	296	49	11
0.015 Hz	791500	285000	30400	3535	430	73	17
0.02 Hz	1010000	361500	39600	4605	575	97	22
0.05 Hz	1820000	697000	89000	11250	1385	241	56
0.1 Hz	2885000	1170000	160000	21900	2750	484	112
0.15 Hz	3840000	1545000	227000	31400	4155	720	167
0.2 Hz	4540000	1870000	287000	40050	5485	949	224
0.5 Hz	7630000	3385000	579000	89250	13050	2315	554
1 Hz	10950000	5130000	938000	161000	24800	4535	1090
1.5 Hz	13450000	6465000	1200000	224500	35950	6680	1615
2 Hz	15350000	7595000	1420000	282500	46700	8820	2130
5 Hz	23000000	12300000	2170000	576000	104500	20850	5170
10 Hz	30250000	17050000	2690000	932500	186000	38950	9930
15 Hz	34800000	20450000	2890000	1170000	246000	56050	14650

Freq\Temp	10°C	15°C	25°C	35°C	45°C	55°C	65°C
0.01 Hz	67	73	81	83	86	88	89
0.015 Hz	65	70	80	85	87	89	90
0.02 Hz	63	69	79	84	87	89	90
0.05 Hz	59	66	76	83	87	88	89
0.1 Hz	57	63	74	81	86	88	89
0.15 Hz	55	61	73	80	85	88	89
0.2 Hz	53	60	72	80	85	87	89
0.5 Hz	49	56	69	78	83	87	88
1 Hz	46	53	66	76	82	86	88
1.5 Hz	44	51	65	75	81	85	87
2 Hz	43	50	64	74	80	85	87
5 Hz	39	46	60	72	78	83	86
10 Hz	36	43	57	69	75	82	85
15 Hz	34	41	55	66	74	81	85

Table B4: Complex modulus and phase angle of the PAV aged Russian 80 penetration grade bitumen [Airey, 1997]

Freq\Temp	10°C	15°C	25°C	35°C	45°C	55°C	65°C	75°C
0.01 Hz	2280000	911500	100400	12300	1435	192	37	9
0.015 Hz	2900000	1225000	140500	18400	2100	286	55	13
0.02 Hz	3510000	1475000	174500	21400	2815	395	73	18
0.05 Hz	5870000	2615000	345500	52200	6665	973	183	44
0.1 Hz	8385000	3985000	575500	95400	12650	1915	363	87
0.15 Hz	10180000	5115000	775000	128000	17650	2825	541	132
0.2 Hz	11700000	6010000	933500	161000	22650	3690	720	176
0.5 Hz	17850000	9670000	1720000	325000	50050	8665	1760	439
1 Hz	23800000	13450000	2650000	532000	89800	16250	3415	870
1.5 Hz	28100000	16100000	3370000	694000	125500	23400	5030	1295
2 Hz	31450000	18350000	4010000	835000	159000	30200	6570	1720
5 Hz	43600000	26550000	6685000	1410000	323000	65900	15350	4160
10 Hz	54000000	34250000	9535000	1940000	533000	116000	28400	7940
15 Hz	60250000	38750000	11400000	2230000	699000	154500	40750	11450

Freq\Temp	10°C	15°C	25°C	35°C	45°C	55°C	65°C	75°C
0.01 Hz	57	63	73	81	86	88	89	89
0.015 Hz	53	58	70	79	85	88	89	89
0.02 Hz	52	57	69	78	84	88	89	89
0.05 Hz	48	54	66	76	82	87	89	89
0.1 Hz	45	51	63	73	81	86	88	89
0.15 Hz	44	49	62	72	80	85	88	89
0.2 Hz	43	48	61	71	79	85	88	89
0.5 Hz	39	45	58	69	76	82	86	88
1 Hz	37	42	55	67	74	81	85	88
1.5 Hz	35	41	54	65	73	80	84	87
2 Hz	34	39	53	64	72	79	84	87
5 Hz	31	36	49	62	67	77	82	85
10 Hz	29	34	47	59	63	74	80	84
15 Hz	27	33	46	58	60	73	80	83

Table B5: Complex modulus and phase angle of the RTFOT aged Venezuelan 70/100 penetration grade bitumen [Airey, 1997]

Freq\Temp	10°C	15°C	25°C	35°C	45°C	55°C	65°C
0.01 Hz	346500	116500	15500	2065	332	63	14
0.015 Hz	479000	163000	23100	3125	493	92	21
0.02 Hz	568500	199500	29500	4040	667	124	28
0.05 Hz	1085000	395500	64400	9325	1515	310	70
0.1 Hz	1710000	640000	110000	17350	2905	608	140
0.15 Hz	2255000	858500	147000	24550	4200	903	209
0.2 Hz	2685000	1045000	183000	30900	5470	1185	276
0.5 Hz	4705000	1930000	359000	65150	12350	2815	678
1 Hz	7040000	3005000	582000	113000	22500	5335	1325
1.5 Hz	8895000	3880000	760000	155000	31850	7685	1950
2 Hz	10450000	4605000	907000	192500	40600	9915	2555
5 Hz	16850000	7850000	1510000	379500	86500	22050	5980
10 Hz	23350000	11400000	2020000	612000	149500	39250	11100
15 Hz	27650000	14000000	2270000	767500	206000	53200	16050

Freq\Temp	10°C	15°C	25°C	35°C	45°C	55°C	65°C
0.01 Hz	68	68	76	83	87	88	89
0.015 Hz	64	67	74	82	87	89	89
0.02 Hz	63	67	74	81	86	89	89
0.05 Hz	61	64	71	78	84	88	89
0.1 Hz	58	63	70	77	83	86	89
0.15 Hz	58	62	69	75	82	86	88
0.2 Hz	57	61	69	75	81	85	88
0.5 Hz	53	59	67	73	79	83	87
1 Hz	51	57	66	72	77	82	85
1.5 Hz	49	55	64	71	76	81	85
2 Hz	48	54	64	70	75	80	84
5 Hz	45	51	61	69	73	78	82
10 Hz	42	49	59	68	71	77	81
15 Hz	40	47	58	67	69	76	80

Table B6: Complex modulus and phase angle of the RTFOT aged Venezuelan 70/100 penetration grade bitumen [Airey, 1997]

Freq\Temp	10°C	15°C	25°C	35°C	45°C	55°C	65°C	75°C
0.01 Hz	1255000	489500	67000	11600	1775	289	54	13
0.015 Hz	1600000	597500	93150	15800	2565	431	80	19
0.02 Hz	1910000	725000	113500	20900	3385	553	107	26
0.05 Hz	3205000	1290000	215000	42400	7415	1295	266	63
0.1 Hz	4645000	1935000	348500	71900	13250	2505	523	124
0.15 Hz	5895000	2465000	457500	95100	18950	3655	774	187
0.2 Hz	6815000	2885000	552000	117000	23900	4705	1019	249
0.5 Hz	10650000	4780000	997000	223000	49650	10450	2400	604
1 Hz	14750000	6870000	1535000	356000	84250	18550	4510	1170
1.5 Hz	17700000	8420000	1965000	464000	114500	25850	6495	1710
2 Hz	20150000	9735000	2330000	555000	141000	32700	8360	2245
5 Hz	29250000	15000000	3945000	952000	271500	66800	18350	5160
10 Hz	37650000	20350000	5715000	1340000	434000	113000	32500	9500
15 Hz	42650000	23750000	6930000	1580000	555500	151500	44150	13600

Freq\Temp	10°C	15°C	25°C	35°C	45°C	55°C	65°C	75°C
0.01 Hz	60	61	67	76	82	86	89	90
0.015 Hz	53	58	64	73	81	86	89	89
0.02 Hz	52	57	64	72	80	85	89	90
0.05 Hz	50	54	61	69	77	83	87	89
0.1 Hz	47	53	60	67	75	82	86	88
0.15 Hz	46	52	59	66	73	80	85	88
0.2 Hz	46	51	59	66	72	79	84	87
0.5 Hz	43	48	57	64	70	77	82	86
1 Hz	41	46	55	62	68	75	80	85
1.5 Hz	40	45	54	62	66	73	79	84
2 Hz	39	44	54	61	65	73	78	83
5 Hz	36	42	51	59	62	70	76	81
10 Hz	34	40	50	57	59	68	74	79
15 Hz	33	39	48	56	58	68	73	78

# Appendix C

Dynamic Shear Rheometer Data for Unaged  
Polymer-Modified Bitumens

Table C1: Complex modulus and phase angle of 3% EVA with 97% Middle East 80/100 penetration grade bitumen [Airey, 1997]

Freq\Temp	10°C	15°C	25°C	35°C	45°C	55°C	65°C	75°C
0.01 Hz	676000	256500	33300	4395	563	94	23	5
0.015 Hz	859000	341500	44750	6155	826	139	34	8
0.02 Hz	1070000	408500	56150	7865	1090	184	45	11
0.05 Hz	1940000	745500	104000	16450	2495	444	110	27
0.1 Hz	2950000	1200000	169500	28050	4630	875	217	54
0.15 Hz	3690000	1570000	230500	37800	6715	1290	325	82
0.2 Hz	4310000	1870000	286000	47250	8675	1685	431	109
0.5 Hz	7150000	3285000	545500	94150	18950	3890	1020	268
1 Hz	10200000	4920000	879000	157500	33400	7180	1920	524
1.5 Hz	12600000	6170000	1160000	211500	46300	10200	2760	775
2 Hz	14600000	7205000	1405000	261000	57800	13050	3540	1020
5 Hz	22500000	11700000	2535000	503500	117000	28100	7830	2400
10 Hz	30200000	16300000	3850000	819000	194000	48950	13900	4490
15 Hz	35100000	18900000	4740000	1075000	257000	66850	18800	6270

Freq\Temp	10°C	15°C	25°C	35°C	45°C	55°C	65°C	75°C
0.01 Hz	58	63	69	78	84	85	88	88
0.015 Hz	58	61	67	78	85	87	88	88
0.02 Hz	57	60	67	78	84	86	87	87
0.05 Hz	54	58	65	74	82	85	87	88
0.1 Hz	53	57	64	72	80	84	86	88
0.15 Hz	52	56	63	71	79	83	85	88
0.2 Hz	51	56	63	70	78	82	85	88
0.5 Hz	48	53	61	68	75	80	83	87
1 Hz	46	51	60	66	73	78	81	87
1.5 Hz	44	50	59	66	72	77	80	86
2 Hz	43	49	59	65	71	76	80	86
5 Hz	40	46	57	64	69	74	78	84
10 Hz	37	43	55	62	67	73	77	82
15 Hz	36	42	54	61	65	72	76	80

Table C2: Complex modulus and phase angle of 5% EVA with 95% Middle East 80/100 penetration grade bitumen [Airey, 1997]

Freq\Temp	10°C	15°C	25°C	35°C	45°C	55°C	65°C	75°C
0.01 Hz	899000	368500	55150	8810	1045	182	44	9
0.015 Hz	1170000	486000	70500	11750	1505	253	62	14
0.02 Hz	1355000	595000	87450	14350	1970	330	81	18
0.05 Hz	2385000	1013500	156500	27500	4300	769	190	44
0.1 Hz	3350000	1540000	251000	43150	7530	1420	360	86
0.15 Hz	4050000	1900000	330500	58350	10600	2070	523	128
0.2 Hz	4630000	2220000	392500	71600	13350	2670	681	171
0.5 Hz	7305000	3655000	691500	132000	26750	5880	1540	416
1 Hz	10150000	5210000	1055000	208000	44450	10400	2800	807
1.5 Hz	12250000	6390000	1345000	271000	59700	14400	3940	1185
2 Hz	14000000	7370000	1590000	325000	73150	18050	5005	1560
5 Hz	20600000	11450000	2695000	587000	138000	36250	10450	3620
10 Hz	27000000	15450000	3905000	902000	218500	60050	18050	6675
15 Hz	31200000	18050000	4760000	1175000	282500	78000	24250	9230

Freq\Temp	10°C	15°C	25°C	35°C	45°C	55°C	65°C	75°C
0.01 Hz	56	57	62	71	79	82	85	85
0.015 Hz	52	54	59	70	79	82	83	87
0.02 Hz	51	54	58	69	78	82	83	86
0.05 Hz	49	52	58	66	76	81	82	87
0.1 Hz	47	51	57	64	73	80	82	87
0.15 Hz	46	50	57	62	72	79	81	87
0.2 Hz	46	50	56	62	71	78	80	87
0.5 Hz	43	47	55	60	68	75	78	86
1 Hz	41	46	54	59	66	73	77	85
1.5 Hz	40	45	54	59	64	72	75	84
2 Hz	39	44	53	59	64	71	75	83
5 Hz	37	41	51	58	62	68	73	81
10 Hz	35	39	50	58	60	67	71	79
15 Hz	34	38	49	57	59	66	71	78

Table C3: Complex modulus and phase angle of 7% EVA with 93% Middle East 80/100 penetration grade bitumen [Airey, 1997]

Freq\Temp	10°C	15°C	25°C	35°C	45°C	55°C	65°C	75°C
0.01 Hz	1420000	643500	105500	18700	2085	351	71	16
0.015 Hz	1675000	778000	140000	24300	2900	498	116	23
0.02 Hz	2010000	911000	163000	29600	3700	635	153	31
0.05 Hz	3095000	1495000	273000	54200	7780	1400	346	76
0.1 Hz	4380000	2155000	416500	83700	13050	2490	633	150
0.15 Hz	5430000	2730000	535500	106000	17400	3480	912	222
0.2 Hz	6140000	3110000	630500	125000	21600	4440	1180	292
0.5 Hz	9165000	4775000	1055000	218500	42500	9320	2540	700
1 Hz	12200000	6500000	1540000	332000	68800	16000	4470	1350
1.5 Hz	14400000	7735000	1915000	423000	90550	21850	6200	1950
2 Hz	16100000	8715000	2235000	502500	109500	27100	7765	2540
5 Hz	23000000	12850000	3605000	866500	193500	52900	15700	5650
10 Hz	29450000	16900000	5055000	1300000	292000	85750	25900	9890
15 Hz	33950000	19800000	6045000	1610000	366000	112000	34050	12900

Freq\Temp	10°C	15°C	25°C	35°C	45°C	55°C	65°C	75°C
0.01 Hz	51	50	55	68	72	69	75	84
0.015 Hz	46	49	54	65	73	75	79	85
0.02 Hz	46	48	53	65	73	75	79	85
0.05 Hz	44	46	52	61	71	75	79	86
0.1 Hz	42	46	52	58	69	75	78	86
0.15 Hz	41	45	51	56	68	74	77	86
0.2 Hz	41	44	51	55	67	74	77	85
0.5 Hz	39	43	50	54	63	71	74	84
1 Hz	38	41	49	54	61	69	73	83
1.5 Hz	37	40	48	54	59	68	71	82
2 Hz	36	40	48	54	58	67	71	81
5 Hz	34	38	46	53	56	65	68	78
10 Hz	33	37	45	53	54	63	66	75
15 Hz	32	36	44	52	53	62	65	73

Table C4: Complex modulus and phase angle of 3% EVA with 97% Russian penetration grade bitumen [Airey, 1997]

Freq\Temp	10°C	15°C	25°C	35°C	45°C	55°C	65°C	75°C
0.01 Hz	486000	159000	16450	2280	400	111	11	3
0.015 Hz	705500	225500	23100	3350	639	152	18	4
0.02 Hz	860000	280500	29700	4380	796	181	24	5
0.05 Hz	1700000	546500	62250	8950	1615	340	58	13
0.1 Hz	2760000	956000	107500	15800	2780	594	106	26
0.15 Hz	3565000	1275000	148500	22400	3930	837	154	39
0.2 Hz	4230000	1565000	189000	28400	4980	1045	202	52
0.5 Hz	7365000	2950000	385500	60600	10750	2245	473	127
1 Hz	10850000	4610000	655000	107000	19200	4050	905	250
1.5 Hz	13600000	5930000	894000	148000	26900	5725	1310	372
2 Hz	15850000	7125000	1110000	186000	34200	7360	1710	490
5 Hz	24550000	12000000	2120000	378000	73100	16250	3970	1190
10 Hz	32850000	17150000	3375000	620000	128000	29350	7365	2310
15 Hz	37900000	20650000	4280000	803000	176500	41100	10400	3370

Freq\Temp	10°C	15°C	25°C	35°C	45°C	55°C	65°C	75°C
0.01 Hz	69	72	71	73	61	11	74	90
0.015 Hz	65	69	71	72	64	53	82	90
0.02 Hz	65	69	72	73	65	55	83	89
0.05 Hz	61	66	71	73	69	64	83	89
0.1 Hz	59	64	71	74	72	69	83	89
0.15 Hz	57	63	71	74	73	71	83	90
0.2 Hz	56	62	70	73	73	72	83	89
0.5 Hz	52	59	69	73	75	75	83	89
1 Hz	49	56	67	73	75	76	83	88
1.5 Hz	47	54	66	72	75	77	82	88
2 Hz	46	53	65	72	75	77	82	87
5 Hz	42	49	62	71	74	77	81	85
10 Hz	39	46	60	69	73	77	81	84
15 Hz	37	44	58	67	72	77	80	82

Table C5: Complex modulus and phase angle of 5% EVA with 95% Russian penetration grade bitumen [Airey, 1997]

Freq\Temp	10°C	15°C	25°C	35°C	45°C	55°C	65°C	75°C
0.01 Hz	613500	224500	29800	6315	2100	842	47	4
0.015 Hz	791500	295500	40450	7875	2330	906	65	6
0.02 Hz	960500	359500	48850	9195	2570	948	77	8
0.05 Hz	1765000	665000	91200	16900	3760	1185	138	20
0.1 Hz	2715000	1055000	146500	26950	5815	1535	230	40
0.15 Hz	3495000	1380000	198500	35100	7520	1915	315	61
0.2 Hz	4140000	1660000	246000	42800	9090	2265	393	80
0.5 Hz	7020000	2965000	469500	81200	17350	4160	823	197
1 Hz	10250000	4510000	755500	133000	28600	6850	1455	390
1.5 Hz	12650000	5760000	991000	178500	38550	9340	2040	576
2 Hz	14750000	6815000	1205000	219500	47850	11600	2590	761
5 Hz	22900000	11250000	2210000	423500	94000	23200	5555	1800
10 Hz	30800000	16000000	3420000	690000	155500	39150	9755	3350
15 Hz	35700000	19050000	4350000	918000	204000	51750	13400	4690

Freq\Temp	10°C	15°C	25°C	35°C	45°C	55°C	65°C	75°C
0.01 Hz	61	60	59	44	24	13	36	88
0.015 Hz	59	60	59	52	28	17	48	87
0.02 Hz	58	60	59	54	33	19	51	88
0.05 Hz	56	58	61	59	45	29	60	88
0.1 Hz	55	59	62	61	52	41	65	88
0.15 Hz	54	58	62	62	55	47	68	88
0.2 Hz	53	57	62	63	58	51	69	88
0.5 Hz	50	55	62	64	62	60	72	88
1 Hz	48	53	61	64	65	64	73	86
1.5 Hz	46	52	60	64	65	65	73	86
2 Hz	45	51	60	64	66	66	74	85
5 Hz	41	48	58	64	66	68	74	83
10 Hz	38	45	56	64	66	69	74	81
15 Hz	37	43	55	63	65	69	74	79

Table C6: Complex modulus and phase angle of 7% EVA with 93% Russian penetration grade bitumen [Airey, 1997]

Freq\Temp	10°C	15°C	25°C	35°C	45°C	55°C	65°C	75°C
0.01 Hz	808500	330000	62500	16300	4565	1535	166	7
0.015 Hz	1035000	442000	80450	19550	5070	1650	167	10
0.02 Hz	1270000	505000	93700	22150	5635	1760	187	14
0.05 Hz	2090000	853000	147500	34700	8055	2210	303	36
0.1 Hz	3245000	1330000	227000	52050	11550	2885	486	69
0.15 Hz	4135000	1680000	289500	66150	14600	3535	639	102
0.2 Hz	4920000	1970000	342500	77800	17000	4100	776	135
0.5 Hz	8245000	3410000	596000	133500	29050	6995	1495	329
1 Hz	11900000	5090000	909000	202500	44100	10850	2480	634
1.5 Hz	14800000	6400000	1165000	259000	56750	14200	3355	925
2 Hz	17050000	7540000	1400000	310000	67850	17200	4150	1200
5 Hz	26550000	12500000	2455000	551000	121500	32000	8315	2700
10 Hz	35750000	17700000	3715000	852000	188000	51050	13750	4780
15 Hz	40750000	21300000	4640000	1085000	239000	66600	18400	6460

Freq\Temp	10°C	15°C	25°C	35°C	45°C	55°C	65°C	75°C
0.01 Hz	51	55	46	42	29	18	12	86
0.015 Hz	52	50	46	42	31	19	36	88
0.02 Hz	52	50	46	43	33	21	41	87
0.05 Hz	51	52	48	46	39	29	51	88
0.1 Hz	52	52	51	49	45	38	57	87
0.15 Hz	51	53	52	50	47	43	59	87
0.2 Hz	51	53	53	51	49	46	61	87
0.5 Hz	49	52	54	53	53	53	64	85
1 Hz	47	51	55	55	55	57	65	84
1.5 Hz	46	50	55	56	56	58	66	82
2 Hz	45	50	55	56	56	59	66	82
5 Hz	42	48	55	58	57	61	67	78
10 Hz	39	46	55	59	58	62	67	75
15 Hz	38	44	54	59	58	63	67	73

Table C7: Complex modulus and phase angle of 3% EVA with 97% Venezuelan 70/100 penetration grade bitumen [Airey, 1997]

Freq\Temp	10°C	15°C	25°C	35°C	45°C	55°C	65°C	75°C
0.01 Hz	313000	103500	15100	2685	447	80	15	5
0.015 Hz	393500	143000	20500	3605	610	117	26	7
0.02 Hz	481000	178500	26200	4400	797	155	35	9
0.05 Hz	897000	332500	52000	9395	1780	369	85	22
0.1 Hz	1380000	532000	87000	16550	3225	696	160	44
0.15 Hz	1790000	705500	125000	22400	4425	1008	233	66
0.2 Hz	2160000	856500	156000	27800	5615	1315	305	87
0.5 Hz	3795000	1570000	301000	56400	11950	2930	711	216
1 Hz	5690000	2425000	486000	95500	20900	5270	1340	426
1.5 Hz	7175000	3120000	640000	130000	29050	7385	1950	633
2 Hz	8410000	3730000	767000	162000	36450	9380	2520	837
5 Hz	13650000	6360000	1310000	319000	74600	19700	5690	1990
10 Hz	19100000	9265000	1830000	521000	125500	34150	10300	3770
15 Hz	22650000	11300000	2110000	680000	168000	46150	13800	5560

Freq\Temp	10°C	15°C	25°C	35°C	45°C	55°C	65°C	75°C
0.01 Hz	64	64	70	74	79	82	77	88
0.015 Hz	61	63	69	74	81	85	84	88
0.02 Hz	61	63	69	74	81	85	83	88
0.05 Hz	58	61	67	72	78	83	83	88
0.1 Hz	57	61	66	71	76	81	83	89
0.15 Hz	57	60	65	70	75	80	83	89
0.2 Hz	56	60	65	70	75	79	83	89
0.5 Hz	53	58	64	68	73	77	83	88
1 Hz	51	56	64	68	72	76	82	87
1.5 Hz	50	55	63	67	71	75	81	86
2 Hz	49	54	63	67	71	75	81	85
5 Hz	46	51	61	67	70	73	79	83
10 Hz	43	49	59	65	69	73	78	81
15 Hz	42	48	58	63	68	72	76	81

Table C8: Complex modulus and phase angle of 5% EVA with 95% Venezuelan 70/100 penetration grade bitumen [Airey, 1997]

Freq\Temp	10°C	15°C	25°C	35°C	45°C	55°C	65°C	75°C
0.01 Hz	491000	217000	40250	8730	1305	237	62	9
0.015 Hz	620000	266000	49500	10400	1790	359	83	14
0.02 Hz	723500	319000	60400	13000	2240	459	106	19
0.05 Hz	1235000	548000	103500	22100	4640	976	226	49
0.1 Hz	1860000	815000	154000	34200	7350	1700	400	98
0.15 Hz	2410000	1040000	211500	44000	9805	2350	560	146
0.2 Hz	2825000	1215000	257000	53000	11900	2935	707	193
0.5 Hz	4670000	2065000	454000	96900	22650	5995	1480	467
1 Hz	6720000	3065000	696500	152000	36400	10150	2570	897
1.5 Hz	8290000	3860000	900000	197000	48050	13650	3550	1310
2 Hz	9545000	4545000	1075000	237000	58800	16900	4470	1700
5 Hz	14950000	7485000	1870000	428000	109500	32650	9100	3790
10 Hz	20550000	10700000	2810000	669000	172000	52650	15100	6670
15 Hz	23800000	12950000	3405000	867000	221500	68600	19800	8330

Freq\Temp	10°C	15°C	25°C	35°C	45°C	55°C	65°C	75°C
0.01 Hz	55	57	53	60	68	66	36	88
0.015 Hz	52	53	54	59	69	74	74	88
0.02 Hz	52	53	54	58	69	74	75	87
0.05 Hz	51	53	54	56	66	73	74	88
0.1 Hz	51	52	56	56	65	71	73	87
0.15 Hz	50	52	55	57	64	71	73	87
0.2 Hz	50	52	55	57	64	70	73	86
0.5 Hz	48	51	55	58	62	69	72	85
1 Hz	47	50	55	58	62	67	72	84
1.5 Hz	46	50	55	58	61	67	71	82
2 Hz	46	49	55	58	61	66	71	81
5 Hz	44	48	54	59	60	65	69	78
10 Hz	42	46	53	59	59	64	68	75
15 Hz	41	45	52	57	59	64	67	73

Table C9: Complex modulus and phase angle of 7% EVA with 93% Venezuelan 70/100 penetration grade bitumen [Airey, 1997]

Freq\Temp	10°C	15°C	25°C	35°C	45°C	55°C	65°C	75°C
0.01 Hz	455500	236000	59050	15750	4110	677	145	11
0.015 Hz	586000	274000	73250	19500	5150	873	185	17
0.02 Hz	672500	327500	84850	23000	5930	1055	223	22
0.05 Hz	1065000	526500	133500	35550	9520	1900	416	52
0.1 Hz	1595000	750000	196500	51850	14400	2950	682	106
0.15 Hz	1990000	928000	243500	67100	18400	3855	903	163
0.2 Hz	2310000	1080000	282000	79050	21700	4630	1095	217
0.5 Hz	3800000	1780000	457500	132500	36700	8380	2075	522
1 Hz	5515000	2620000	662500	194500	55000	13050	3380	1000
1.5 Hz	6895000	3295000	827500	243000	70000	16950	4510	1460
2 Hz	8070000	3860000	968000	286000	82800	20350	5510	1890
5 Hz	13000000	6420000	1620000	482000	143000	36350	10400	4110
10 Hz	18250000	9260000	2395000	719000	194000	55400	16550	6930
15 Hz	22200000	11450000	3045000	903000	397000	69750	20700	8310

Freq\Temp	10°C	15°C	25°C	35°C	45°C	55°C	65°C	75°C
0.01 Hz	46	51	47	47	51	50	61	89
0.015 Hz	47	46	46	46	51	54	61	88
0.02 Hz	47	47	46	46	51	55	61	88
0.05 Hz	46	48	46	47	50	57	61	87
0.1 Hz	49	47	48	49	51	57	62	87
0.15 Hz	48	48	48	49	51	57	62	86
0.2 Hz	49	49	48	49	51	58	63	86
0.5 Hz	49	49	49	50	52	58	64	84
1 Hz	48	49	50	51	52	58	64	82
1.5 Hz	48	49	50	51	52	58	64	81
2 Hz	48	49	50	51	52	58	64	80
5 Hz	46	49	51	52	53	57	63	75
10 Hz	44	48	51	52	53	58	63	72
15 Hz	43	47	51	51	53	58	62	69

Table C10: Complex modulus and phase angle of 3% SBS with 97% Russian 80 penetration grade bitumen [Airey, 1997]

Freq\Temp	10°C	15°C	25°C	35°C	45°C	55°C	65°C	75°C
0.01 Hz	387500	140500	15100	2360	402	60	29	11
0.015 Hz	555000	192500	21300	3330	564	118	32	13
0.02 Hz	705500	242500	28300	4320	724	153	42	17
0.05 Hz	1325000	491000	57500	9210	1660	355	97	36
0.1 Hz	2200000	816000	99200	16050	3080	668	181	65
0.15 Hz	2880000	1100000	134000	21900	4400	968	260	89
0.2 Hz	3465000	1345000	168000	27600	5645	1260	336	114
0.5 Hz	6045000	2525000	343000	58500	12050	2825	777	255
1 Hz	8905000	3965000	576000	103000	21100	5150	1455	474
1.5 Hz	11050000	5105000	765000	143000	29500	7275	2080	682
2 Hz	12900000	6060000	927000	180500	37300	9225	2685	884
5 Hz	20100000	10100000	1560000	370000	79300	19650	5925	2000
10 Hz	26950000	14400000	2090000	614500	139000	34300	10500	3660
15 Hz	31150000	17150000	2360000	795500	190000	46500	14200	5150

Freq\Temp	10°C	15°C	25°C	35°C	45°C	55°C	65°C	75°C
0.01 Hz	69	72	72	79	72	72	40	78
0.015 Hz	67	70	72	78	80	81	77	74
0.02 Hz	65	69	71	77	80	81	78	73
0.05 Hz	62	67	71	74	79	81	80	75
0.1 Hz	60	65	71	73	77	81	80	76
0.15 Hz	58	64	71	72	76	80	81	77
0.2 Hz	57	63	71	72	76	80	81	78
0.5 Hz	52	59	69	72	74	78	81	79
1 Hz	49	56	67	72	73	77	80	80
1.5 Hz	47	54	66	72	73	76	80	80
2 Hz	46	53	65	72	73	76	79	80
5 Hz	42	49	63	71	73	75	77	79
10 Hz	39	46	60	82	72	74	76	77
15 Hz	37	44	58	25	71	74	75	76

Table C11: Complex modulus and phase angle of 5% SBS with 95% Russian 80 penetration grade bitumen [Airey, 1997]

Freq\Temp	10°C	15°C	25°C	35°C	45°C	55°C	65°C	75°C
0.01 Hz	428500	150000	19500	3050	653	132	40	18
0.015 Hz	587000	203500	26400	4575	907	229	84	46
0.02 Hz	724500	259500	33700	5770	1145	285	98	54
0.05 Hz	1385000	498000	65900	12000	2365	569	182	90
0.1 Hz	2205000	815000	105000	20500	4165	1010	301	135
0.15 Hz	2875000	1115000	152000	28000	5745	1390	416	180
0.2 Hz	3415000	1365000	192000	34800	7225	1740	519	219
0.5 Hz	5865000	2500000	385000	70150	15000	3670	1100	435
1 Hz	8535000	3835000	629000	118500	25700	6460	1950	751
1.5 Hz	10550000	4870000	825000	161000	35150	8985	2745	1050
2 Hz	12150000	5700000	984000	200000	43800	11300	3490	1320
5 Hz	18600000	9315000	1640000	393500	88400	23400	7440	2805
10 Hz	24850000	13050000	2180000	639500	148500	39650	12950	4905
15 Hz	28750000	15300000	2450000	823000	199500	53450	17800	6695

Freq\Temp	10°C	15°C	25°C	35°C	45°C	55°C	65°C	75°C
0.01 Hz	67	67	70	68	59	40	50	45
0.015 Hz	64	66	69	71	67	62	55	49
0.02 Hz	63	66	69	71	69	63	57	49
0.05 Hz	60	64	67	70	70	68	63	53
0.1 Hz	57	63	67	69	71	71	68	58
0.15 Hz	56	61	67	69	71	72	69	61
0.2 Hz	55	61	67	69	71	72	71	63
0.5 Hz	51	57	66	68	71	73	73	68
1 Hz	48	54	65	68	70	73	74	71
1.5 Hz	46	53	64	68	69	72	74	72
2 Hz	45	51	63	68	69	72	74	72
5 Hz	41	48	60	68	68	71	73	73
10 Hz	38	45	58	67	68	70	72	73
15 Hz	36	43	57	65	67	70	72	72

Table C12: Complex modulus and phase angle of 7% SBS with 93% Russian 80 penetration grade bitumen [Airey, 1997]

Freq\Temp	10°C	15°C	25°C	35°C	45°C	55°C	65°C	75°C
0.01 Hz	406500	164000	24050	4560	926	352	133	53
0.015 Hz	529500	210000	32000	5970	1355	438	199	105
0.02 Hz	642500	260000	39550	7360	1700	514	225	118
0.05 Hz	1145000	475000	75450	14400	3150	882	363	178
0.1 Hz	1750000	737000	124000	24100	5250	1495	538	254
0.15 Hz	2245000	967000	166000	32200	7265	2050	720	325
0.2 Hz	2650000	1170000	202500	39800	9080	2540	871	386
0.5 Hz	4370000	2030000	378000	77500	18050	5090	1695	705
1 Hz	6205000	3020000	600000	127000	30300	8565	2860	1155
1.5 Hz	7590000	3790000	784000	170000	41050	11600	3900	1555
2 Hz	8660000	4440000	940000	210000	50800	14350	4850	1935
5 Hz	13000000	7130000	1660000	396000	99050	28050	9780	3875
10 Hz	17100000	9810000	2485000	621000	161500	46350	16300	6540
15 Hz	19850000	11500000	3070000	791000	211500	61250	21550	8765

Freq\Temp	10°C	15°C	25°C	35°C	45°C	55°C	65°C	75°C
0.01 Hz	61	62	67	59	49	33	44	28
0.015 Hz	58	61	64	64	60	49	42	44
0.02 Hz	58	61	68	64	62	51	44	44
0.05 Hz	55	58	64	65	64	58	49	47
0.1 Hz	53	58	63	65	65	63	57	51
0.15 Hz	52	56	62	65	66	64	59	54
0.2 Hz	51	56	62	65	66	65	61	56
0.5 Hz	48	53	61	64	66	67	65	61
1 Hz	45	51	59	64	66	67	67	64
1.5 Hz	44	49	58	63	66	67	67	66
2 Hz	43	48	57	63	65	67	68	66
5 Hz	39	45	55	62	65	67	68	68
10 Hz	37	42	53	59	64	66	67	68
15 Hz	36	41	51	56	63	66	67	67

Table C13: Complex modulus and phase angle of 3% SBS with 97% Venezuelan 70/100 penetration grade bitumen [Airey, 1997]

Freq\Temp	10°C	15°C	25°C	35°C	45°C	55°C	65°C	75°C
0.01 Hz	255500	88750	14700	2570	390	85	23	7
0.015 Hz	334500	118500	19900	3530	608	132	33	11
0.02 Hz	422500	147000	24500	4470	798	174	44	14
0.05 Hz	805000	292500	49300	9345	1850	424	111	34
0.1 Hz	1275000	482000	84450	16200	3420	830	218	67
0.15 Hz	1695000	641500	112000	22200	4830	1220	325	97
0.2 Hz	2060000	788000	139000	27600	6105	1590	430	128
0.5 Hz	3685000	1495000	275500	55450	12700	3620	1011	308
1 Hz	5565000	2370000	452500	94050	21750	6545	1915	594
1.5 Hz	7030000	3080000	599000	128000	29750	9145	2755	872
2 Hz	8225000	3695000	726500	159000	37050	11550	3555	1140
5 Hz	13350000	6415000	1255000	313500	75050	23700	7755	2630
10 Hz	18600000	9400000	1740000	511000	126500	40050	13600	4770
15 Hz	22050000	11450000	2005000	657000	168500	53550	18100	6730

Freq\Temp	10°C	15°C	25°C	35°C	45°C	55°C	65°C	75°C
0.01 Hz	67	69	70	79	83	81	89	85
0.015 Hz	65	66	69	77	83	87	88	87
0.02 Hz	64	66	69	76	83	86	87	87
0.05 Hz	62	65	68	72	80	85	87	87
0.1 Hz	60	64	68	71	77	83	86	86
0.15 Hz	59	63	67	70	76	82	85	86
0.2 Hz	58	63	67	69	75	81	85	86
0.5 Hz	55	60	67	69	72	78	83	85
1 Hz	52	58	66	69	70	75	81	84
1.5 Hz	51	57	65	68	70	74	79	83
2 Hz	50	56	64	69	70	73	79	82
5 Hz	46	52	62	68	69	71	76	80
10 Hz	43	50	60	79	68	70	74	77
15 Hz	42	48	59		68	70	73	76

Table C14: Complex modulus and phase angle data of 5% SBS with 95% Venezuelan 70/100 penetration grade bitumen [Airey, 1997]

Freq\Temp	10°C	15°C	25°C	35°C	45°C	55°C	65°C	75°C
0.01 Hz	335250	119000	23100	4340	704	174	46	11
0.015 Hz	436750	155000	31100	5640	1050	220	55	20
0.02 Hz	532500	197500	37800	7240	1370	285	73	27
0.05 Hz	969000	375500	70700	14700	3170	664	171	60
0.1 Hz	1530000	593500	116000	24700	5650	1240	327	113
0.15 Hz	2010000	753500	155000	33000	7620	1790	473	163
0.2 Hz	2387500	910500	190000	40300	9700	2290	613	212
0.5 Hz	4112500	1655000	357000	76800	19800	5040	1420	486
1 Hz	6052500	2555000	566000	125000	32900	8910	2640	911
1.5 Hz	7550000	3270000	734000	166000	44500	12200	3750	1310
2 Hz	8767500	3885000	881000	204000	54600	15200	4820	1700
5 Hz	13725000	6490000	1460000	387000	106000	29800	10300	3770
10 Hz	18750000	9285000	1990000	615000	172000	48800	17700	6650
15 Hz	21750000	11260000	2280000	793000	223000	62800	24000	9100

Freq\Temp	10°C	15°C	25°C	35°C	45°C	55°C	65°C	75°C
0.01 Hz	63	67	65	73	83	73	63	67
0.015 Hz	61	62	64	73	80	80	81	78
0.02 Hz	60	62	63	72	79	81	82	79
0.05 Hz	58	62	63	68	76	80	82	79
0.1 Hz	56	60	63	66	74	79	82	80
0.15 Hz	55	59	63	65	72	79	82	80
0.2 Hz	54	59	63	64	71	78	81	81
0.5 Hz	51	56	63	63	68	75	80	80
1 Hz	49	55	62	63	66	72	78	80
1.5 Hz	47	53	61	63	65	71	77	79
2 Hz	46	52	61	62	65	69	76	78
5 Hz	43	49	59	60	64	67	72	76
10 Hz	40	47	57	57	64	65	70	74
15 Hz	39	45	56	54	63	65	69	73

Table C15: Complex modulus and phase angle data of 7% SBS with 93% Venezuelan 70/100 penetration grade bitumen [Airey, 1997]

Freq\Temp	10°C	15°C	25°C	35°C	45°C	55°C	65°C	75°C
0.01 Hz	446000	174000	28700	5610	1180	179	74	25
0.015 Hz	585500	227000	38300	8080	1600	347	92	30
0.02 Hz	713500	270000	45900	10400	2060	455	122	39
0.05 Hz	1300000	499000	82300	19300	4480	1030	280	88
0.1 Hz	1990000	789000	133000	30200	7780	1900	533	167
0.15 Hz	2520000	1030000	174000	39800	10600	2690	764	239
0.2 Hz	2945000	1220000	213000	48500	13000	3450	985	309
0.5 Hz	4895000	2150000	396000	88700	24600	7260	2230	716
1 Hz	7025000	3230000	626000	140000	38900	12400	4040	1340
1.5 Hz	8640000	4040000	815000	183000	50900	16600	5650	1920
2 Hz	9945000	4750000	986000	221000	61200	20400	7150	2470
5 Hz	15300000	7690000	1750000	404000	113000	37900	14400	5380
10 Hz	20500000	10800000	2640000	622000	178000	59800	23300	9270
15 Hz	23750000	12900000	3270000	784000	232000	77400	29900	12500

Freq\Temp	10°C	15°C	25°C	35°C	45°C	55°C	65°C	75°C
0.01 Hz	58	64	61	68	80	70	79	68
0.015 Hz	58	59	57	69	77	79	79	79
0.02 Hz	57	59	57	67	76	79	80	79
0.05 Hz	54	59	59	62	72	78	80	81
0.1 Hz	54	57	60	60	69	76	80	81
0.15 Hz	52	56	60	60	67	75	80	81
0.2 Hz	51	56	60	59	66	74	79	81
0.5 Hz	49	53	60	60	62	70	77	80
1 Hz	46	52	59	61	60	67	74	79
1.5 Hz	45	50	58	61	60	65	73	78
2 Hz	44	49	58	61	60	64	71	77
5 Hz	41	46	56	61	60	61	67	73
10 Hz	38	44	54	61	60	61	64	70
15 Hz	37	43	54	61	60	61	63	68

# Appendix D

Dynamic Shear Rheometer Data for Aged  
Polymer-Modified Bitumens

Table D1: Complex modulus and phase angle data of RTFOT aged 3% EVA with 97% Middle East 80/100 penetration grade bitumen [Airey, 1997]

Freq\Temp	10°C	15°C	25°C	35°C	45°C	55°C	65°C	75°C
0.01 Hz	1260000	551000	70100	9760	1160	205	43	11
0.015 Hz	1585000	667000	95750	13400	1695	297	64	17
0.02 Hz	1890000	799000	119000	16800	2225	395	83	23
0.05 Hz	3185000	1390000	219000	33900	5125	957	205	55
0.1 Hz	4640000	2090000	347500	58900	9425	1840	403	111
0.15 Hz	5780000	2670000	453000	76500	13300	2680	597	166
0.2 Hz	6650000	3120000	548000	94200	16900	3505	790	221
0.5 Hz	10450000	5130000	986000	182000	35600	7890	1860	536
1 Hz	14400000	7330000	1510000	294000	60850	14350	3505	1040
1.5 Hz	17200000	9010000	1925000	386000	82200	20150	5040	1520
2 Hz	19400000	10300000	2285000	471000	101500	25500	6465	1990
5 Hz	28250000	15900000	3855000	864000	194500	52600	14050	4615
10 Hz	36350000	21400000	5585000	1340000	309500	88650	24500	8555
15 Hz	41450000	25000000	6750000	1720000	397000	118000	33200	11700

Freq\Temp	10°C	15°C	25°C	35°C	45°C	55°C	65°C	75°C
0.01 Hz	58	61	65	78	84	88	89	84
0.015 Hz	52	56	64	76	83	87	89	86
0.02 Hz	52	56	63	75	83	87	89	86
0.05 Hz	49	53	60	70	79	85	88	86
0.1 Hz	47	51	59	68	77	83	86	86
0.15 Hz	46	51	58	66	76	82	86	86
0.2 Hz	45	50	58	65	74	81	85	86
0.5 Hz	43	47	56	63	71	78	82	85
1 Hz	41	45	55	62	68	76	80	85
1.5 Hz	39	44	54	61	67	74	79	84
2 Hz	38	43	53	61	66	74	78	83
5 Hz	36	41	51	59	63	70	75	81
10 Hz	34	39	49	58	60	68	73	80
15 Hz	33	38	49	58	59	68	73	79

Table D2: Complex modulus and phase angle data of PAV aged 3% EVA with 97% Middle East 80/100 penetration grade bitumen [Airey, 1997]

Freq\Temp	10°C	15°C	25°C	35°C	45°C	55°C	65°C	75°C	85°C
0.01 Hz	3045000	1430000	237500	39200	5960	938	178	44	13
0.015 Hz	3695000	1730000	316500	51200	8400	1345	261	72	21
0.02 Hz	4355000	2070000	364500	62300	10800	1780	347	94	27
0.05 Hz	6450000	3220000	636500	117000	22500	4060	826	225	64
0.1 Hz	8700000	4490000	955500	183500	39000	7450	1590	434	123
0.15 Hz	10350000	5440000	1195000	239500	53100	10600	2335	631	182
0.2 Hz	11600000	6180000	1400000	284000	66000	13550	3050	821	244
0.5 Hz	16550000	9240000	2285000	497000	126000	28750	6855	1925	597
1 Hz	21250000	12300000	3255000	749000	200000	49200	12300	3595	1160
1.5 Hz	24650000	14400000	3985000	951000	260000	66750	17050	5160	1720
2 Hz	27250000	16200000	4580000	1115000	312000	82400	21550	6640	2260
5 Hz	36700000	22800000	7020000	1875000	540000	155500	43400	14500	5270
10 Hz	44950000	28700000	9480000	2715000	789000	242000	71550	25500	9610
15 Hz	50000000	32600000	11100000	3320000	958000	304000	92400	35000	13400

Freq\Temp	10°C	15°C	25°C	35°C	45°C	55°C	65°C	75°C	85°C
0.01 Hz	45	55	60	66	78	85	87	74	84
0.015 Hz	43	47	56	64	76	84	87	84	83
0.02 Hz	42	47	55	63	75	83	87	84	82
0.05 Hz	39	45	52	60	71	80	85	84	85
0.1 Hz	38	42	51	59	69	78	83	84	86
0.15 Hz	37	41	50	57	67	76	82	84	86
0.2 Hz	37	41	49	57	66	75	80	83	87
0.5 Hz	34	38	47	55	62	71	77	82	86
1 Hz	33	37	46	53	60	68	74	80	85
1.5 Hz	31	36	45	52	59	67	73	79	84
2 Hz	31	35	44	52	58	65	72	78	83
5 Hz	29	33	42	50	57	62	68	76	81
10 Hz	27	31	41	49	56	60	66	74	79
15 Hz	27	30	40	48	55	58	66	73	78

Table D3: Complex modulus and phase angle data of RTFOT aged 5% EVA with 95% Middle East 80/100 penetration grade bitumen [Airey, 1997]

Freq\Temp	10°C	15°C	25°C	35°C	45°C	55°C	65°C	75°C
0.01 Hz	1970000	847500	142000	23050	2555	387	77	20
0.015 Hz	2280000	1100000	185500	30450	3615	566	118	30
0.02 Hz	2750000	1275000	221000	36950	4675	722	157	42
0.05 Hz	4425000	2060000	386000	68100	10200	1715	378	103
0.1 Hz	5985000	3045000	591500	107000	17800	3225	723	200
0.15 Hz	7385000	3780000	756500	138500	24400	4695	1050	297
0.2 Hz	8330000	4355000	888500	166000	30150	6070	1370	389
0.5 Hz	12450000	6795000	1500000	296000	58500	13150	3095	932
1 Hz	16650000	9300000	2200000	453500	94050	22750	5570	1775
1.5 Hz	19600000	11150000	2745000	582000	123500	30900	7765	2570
2 Hz	21900000	12650000	3205000	697000	149000	38300	9780	3335
5 Hz	30750000	18450000	5140000	1215000	266500	73050	19950	7505
10 Hz	38800000	24050000	7175000	1815000	407000	117000	33550	13350
15 Hz	43900000	27550000	8560000	2265000	510500	147500	44650	17850

Freq\Temp	10°C	15°C	25°C	35°C	45°C	55°C	65°C	75°C
0.01 Hz	51	51	59	71	80	83	84	77
0.015 Hz	47	50	56	68	78	84	86	84
0.02 Hz	47	49	55	67	77	83	86	85
0.05 Hz	44	46	54	63	73	81	84	86
0.1 Hz	42	46	53	60	71	79	83	86
0.15 Hz	41	45	52	59	69	78	82	85
0.2 Hz	41	45	52	58	67	76	81	85
0.5 Hz	38	42	51	56	64	73	77	84
1 Hz	37	41	50	56	62	70	75	83
1.5 Hz	36	40	49	55	60	68	73	82
2 Hz	35	39	48	55	59	67	72	81
5 Hz	33	37	46	54	57	64	70	79
10 Hz	31	35	45	53	55	63	68	77
15 Hz	30	34	44	52	53	62	67	75

Table D4: Complex modulus and phase angle data of PAV aged 5% EVA with 95% Middle East 80/100 penetration grade bitumen [Airey, 1997]

Freq\Temp	10°C	15°C	25°C	35°C	45°C	55°C	65°C	75°C	85°C
0.01 Hz	5095000	2540000	498000	89000	13600	1590	327	85	21
0.015 Hz	6310000	3160000	610500	111000	18600	2340	480	124	37
0.02 Hz	7165000	3570000	707000	135500	22800	3060	629	162	50
0.05 Hz	9970000	5450000	1165000	235000	44800	6615	1470	387	121
0.1 Hz	13650000	7545000	1655000	355000	72500	11900	2760	749	242
0.15 Hz	16250000	8775000	2110000	453500	94500	16350	3875	1080	361
0.2 Hz	18050000	9840000	2445000	537500	114000	20600	4935	1405	478
0.5 Hz	24900000	14150000	3830000	906500	205000	41450	10500	3220	1150
1 Hz	31100000	18250000	5295000	1325000	313000	68100	18100	5925	2190
1.5 Hz	35350000	21100000	6395000	1655000	394000	89850	24500	8395	3170
2 Hz	38650000	23450000	7250000	1930000	467000	109000	30300	10700	4110
5 Hz	50650000	31900000	10700000	3085000	792000	195500	57650	22550	9130
10 Hz	60750000	39550000	14100000	4320000	1160000	295500	91250	38150	16300
15 Hz	66600000	44300000	16250000	5145000	1450000	365500	116500	47350	21300

Freq\Temp	10°C	15°C	25°C	35°C	45°C	55°C	65°C	75°C	85°C
0.01 Hz	44	48	54	61	74	81	84	75	83
0.015 Hz	38	43	52	59	72	80	84	82	83
0.02 Hz	38	42	51	58	71	79	84	83	84
0.05 Hz	36	40	48	55	67	76	81	83	86
0.1 Hz	34	38	47	54	64	73	79	82	86
0.15 Hz	33	37	46	53	63	72	77	82	86
0.2 Hz	33	37	45	52	61	71	76	81	86
0.5 Hz	31	35	43	50	57	67	72	79	84
1 Hz	30	34	42	49	55	64	70	78	83
1.5 Hz	29	32	41	48	54	62	68	76	82
2 Hz	28	32	40	48	54	61	67	76	81
5 Hz	26	30	38	46	53	57	64	73	78
10 Hz	25	29	37	45	52	55	62	71	76
15 Hz	25	28	36	45	52	54	61	69	75

Table D5: Complex modulus and phase angle data of RTFOT aged 7% EVA with 93% Middle East 80/100 penetration grade bitumen [Airey, 1997]

Freq\Temp	10°C	15°C	25°C	35°C	45°C	55°C	65°C	75°C	85°C
0.01 Hz	2025000	895000	182000	31000	5920	842	167	28	9
0.015 Hz	2295000	1140000	216000	38700	7880	1170	252	45	14
0.02 Hz	2720000	1320000	248000	46400	9560	1390	329	62	19
0.05 Hz	4025000	1990000	396000	81900	17600	3030	745	154	48
0.1 Hz	5360000	2770000	599000	122000	28500	5340	1350	301	97
0.15 Hz	6485000	3330000	773000	157000	36700	7400	1890	441	145
0.2 Hz	7340000	3760000	892000	184000	43900	9220	2400	578	193
0.5 Hz	10600000	5590000	1420000	313000	76900	18400	5050	1370	472
1 Hz	13750000	7420000	1990000	460000	116000	30100	8610	2600	920
1.5 Hz	16000000	8790000	2420000	577000	148000	39800	11600	3730	1350
2 Hz	17750000	9880000	2770000	675000	177000	48400	14400	4830	1760
5 Hz	24400000	14000000	4240000	1110000	303000	87700	27100	10500	4060
10 Hz	30450000	17900000	5730000	1590000	452000	133000	43300	18200	7320
15 Hz	34150000	20300000	6690000	1950000	564000	166000	54800	22200	9420

Freq\Temp	10°C	15°C	25°C	35°C	45°C	55°C	65°C	75°C	85°C
0.01 Hz	49	45	53	64	70	75	81	75	85
0.015 Hz	41	45	52	61	71	76	80	85	86
0.02 Hz	41	43	51	60	70	75	80	85	86
0.05 Hz	39	40	51	57	66	74	78	86	87
0.1 Hz	37	41	48	54	63	72	76	85	88
0.15 Hz	37	40	47	53	61	70	75	85	87
0.2 Hz	36	40	47	52	60	69	73	84	87
0.5 Hz	34	38	45	51	57	66	70	83	86
1 Hz	34	37	44	50	55	63	68	81	85
1.5 Hz	33	36	43	50	54	61	66	80	84
2 Hz	32	36	43	49	54	60	65	79	83
5 Hz	31	35	41	48	53	57	63	76	80
10 Hz	30	33	40	47	53	56	61	73	78
15 Hz	29	33	40	46	52	55	61	71	75

Table D6: Complex modulus and phase angle data of PAV aged 7% EVA with 93% Middle East 80/100 penetration grade bitumen [Airey, 1997]

Freq\Temp	10°C	15°C	25°C	35°C	45°C	55°C	65°C	75°C	85°C
0.01 Hz	6040000	3010000	605000	125000	25100	5110	692	163	43
0.015 Hz	6660000	3320000	781000	162000	32200	7050	1040	247	75
0.02 Hz	7430000	3860000	922000	189000	39300	8880	1330	337	99
0.05 Hz	10500000	5680000	1410000	316000	71400	15800	2870	763	257
0.1 Hz	13100000	7250000	2030000	476000	107000	26500	5100	1420	495
0.15 Hz	15300000	8520000	2440000	600000	141000	34900	7150	2090	726
0.2 Hz	16500000	9500000	2780000	705000	166000	42800	8910	2710	972
0.5 Hz	22100000	13300000	4160000	1130000	286000	75300	17600	5970	2340
1 Hz	27600000	16900000	5550000	1590000	422000	115000	28700	10600	4280
1.5 Hz	31600000	19500000	6550000	1940000	523000	148000	38200	14400	6020
2 Hz	34400000	21400000	7390000	2230000	605000	174000	45800	18100	7800
5 Hz	44800000	28700000	10500000	3400000	954000	294000	81800	36000	16400
10 Hz	53700000	35200000	13500000	4600000	1350000	438000	124000	57200	27100
15 Hz	58000000	39200000	15400000	5360000	1620000	557000	155000	60300	29400

Freq\Temp	10°C	15°C	25°C	35°C	45°C	55°C	65°C	75°C	85°C
0.01 Hz	37	43	49	54	67	74	78	81	77
0.015 Hz	36	40	47	54	65	72	77	81	83
0.02 Hz	35	39	46	53	64	72	77	81	85
0.05 Hz	31	36	43	49	61	68	74	80	85
0.1 Hz	31	35	43	50	58	66	72	79	85
0.15 Hz	31	34	41	48	56	65	71	79	84
0.2 Hz	31	34	41	48	55	64	69	78	83
0.5 Hz	29	32	39	46	51	60	65	75	81
1 Hz	28	31	38	44	50	57	62	73	79
1.5 Hz	27	30	37	43	49	56	61	72	78
2 Hz	27	29	36	43	49	55	60	71	77
5 Hz	25	28	35	41	48	52	57	68	73
10 Hz	24	28	34	41	47	51	55	66	71
15 Hz	24	27	33	40	47	49	54	64	70

Table D7: Complex modulus and phase angle data of RTFOT aged 3% EVA with 97% Russian 80 penetration grade bitumen [Airey, 1997]

Freq\Temp	10°C	15°C	25°C	35°C	45°C	55°C	65°C	75°C
0.01 Hz	1100000	408500	45150	5830	870	161	26	5
0.015 Hz	1500000	529000	61050	8090	1220	222	41	8
0.02 Hz	1890000	655000	74350	10200	1610	288	55	10
0.05 Hz	3195000	1190000	140000	21300	3470	662	128	25
0.1 Hz	4920000	1855000	231500	35800	6120	1220	245	51
0.15 Hz	6255000	2430000	324500	48800	8555	1740	358	76
0.2 Hz	7345000	2870000	400000	61400	10900	2235	465	101
0.5 Hz	11900000	4950000	767500	124000	22750	4925	1055	251
1 Hz	16700000	7325000	1235000	206000	39450	8870	1950	496
1.5 Hz	20200000	9190000	1620000	274000	54300	12450	2780	737
2 Hz	23150000	10700000	1950000	339000	68000	15800	3565	975
5 Hz	34050000	17000000	3500000	638000	139000	33700	7925	2350
10 Hz	44250000	23300000	5305000	984000	233000	58700	14250	4455
15 Hz	50600000	27750000	6750000	1220000	309000	79900	19450	6445

Freq\Temp	10°C	15°C	25°C	35°C	45°C	55°C	65°C	75°C
0.01 Hz	63	62	68	71	74	72	81	88
0.015 Hz	57	61	67	72	77	81	83	88
0.02 Hz	56	61	66	71	77	81	83	88
0.05 Hz	54	58	66	71	75	80	82	89
0.1 Hz	51	57	65	69	74	79	82	89
0.15 Hz	50	56	64	69	74	78	82	89
0.2 Hz	49	55	64	69	73	78	81	88
0.5 Hz	46	52	62	68	72	76	80	88
1 Hz	43	50	61	67	71	76	80	87
1.5 Hz	42	48	60	67	71	75	79	87
2 Hz	41	47	59	66	70	75	79	86
5 Hz	37	44	56	65	69	74	79	84
10 Hz	34	41	54	63	67	73	78	83
15 Hz	33	39	53	61	65	73	77	83

Table D8: Complex modulus and phase angle data of RTFOT aged 5% EVA with 95% Russian 80 penetration grade bitumen [Airey, 1997]

Freq\Temp	10°C	15°C	25°C	35°C	45°C	55°C	65°C	75°C
0.01 Hz	1180000	510500	82850	13850	2295	422	77	10
0.015 Hz	1435000	650000	102500	17650	3050	576	102	15
0.02 Hz	1725000	762500	124500	21300	3690	686	129	19
0.05 Hz	2825000	1295000	222000	39250	7125	1385	274	48
0.1 Hz	4065000	1930000	333000	61400	11700	2410	494	98
0.15 Hz	5050000	2425000	433000	79100	16000	3310	693	144
0.2 Hz	5855000	2850000	513000	94750	19600	4105	884	190
0.5 Hz	9235000	4700000	888500	172000	37150	8315	1880	463
1 Hz	12850000	6725000	1340000	271000	59650	14050	3335	897
1.5 Hz	15450000	8280000	1705000	353500	78750	19050	4660	1315
2 Hz	17600000	9565000	2005000	422500	95750	23600	5870	1710
5 Hz	25900000	14700000	3380000	758500	177000	46100	12300	3930
10 Hz	33750000	19850000	4910000	1170000	278000	75450	21050	7055
15 Hz	38800000	23000000	5980000	1480000	354500	98600	28550	9310

Freq\Temp	10°C	15°C	25°C	35°C	45°C	55°C	65°C	75°C
0.01 Hz	54	54	57	57	65	56	51	87
0.015 Hz	50	52	55	57	65	64	70	87
0.02 Hz	50	51	55	58	65	65	71	87
0.05 Hz	48	50	55	57	65	68	73	87
0.1 Hz	47	50	54	58	64	68	74	87
0.15 Hz	46	49	55	58	64	69	74	87
0.2 Hz	45	49	55	58	63	69	74	87
0.5 Hz	43	47	54	58	62	68	74	86
1 Hz	42	46	53	59	62	68	73	84
1.5 Hz	40	44	53	58	61	67	73	83
2 Hz	40	44	52	58	61	67	73	82
5 Hz	37	41	51	58	60	66	71	80
10 Hz	35	40	50	58	59	66	71	78
15 Hz	33	39	49	57	58	66	71	75

Table D9: Complex modulus and phase angle data of PAV aged 5% EVA with 95% Russian 80 penetration grade bitumen [Airey, 1997]

Freq\Temp	10°C	15°C	25°C	35°C	45°C	55°C	65°C	75°C	85°C
0.01 Hz	3650000	1670000	323000	44900	6200	990	202	50	14
0.015 Hz	4215000	2090000	376000	57200	8530	1410	279	68	21
0.02 Hz	4960000	2470000	445000	70700	11000	1810	367	89	27
0.05 Hz	7495000	3810000	758000	128000	22400	3840	858	213	68
0.1 Hz	9935000	5440000	1090000	198000	37200	7020	1580	418	133
0.15 Hz	12000000	6630000	1380000	254000	50400	10000	2270	617	198
0.2 Hz	13550000	7500000	1610000	303000	61100	12800	2920	821	261
0.5 Hz	19450000	11100000	2600000	528000	115000	26600	6450	1940	638
1 Hz	25200000	14700000	3700000	793000	182000	44900	11500	3670	1250
1.5 Hz	29150000	17200000	4520000	1010000	235000	60100	15900	5320	1840
2 Hz	32200000	19200000	5220000	1190000	281000	73900	20000	6880	2430
5 Hz	43400000	27100000	8010000	2000000	485000	139000	40000	15100	5570
10 Hz	53150000	34100000	10800000	2880000	709000	218000	65900	26400	10200
15 Hz	58800000	38100000	12700000	3540000	863000	277000	87600	32900	13400

Freq\Temp	10°C	15°C	25°C	35°C	45°C	55°C	65°C	75°C	85°C
0.01 Hz	49	52	59	65	74	77	82	80	84
0.015 Hz	42	45	54	61	73	78	81	84	84
0.02 Hz	42	44	53	60	72	78	81	84	84
0.05 Hz	40	43	51	58	69	76	80	85	87
0.1 Hz	37	41	49	56	66	74	79	85	88
0.15 Hz	37	40	49	55	65	73	78	85	88
0.2 Hz	36	40	48	55	64	72	77	84	87
0.5 Hz	34	38	46	53	60	69	75	83	86
1 Hz	33	36	45	53	58	67	73	81	85
1.5 Hz	32	36	44	52	58	65	71	80	84
2 Hz	31	35	44	51	58	64	70	79	84
5 Hz	29	33	42	50	57	61	68	76	81
10 Hz	27	31	41	49	57	59	66	74	79
15 Hz	27	31	40	48	56	58	65	73	77

Table D10: Complex modulus and phase angle data of RTFOT aged 7% EVA with 93% Russian 80 penetration grade bitumen [Airey, 1997]

Freq\Temp	10°C	15°C	25°C	35°C	45°C	55°C	65°C	75°C	85°C
0.01 Hz	1495000	707000	138000	30600	7210	1560	266	15	4
0.015 Hz	1830000	850000	176000	39000	9120	1930	335	24	7
0.02 Hz	2045000	986000	202000	44800	10600	2260	402	33	9
0.05 Hz	3285000	1500000	303000	70100	17000	3940	753	78	24
0.1 Hz	4735000	2090000	446000	103000	25300	6030	1230	152	48
0.15 Hz	5705000	2610000	544000	127000	31900	7670	1640	224	69
0.2 Hz	6440000	3010000	635000	146000	37500	9100	2000	298	93
0.5 Hz	9960000	4760000	1020000	234000	61300	16100	3780	715	232
1 Hz	13750000	6670000	1450000	338000	88200	24500	6080	1360	459
1.5 Hz	16550000	8180000	1790000	424000	110000	31300	8040	1960	685
2 Hz	18900000	9400000	2070000	500000	129000	37600	9760	2530	905
5 Hz	28100000	14400000	3360000	841000	216000	66000	18300	5410	2110
10 Hz	36750000	19500000	4790000	1240000	318000	101000	28900	9230	3860
15 Hz	42100000	23000000	5860000	1540000	394000	127000	36900	11500	5160

Freq\Temp	10°C	15°C	25°C	35°C	45°C	55°C	65°C	75°C	85°C
0.01 Hz	50	41	45	48	52	52	61	88	87
0.015 Hz	42	43	42	45	51	53	60	87	88
0.02 Hz	43	43	42	45	50	53	61	87	88
0.05 Hz	44	41	43	46	48	55	61	87	89
0.1 Hz	43	45	45	47	50	55	63	86	89
0.15 Hz	43	44	45	47	50	55	62	86	88
0.2 Hz	43	44	45	47	50	55	62	85	88
0.5 Hz	42	44	46	48	51	55	62	83	87
1 Hz	41	44	47	49	51	55	62	81	86
1.5 Hz	40	43	47	49	52	55	62	80	85
2 Hz	39	43	48	50	52	55	62	79	84
5 Hz	37	42	48	51	54	55	62	75	81
10 Hz	35	40	48	52	54	56	62	72	78
15 Hz	33	39	47	52	53	56	62	70	75

Table D11: Complex modulus and phase angle data of PAV aged 7% EVA with 93% Russian 80 penetration grade bitumen [Airey, 1997]

Freq\Temp	10°C	15°C	25°C	35°C	45°C	55°C	65°C	75°C	85°C
0.01 Hz	5120000	2460000	474000	89500	16000	3270	443	74	16
0.015 Hz	5426667	3010000	613000	118000	21100	4290	634	115	25
0.02 Hz	6096667	3350000	712000	137000	25400	5170	822	146	37
0.05 Hz	8740000	4670000	1090000	229000	45700	10000	1790	345	94
0.1 Hz	11200000	6280000	1560000	336000	68000	16100	3150	671	187
0.15 Hz	13533333	7380000	1900000	429000	86400	21400	4250	923	279
0.2 Hz	14933333	8250000	2180000	504000	103000	25700	5280	1200	371
0.5 Hz	20733333	11800000	3330000	820000	178000	45600	10400	2760	914
1 Hz	26233333	15100000	4490000	1170000	266000	70300	17200	4960	1755
1.5 Hz	30000000	17600000	5350000	1430000	339000	90200	22800	6880	2540
2 Hz	33000000	19500000	6070000	1650000	400000	107000	27700	8750	3290
5 Hz	43866667	26800000	8900000	2580000	674000	188000	51500	18100	7400
10 Hz	53333333	33500000	11700000	3560000	992000	286000	80400	29900	13000
15 Hz	58833333	37600000	13400000	4220000	1230000	361000	100000	33500	15950

Freq\Temp	10°C	15°C	25°C	35°C	45°C	55°C	65°C	75°C	85°C
0.01 Hz	39	40	48	54	65	70	74	85	88
0.015 Hz	37	39	47	53	64	69	73	81	88
0.02 Hz	36	38	46	52	63	69	73	81	88
0.05 Hz	34	35	43	50	60	67	72	82	87
0.1 Hz	34	37	44	50	57	66	71	81	87
0.15 Hz	33	36	42	49	56	64	70	81	87
0.2 Hz	33	35	42	48	55	63	69	80	87
0.5 Hz	31	34	41	47	52	60	66	79	85
1 Hz	30	33	40	46	52	58	64	77	83
1.5 Hz	29	32	39	46	51	57	63	76	82
2 Hz	29	32	39	46	51	56	62	75	81
5 Hz	27	31	38	44	51	54	60	72	78
10 Hz	26	30	36	44	50	52	59	70	75
15 Hz	25	29	36	43	49	51	58	67	73

Table D12: Complex modulus and phase angle data of RTFOT aged 3% EVA with 97% Venezuelan 70/100 penetration grade bitumen [Airey, 1997]

Freq\Temp	10°C	15°C	25°C	35°C	45°C	55°C	65°C	75°C
0.01 Hz	624000	277000	45450	7270	1115	213	57	13
0.015 Hz	776000	368000	58200	9770	1590	299	78	19
0.02 Hz	952500	429000	70250	12100	2025	389	102	25
0.05 Hz	1610000	750500	130500	23500	4335	905	230	64
0.1 Hz	2420000	1155000	206500	39000	7600	1690	425	125
0.15 Hz	3110000	1475000	268000	51000	10500	2390	610	187
0.2 Hz	3640000	1745000	323500	62300	13100	3030	783	247
0.5 Hz	5885000	2930000	587500	117000	26050	6435	1755	596
1 Hz	8310000	4265000	910500	187000	43350	11150	3205	1145
1.5 Hz	10150000	5265000	1170000	245000	58250	15300	4515	1660
2 Hz	11600000	6135000	1400000	297000	71550	19050	5775	2150
5 Hz	17600000	9670000	2410000	532000	136500	38250	12350	4860
10 Hz	23500000	13350000	3560000	800000	218500	63350	21400	8780
15 Hz	27400000	15750000	4360000	998000	282000	84300	28400	11750

Freq\Temp	10°C	15°C	25°C	35°C	45°C	55°C	65°C	75°C
0.01 Hz	56	61	63	69	79	84	79	86
0.015 Hz	54	55	61	68	78	84	82	87
0.02 Hz	53	55	60	67	77	83	81	87
0.05 Hz	51	54	59	65	74	81	79	87
0.1 Hz	50	52	59	64	71	79	79	87
0.15 Hz	49	52	58	63	70	77	79	87
0.2 Hz	48	51	58	63	69	76	78	86
0.5 Hz	46	49	57	62	67	73	78	85
1 Hz	44	48	56	61	66	71	77	83
1.5 Hz	43	47	55	61	65	70	76	82
2 Hz	42	46	55	61	65	70	76	82
5 Hz	40	44	53	60	63	68	74	79
10 Hz	38	42	51	59	62	67	72	77
15 Hz	37	41	51	59	61	67	72	76

Table D13: Complex modulus and phase angle data of RTFOT aged 5% EVA with 95% Venezuelan 70/100 penetration grade bitumen [Airey, 1997]

Freq\Temp	10°C	15°C	25°C	35°C	45°C	55°C	65°C	75°C
0.01 Hz	1015000	451000	91500	17600	3210	479	106	17
0.015 Hz	1225000	547000	116000	22400	4070	698	173	28
0.02 Hz	1385000	663000	140000	27600	5210	891	217	40
0.05 Hz	2220000	1030000	222000	46900	9770	1850	451	99
0.1 Hz	3140000	1540000	333000	72900	15100	3140	769	198
0.15 Hz	3900000	1930000	417000	97600	19800	4260	1040	299
0.2 Hz	4485000	2190000	494000	116000	23800	5280	1300	397
0.5 Hz	6945000	3480000	828000	198000	43100	10200	2660	934
1 Hz	9570000	4880000	1200000	297000	67000	16500	4520	1750
1.5 Hz	11550000	5900000	1490000	377000	87100	21700	6160	2500
2 Hz	13100000	6790000	1740000	445000	105000	26200	7620	3200
5 Hz	19600000	10400000	2810000	755000	187000	47600	14900	6790
10 Hz	26050000	14200000	4010000	1120000	287000	73300	23900	11300
15 Hz	30200000	16700000	4890000	1330000	369000	93100	30300	12400

Freq\Temp	10°C	15°C	25°C	35°C	45°C	55°C	65°C	75°C
0.01 Hz	50	54	56	60	68	73	61	88
0.015 Hz	45	47	51	57	66	74	72	87
0.02 Hz	46	48	51	56	65	73	72	87
0.05 Hz	45	47	51	55	61	71	70	86
0.1 Hz	44	46	50	54	60	68	70	85
0.15 Hz	44	46	50	54	59	67	70	84
0.2 Hz	43	45	49	54	59	66	69	84
0.5 Hz	42	45	49	53	58	64	69	82
1 Hz	42	44	49	53	57	62	68	80
1.5 Hz	41	44	49	53	57	61	68	78
2 Hz	40	43	48	53	57	61	67	77
5 Hz	39	42	48	53	57	59	66	74
10 Hz	38	41	47	53	57	59	65	72
15 Hz	37	41	47	53	56	59	64	70

Table D14: Complex modulus and phase angle data of PAV aged 5% EVA with 95% Venezuelan 70/100 penetration grade bitumen [Airey, 1997]

Freq\Temp	10°C	15°C	25°C	35°C	45°C	55°C	65°C	75°C	85°C
0.01 Hz	3170000	1480000	351500	74100	13500	2535	603	166	48
0.015 Hz	3385000	1730000	405000	86600	18200	3450	836	249	66
0.02 Hz	3950000	2010000	474000	103000	21800	4380	1055	330	88
0.05 Hz	5780000	2970000	764000	175000	37100	8120	2070	772	201
0.1 Hz	7380000	3990000	1050000	255000	57400	13350	3395	1420	396
0.15 Hz	8875000	4750000	1325000	309000	77100	18100	4555	2035	580
0.2 Hz	9890000	5310000	1530000	352000	92300	22300	5625	2595	755
0.5 Hz	13900000	7720000	2355000	571000	158000	40450	10800	5520	1710
1 Hz	17900000	10200000	3210000	816000	233000	62000	17450	9475	3090
1.5 Hz	20800000	11900000	3860000	1010000	292000	79550	22800	12750	4290
2 Hz	22900000	13300000	4370000	1180000	343000	94450	27650	15700	5450
5 Hz	31300000	18700000	6445000	1870000	566000	160000	49850	29300	11100
10 Hz	39000000	23800000	8545000	2630000	825000	234000	76150	45150	18200
15 Hz	43600000	27100000	9880000	3290000	1010000	280000	93900	44650	20700

Freq\Temp	10°C	15°C	25°C	35°C	45°C	55°C	65°C	75°C	85°C
0.01 Hz	41	49	50	56	63	70	70	80	84
0.015 Hz	39	41	48	53	60	68	71	82	85
0.02 Hz	38	41	47	53	59	67	70	82	84
0.05 Hz	35	40	45	50	57	64	68	80	84
0.1 Hz	35	38	44	49	56	62	67	78	83
0.15 Hz	35	38	44	49	54	61	66	76	82
0.2 Hz	35	37	43	49	54	60	65	76	81
0.5 Hz	33	36	42	47	52	57	63	73	78
1 Hz	32	35	41	46	52	56	62	70	76
1.5 Hz	32	35	40	46	51	54	61	69	75
2 Hz	32	34	40	46	51	54	61	68	74
5 Hz	31	34	39	45	50	52	59	66	71
10 Hz	30	33	39	44	50	51	58	64	69
15 Hz	29	32	39	44	50	51	58	64	68

Table D15: Complex modulus and phase angle data of RTFOT aged 7% EVA with 93% Venezuelan 70/100 penetration grade bitumen [Airey, 1997]

Freq\Temp	10°C	15°C	25°C	35°C	45°C	55°C	65°C	75°C	85°C
0.01 Hz	789500	425000	114000	31100	8120	2100	267	24	7
0.015 Hz	910000	470000	125000	36000	9670	2430	376	39	10
0.02 Hz	1030000	548000	148000	42300	11300	2890	454	52	13
0.05 Hz	1600000	848000	231000	68000	18900	4970	811	126	32
0.1 Hz	2220000	1130000	317000	94600	26600	7510	1240	241	64
0.15 Hz	2705000	1410000	392000	119000	33200	9340	1650	345	97
0.2 Hz	3065000	1600000	448000	136000	38600	10800	1990	447	129
0.5 Hz	4740000	2470000	697000	217000	63700	18300	3660	1030	314
1 Hz	6610000	3440000	975000	309000	92800	27200	5790	1890	609
1.5 Hz	8025000	4200000	1180000	381000	116000	34200	7590	2650	895
2 Hz	9235000	4810000	1360000	441000	136000	40400	9120	3370	1170
5 Hz	14250000	7520000	2140000	703000	222000	68500	16500	6840	2610
10 Hz	19550000	10400000	3010000	993000	322000	101000	25200	11300	4620
15 Hz	23150000	12500000	3650000	1200000	392000	450000	30300	12900	5830

Freq\Temp	10°C	15°C	25°C	35°C	45°C	55°C	65°C	75°C	85°C
0.01 Hz	47	44	49	49	51	57	61	79	86
0.015 Hz	40	43	44	46	49	53	59	86	88
0.02 Hz	41	42	44	46	49	53	59	86	88
0.05 Hz	42	41	44	46	48	53	58	85	88
0.1 Hz	42	42	43	45	48	52	59	83	87
0.15 Hz	42	42	44	45	48	53	59	83	87
0.2 Hz	42	43	44	45	48	53	60	82	87
0.5 Hz	43	43	44	45	48	53	60	80	86
1 Hz	43	44	44	46	49	52	61	78	84
1.5 Hz	43	44	44	46	49	53	61	77	83
2 Hz	43	44	45	46	49	52	61	76	82
5 Hz	42	44	45	47	49	53	60	72	78
10 Hz	41	44	46	48	50	53	60	69	75
15 Hz	41	43	47	48	48		59	68	73

Table D16: Complex modulus and phase angle data of PAV aged 7% EVA with 93% Venezuelan 70/100 penetration grade bitumen [Airey, 1997]

Freq\Temp	10°C	15°C	25°C	35°C	45°C	55°C	65°C	75°C	85°C
0.01 Hz	3285000	1825000	521000	115000	28400	6360	1210	343	89
0.015 Hz	3955000	2115000	569000	145000	34300	8330	1630	510	130
0.02 Hz	4310000	2435000	663000	168000	41300	10000	1960	683	173
0.05 Hz	5795000	3450000	1020000	264000	66700	18100	3640	1530	404
0.1 Hz	7770000	4560000	1370000	384000	98800	27900	5790	2730	731
0.15 Hz	8945000	5370000	1660000	461000	124000	35800	7600	3690	1050
0.2 Hz	9910000	5945000	1870000	526000	144000	41200	9150	4620	1320
0.5 Hz	13650000	8320000	2730000	808000	227000	70400	16500	9210	2840
1 Hz	17200000	10650000	3610000	1100000	322000	103000	25500	15100	4880
1.5 Hz	19750000	12350000	4240000	1330000	399000	127000	33000	19800	6690
2 Hz	21800000	13650000	4740000	1510000	457000	148000	39100	23500	8260
5 Hz	29550000	18850000	6770000	2260000	717000	242000	67000	40100	15500
10 Hz	36650000	23750000	8800000	3040000	1010000	345000	99100	57900	24200
15 Hz	41050000	26800000	10200000	3580000	1240000	413000	117000	48900	25400

Freq\Temp	10°C	15°C	25°C	35°C	45°C	55°C	65°C	75°C	85°C
0.01 Hz	38	41	49	53	53	62	63	80	84
0.015 Hz	33	37	43	47	53	59	63	79	84
0.02 Hz	33	36	43	47	52	59	63	78	83
0.05 Hz	32	35	41	46	49	57	61	75	80
0.1 Hz	32	34	39	44	49	54	61	73	79
0.15 Hz	32	34	39	43	48	53	60	72	78
0.2 Hz	32	34	39	43	48	53	60	71	77
0.5 Hz	31	33	37	42	46	51	59	67	74
1 Hz	31	33	37	41	46	50	58	65	72
1.5 Hz	30	32	36	41	45	50	58	64	70
2 Hz	30	32	36	41	45	49	57	64	69
5 Hz	30	32	36	40	45	49	56	62	67
10 Hz	29	31	35	40	45	49	55	60	65
15 Hz	29	31	35	40	44	48	55	61	65

Table D17: Complex modulus and phase angle data of RTFOT aged 3% SBS with 97% Russian 80 penetration grade bitumen [Airey, 1997]

Freq\Temp	10°C	15°C	25°C	35°C	45°C	55°C	65°C	75°C
0.01 Hz	848000	329000	37450	4890	703	136	31	10
0.015 Hz	1150000	451000	50950	7090	1050	183	45	15
0.02 Hz	1450000	546500	62500	9170	1345	242	59	19
0.05 Hz	2640000	1040000	130500	18800	3045	570	139	45
0.1 Hz	4010000	1685000	219000	31000	5595	1085	268	84
0.15 Hz	5165000	2225000	293500	44600	8090	1565	391	123
0.2 Hz	6065000	2650000	363000	56500	10400	2030	510	159
0.5 Hz	9930000	4625000	714000	117000	22150	4610	1185	370
1 Hz	14050000	6850000	1165000	198000	38750	8445	2220	700
1.5 Hz	17000000	8545000	1540000	269000	53650	11950	3190	1015
2 Hz	19450000	9960000	1870000	334000	67250	15250	4125	1320
5 Hz	28800000	15700000	3355000	644000	138000	32700	9080	3010
10 Hz	37300000	21350000	5065000	1010000	234000	56600	16150	5515
15 Hz	42400000	25100000	6265000	1280000	306000	77900	22100	7730

Freq\Temp	10°C	15°C	25°C	35°C	45°C	55°C	65°C	75°C
0.01 Hz	66	69	72	77	78	83	76	74
0.015 Hz	61	65	70	76	81	84	85	82
0.02 Hz	60	64	69	75	80	84	84	81
0.05 Hz	56	62	68	73	79	82	84	82
0.1 Hz	53	59	67	72	77	82	83	82
0.15 Hz	52	58	67	71	76	81	83	82
0.2 Hz	51	57	66	71	75	80	83	82
0.5 Hz	47	53	64	70	73	78	82	82
1 Hz	44	50	62	69	72	77	80	82
1.5 Hz	42	48	61	69	71	76	80	81
2 Hz	41	47	60	69	71	75	79	81
5 Hz	37	43	57	67	70	73	77	79
10 Hz	34	41	54	64	68	73	76	78
15 Hz	33	39	53	62	67	72	75	77

Table D18: Complex modulus and phase angle data of PAV aged 3% SBS with 97% Russian 80 penetration grade bitumen [Airey, 1997]

Freq\Temp	10°C	15°C	25°C	35°C	45°C	55°C	65°C	75°C	85°C
0.01 Hz	2405000	930000	136000	18800	2860	444	91	20	6
0.015 Hz	3035000	1250000	188000	25800	3980	689	127	30	9
0.02 Hz	3525000	1490000	227000	33100	5000	876	167	39	11
0.05 Hz	5570000	2510000	410000	61100	10300	1920	406	97	29
0.1 Hz	7900000	3720000	659000	104000	18100	3510	777	193	59
0.15 Hz	9525000	4520000	842000	141000	24700	5060	1140	287	85
0.2 Hz	10800000	5240000	1010000	171000	30900	6440	1470	376	113
0.5 Hz	15750000	8200000	1780000	326000	60800	13400	3300	891	273
1 Hz	20600000	11100000	2640000	523000	103000	23000	5920	1680	531
1.5 Hz	24000000	13200000	3310000	683000	139000	31400	8310	2380	777
2 Hz	26600000	14900000	3880000	824000	169000	39100	10500	3070	1020
5 Hz	36000000	21300000	6220000	1460000	328000	78300	22000	6720	2340
10 Hz	44300000	27200000	8600000	2200000	529000	130000	37300	11600	4230
15 Hz	48950000	30900000	10200000	2750000	681000	170000	49300	15300	5690

Freq\Temp	10°C	15°C	25°C	35°C	45°C	55°C	65°C	75°C	85°C
0.01 Hz	52	57	64	70	75	83	85	87	89
0.015 Hz	48	53	62	67	74	82	86	88	89
0.02 Hz	47	52	61	68	73	81	86	88	89
0.05 Hz	43	49	59	66	71	78	84	87	88
0.1 Hz	42	47	58	65	70	76	82	86	88
0.15 Hz	40	46	56	64	69	75	81	86	88
0.2 Hz	39	45	56	63	69	73	80	85	87
0.5 Hz	36	42	53	62	67	71	77	83	86
1 Hz	34	40	51	60	66	70	75	81	85
1.5 Hz	33	38	49	59	66	69	74	79	84
2 Hz	32	38	49	58	65	69	73	78	83
5 Hz	30	35	46	56	64	68	71	76	81
10 Hz	28	33	43	54	62	66	70	74	79
15 Hz	27	32	42	52	60	65	70	72	76

Table D19: Complex modulus and phase angle data of RTFOT aged 5% SBS with 95% Russian 80 penetration grade bitumen [Airey, 1997]

Freq\Temp	10°C	15°C	25°C	35°C	45°C	55°C	65°C	75°C
0.01 Hz	906500	353000	43750	7170	1195	217	46	14
0.015 Hz	1155000	447000	56350	9420	1720	314	71	22
0.02 Hz	1440000	552000	72750	11900	2210	409	94	29
0.05 Hz	2500000	1050000	139500	23400	4700	936	222	69
0.1 Hz	3665000	1610000	229500	39200	8070	1735	425	133
0.15 Hz	4780000	2095000	309000	53000	11000	2485	619	192
0.2 Hz	5630000	2500000	378000	65200	13800	3175	807	253
0.5 Hz	9125000	4290000	720500	129000	27550	6720	1830	587
1 Hz	12750000	6290000	1155000	214000	46250	11550	3325	1100
1.5 Hz	15450000	7810000	1505000	288000	62350	15650	4660	1580
2 Hz	17450000	9020000	1815000	354000	77250	19450	5910	2030
5 Hz	25550000	14050000	3205000	657000	152500	38550	12200	4450
10 Hz	32950000	19000000	4755000	999000	250500	64250	20600	7745
15 Hz	37200000	22200000	5875000	1240000	326500	86500	27450	10350

Freq\Temp	10°C	15°C	25°C	35°C	45°C	55°C	65°C	75°C
0.01 Hz	60	65	68	71	75	80	85	81
0.015 Hz	59	62	66	69	77	82	85	84
0.02 Hz	58	62	66	69	76	82	84	84
0.05 Hz	53	59	65	68	73	79	83	84
0.1 Hz	52	57	64	67	70	78	82	83
0.15 Hz	50	56	64	67	69	76	82	83
0.2 Hz	49	55	63	67	69	75	81	83
0.5 Hz	45	51	61	66	67	72	78	81
1 Hz	42	48	60	66	67	70	76	80
1.5 Hz	41	47	59	65	67	69	75	79
2 Hz	40	46	58	65	67	69	74	78
5 Hz	36	42	55	64	66	68	71	75
10 Hz	34	40	52	63	65	68	70	73
15 Hz	33	38	51	62	64	68	70	72

Table D20: Complex modulus and phase angle data of PAV aged 5% SBS with 95% Russian 80 penetration grade bitumen [Airey, 1997]

Freq\Temp	10°C	15°C	25°C	35°C	45°C	55°C	65°C	75°C	85°C
0.01 Hz	2075000	911000	137000	25000	4360	703	145	38	10
0.015 Hz	2760000	1230000	170000	33600	5890	1050	215	52	15
0.02 Hz	3205000	1440000	208000	41300	7370	1400	284	69	20
0.05 Hz	5015000	2390000	388000	78900	14900	3080	672	169	51
0.1 Hz	7235000	3510000	595000	129000	24700	5400	1260	329	99
0.15 Hz	8655000	4320000	774000	172000	33300	7430	1800	484	142
0.2 Hz	9730000	4970000	917000	206000	40400	9230	2310	637	187
0.5 Hz	14350000	7760000	1600000	377000	78400	18500	4980	1460	451
1 Hz	18800000	10600000	2380000	581000	129000	30800	8670	2700	864
1.5 Hz	21850000	12600000	2960000	745000	172000	41500	11900	3830	1260
2 Hz	24350000	14100000	3460000	876000	211000	51300	14900	4860	1620
5 Hz	33200000	20200000	5560000	1390000	393000	99300	29600	10200	3620
10 Hz	40950000	25700000	7710000	1840000	607000	161000	48500	17300	6410
15 Hz	45550000	29000000	9280000	2100000	759000	208000	65500	23500	8860

Freq\Temp	10°C	15°C	25°C	35°C	45°C	55°C	65°C	75°C	85°C
0.01 Hz	52	54	66	67	72	78	81	88	88
0.015 Hz	47	53	61	65	70	80	85	88	89
0.02 Hz	47	52	61	65	70	79	84	87	89
0.05 Hz	44	48	59	64	68	75	82	86	88
0.1 Hz	42	47	57	63	66	72	79	85	87
0.15 Hz	40	45	56	63	66	71	78	84	87
0.2 Hz	39	45	55	62	66	70	77	83	87
0.5 Hz	36	42	53	61	65	68	73	80	85
1 Hz	34	40	51	59	64	67	71	77	83
1.5 Hz	33	38	49	59	64	66	70	76	81
2 Hz	32	37	48	58	64	66	69	75	80
5 Hz	29	35	46	56	62	65	68	72	77
10 Hz	28	33	44	54	61	63	67	70	75
15 Hz	26	32	42	52	58	63	67	69	73

Table D21: Complex modulus and phase angle data of RTFOT aged 7% SBS with 93% Russian 80 penetration grade bitumen [Airey, 1997]

Freq\Temp	10°C	15°C	25°C	35°C	45°C	55°C	65°C	75°C	85°C
0.01 Hz	788000	296000	41100	7680	1200	321	48	16	9
0.015 Hz	970000	404000	59000	10500	2000	422	111	37	17
0.02 Hz	1200000	490000	66700	12900	2510	555	149	47	22
0.05 Hz	1985000	864000	133000	25100	5100	1180	333	104	45
0.1 Hz	2870000	1350000	217000	40600	8760	2080	604	192	79
0.15 Hz	3610000	1700000	283000	51600	11900	2930	860	275	110
0.2 Hz	4190000	2000000	339000	63300	14900	3700	1100	355	142
0.5 Hz	6575000	3310000	611000	122000	28700	7600	2400	786	307
1 Hz	9040000	4740000	938000	198000	46900	12800	4260	1440	555
1.5 Hz	10900000	5820000	1200000	263000	62400	17200	5910	2040	791
2 Hz	12400000	6730000	1430000	318000	76200	21000	7420	2610	1010
5 Hz	17850000	10200000	2410000	581000	145000	40100	15000	5540	2200
10 Hz	23050000	13600000	3500000	875000	233000	64900	24600	9470	3930
15 Hz	26300000	15900000	4260000	1060000	300000	85400	32200	12400	5400

Freq\Temp	10°C	15°C	25°C	35°C	45°C	55°C	65°C	75°C	85°C
0.01 Hz	56	61	64	68	69	80	67	56	52
0.015 Hz	55	58	62	66	72	75	75	75	71
0.02 Hz	53	57	61	65	71	74	75	74	71
0.05 Hz	50	55	61	64	69	74	76	76	72
0.1 Hz	49	53	60	63	67	73	77	77	73
0.15 Hz	47	52	59	63	66	72	77	78	74
0.2 Hz	46	51	59	63	65	72	76	78	75
0.5 Hz	43	48	57	62	64	69	75	77	76
1 Hz	41	46	56	62	63	67	73	77	76
1.5 Hz	39	45	55	61	63	66	71	76	76
2 Hz	39	44	54	61	63	65	71	75	76
5 Hz	36	41	52	59	63	64	68	72	75
10 Hz	34	39	50	58	62	64	66	71	74
15 Hz	33	38	49	57	61	64	66	69	73

Table D22: Complex modulus and phase angle data of PAV aged 7% SBS with 93% Russian 80 penetration grade bitumen [Airey, 1997]

Freq\Temp	10°C	15°C	25°C	35°C	45°C	55°C	65°C	75°C	85°C
0.01 Hz	3090000	1470000	213000	34300	6190	1190	236	58	16
0.015 Hz	3800000	1730000	288000	43800	8330	1650	356	81	24
0.02 Hz	4460000	2070000	368000	54000	10300	2110	463	108	33
0.05 Hz	7000000	3560000	664000	102000	19700	4450	1100	262	81
0.1 Hz	9665000	5090000	997000	162000	31500	7630	1990	513	162
0.15 Hz	11700000	6180000	1160000	215000	43100	10200	2810	752	237
0.2 Hz	13200000	6980000	1380000	260000	51800	12600	3550	973	315
0.5 Hz	19150000	10600000	2350000	476000	97500	24200	7330	2190	752
1 Hz	24800000	14400000	3420000	741000	157000	39100	12300	3950	1410
1.5 Hz	28800000	17000000	4260000	959000	204000	51400	16500	5470	2010
2 Hz	31850000	19200000	4960000	1140000	247000	63000	20200	6850	2590
5 Hz	42900000	27200000	7830000	1980000	455000	118000	38300	13600	5510
10 Hz	52400000	34500000	10800000	2910000	709000	188000	60600	22300	9220
15 Hz	58000000	38900000	12900000	3580000	891000	245000	76200	29800	11900

Freq\Temp	10°C	15°C	25°C	35°C	45°C	55°C	65°C	75°C	85°C
0.01 Hz	49	58	61	65	68	77	84	84	87
0.015 Hz	47	51	58	61	66	77	84	87	88
0.02 Hz	45	50	57	61	65	76	83	87	88
0.05 Hz	42	48	56	61	63	71	80	85	88
0.1 Hz	40	44	54	60	62	68	77	83	87
0.15 Hz	39	44	54	60	62	66	75	82	86
0.2 Hz	38	43	53	60	62	65	74	81	85
0.5 Hz	35	40	51	58	62	63	69	77	83
1 Hz	33	38	49	57	62	63	67	74	80
1.5 Hz	32	37	47	56	61	62	66	72	78
2 Hz	31	36	47	55	61	62	65	71	77
5 Hz	29	33	44	53	60	62	64	67	73
10 Hz	27	31	42	52	59	61	63	65	70
15 Hz	26	30	41	51	58	60	63	65	68

Table D23: Complex modulus and phase angle data of RTFOT aged 3% SBS with 97% Venezuelan 70/100 penetration grade bitumen [Airey, 1997]

Freq\Temp	10°C	15°C	25°C	35°C	45°C	55°C	65°C	75°C
0.01 Hz	451000	170500	33800	5480	982	179	40	11
0.015 Hz	618000	234000	42500	7860	1425	271	60	16
0.02 Hz	748500	285500	55300	9830	1825	365	80	22
0.05 Hz	1335000	525500	108000	20200	4010	850	196	53
0.1 Hz	2075000	860500	173000	32200	6990	1535	382	105
0.15 Hz	2645000	1125000	232000	42600	9580	2180	560	158
0.2 Hz	3115000	1355000	283000	52600	11950	2800	732	209
0.5 Hz	5245000	2395000	521000	105000	23950	5955	1670	502
1 Hz	7580000	3605000	802000	174000	40200	10350	3055	959
1.5 Hz	9345000	4530000	1020000	234000	54700	14200	4285	1385
2 Hz	10800000	5310000	1190000	288000	67800	17700	5430	1805
5 Hz	16750000	8610000	1840000	539000	134000	35750	11400	3995
10 Hz	22650000	12050000	2350000	832000	220500	59650	19350	7065
15 Hz	26300000	14200000	2590000	1030000	291000	79700	25900	9620

Freq\Temp	10°C	15°C	25°C	35°C	45°C	55°C	65°C	75°C
0.01 Hz	62	67	69	72	79	84	88	88
0.015 Hz	59	62	66	70	79	85	88	88
0.02 Hz	58	62	66	70	78	84	87	88
0.05 Hz	56	60	65	69	74	81	86	88
0.1 Hz	54	58	64	67	72	79	84	87
0.15 Hz	53	57	64	67	71	78	83	86
0.2 Hz	52	57	63	67	70	76	82	86
0.5 Hz	50	54	62	66	68	73	79	84
1 Hz	47	52	61	66	68	71	77	82
1.5 Hz	46	51	60	65	67	70	76	81
2 Hz	45	50	59	65	67	70	75	80
5 Hz	42	47	57	64	66	69	72	77
10 Hz	39	45	55	63	64	68	71	75
15 Hz	38	44	54	61	63	68	70	73

Table D24: Complex modulus and phase angle data of PAV aged 3% SBS with 97% Venezuelan 70/100 penetration grade bitumen [Airey, 1997]

Freq\Temp	10°C	15°C	25°C	35°C	45°C	55°C	65°C	75°C	85°C
0.01 Hz	1470000	694000	110000	18100	3980	784	187	40	12
0.015 Hz	1970000	831000	137000	25200	5170	1120	259	62	17
0.02 Hz	2305000	983000	173000	30600	6630	1430	338	83	23
0.05 Hz	3545000	1690000	311000	58900	12900	3120	760	195	52
0.1 Hz	5190000	2460000	473000	99000	21800	5390	1350	377	109
0.15 Hz	6435000	3030000	614000	127000	29000	7200	1920	565	166
0.2 Hz	7430000	3510000	734000	157000	35500	8920	2440	736	221
0.5 Hz	11400000	5610000	1280000	286000	68000	17600	5160	1650	533
1 Hz	15300000	7830000	1920000	444000	110000	29200	8890	2960	1010
1.5 Hz	18150000	9470000	2420000	575000	145000	39400	12200	4120	1440
2 Hz	20400000	10700000	2840000	692000	177000	48300	15200	5190	1840
5 Hz	28950000	16000000	4660000	1210000	322000	93600	30500	10800	3950
10 Hz	36750000	21200000	6570000	1820000	492000	151000	50600	18300	6870
15 Hz	41100000	24500000	7880000	2240000	611000	196000	66700	23900	9440

Freq\Temp	10°C	15°C	25°C	35°C	45°C	55°C	65°C	75°C	85°C
0.01 Hz	52	59	63	66	72	78	84	82	89
0.015 Hz	49	53	59	63	69	77	83	87	89
0.02 Hz	48	53	59	63	69	76	82	86	88
0.05 Hz	45	51	57	62	67	72	79	84	87
0.1 Hz	45	48	56	61	65	70	77	82	86
0.15 Hz	43	48	55	60	65	69	75	81	85
0.2 Hz	42	47	55	60	64	69	74	80	85
0.5 Hz	40	45	53	59	63	67	72	77	82
1 Hz	38	43	51	58	62	66	70	75	80
1.5 Hz	37	42	51	57	62	65	69	74	78
2 Hz	36	41	50	57	62	65	69	73	78
5 Hz	34	39	48	55	61	63	67	71	75
10 Hz	32	37	46	53	60	62	67	70	74
15 Hz	31	36	45	52	58	61	66	70	73

Table D25: Complex modulus and phase angle data of RTFOT aged 5% SBS with 95% Venezuelan 70/100 penetration grade bitumen [Airey, 1997]

Freq\Temp	10°C	15°C	25°C	35°C	45°C	55°C	65°C	75°C	85°C
0.01 Hz	459000	201000	43700	8240	1810	393	80	28	9
0.015 Hz	600000	246000	57800	11700	2390	540	128	34	13
0.02 Hz	733000	299000	71500	13600	3020	691	168	46	16
0.05 Hz	1285000	544000	130000	27100	6080	1530	396	109	40
0.1 Hz	1965000	843000	204000	43800	10200	2780	738	211	78
0.15 Hz	2455000	1080000	268000	57600	14000	3870	1040	309	115
0.2 Hz	2870000	1280000	325000	69700	17300	4810	1340	403	150
0.5 Hz	4700000	2220000	576000	131000	33400	9590	2900	924	351
1 Hz	6670000	3280000	859000	210000	54200	15900	5080	1700	660
1.5 Hz	8125000	4080000	1070000	274000	72000	21300	7030	2390	947
2 Hz	9335000	4770000	1230000	332000	87600	26200	8750	3060	1220
5 Hz	14100000	7570000	1820000	593000	165000	50600	17300	6400	2670
10 Hz	18800000	10400000	2250000	884000	262000	81400	28800	10900	4640
15 Hz	21800000	12400000	2450000	1080000	337000	105000	38800	14600	6110

Freq\Temp	10°C	15°C	25°C	35°C	45°C	55°C	65°C	75°C	85°C
0.01 Hz	60	64	66	66	72	78	76	82	85
0.015 Hz	56	58	61	66	73	79	83	85	85
0.02 Hz	55	58	62	65	72	79	83	85	84
0.05 Hz	53	57	61	64	68	76	81	84	84
0.1 Hz	51	55	60	62	66	73	79	83	84
0.15 Hz	50	54	60	63	65	72	78	83	83
0.2 Hz	50	54	60	62	65	71	77	82	83
0.5 Hz	47	51	58	62	64	68	74	79	82
1 Hz	45	50	57	62	64	66	71	77	80
1.5 Hz	44	49	57	61	64	65	70	76	79
2 Hz	43	48	56	61	63	65	69	75	78
5 Hz	40	45	54	60	63	64	67	71	76
10 Hz	38	43	52	59	62	64	66	69	74
15 Hz	37	42	51	58	60	64	66	68	72

Table D26: Complex modulus and phase angle data of PAV aged 5% SBS with 95% Venezuelan 70/100 penetration grade bitumen [Airey, 1997]

Freq\Temp	10°C	15°C	25°C	35°C	45°C	55°C	65°C	75°C	85°C
0.01 Hz	1385000	648000	125000	29200	6540	1470	357	92	29
0.015 Hz	1755000	846000	155000	38700	9040	2100	498	142	33
0.02 Hz	2055000	995000	187000	46500	10500	2690	645	195	44
0.05 Hz	3230000	1630000	329000	81400	20100	5260	1360	448	109
0.1 Hz	4585000	2400000	493000	134000	32600	8580	2410	791	208
0.15 Hz	5620000	2950000	650000	177000	42400	11400	3310	1130	301
0.2 Hz	6465000	3410000	766000	209000	51200	14000	4050	1440	394
0.5 Hz	9770000	5360000	1300000	364000	93700	26400	7980	3050	893
1 Hz	13100000	7380000	1900000	538000	147000	42200	13100	5240	1595
1.5 Hz	15450000	8810000	2380000	666000	191000	55400	17300	7070	2220
2 Hz	17300000	10000000	2750000	773000	228000	67600	21400	9140	2790
5 Hz	24400000	14700000	4410000	1200000	402000	124000	39900	17400	5710
10 Hz	30950000	19200000	6120000	1590000	596000	193000	63500	28000	9580
15 Hz	34800000	21900000	7280000	1790000	734000	243000	83100	34300	12650

Freq\Temp	10°C	15°C	25°C	35°C	45°C	55°C	65°C	75°C	85°C
0.01 Hz	51	57	59	60	65	70	74	84	86
0.015 Hz	47	50	57	60	63	71	78	83	86
0.02 Hz	46	50	56	60	63	69	77	81	86
0.05 Hz	44	48	54	58	61	66	73	79	84
0.1 Hz	43	46	53	58	61	64	70	77	82
0.15 Hz	42	45	53	58	61	63	69	75	81
0.2 Hz	41	45	52	57	61	63	68	74	80
0.5 Hz	39	42	50	56	60	62	66	70	77
1 Hz	37	41	49	55	59	61	65	68	75
1.5 Hz	36	40	48	55	59	61	64	67	73
2 Hz	35	39	48	54	59	60	63	67	72
5 Hz	33	37	46	53	57	59	63	65	70
10 Hz	31	35	44	51	56	58	62	64	68
15 Hz	30	34	43	50	53	57	62	64	68

Table D27: Complex modulus and phase angle data of RTFOT aged 7% SBS with 93% Venezuelan 70/100 penetration grade bitumen [Airey, 1997]

Freq\Temp	10°C	15°C	25°C	35°C	45°C	55°C	65°C	75°C	85°C
0.01 Hz	718500	293000	50200	11000	2400	563	114	29	11
0.015 Hz	935000	393000	65800	14000	3590	804	180	48	17
0.02 Hz	1120000	469000	84100	17000	4380	1020	237	64	22
0.05 Hz	1835000	800000	146000	30700	8540	2200	549	153	52
0.1 Hz	2690000	1230000	230000	48900	13600	3830	1010	292	100
0.15 Hz	3350000	1550000	295000	63200	17800	5240	1420	424	148
0.2 Hz	3865000	1810000	354000	75400	21300	6490	1820	549	194
0.5 Hz	6110000	2980000	629000	138000	38900	12400	3770	1240	450
1 Hz	8450000	4250000	961000	217000	61400	19700	6340	2240	839
1.5 Hz	10200000	5220000	1240000	280000	80400	25800	8540	3130	1200
2 Hz	11600000	6020000	1480000	337000	97000	31400	10500	3930	1540
5 Hz	17100000	9260000	2500000	601000	176000	57300	19600	7970	3310
10 Hz	22300000	12600000	3620000	916000	271000	89800	30900	13000	5670
15 Hz	25700000	14800000	4450000	1180000	342000	114000	39400	17100	7630

Freq\Temp	10°C	15°C	25°C	35°C	45°C	55°C	65°C	75°C	85°C
0.01 Hz	53	57	60	60	63	72	78	73	77
0.015 Hz	52	54	57	60	70	78	82	85	84
0.02 Hz	51	54	58	59	67	77	82	84	84
0.05 Hz	48	52	57	59	64	73	80	83	84
0.1 Hz	48	52	57	58	61	69	77	82	83
0.15 Hz	46	50	56	59	60	67	76	81	83
0.2 Hz	46	50	56	59	60	66	74	80	82
0.5 Hz	43	48	55	59	59	63	70	77	80
1 Hz	42	46	54	59	59	61	67	74	79
1.5 Hz	40	45	53	58	59	61	65	72	77
2 Hz	40	44	52	58	58	60	65	71	76
5 Hz	37	42	50	57	58	60	62	68	73
10 Hz	35	40	49	56	56	60	61	65	70
15 Hz	35	39	48	55	56	59	61	64	69

Table D28: Complex modulus and phase angle data of PAV aged 7% SBS with 93% Venezuelan 70/100 penetration grade bitumen [Airey, 1997]

Freq\Temp	10°C	15°C	25°C	35°C	45°C	55°C	65°C	75°C	85°C
0.01 Hz	1900000	847000	145000	29500	7320	1840	438	102	28
0.015 Hz	2335000	1010000	191000	38200	9520	2480	625	157	42
0.02 Hz	2645000	1200000	226000	45800	11500	3020	777	211	54
0.05 Hz	4095000	1950000	381000	83900	20200	5630	1670	477	130
0.1 Hz	5700000	2740000	599000	128000	32300	9140	2840	865	252
0.15 Hz	6985000	3430000	777000	167000	42600	11900	3910	1230	372
0.2 Hz	7930000	3930000	904000	199000	51100	14400	4790	1550	487
0.5 Hz	11700000	6060000	1500000	353000	91600	26400	8930	3190	1080
1 Hz	15400000	8220000	2170000	538000	141000	41500	14200	5350	1900
1.5 Hz	18100000	9830000	2650000	688000	182000	53800	18600	7160	2610
2 Hz	20100000	11100000	3080000	811000	217000	65100	22300	8770	3230
5 Hz	27900000	16100000	4820000	1380000	375000	116000	40700	16500	6410
10 Hz	34850000	20700000	6640000	1990000	552000	178000	63200	26000	10400
15 Hz	39050000	23700000	8030000	2450000	673000	224000	81800	33000	13700

Freq\Temp	10°C	15°C	25°C	35°C	45°C	55°C	65°C	75°C	85°C
0.01 Hz	46	50	60	59	60	68	79	80	87
0.015 Hz	46	50	54	58	60	67	77	83	86
0.02 Hz	45	49	54	58	59	66	76	82	86
0.05 Hz	41	45	53	56	58	62	71	79	84
0.1 Hz	41	45	52	56	59	60	68	76	82
0.15 Hz	40	44	51	56	58	60	66	74	80
0.2 Hz	39	44	51	56	58	60	65	73	79
0.5 Hz	37	42	49	55	58	59	63	69	75
1 Hz	35	40	48	54	58	59	62	66	73
1.5 Hz	34	39	47	53	57	58	61	65	71
2 Hz	34	38	46	53	57	58	61	64	70
5 Hz	32	36	44	52	56	57	60	63	67
10 Hz	30	34	43	50	55	56	60	62	65
15 Hz	29	34	42	50	54	56	60	62	64

# Appendix E

Dynamic Shear Rheometer Data for the Unaged  
Bitumen-Filler Mastics

Table E1: Complex modulus and phase angle of 15% limestone bitumen-filler mastic (by mass)

Fre/Temp	10°C	15°C	25°C	35°C	45°C	55°C	65°C	75°C	80°C
0.1	5206600	1930800	216020	33557	5277.3	1020	231.83	62.491	35.316
0.13216	6480200	2335200	269080	42522	6814.1	1329.7	304.39	82.659	47.003
0.17467	7361700	2829300	334290	53833	8803.2	1738	400.67	109.1	62.204
0.23085	8721100	3427600	415500	68103	11369	2270.8	526.84	144.4	82.652
0.30509	10317000	4150200	515390	86197	14622	2955.8	692.2	191.18	109.22
0.40321	12163000	4961000	639750	108570	18782	3838.2	907.86	252.2	143.36
0.53289	14341000	6012400	792120	136710	24031	4964.6	1189.9	332.2	189.25
0.70428	16831000	7150600	975320	171600	30710	6436.9	1554.9	437.81	250.15
0.9308	19582000	8510800	1201300	215070	39112	8296.9	2029.1	575.48	329.1
1.2302	22786000	10133000	1475000	269340	49737	10696	2644.7	756.71	433.72
1.6258	26294000	11986000	1804800	336580	63162	13757	3444.1	994.22	571.82
2.1487	30412000	14120000	2202300	419160	80026	17613	4474.6	1302.4	752.05
2.8398	34966000	16540000	2680200	521220	101000	22538	5801.8	1701.5	986.91
3.7531	40343000	19381000	3247400	647030	127140	28759	7504	2217.5	1292.2
4.9602	46016000	22646000	3918600	799390	159470	36695	9687.2	2888.6	1688.1
6.5555	52192000	26271000	4712500	987430	199990	46771	12468	3757.1	2195.4
8.6638	59229000	30427000	5661000	1215600	249180	59416	16029	4862.2	2856
11.45	66785000	35055000	6757300	1488700	306140	75226	20559	6277.8	3684.3
15.133	74898000	40197000	8016300	1810800	370920	95316	26317	8054	4732.4
20	83484000	45853000	9452000	2177100	428200	120030	33493	10256	5985.5

	10°C	15°C	25°C	35°C	45°C	55°C	65°C	75°C	80°C
0.1	59.1	64.1	72.5	77.9	83.1	86.6	88.6	89.3	89.5
0.13216	57.4	62.6	71.2	76.8	82.1	85.9	88.3	89.4	89.7
0.17467	56.1	61.8	70.7	76.3	81.5	85.4	88	89.2	89.4
0.23085	54.7	60.9	70	75.7	80.9	85	87.7	88.9	89.5
0.30509	54	60.1	69.5	75.2	80.4	84.5	87.3	89	89.3
0.40321	52.6	58.5	68.9	74.6	79.8	84	86.9	88.7	89.2
0.53289	51.7	58.2	68.2	74.1	79.2	83.4	86.6	88.5	89.1
0.70428	50.7	56.9	67.5	73.6	78.7	82.9	86.1	88.3	88.9
0.9308	49.4	55.9	66.9	73.2	78.3	82.3	85.7	88	88.8
1.2302	48.2	55	66.1	72.6	77.7	81.7	85.2	87.6	88.5
1.6258	47.4	53.7	65.4	72.2	77.4	81.1	84.7	87.3	88.2
2.1487	46.1	52.8	64.6		77	80.6	84.3	86.9	88
2.8398	44.9	51.8	63.9			80.1	83.9	86.6	87.8
3.7531	43.9	50.6	63.3			79.7	83.5	86.3	
4.9602	42.7	49.6	62.6			79.2	83.2		
6.5555	41.6		61.7			78.8	82.9		
8.6638			61			78.4			
11.45			60.4			78.1			
15.133						77.9			
20						77.9			

Table E2: Complex modulus and phase angle of 35% limestone bitumen-filler mastic (by mass)

Fre/Temp	10°C	15°C	25°C	35°C	45°C	55°C	65°C	75°C	80°C
0.1	8930100	3552300	359520	53942	8892.9	1449.2	294.15	89.012	47.24
0.13216	9937400	4391400	446120	68557	11421	1896.7	385.98	118.96	62.729
0.17467	12834000	5193500	553590	86751	14686	2473.5	511.93	156.17	83.699
0.23085	14797000	6215700	687930	109380	18916	3223.5	671.87	206.81	110.48
0.30509	17556000	7497200	849910	138330	24309	4199.1	886.12	273.69	145.65
0.40321	19774000	8968400	1050700	174200	31206	5459.4	1159.2	358.77	192.06
0.53289	24150000	10705000	1298200	218870	39890	7081.3	1518.4	473.14	253.83
0.70428	28085000	12726000	1598700	274550	50740	9168.8	1988	625.26	334.46
0.9308	32658000	15030000	1957200	344400	64417	11857	2597.9	827.11	443
1.2302	37809000	17714000	2403700	430490	81613	15246	3385.3	1090.6	583.45
1.6258	43672000	20832000	2929300	536840	103200	19551	4411.4	1428.9	765.96
2.1487	49494000	24462000	3565500	667210	130280	25086	5734.3	1864.6	1011.7
2.8398	56908000	28724000	4317200	827720	164290	32145	7434.8	2431.9	1333.5
3.7531	64539000	33426000	5207300	1025100	206630	40958	9617.2	3177	1743
4.9602	73129000	38470000	6286200	1265500	258870	52275	12430	4130.9	2278.7
6.5555	82350000	44253000	7583200	1557100	322670	66464	15999	5346.7	2953.5
8.6638	92178000	50913000	9084200	1920200	403700	84414	20554	6931.5	3829.6
11.45	103240000	58023000	10837000	2349400	481110	106800	26386	8951.2	4948.2
15.133	114890000	66054000	12850000	2860400	608870	135260	33739	11502	6349.6
20	126840000	74571000	15145000	3450600	727550	170250	42961	14638	8065.7

Fre/Temp	10°C	15°C	25°C	35°C	45°C	55°C	65°C	75°C	80°C
0.1	57.9	63.2	71.9	77.5	82.6	86.6	88.7	89.7	89.8
0.13216	54.4	61.4	70.7	76.5	81.6	85.9	88.2	89.4	89.6
0.17467	54.8	60.9	70.1	76	80.9	85.5	88.2	89.4	89.3
0.23085	52.6	59.3	69.6	75.2	80.4	85	87.8	89.2	89.4
0.30509	52.4	58.7	69	74.8	79.8	84.5	87.5	88.9	89.4
0.40321	48.3	57.6	68.3	74.2	79.2	84	87		89.1
0.53289	49.8	56.5	67.7	73.6	78.5	83.4	86.6	88.6	89.1
0.70428	48.1	55.5	67	73.1	78.1	82.9	86.2	88.3	88.9
0.9308	48.2	54.5	66.3	72.7	77.5	82.4	85.8		88.8
1.2302	46.2	53.3	65.4	72.1	76.9	81.7	85.3		88.4
1.6258	44.4	52.4	64.8	71.6	76.5	81.1	84.8		88.2
2.1487	45.7	50.9	64	71.1	76	80.6	84.4		87.9
2.8398	43	49.7	63.3	70.7	75.7	80	83.9		87.7
3.7531	41.6	48.7	62.5	70.3	75.4	79.6	83.5		87.4
4.9602	40.2	47.6	61.7			79.1	83.2		87.4
6.5555	38.6	46.6	60.8			78.6	82.8		87.1
8.6638	37.6		60.1			78.2	82.5		
11.45	36.7					77.8			
15.133	35.8								
20	35.2								

Table E3: Complex modulus and phase angle of 65% limestone bitumen-filler mastic (by mass)

Fre/Temp	10°C	15°C	25°C	35°C	45°C	55°C	65°C	75°C	80°C
0.1	27254000	10470000	1568000	245210	45902	8456.5	1802.7	495.9	279.44
0.13216	29473000	13004000	1889700	305200	57837	10939	2280.7	643.22	370.04
0.17467	38410000	15019000	2323300	378480	73826	14071	3006.7	852.17	496.14
0.23085	44060000	17967000	2834600	471140	94023	18217	3991.7	1110.1	641.81
0.30509	50811000	21590000	3455800	590360	118520	23516	5273.9	1456.8	822.56
0.40321	59952000	24625000	4226800	738950	152000	30327	6732.9	1898.6	1101.2
0.53289	69454000	28758000	5255700	922140	190640	39329	8866.2	2453	1435
0.70428	83710000	35336000	6361500	1144600	242910	50167	11336	3254.1	1909.1
0.9308	92915000	42271000	7693100	1424300	307570	63901	14782	4273.5	2500.8
1.2302	107600000	49207000	9303300	1768200	385360	82087	19082	5592	3254.2
1.6258	122620000	57394000	11254000	2186700	485240	105410	24739	7243.3	4263.8
2.1487	135630000	70089000	13448000	2700800	606550	133010	31885	9431.6	5555.7
2.8398	151730000	77360000	16287000	3333300	760620	169740	41463	12263	7270.6
3.7531	166220000	87930000	19526000	4093300	949550	218730	52888	15970	9462.6
4.9602	186410000	101370000	23424000	5010300	1188000	264310	67823	20710	12334
6.5555	205940000	115410000	27821000	6166500	1472100	342470	86765	26776	15969
8.6638	226750000	130310000	32990000	7546600	1831200	426460	110860	34479	20648
11.45	247960000	146940000	38917000	9185400	2265600	530960	140830	44505	26728
15.133	269930000	164510000	45632000	11163000	2793300	659430	178810	57074	34501
20	291920000	182640000	53178000	13459000	3412900	794650	225970	73200	44131

Fre/Temp	10°C	15°C	25°C	35°C	45°C	55°C	65°C	75°C	80°C
0.1	54.5	61.8	68.6	74.3	79.2	82.4			87.4
0.13216	53.5		68	73.4	78.6	82.6	85.8	86.7	86.7
0.17467	52.7	58.4	68	73.1	78.2	82.1			88.4
0.23085	50.7	57.7	67.1	72.2	78.1	82.6	86.2	86.8	87.9
0.30509	49.9	56.8	66.7	72.3	77.3	81.8	85.7	86.9	86.7
0.40321			66	71.6	76.7	81.4	85.1	86.7	89.2
0.53289	47.2	54.4	65.5	71.4	76.1	81	84.4	85.6	87
0.70428		52.8	64.7	70.9	75.9	80.4	83.5	86.5	87.8
0.9308		53.1	64.1	70.6	75.5	80	83.5	86.1	86.5
1.2302	43.9	50.7	63.2	70	74.9	79.4	83	86.4	86.8
1.6258	44.2	49.4	62.3	69.6	74.4	78.9	82.7	85.7	86.7
2.1487	39.6	50.2	61.6	69.1	74.1	78.9	82.1	85.3	86
2.8398	37.7	46.7	60.5	68.4	73.7	78.6	81.6	84.8	86.1
3.7531	36.6	45.4	59.8	68.2	73.5	78.5	81	83.8	86
4.9602	34.9	43.9	58.4	67.4	73.2		80.5	84	85.2
6.5555	33.6	42.4	57.3	66.9			79.9		
8.6638	32.4	41	56.4				79.4		
11.45			55.4				78.9		
15.133			54.3						
20			53.4						

Table E4: Complex modulus and phase angle of 35% cement bitumen-filler mastic (by mass)

Fre/Temp	10°C	15°C	25°C	35°C	45°C	55°C	65°C	75°C	80°C
0.1	6089400	2908600	334740	49399	7522.1	1516.2	370.92	113.18	62.614
0.13216	7427600	3593000	416190	62681	9673.1	1982.8	486.08	150.14	82.078
0.17467	8482500	4291600	516960	79117	12481	2586.6	642.07	196.6	108.52
0.23085	10068000	5180000	641070	100260	16058	3385.3	843.72	259.21	143.91
0.30509	11770000	6244800	796750	127090	20708	4402.9	1113.5	340.84	190.47
0.40321	13693000	7524700	985600	159630	26546	5731.9	1453.8	449.87	251.84
0.53289	16502000	9015200	1217300	200890	34004	7427.5	1901	594.52	333.34
0.70428	18979000	10806000	1503400	253090	43473	9589.3	2487.5	782.95	439.16
0.9308	21948000	12813000	1845200	316470	55526	12406	3247.1	1029.7	578.26
1.2302	25246000	15204000	2259400	396450	70724	15963	4249	1351.2	760.63
1.6258	29136000	17913000	2767900	494620	89535	20541	5514.4	1774	998.19
2.1487	33489000	21077000	3366600	615920	112920	26403	7157.6	2323.4	1313
2.8398	37601000	24696000	4077700	765100	142480	33833	9293	3031.6	1723.3
3.7531	43309000	28674000	4920900	947790	179150	43319	12016	3958.5	2245.6
4.9602	48932000	33441000	5943600	1170300	225400	55291	15530	5148.8	2937.9
6.5555	55061000	38624000	7183300	1440400	281330	70491	19938	6686.2	3833.6
8.6638	61522000	44342000	8611800	1773500	350510	89814	25626	8662.9	4975.9
11.45	68295000	50669000	10276000	2171100	430420	114160	32831	11170	6474.6
15.133	75222000	57555000	12184000	2641700	525070	144370	41982	14367	8325.3
20	82622000	64872000	14377000	3181700	618270	181950	53404	18396	10620

Fre/Temp	10°C	15°C	25°C	35°C	45°C	55°C	65°C	75°C	80°C
0.1	58.6	64.7	72.3	77.9	83.2	86.5	88.3	89.5	
0.13216	56.7	62.9	71	76.9	82.3	86.2	88.3	89.3	89.4
0.17467	54.8	62.2	70.6	76.3	81.8	85.7	88.1	89.1	89.2
0.23085	53.9	60.8	69.8	75.7	81.2	85.4	87.6	89	89.5
0.30509	53.2	60.1	69.3	75.2	80.6	84.7	87.4	88.8	89.2
0.40321	50.7	59.2	68.6	74.6	79.9	84.3	87.1	88.5	89
0.53289	51.4	57.8	67.9	74	79.4	83.7	86.5	88.3	89
0.70428	49.5	56.8	67.2	73.6	78.9	83.1	86.1	88.1	88.8
0.9308	47.6	55.7	66.5	73.1	78.3	82.7	85.6	87.8	88.5
1.2302	47.3	54.5	65.7	72.4	77.8	81.9	85.1	87.4	88.2
1.6258	45.5	53.4	64.9	71.9	77.3	81.2	84.7	87.1	87.9
2.1487	44.1	52.1	64.1	71.5	76.9	80.8	84.1	86.7	87.7
2.8398	43.4	50.9	63.3	71	76.6	80.2	83.8	86.5	87.4
3.7531	41.7	49.6	62.6	70.6	76.4	79.7	83.4	85.9	87.1
4.9602	40.5	48.3	61.8	70.2	76.3	79.1	83	85.7	86.9
6.5555	39.4	47	60.9			78.5	82.6	85.4	
8.6638			60.2			78.1	82.4	85.3	
11.45			59.5			77.6	82.1		
15.133						77.1			
20						77			

Table E5: Complex modulus and phase angle of 65% cement bitumen-filler mastic (by mass)

Fre/Temp	10°C	15°C	25°C	35°C	45°C	55°C	65°C	75°C	80°C
0.1	27784000	11186000	2157700	358310	66781	12696	2093.7	584.28	325.58
0.13216	30912000	14182000	2615400	446920	82822	16295	2765.5	727.63	419.92
0.17467	37124000	15768000	3180300	555620	102850	20490	3539.6	981.03	551.06
0.23085	44386000	18608000	3867600	684340	129840	26107	4617.5	1308.2	719.4
0.30509	49062000	21886000	4661300	842520	165060	33245	6127.5	1674	944.89
0.40321	55294000	26820000	5752500	1054600	205060	42116	7770.6	2244.5	1231.8
0.53289	67142000	30190000	7029500	1288800	255550	52639	10178	2932.2	1629
0.70428	64001000	35080000	8448500	1596900	319640	67764	13451	3759.9	2110.5
0.9308	77280000	29395000	10186000	2002000	398800	84812	17279	4938.9	2795.3
1.2302	88049000	48256000	12239000	2445000	496450	108370	22267	6442.2	3644
1.6258	108230000	53383000	14664000	2983400	623910	137140	28879	8422	4798.8
2.1487	123550000	66934000	17462000	3650200	777260	173210	36898	10982	6262.9
2.8398	136460000	71848000	20726000	4437300	968690	219850	47114	14262	8114.2
3.7531	148980000	82289000	25015000	5474000	1203400	272970	60584	18352	10581
4.9602	166610000	93531000	29461000	6623300	1499800	336630	76955	23823	13756
6.5555	182610000	105760000	34682000	8079300	1842600	439070	98258	30614	17810
8.6638	199750000	118970000	40875000	9806400	2287700	543510	125290	39507	23022
11.45	217290000	132810000	47764000	11893000	2817900	673020	157850	50894	29832
15.133	237560000	147560000	55535000	14278000	3449900	852520	200820	65213	38238
20	255630000	162760000	64026000	17225000	4220600	1034900	252370	83152	49141

Fre/Temp	10°C	15°C	25°C	35°C	45°C	55°C	65°C	75°C	80°C
0.1			65	72.8			85.7		86.7
0.13216			65.2	70.7			86.4		86.6
0.17467	49.1	56.2	64.1	70.5			85.1	87.1	87.3
0.23085		55.5	63.2	69.3	74.7		84.7	87.7	86.7
0.30509	46.1	53.7	62.9	69.3	74.7		85	86.5	86.9
0.40321		51.4	61.5	68.9	74.7		83.9	87.3	86.4
0.53289	47.2	51.3	61.7	67.9	73.3		83.8	86.4	87.3
0.70428		49.5	60.9	67.6	73.3		83.5	86	87
0.9308	44.1		60.2	68.7	72.6		83.1	85.7	86.7
1.2302	44.3	46	59.1	67	71.7		82.1	85.5	86.5
1.6258	38	46.4	58.2	66.3	72.1	76.4	81.2	85	85.9
2.1487	35.8	44.9	57.7	65.8	71.4	75.6	81	84.6	85.6
2.8398	35.7	43.5	56.3	65.3	70.8	73.7	80.4	84	85.5
3.7531	34.4	42.5	55.5	64.5	70.4	75.4	79.5	83.4	84.7
4.9602	33.1	40.8	54.3	64.1	70	75.5	78.9	83.2	84.5
6.5555	31.9	40	53	63.4	69.7	73.9	78.6	82.5	84.3
8.6638	30.6	38.5	52.1		69.2	73.2	77.8	82.4	83.6
11.45	30		51.1			72.1	77.3		
15.133	28.9					71.5	76.5		
20	28.3					69.5	75.9		

Table E6: Complex modulus and phase angle of 35% gritstone bitumen-filler mastic (by mass)

Fre/Temp	10°C	15°C	25°C	35°C	45°C	55°C	65°C	75°C	80°C
0.1	8408000	3109200	484850	76131	8412.7	1757.2	445.79	119.28	67.679
0.13216	10354000	3816400	600920	96340	10882	2296.7	587.63	156.88	89.718
0.17467	11851000	4582100	744160	121110	14066	3009.3	769.56	207.48	118.3
0.23085	14007000	5525400	921450	152270	18142	3914	1013.1	273.4	156.54
0.30509	15184000	6664800	1140200	192160	23315	5099.9	1333.5	360.27	206.82
0.40321	19451000	7974300	1408200	240760	29833	6619.5	1741.8	477.14	272.33
0.53289	22743000	9528300	1739300	301230	38183	8580.8	2284.7	630.47	360.16
0.70428	26495000	11369000	2137000	377450	48723	11070	2990.4	829.4	475.05
0.9308	30857000	13493000	2614000	471460	62129	14338	3877.9	1088.1	626.84
1.2302	35593000	15969000	3197700	587650	78800	18463	5053.4	1424.7	823.63
1.6258	40991000	18712000	3889600	729850	100020	23700	6566.5	1861.6	1083.9
2.1487	47298000	22000000	4720600	905880	126680	30309	8499.8	2434.9	1420.9
2.8398	53306000	25768000	5691200	1120600	160500	38745	10983	3176.8	1860.1
3.7531	60608000	29970000	6874800	1383800	201930	49367	14168	4145.4	2433.1
4.9602	68874000	34575000	8290000	1705900	252180	62593	18251	5396.6	3182.8
6.5555	77581000	39842000	9953300	2092100	315360	79486	23364	7018.6	4144.5
8.6638	86641000	45582000	11896000	2566100	391170	100870	29958	9077.5	5367.5
11.45	96175000	51776000	14162000	3130500	480410	127810	38240	11693	6925.2
15.133	105670000	58634000	16767000	3806000	584260	161060	48705	15051	8880.7
20	115470000	65828000	19733000	4592100	693400	201570	61811	19178	11282

Fre/Temp	10°C	15°C	25°C	35°C	45°C	55°C	65°C	75°C	80°C
0.1	59.1	64.5	71.5	76.8	83.2	86.4	88.5	89.4	
0.13216	57	62.5	70.2	75.7	82.4	85.8	88.1		89.6
0.17467	55.5	61.8	69.6	75.1	81.6	85.4	87.7	89.3	89.4
0.23085	54.4	60.6	68.8	74.4	81.2	84.8	87.5	89.2	89.4
0.30509	53.9	59.6	68.4	74	80.6	84.3	87.1	88.9	89.2
0.40321	52	58.2	67.5	73.4	80	83.9	86.5	88.7	89.1
0.53289	51	57.4	67	72.9	79.5	83.2	86.3	88.3	89
0.70428	49.5	56.1	66.3	72.4	79	82.6	85.8	88.1	88.8
0.9308	48.3	55.1	65.5	71.9	78.5	82.1	85.4	87.9	88.7
1.2302	46.9	53.9	64.7	71.3	78	81.3	84.9	87.4	88.3
1.6258	45.6	52.7	63.9	70.8	77.6	80.8	84.4	87	88
2.1487	44.1	51.4	63.1	70.3	77.2	80.2	83.9	86.7	87.7
2.8398	43.1	50.3	62.2	69.8	77	79.7	83.5	86.4	
3.7531	42	49	61.3	69.3	77	79.2	83	86.1	
4.9602	40.4	47.7	60.4	68.9		78.6	82.7	85.8	
6.5555	39.1	46.5	59.4	68.5		78	82.3		
8.6638	38	45.3	58.6			77.5	82		
11.45		44.3				77.1	81.8		
15.133		43.3				76.7			
20						76.3			

Table E7: Complex modulus and phase angle of 65% gritstone bitumen-filler mastic (by mass)

Fre/Temp	10°C	15°C	25°C	35°C	45°C	55°C	65°C	75°C	80°C
0.1	23668000	11807000	4751200	715560	113300	19196	3427.1	906.1	484.4
0.13216	26406000	13780000	5658100	854370	138320	23963	4350.6	1195.3	630.1
0.17467	31087000	16032000	6397300	1014300	168880	30251	5709	1538.2	838.51
0.23085	35977000	18630000	7481800	1224900	206150	38069	7479	2013.8	1083.7
0.30509	41031000	21862000	8757800	1484800	258190	48697	9534.8	2628.4	1430.1
0.40321	46288000	26790000	10398000	1776200	317320	61082	12342	3472.2	1856.7
0.53289	53908000	29803000	12385000	2141500	394380	78159	16229	4539.9	2434.6
0.70428	50440000	30973000	14536000	2630600	490740	98838	20886	5850.1	3200.5
0.9308	66574000	40887000	16953000	3219100	619850	124890	26750	7643	4187.5
1.2302	74502000	46558000	19827000	3853100	759780	156590	34553	10051	5457.4
1.6258	85717000	53560000	23287000	4644000	932340	202470	43984	12970	7129.5
2.1487	101090000	61842000	28146000	5627400	1149100	252060	56519	16714	9311.1
2.8398	106340000	70585000	32757000	6736300	1425300	317650	71996	21549	12113
3.7531	116950000	79569000	38783000	8193000	1765300	398480	92131	27864	15602
4.9602	130440000	89246000	45125000	9991300	2191500	511770	117760	35831	20336
6.5555	141520000	99967000	52446000	12044000	2689300	637050	149900	46063	26341
8.6638	154460000	110630000	60618000	14527000	3313300	801270	188640	59539	33933
11.45	165490000	121390000	69648000	17394000	4084800	987180	238510	76077	43935
15.133	178450000	128970000	79556000	20853000	4998700	1231600	300460	97535	56280
20	189550000	135710000	90702000	24756000	6093200	1493100	375390	123400	71612

Fre/Temp	10°C	15°C	25°C	35°C	45°C	55°C	65°C	75°C	80°C
0.1							85.2		86.6
0.13216							84.6		87
0.17467						77.9	84.3	87.2	87.7
0.23085						77.8	84.9	87.2	87.3
0.30509			59	67	72.9	77.8	84	86.6	87.6
0.40321			59.6	66.8	72.3	77.3	82.2	86.9	86.6
0.53289	44.4		58.8	66.4	72.5	77.4	83.4	86.2	86.9
0.70428		54.3	57.8	66.2	72.5	77.2	82.9	85.2	87.1
0.9308	40.8	47.1	57.8	66	72.4	77.1	82.3	85.3	86.7
1.2302	40.2	47.1	56.9	65.5	71.6	77	81.6	85	85.9
1.6258	37	44.6	56	65.3	71.4	75.7	80.5	83.9	86.2
2.1487	35.4	43.7	54.5	64.8	71.1	75.8	80.1	84.2	85.3
2.8398	34.7	42.1	53.4	64.6	70.7	75	79.7	83.9	85
3.7531	33.5	41.8	52.1	63.9	70.2	75.1	78.9	83	84.8
4.9602	33.1	40.2	50.9	63.1	70.2	74.7	78.3	82.7	84.3
6.5555	31.7	39.2	49.8	62.4	69.7	74.3	77.1	82	83.8
8.6638	30.3	38.1	48.6	61.8	69.2	74.1	76.7	81.6	83.5
11.45	29.6	37	47.5	61	69	73.9	75.9		83.3
15.133	28.7	36.6	46.2	60.3	68.8	74	75		
20	28	35.6	45.3	59.8	68.6	72.9	74.2		

Table E8: Complex modulus and phase angle of 40% gritstone bitumen-filler mastics (by volume)

Freq/Temp	10°C	15°C	25°C	35°C	45°C	55°C	60°C	65°C	70°C
0.1 Hz	16787000	7038000	954540	121710	19580	5764.1	7252.3	9139.6	10171
0.15849 Hz	19750000	10062000	1317100	173210	27935	6463.8	7349.4	9231.4	9794.5
0.25119 Hz	27893000	12004000	1827400	250460	40510	8143.9	7944.4	8894.5	9201.9
0.39811 Hz	34039000	15933000	2517400	361810	59409	11492	8366	9318.5	9585.4
0.63096 Hz	43731000	20726000	3490300	517870	86926	15480	10870	10068	10172
1 Hz	54758000	26583000	4784200	741480	128650	22066	14134	11683	11131
1.5849 Hz	68455000	34213000	6491800	1059600	188920	31550	19487	14369	12741
2.5119 Hz	83522000	43811000	8764200	1504000	276620	46471	28640	19620	15395
3.9811 Hz	100770000	55245000	11820000	2130300	404600	69489	39841	26177	18874
6.3096 Hz	119870000	68416000	15825000	2996500	592930	104630	60055	37549	25073
10 Hz	141000000	84044000	21005000	4198600	850970	155610	88453	54749	35991

Freq/Temp	10°C	15°C	25°C	35°C	45°C	55°C	60°C	65°C	70°C
0.1 Hz	53.99	58.25	67.27	74.22	75.48	49.94	35.34	26.7	23.97
0.15849 Hz	51.48	62.97	66.08	73.29	75.94	56.34	37.79	29.5	24.42
0.25119 Hz	49.04	56.01	65.48	73.02	76.61	63.45	43.64	31.92	24.36
0.39811 Hz	47.05	54.5	64.62	72.7	76.91	69.76	50.51	35.25	28.43
0.63096 Hz	46.96	52.52	63.35	71.8	76.99	72.59	60.62	43.61	32.67
1 Hz	44.5	51.22	62.58	71.12	76.83	75.52	66.88	51.53	38.83
1.5849 Hz	41.69	49.21	61.68	70.3	76.22	78.57	71.67	60.06	46.16
2.5119 Hz	39.91	47.46	60.6	69.46	76.09	79.66	73.97	66	53.4
3.9811 Hz	37.43	45.69	58.9	68.74	75.25	79.49	77.73	71.36	62.3
6.3096 Hz	35.26	43.5	57.71	68.03	75	78.96	78.25	74.51	68.59
10 Hz	33.41	41.66	56.36	67.23	74.27	78.56	79.03	76.8	72.34

Table E9: Complex modulus and phase angle of 40% limestone bitumen-filler mastics (by volume)

Freq/Temp	10°C	15°C	25°C	35°C	45°C	55°C	65°C	75°C	80°C
0.1 Hz	14164000	6129500	840970	110940	17907	2409.5	638.84	210.1	124.78
0.15849 Hz	19808000	8603900	1193100	162390	26031	3755.4	979.5	317.39	186.55
0.25119 Hz	24087000	10850000	1667300	233500	38871	5843.7	1542.3	487.12	279.66
0.39811 Hz	30313000	14564000	2301700	340320	57479	8998.2	2416.1	762.71	435.91
0.63096 Hz	39772000	19227000	3244400	489620	84251	13785	3697.1	1182.2	680.08
1 Hz	50060000	25001000	4489500	707090	125820	20877	5716	1829.2	1060.2
1.5849 Hz	63296000	32671000	6157000	1011000	184880	32447	8836.2	2859.4	1662.6
2.5119 Hz	79228000	42299000	8366600	1445400	273300	49515	13607	4435.5	2554.7
3.9811 Hz	96508000	53686000	11359000	2056700	397320	74896	20942	6922.6	4047.9
6.3096 Hz	117140000	67295000	15395000	2900300	588010	113090	32156	10772	6275.8
10 Hz	139250000	83777000	20506000	4080000	845760	167950	49190	16579	9665.3

Freq/Temp	10°C	15°C	25°C	35°C	45°C	55°C	65°C	75°C	80°C
0.1 Hz	56.54	60.48	69.82	76.15	78.88	85.53	86.38	83.64	83.86
0.15849 Hz	62.17	59.51	67.79	74.89	78.6	85.52	85.85	83.92	84.44
0.25119 Hz	52.46	58.38	67.09	74.47	78.48	84.59	85.69	85.02	85.71
0.39811 Hz	49.51	56.69	65.71	73.95	78.79	85.32	87	86.33	85.43
0.63096 Hz	48.87	54.77	64.94	72.9	78.57	84.07	85.99	86.22	86.76
1 Hz	47.05	53.37	63.9	71.64	77.4	82.25	85.94	86.6	86.57
1.5849 Hz	44.14	51.44	62.93	71.23	77.11	82.51	85.45	86.5	86.92
2.5119 Hz	42.13	49.26	61.89	70.47	76.58	81.68	85.23	86.86	86.91
3.9811 Hz	39.96	47.47	60.46	69.67	76.04	80.62	84.55	86.7	87.1
6.3096 Hz	38	45.67	59.16	68.89	75.39	79.6	84.09	86.34	86.84
10 Hz	36.21	43.65	57.89	68.15	74.61	78.54	83.51	86.25	87

Table E10: Complex modulus and phase angle of 40% cement bitumen-filler mastics (by volume)

Freq/Temp	10°C	15°C	25°C	35°C	45°C	55°C	65°C	75°C	80°C
0.1 Hz	14616000	6453200	904310	113620	16563	2490.6	657.58	257.71	222.49
0.15849 Hz	17897000	9116300	1271300	165880	24679	3898.4	1042.2	366.22	273.55
0.25119 Hz	25150000	11336000	1766900	241360	36744	6150.8	1573.4	530.05	374.56
0.39811 Hz	31022000	15150000	2454800	351980	55614	9386.7	2442.7	800.08	533.34
0.63096 Hz	40334000	19921000	3422300	511390	83474	14198	3786.5	1205.8	788.47
1 Hz	51282000	25783000	4721000	735130	124370	21873	5881.5	1893.9	1197.1
1.5849 Hz	64103000	33570000	6469500	1055400	185020	33520	9205	2971.4	1847.5
2.5119 Hz	80999000	43555000	8746600	1502600	273490	51297	14248	4575.7	2832.2
3.9811 Hz	97744000	54716000	11879000	2133100	403770	77809	21962	7158.9	4432.7
6.3096 Hz	118150000	68502000	15940000	3010100	588950	116830	33684	11056	6814
10 Hz	140810000	84316000	21186000	4225600	854000	174950	51299	17053	10492

Freq/Temp	10°C	15°C	25°C	35°C	45°C	55°C	65°C	75°C	80°C
0.1 Hz	55.25	59.8	68.23	76.03	80.37	84.51	84.04	69.69	53.81
0.15849 Hz	54.29	58.85	67.03	75.03	79.91	85.55	84.69	73.81	61.72
0.25119 Hz	50.84	57.35	66.39	74.32	79.89	84.73	85.82	78.35	67.67
0.39811 Hz	48.47	55.73	65.3	73.51	79.39	85.7	86.66	81.92	73.58
0.63096 Hz	48.75	53.84	64.26	72.32	78.56	84.45	86.24	84.76	78.15
1 Hz	46.01	52.56	63.03	71.65	77.98	83.45	85.86	85.39	80.92
1.5849 Hz	43.34	50.46	61.97	70.74	77.19	82.86	85.62	85.56	83.07
2.5119 Hz	41.54	48.07	60.93	69.95	76.66	81.92	85.26	86	84.65
3.9811 Hz	39.24	46.59	59.57	69.13	75.69	80.95	84.51	86.25	85.53
6.3096 Hz	37.42	44.74	58.17	68.3	75.05	79.9	84.22	86.24	86.09
10 Hz	35.52	43.08	56.92	67.49	74.74	78.82	83.86	86.09	86.39

# Appendix F

Dynamic Shear Rheometer Data for the Aged  
Bitumen-Filler Mastics

Table F1: Complex modulus and phase angle of the 1 hour aged gritstone bitumen-filler mastics

Freq/Temp	10°C	15°C	25°C	35°C	45°C	55°C	65°C	75°C	80°C
0.1 Hz	16401000	7211400	1063400	139830	22261	3783.6	1159.7	463.26	365.16
0.15849 Hz	19356000	10345000	1466400	199870	31932	5383	1618.9	617.05	443.76
0.25119 Hz	27022000	12406000	2035900	287450	46398	8199.1	2349.5	846.53	580.89
0.39811 Hz	32968000	16334000	2804900	413070	67768	12274	3421.2	1189.7	799.94
0.63096 Hz	42393000	21168000	3843400	591830	99359	18392	5050.8	1736.8	1103
1 Hz	53505000	27164000	5245400	845280	145420	27823	7709.1	2596.2	1650.4
1.5849 Hz	66550000	35534000	7073400	1197900	214590	41891	11536	3909.4	2416.6
2.5119 Hz	82113000	44851000	9485100	1697700	313490	62803	17817	5868.9	3586.4
3.9811 Hz	99584000	56450000	12860000	2387700	459480	94538	27045	9028.5	5538
6.3096 Hz	119450000	70191000	17161000	3341500	663150	141990	41055	13789	8383.9
10 Hz	141350000	86228000	22607000	4664400	956430	212170	62463	21149	12840

Freq/Temp	10°C	15°C	25°C	35°C	45°C	55°C	65°C	75°C	80°C
0.1 Hz	53.71	58.19	66.86	73.84	76.57	78.67	76.7	66.49	59.64
0.15849 Hz	51.4	62.46	65.44	72.91	76.35	81.96	77.91	69.7	62.12
0.25119 Hz	49.33	55.57	64.72	72.56	76.79	81.99	79.82	73.39	66.47
0.39811 Hz	47.47	54.21	63.93	72.07	76.58	83	81.66	76.77	71.39
0.63096 Hz	47.34	52.48	62.93	70.95	76.58	82.28	83.68	79.09	75.44
1 Hz	44.81	51.4	61.86	70.58	76.03	81.24	83.32	81.15	76.99
1.5849 Hz	42.24	49.04	61.2	69.66	75.55	81.28	83.79	82.63	79.98
2.5119 Hz	40.48	47.31	59.76	68.78	75.25	80.6	83.57	84.07	82.57
3.9811 Hz	37.91	45.36	58.51	68.06	74.72	79.58	83.14	84.43	83.01
6.3096 Hz	36.25	43.58	57.04	67.41	73.92	78.44	83.11	84.87	84.3
10 Hz	34.48	41.87	55.84	66.61	73.36	77.41	82.5	84.75	84.75

Table F2 Complex modulus and phase angle of the 3 hour aged gritstone bitumen-filler mastics

Freq/Temp	10°C	15°C	25°C	35°C	45°C	55°C	65°C	75°C	80°C
0.1 Hz	18980000	8721500	1366500	189350	29941	10253	12917	14786	14620
0.15849 Hz	21874000	12411000	1866700	269760	43158	12592	13220	16006	15377
0.25119 Hz	31083000	14477000	2551800	380380	62583	15435	13072	15232	14131
0.39811 Hz	36976000	18832000	3455400	537640	91655	20668	13725	15155	15099
0.63096 Hz	46945000	24192000	4701100	764100	132930	29664	15332	16237	16845
1 Hz	58375000	30632000	6315200	1076600	193120	42161	18239	16457	15995
1.5849 Hz	72165000	38972000	8451300	1508500	280840	60437	24139	17399	17053
2.5119 Hz	87901000	49054000	11150000	2108100	405610	87675	32272	19574	17781
3.9811 Hz	105230000	61140000	14837000	2931200	583500	130580	41751	22808	18862
6.3096 Hz	124910000	74692000	19508000	4034800	838090	191770	61487	29799	23022
10 Hz	145990000	90665000	25331000	5547000	1195500	275340	88010	39930	29293

Freq/Temp	10°C	15°C	25°C	35°C	45°C	55°C	65°C	75°C	80°C
0.1 Hz	51	55.48	64.49	71.94	76.47	45.47	17.22	9.77	10.54
0.15849 Hz	44.74	57.34	62.86	70.77	75.98	57.22	18.63	10.64	9.03
0.25119 Hz	46.41	53.14	62.17	70.3	75.87	63.27	24.46	9.2	8.07
0.39811 Hz	43.99	51.4	60.98	69.42	75.38	67.82	29.93	11.34	8.47
0.63096 Hz	44.92	49.64	60.68	68.48	75.18	71	39.43	13.84	11.21
1 Hz	43.17	48.58	58.91	68	74.39	74.12	48.64	22.04	13.01
1.5849 Hz	39.65	46.42	57.9	66.95	73.87	75.58	55.16	27.21	19.18
2.5119 Hz	38.15	44.69	56.81	66.12	73.07	75.93	62.51	36.06	25.39
3.9811 Hz	35.88	43.3	55.42	65.34	72.32	75.53	70.56	47.08	35.18
6.3096 Hz	34.06	41.03	54.23	64.57	71.58	74.09	72.1	55.99	44.55
10 Hz	32.5	39.46	53.01	63.79	71.15	73.45	74.37	63.18	54.06

Table F3: Complex modulus and phase angle of the 5 hour aged gritstone bitumen-filler mastics

Freq/Temp	10°C	15°C	25°C	35°C	45°C	55°C	65°C	70°C	75°C
0.1 Hz	24348000	11197000	1749500	240870	37098	11402	10454	8119.9	7884.3
0.15849 Hz	25166000	12812000	2367100	340000	53576	15605	11406	8346.1	7966.1
0.25119 Hz	38047000	18589000	3197700	480860	77869	17808	11330	8308	7446.7
0.39811 Hz	45798000	23052000	4275600	680760	114080	24621	12383	8509.5	7573.3
0.63096 Hz	56833000	29697000	5795000	956590	166490	34246	14436	9527.9	8237.1
1 Hz	67375000	37258000	7719900	1336700	241900	49023	17720	10909	8569
1.5849 Hz	86280000	46556000	10124000	1862700	349390	68941	24435	13915	9891.2
2.5119 Hz	103130000	56181000	13431000	2576600	502530	101900	34234	19232	12467
3.9811 Hz	119700000	70522000	17567000	3533200	721560	147710	45798	26225	16565
6.3096 Hz	139920000	85830000	22830000	4847500	1028200	214000	66861	37845	22809
10 Hz	162290000	102700000	29456000	6606500	1450400	308450	97527	55257	33401

Freq/Temp	10°C	15°C	25°C	35°C	45°C	55°C	65°C	70°C	75°C
0.1 Hz	48.13	53.41	62.97	70.99	76.47	41.6	18.32	16.51	15.43
0.15849 Hz	15.87	44.61	61.3	69.72	75.94	55.02	23.18	17.54	15.27
0.25119 Hz	44.33	49.79	60.56	69.09	75.56	59.35	28.61	22.39	19.16
0.39811 Hz	40.67	48.28	59.19	68.19	74.93	66.42	37.2	27.35	21.32
0.63096 Hz	41.32	47.56	58.36	67.08	74.21	70.26	45.84	37.27	27.1
1 Hz	39.9	45.82	57.34	66.49	73.46	72.84	55.64	47.07	35.8
1.5849 Hz	38.55	44.01	56.29	65.33	72.67	74.62	61.22	56.96	45.74
2.5119 Hz	35.45	42.83	54.68	64.53	71.84	74.42	66.56	63.17	54.74
3.9811 Hz	33.47	40.4	53.45	63.71	70.91	73.94	73.41	71.21	64.62
6.3096 Hz	32.1	38.92	52.31	62.87	70.4	73.13	74.23	74.47	71.72
10 Hz	30.5	37.32	51.04	62.06	69.71	72.42	75.06	76.18	74.71

Table F4: Complex modulus and phase angle of the 10 hour aged gritstone bitumen-filler mastics

Freq/Temp	10°C	15°C	25°C	35°C	45°C	55°C	65°C	75°C	80°C
0.1 Hz	26623000	12813000	2190300	331850	52823	10346	2692.4	1046.6	987.83
0.15849 Hz	28481000	17496000	2931500	461120	74570	14835	3779.3	1387.7	1094.2
0.25119 Hz	40682000	20059000	3966300	642930	105970	22222	5592.4	1824.7	1408.5
0.39811 Hz	47901000	25246000	5129400	889730	153070	33038	8124.6	2580.8	1819.8
0.63096 Hz	58322000	31736000	6834400	1240400	221010	49289	11992	3723.8	2452.6
1 Hz	69143000	39490000	8944700	1712100	316650	72275	17915	5549.2	3528.7
1.5849 Hz	86291000	49632000	11644000	2339400	451600	105730	26730	8309.3	5191.7
2.5119 Hz	102860000	60756000	15099000	3183800	641790	153940	40317	12444	7716.3
3.9811 Hz	120160000	73735000	19634000	4304300	909680	222650	59438	18721	11499
6.3096 Hz	140180000	88589000	25181000	5834900	1276900	316980	88128	28192	17268
10 Hz	160880000	104830000	32115000	7829900	1789000	453030	129810	42330	25934

Freq/Temp	10°C	15°C	25°C	35°C	45°C	55°C	65°C	75°C	80°C
0.1 Hz	47.22	52.34	61.35	69.23	73.57	77.84	69.86	54.92	44.32
0.15849 Hz	33.38	52.49	59.64	67.72	73.65	78.37	74.42	60.51	50.66
0.25119 Hz	43.42	49.89	58.13	67.17	73.71	78.99	75.95	68.42	55.23
0.39811 Hz	41.29	48.12	57.85	66.27	72.94	77.97	78.69	73.3	63.65
0.63096 Hz	41.71	46.8	56.97	65.12	72.28	76.74	79.83	77.59	70.65
1 Hz	42.45	45.19	55.89	64.66	71.79	75.51	80.02	79.81	74.92
1.5849 Hz	36.64	43.57	54.83	63.82	70.99	74.55	79.93	80.31	77.65
2.5119 Hz	34.78	41.56	53.8	62.93	70.29	73.47	78.44	81.31	79.44
3.9811 Hz	33.72	39.82	52.81	62.24	69.56	71.85	78.3	81.42	81.05
6.3096 Hz	31.64	38.32	51.44	61.42	68.95	70.31	77.32	81.34	81.63
10 Hz	30.15	36.93	50.12	60.64	68.33	68.19	76.54	81.16	82.05

Table F5: Complex modulus and phase angle of the 20 hour aged gritstone bitumen-filler mastics

Freq/Temp	10°C	15°C	25°C	35°C	45°C	55°C	65°C	75°C	80°C
0.1 Hz	51400000	27888000	6094900	1157200	211040	21028	4521.7	1710.4	1044.9
0.15849 Hz	42011000	26230000	7516800	1553700	292180	32484	6775.9	2172.6	1293.5
0.25119 Hz	72323000	40982000	10018000	2040100	402530	44757	10321	3094.9	1862.5
0.39811 Hz	85763000	48667000	12367000	2708300	556400	68618	15280	4612.9	2650
0.63096 Hz	100300000	59090000	15672000	3536700	764610	96766	23121	6786.1	3863.6
1 Hz	109600000	66949000	19557000	4635700	1039200	140030	34508	10231	5834.8
1.5849 Hz	137050000	84199000	24368000	6008500	1405200	200730	50842	15268	8796.5
2.5119 Hz	145970000	98932000	30329000	7769500	1900400	278180	75373	23019	13211
3.9811 Hz	170690000	113670000	37738000	10042000	2545900	401840	109770	34360	19933
6.3096 Hz	191180000	131260000	46011000	12958000	3402400	558950	159510	51396	30021
10 Hz	213500000	150630000	55737000	16515000	4522300	766000	229980	75926	44920

Freq/Temp	10°C	15°C	25°C	35°C	45°C	55°C	65°C	75°C	80°C
0.1 Hz	37.61	42.43	51.65	59.51	67.07	78.36	79.44	57.46	49.67
0.15849 Hz	1.47	3.9	53.93	57.28	65.14	78.29	80.71	64.09	60.95
0.25119 Hz	33.84	38.83	47.99	56.65	64.31	76.25	79.94	71.76	67.33
0.39811 Hz	32.81	36.22	47.07	55.93	63.44	75.58	79.45	75.28	72.33
0.63096 Hz	30.58	36.26	46.69	54.92	61.75	71.3	78.7	77.89	77.48
1 Hz	28.76	36.21	45.78	53.93	61.3	71.02	77.51	79.21	78.74
1.5849 Hz	30.76	33.33	44.34	53.13	60.4	69.34	76.68	79.91	80.42
2.5119 Hz	26.85	32.05	43.25	52.46	59.42	67.87	75.33	79.56	80.5
3.9811 Hz	25.79	30.46	42.29	51.45	58.87	65.5	73.84	79.07	80.49
6.3096 Hz	24.15	29.67	41.26	50.63	58.18	63.31	72.64	78.27	80.12
10 Hz	23.19	28.5	40.09	50.05	57.71	60.74	71.4	77.47	79.62

Table F6: Complex modulus and phase angle of the 1 hour aged limestone bitumen-filler mastics

Freq/Temp	10°C	15°C	25°C	35°C	45°C	55°C	65°C	75°C	80°C
0.1 Hz	13134000	5931200	875490	115720	17310	2206.2	598.29	178.81	105.44
0.15849 Hz	17366000	8553900	1217400	166390	25393	3449.5	926.71	271.71	163.48
0.25119 Hz	21900000	10177000	1672500	240920	37186	5434	1411.6	419.79	252.01
0.39811 Hz	27506000	13564000	2280700	342150	55056	8379.8	2236.4	664.45	392.02
0.63096 Hz	35475000	17698000	3170800	489990	81349	12506	3418.8	1028.4	611.59
1 Hz	44746000	22834000	4348700	702180	120470	19240	5306.3	1616.6	973.01
1.5849 Hz	56346000	29312000	5876900	993490	176530	29306	8138.8	2527.4	1514.2
2.5119 Hz	70551000	37927000	7904300	1403800	257810	44316	12540	3942.3	2374.6
3.9811 Hz	85056000	48100000	10647000	1978500	379640	67140	19246	6093.1	3780.3
6.3096 Hz	102840000	60012000	14286000	2768100	547480	100190	29511	9499.6	5825.4
10 Hz	122730000	74233000	18909000	3861600	782310	150100	44933	14591	8980.7

Freq/Temp	10°C	15°C	25°C	35°C	45°C	55°C	65°C	75°C	80°C
0.1 Hz	54.37	58.05	66.39	74.05	78.12	85.59	85.1	85.13	85.2
0.15849 Hz	59.81	60.94	64.9	72.49	77.5	84.89	85.42	85.23	84.38
0.25119 Hz	50.34	56.04	64.45	71.86	77.48	83.89	85.99	86.27	85.87
0.39811 Hz	48.89	54.61	63.34	71.25	77.24	85.4	86.75	86.7	87.02
0.63096 Hz	47.92	52.94	62.58	70.74	76.8	83.08	85.41	87.6	87.77
1 Hz	45.86	51.96	62.08	70.25	76.17	83.17	86.08	87.17	87.69
1.5849 Hz	43.75	49.97	61.01	69.13	75.39	81.66	85.12	86.51	87.56
2.5119 Hz	43.69	47.97	59.89	68.52	75.06	80.79	84.74	86.53	87.17
3.9811 Hz	39.73	45.97	58.65	67.82	74.37	79.68	83.91	86.41	87.25
6.3096 Hz	38.04	44.68	57.45	67.16	74.04	79.06	83.35	85.96	87.24
10 Hz	36.05	43.21	56.37	66.44	73.52	77.7	83.1	85.76	87.34

Table F7: Complex modulus and phase angle of the 3 hour aged limestone bitumen-filler mastics

Freq/Temp	10°C	15°C	25°C	35°C	45°C	55°C	65°C	75°C	80°C
0.1 Hz	14241000	6484800	993290	136440	21131	2974.5	759.95	230.48	132.18
0.15849 Hz	16537000	9037300	1373000	194760	30916	4657.5	1180.2	354.9	194.68
0.25119 Hz	23817000	11283000	1893900	280470	45174	7273.9	1797.7	538.82	313.33
0.39811 Hz	28993000	14763000	2605900	399910	66397	10784	2817.6	845.19	487.4
0.63096 Hz	37525000	19123000	3569100	570070	97634	16576	4324.7	1297.3	741.06
1 Hz	47061000	24592000	4867500	810510	142830	25167	6639.8	2041.5	1179.4
1.5849 Hz	58571000	31710000	6596700	1146600	208500	38351	10261	3157.6	1815
2.5119 Hz	69923000	40748000	8797100	1607300	303200	57513	15510	4922.7	2875.6
3.9811 Hz	87554000	50778000	11816000	2256600	437900	85848	24014	7619	4498.6
6.3096 Hz	105620000	63245000	15669000	3136300	631250	127730	36397	11777	6947.6
10 Hz	125590000	77684000	20603000	4343900	902160	188140	54952	18070	10720

Freq/Temp	10°C	15°C	25°C	35°C	45°C	55°C	65°C	75°C	80°C
0.1 Hz	53.52	58.07	66.2	73.54	77.22	84.37	85.58	83.97	84.57
0.15849 Hz	44.82	63.55	64.54	72.13	76.95	84.44	85.05	85.14	84.63
0.25119 Hz	49.33	54.64	63.9	71.42	76.71	82.91	85.38	85.84	85.39
0.39811 Hz	46.88	53.67	62.75	70.54	76.35	83.51	85.76	86.46	86.89
0.63096 Hz	46.72	52.36	62.11	69.84	75.67	82.04	84.8	86.85	87.63
1 Hz	44.94	50.87	60.86	69.06	75.04	80.73	84.7	87.19	86.94
1.5849 Hz	42.49	49.01	59.83	68.19	74.48	80.27	84.16	86.28	87.18
2.5119 Hz	41.59	47.11	58.86	67.49	73.67	79.42	83.42	86.16	86.64
3.9811 Hz	38.87	45.28	57.61	66.64	73	78.43	82.87	85.71	86.43
6.3096 Hz	37.08	43.68	56.41	66.05	72.37	77.25	82.26	85.36	86.2
10 Hz	35.28	41.99	55.19	65.32	71.8	76.1	81.64	84.98	85.97

Table F8: Complex modulus and phase angle of the 5 hour aged limestone bitumen-filler mastics

Freq/Temp	10°C	15°C	25°C	35°C	45°C	55°C	65°C	75°C	80°C
0.1 Hz	20367000	9033300	1342000	184750	28815	4574.4	1062.8	295.15	174.93
0.15849 Hz		11188000	1824600	262190	41779	6927.2	1617.8	458.41	262.16
0.25119 Hz	32416000	15379000	2493600	370830	60995	10665	2511.7	703.75	409.57
0.39811 Hz	39076000	19423000	3390500	526740	89708	15738	3864.4	1092.7	633.23
0.63096 Hz	49040000	24902000	4591000	744200	130390	24435	5936.7	1690.2	983.93
1 Hz	60664000	31451000	6158900	1045800	190360	36716	9177.1	2629	1552.3
1.5849 Hz	74614000	39955000	8230100	1460100	275240	55660	14100	4104	2394.8
2.5119 Hz	90617000	49902000	10875000	2029100	397400	83323	21420	6355.9	3736.3
3.9811 Hz	108160000	61905000	14372000	2814600	570790	123860	32460	9827.3	5784.6
6.3096 Hz	127950000	75464000	18870000	3875200	813890	182750	49383	15181	8982.1
10 Hz	148760000	91882000	24351000	5314700	1155100	267750	74461	23181	13887

Freq/Temp	10°C	15°C	25°C	35°C	45°C	55°C	65°C	75°C	80°C
0.1 Hz	49.89	54.83	63.9	71.97	76.89	83.04	84.78	85.77	84.56
0.15849 Hz		56.72	62.52	70.42	76.31	83.64	85.59	85.79	85.61
0.25119 Hz	45.95	51.15	61.76	69.86	76.08	82.48	85.34	86.14	86.07
0.39811 Hz	43.21	50.44	60.69	69.02	75.55	82.17	85.7	86.87	87.29
0.63096 Hz	44.07	48.95	59.82	67.92	74.8	80.63	85.56	86.72	87.35
1 Hz	42.78	47.76	58.55	67.26	74.14	80.04	84.83	86.52	87.74
1.5849 Hz	38.81	45.72	57.27	66.42	73.28	79.44	83.79	86.19	87.04
2.5119 Hz	36.84	43.18	56.57	65.46	72.5	78.07	83.3	85.89	86.96
3.9811 Hz	35	41.87	55.13	64.65	71.78	77.05	82.47	85.45	86.38
6.3096 Hz	33.36	40.61	53.75	63.88	71.08	75.64	81.64	85.08	85.94
10 Hz	31.78	38.99	52.73	63.21	70.58	74.16	80.92	84.72	86.04

Table F9: Complex modulus and phase angle of the 10 hour aged limestone bitumen-filler mastics

Freq/Temp	10°C	15°C	25°C	35°C	45°C	55°C	65°C	75°C	80°C
0.1 Hz	21366000	9804100	1637600	243740	37873	6340.8	1589	454.73	256.56
0.15849 Hz	22529000	11266000	2201500	340970	55208	9614.3	2429.6	691.01	392.11
0.25119 Hz	33392000	16283000	2944900	476720	80120	14594	3741.7	1077.9	603.69
0.39811 Hz	39657000	20136000	3913000	667740	116290	21829	5813.5	1647.7	923.05
0.63096 Hz	49580000	25725000	5249500	924980	167860	33067	8571	2548.1	1439.6
1 Hz	60110000	32269000	6950400	1280700	241990	49110	13078	3932.7	2239.3
1.5849 Hz	74499000	40528000	9093500	1761600	346310	72436	19734	6065.3	3443.6
2.5119 Hz	89240000	48205000	11877000	2418600	491730	106410	30087	9242.8	5292.6
3.9811 Hz	105490000	61177000	15601000	3287700	697250	155410	44782	14058	8173
6.3096 Hz	123680000	74611000	20144000	4460000	980800	226740	66282	21424	12539
10 Hz	143430000	89534000	25839000	6032900	1373100	321980	98500	32311	18966

Freq/Temp	10°C	15°C	25°C	35°C	45°C	55°C	65°C	75°C	80°C
0.1 Hz	47.46	52.56	60.96	68.86	75.81	81.16	83.77	84.51	83.09
0.15849 Hz	31.31	47.39	59.28	67.08	74.43	81.51	83.74	84.73	84.81
0.25119 Hz	43.87	48.79	58.64	66.51	73.87	80.57	83.07	84.75	84.87
0.39811 Hz	40.99	47.95	57.57	65.77	72.86	79.13	84.56	84.94	86.27
0.63096 Hz	41.4	46.9	56.72	64.76	72.02	77.85	83.13	84.64	85.18
1 Hz	40.17	45.32	55.67	64.09	70.81	78	81.67	84.12	86.05
1.5849 Hz	38.04	44.06	54.8	63.12	70.16	75.97	81.01	83.98	85.12
2.5119 Hz	35.83	44.46	53.91	62.33	69.39	74.7	80.17	83.59	85.06
3.9811 Hz	34.43	40.76	52.62	61.67	68.66	73.46	79.14	82.86	84.26
6.3096 Hz	32.56	39.43	51.38	60.92	68.07	71.84	78.23	82.33	84.22
10 Hz	31.35	37.7	50.5	60.29	67.71	70.44	77.32	81.89	83.34

Table F10: Complex modulus and phase angle of the 20 hour aged limestone bitumen-filler mastics

Freq/Temp	10°C	15°C	25°C	35°C	45°C	55°C	60°C	65°C	75°C
0.1 Hz	31681000	14638000	2622300	435870	82606	22671	14641	10322	4282.8
0.15849 Hz	30952000	19950000	3457400	585800	112730	32688	20143	13779	4691.7
0.25119 Hz	46504000	23042000	4797900	796280	155720	39610	23779	14499	5434.3
0.39811 Hz	54860000	28086000	5936600	1094200	214770	56412	31724	19899	6757.6
0.63096 Hz	67242000	35752000	7867300	1482800	300810	79820	45520	27135	8897.7
1 Hz	77458000	44294000	10266000	2016600	418280	112450	62942	37208	12017
1.5849 Hz	97843000	55659000	13220000	2740600	580850	158180	87446	51086	16886
2.5119 Hz	116050000	69684000	17345000	3688800	808970	222070	122140	70350	24097
3.9811 Hz	135690000	82477000	22398000	4959100	1124500	312810	173790	99644	34068
6.3096 Hz	156880000	99348000	28687000	6675700	1551500	438630	245200	142610	49210
10 Hz	180400000	117590000	36294000	8922200	2142100	601960	342120	199810	71555

Freq/Temp	10°C	15°C	25°C	35°C	45°C	55°C	60°C	65°C	75°C
0.1 Hz	44.87	50.99	58.8	64.77	68.78	67.65	60.1	56.28	53.46
0.15849 Hz	18.16	57	57.36	63.56	68.31	70.17	68.61	62.97	60.43
0.25119 Hz	42.65	48.2	55.33	63.57	68.22	70.84	67.99	67.85	62.1
0.39811 Hz	39.79	46.6	56.26	63.37	67.88	69.72	68.28	67.27	67.43
0.63096 Hz	40.06	46.18	55.54	62.73	67.5	69.58	69.61	68.32	68.47
1 Hz	42.22	44.89	54.83	61.95	67.33	69.22	69.33	69.78	71.16
1.5849 Hz	35.96	43.02	54.06	61.41	67.19	68.27	69.51	69.91	72.54
2.5119 Hz	34.69	42.49	53.17	61.06	66.93	66.94	70.12	70.92	73.9
3.9811 Hz	32.53	39.9	51.8	60.49	66.57	65.95	68.8	71.07	74.18
6.3096 Hz	31.15	37.89	50.57	59.79	66.27	64.24	68.02	70.52	74.73
10 Hz	29.63	36.55	49.72	59.35	66.12	62.68	67.14	70.46	74.54